

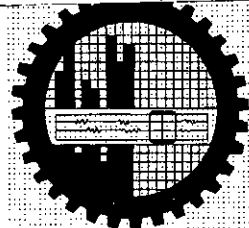
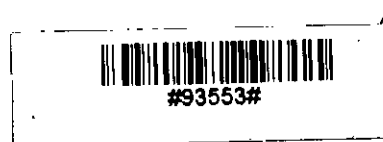
A STUDY OF RADIOACTIVITY AND RADIATION LEVELS IN BANGLADESH FOR ASSESSMENT OF POPULATION EXPOSURE

THESIS SUBMITTED
IN PARTIAL FULFILMENT OF THE REQUIREMENTS
FOR THE DEGREE OF
MASTER OF PHILOSOPHY



BY

SHYAMAL RANJAN CHAKRABORTY



DEPARTMENT OF PHYSICS
BANGLADESH UNIVERSITY OF ENGINEERING AND TECHNOLOGY
DHAKA-1000.
MAY, 1999.

CERTIFICATE

This is to certify that the author is solely responsible for the work reported in this thesis and this work has not been submitted in any university or elsewhere for the award of any degree or diploma.

Shyamal Ranjan Chakraborty

Candidate 12/05/99
(Shyamal Ranjan Chakraborty)

Roll # 9414023 F

Regn. # 9414023

Session: 1993-'94-'95.

BUET, Dhaka-1000.

Gias Uddin Ahmad

Supervisor 12-05-99

(Dr Gias Uddin Ahmad)

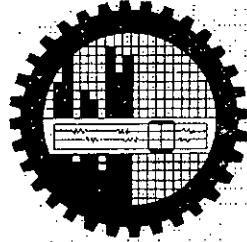
Professor

Department of Physics

BUET

Dhaka-1000.

BANGLADESH UNIVERSITY OF ENGINEERING AND TECHNOLOGY, DHAKA.
DEPARTMENT OF PHYSICS



CERTIFICATION OF THESIS

A Thesis on

**“A STUDY OF RADIOACTIVITY AND RADIATION LEVELS IN BANGLADESH
FOR ASSESSMENT OF POPULATION EXPOSURE”**

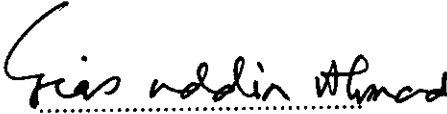
By

SHYAMAL RANJAN CHAKRABORTY

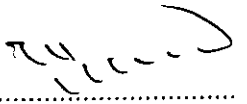
Has been accepted as satisfactory in partial fulfillment for the degree of Master of Philosophy in Physics and certifying that the student has demonstrated a satisfactory knowledge of the field covered by this thesis in an oral examination held on June 17, 1999.

Board of Examiners

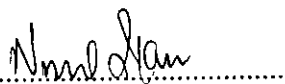
1. Dr Gias Uddin Ahmad
Professor
Department of Physics
BUET, Dhaka-1000.
2. Dr Abdus Sattar Mollah
Principal Scientific Officer
NSRC Division
Bangladesh Atomic Energy Commission
4, Kazi Nazrul Islam Avenue
Ramna, Dhaka-1000.
3. Dr Mominul Huq
Professor & Head
Department of Physics
BUET, Dhaka-1000.
4. Dr Nazma Zaman
Associate Professor
Department of Physics
BUET, Dhaka-1000.
5. Dr Nurul Islam Molla
Director General
Atomic Energy Research Establishment
Bangladesh Atomic Energy Commission
Ganakbari, Savar
Dhaka.


.....
Supervisor & Chairman


.....
Co-supervisor & Member


.....
Member


.....
Member


.....
Member (External)

To
The Memory of My Late Aunt
Mrinaliny Chowdhury

ACKNOWLEDGMENT

This research work has been carried out under the able supervision of **Dr Gias Uddin Ahmad**, Professor of Physics, BUET, and the co-supervision of **Dr Abdus Sattar Mollah**, Principal Scientific Officer, Nuclear Safety & Radiation Control Division, Bangladesh Atomic Energy Commission, Ramna, Dhaka. It is my great pleasure to express my deepest sense of gratitude, sincere appreciation and indebtedness to my reverend teacher & supervisor, and to my revered co-supervisor for their scholastic and indispensable guidance, keen interest, constructive criticism and suggestions, constant inspiration, and hearty assistance throughout the research work for fruitful finishing and in preparing this manuscript with necessary correction.

I'm also indebted and grateful to **Ms Aleya Begum**, Senior Scientific Officer, Radiation Control & Waste Management Division, Institute of Nuclear Science & Technology, Atomic Energy Research Establishment, BAEC, Ganakbari, Savar, Dhaka; for her sincere help, constructive suggestions, perpetual urge and guidance in this research work.

I'm grateful to **Dr Mominul Huq**, Professor and Head, Deptt of Physics, BUET; for his inspiration during this work. I'm also grateful to **Dr Md Ali Asgar**, **Dr Md Tofazzal Hossain**, and **Dr Md Abu Hashan Bhuiyan**, Professors, Deptt of Physics, BUET; for their encouragement. I'm further grateful to **Dr Jiban Podder**, **Dr Nazma Zaman**, and **Ms Dil Afroze Ahmed**, Associate Professors of Physics, BUET; for their constant encouragement and suggestions. I'm also thankful to **Dr Firoze Alam Khan**, **Ms Fahima Khanam**, **Ms Afia Begum**, **Mr Md Ashrafuzzaman**, **Dr Md Nazrul Islam** and all teachers of Physics Deptt, BUET for their encouragement. I'm very grateful to BUET authority for providing the financial grant for this research.

I would like to gratefully acknowledge the heart-felt cooperation of a lot of people meet them in different locations of the present study. Some of them are: **Mr Md Mozammel Haque Babu** and his family members of Race Course, Comilla; **Mr Dhananjay Acharjya** of Saha Bari, Koralia Road, Chandpur; **Mr Tutul Kanti Saha** and his family members of Modhya Modhupur, Feni; **Md Anwar Uddin** and **Md Bahar Uddin** of Ramhorir Taluk, Khalifar Hat, Noakhali; **Mr Kazi Ashraf Hossain** and **Mr Naim Sadek** of Chor King, and the family members of **Mr Tonu Miah** of Chor Kailash, Uchhkhal, Hatiya, Noakhali; **Mr Fasiul Alam**, Assistant Health Inspector of Sandweep thana Health Complex and a resident of Harishpur, Sandweep, Chittagong; **Mr Kanto Prasad Deb**, and his family members of North Balubari, Gaosia Gate, Dinajpur; **Mr A T M Kaosar Jamil**, Ph D student of Physics Deptt, BUET, his younger brother **Babu**, and all of his family members of Master Para, Rangpur; **Md Mojaffar Hossain**, Senior teacher, Kurigram Boy's School, Kurigram; **Mr Abdul Malek** and **Mr Abdul Matin** of Kawak, Ullapara, Sirajgonj; **Mr Md Tajemul Islam**, Ph D Student, Physics Deptt, Rajshahi University; *Headmaster of Srirampur High School* (near Nachole Railway Station), Nachole, Chapai Nawabgonj; **Mr Asim Kumar Dey** of Nokipur, Shyamnagar, Satkhira; **Mr Md Mostafizur Rahman Siyam & Mr Md Ziaur Rahman Niaz**, their family members and neighbours of Horisova, Faridpur; **Ms Mst Hosne-Ara Swopna** and her family members of Chapail, Kalia, Narail; **Mr Md Kamruzzaman Bachchu** of Mazed Villa, Chor Colony, Borguna; **Mr Golam Mortuza Dewan** of Math Para, and **Mr Md Akhtaruzzaman** of Nazim Monjil, Daxin Kut Gaon, Munsigonj; **Mr Ratan** and all of his family members of Etim Khana Road, Old Jhenidah Bus Stand Para, Chuadanga; **Mr Abdul Karim Mollah** and his family members of Diyar Bagal, Roop Pur,

Ishurdi, Pabna; **Mr Md Asgar Ali Sheikh Chunnu Miah** of Sheikh Para, Pirojpur; family members of **Mr Syed Gazi** of Kuakata, Khepupara, Patuakhali; *Villagers of Badalgachhi and Hapunia* of Badalgachhi, Naogaon; *Villagers of Kewa Poshchim Khando*, Maona, Sripur, Gazipur; **Mr Roma Kanto Dhar** of Digar Brahman Gram, Sherpur, Nabigonj, Habigonj; **Mr Azizul Haque Khan** of Sunapur, Sunamgonj; **Mr Babu Bhattacharja** of Munsipara, Kalihati, Tangail; **Mr Hena Miah** and his neighbours of Aricha Ghat, Shibalaya, Manikgonj; **Mr Monwar Hossain Monu Miah** of Chowdhury Para, Teknaf; **Mr Brajendra Das** and his son of Ghonar Para, Cox's Bazar, **Mr Mong Hra Ching Headaram** (Chairman) of Roangchheri, Bandarban; **Mr Priti Kusum Chakma** of Khobong Poria, Khagrachheri; and **Mr Ranjan Chakma** and *Villagers of Diyar Pur, Dewan Para, Rangamati*.

I'm very much grateful to **Mr Anis Uddin Ahmed**, his daughter **Ms Ratna**, and all of his family members of Hazipur, Norsingdi; for their sympathetic cooperation during the field-work at Norsingdi.

I also acknowledge with feelings of gratitude the extended hand of hearty cooperation of **Mr Shamvu Karmakar**, a veteran freedom fighter of our liberation war and now a social worker of Eastern Para, Chorfashion, Bhola; during the field-works at Chorfashion.

I sincerely acknowledge with gratitude the contribution of **Prof Md Abdul Kader Hawlader**, and all of his family members of Khanika, West-Sagardi, Rupatali, Barisal; for their hearty cooperation by providing me all necessary directions and possible facilities during the field works in greater Barisal, Khulna, Faridpur, and Jessore region.

I'm indebted to **Mr Samarendra Bhattacharja Liton**, his father **Prof Satyendra Bhattacharja**, his mother and his sister of Akhra Bazar, Kishoregonj; for their cordial cooperation during the field-works of the present research at Kishoregonj.

I gratefully acknowledge the cooperation of **Mr Moloy Kumar Deb** of North Balubari, Gaosia Gate, Dinajpur; and **Mr Sandip Das Manik**, M Sc Student, Deptt of Computer Science, Bangalore University, Bangalore, and a permanent resident of West-Dinajpur, West Bengal, India; for their sympathetic cooperation at the field-works in Dinajpur, Syedpur, and Panchagarh.

I'm thankful to **Mr Mamun**, lecturer of Botany Deptt. Jahangirnagar University and a permanent resident of Barhatta Bazar, Netrakona; for his kind help at the field-works in Barhatta. Grateful thanks are also due to **Ms Lipika Saha**, Scientific Officer (SO), Nuclear Medicine Centre (NMC), Bogra; **Mr Rashid Ahmed Amiree**, SO, NMC, Faridpur; **Dr Tahmina Begum**, Medical Officer (MO), NMC, Comilla; **Mr Md Jahurul Alam**, Lecturer of Mathematics Deptt, SUST, Sylhet; **Mr Md Nazibul Islam** and **Mr Md Shahjahan Ali**, both are lecturer of Electronics & Applied Physics Deptt, Islamic University, Kushtia; for their sincere and candid cooperation during the field works at Bogra, Faridpur, Comilla, Dinajpur, and Kushtia respectively.

I'm very much grateful to **Dr Mohammed Fazlul Kabir**, PMO & Director, NMC Chittagong for his sympathetic cooperation during the field-works at greater Chittagong region, and encouragement. I'm also grateful to **Prof M A Awal**, **Prof Md Azharul Islam**, and **Prof Mir Md Akramuzzaman** of Physics Deptt, Jahangirnagar University, for their heart-felt help in collecting

few thesis-papers of their department. At the same moment, I would also like to express my sincere gratitude to **Mr Satyajit Ghose**, Scientific Officer, RTL, BAEC, Chittagong; for collecting few papers on environmental radioactivity and radiation level and sending those to me. I would further like to offer my hearty thanks to **Ms Sharmin Nahar Sharmi**, M Sc in Physics, Jahangirnagar University for her candid help in collecting a few papers on low-level radioactivity.

I'm very much indebted to **Dr S M Moinul Islam**, SMO & Director-in-charge, NMC Mymensingh for his constant encouragement, support and endowment of all possible facilities of his establishment. I'm also grateful to **Dr Saiyeeda Mahmood**, **Dr Gazi Abul Hossain**, **Dr Nasim Khan**, **Mr Md Nurul Amin**, and **Dr Nasima Akhter** of NMC Mymensingh for their all possible supports in successful completion of this work.

Grateful thanks are also made to **Mr Md Nasratul Hossain**, M Sc in Physics, Chittagong University; for his friendly cooperation in various ways to crown the conclusion of this research with success. I'm also thankful to all of his family members at Sitakundo, Chittagong.

I also express a lot of thanks from the core of my heart to **Mr Md Zakaria Quadir Sumon**, M Phil Student, Mechanical Engineering Deptt Hongkong University, Hongkong, and my ex-roommate at Shahid Smrity Hall, BUET; and **Dr Ratan Kumar Chakraborty**, MO, NMC Mymensingh; my present housemate; for their relentless encouragement and help in different ways in successful fulfilment of this research.

Hearty thanks are due to **Mr Liakot**, **Mr Azad**, and **Mr Bari**, Scientific Assistants of Health Physics Laboratory, RCWMD, INST, AERE, BAEC, Ganakbari, Savar, Dhaka; for their kind and laborious help in sample preparation, preservation, and readout. I like to offer my sincere thanks to **Mr Lutfur Rahman Sarker**, **Mr Swapon**, **Mr Taher**, **Mr Mozammel**, **Mr Nurul Haque**, and **Mr Mofazzol**, Laboratory assistants; and **Mr Liakot Ali**, Office Assistant; of Physics Deptt, BUET; for their cordial and laborious assistance in different ways of the present research.

Sincere thanks are also due to **Mr Md Manjurul Haque**, **Mr C M Mukammel Wahid**, **Mr Md Tareq Aziz Shuvo**, **Mr Manas Kanti Bishwas**, **Mr Muslehuzzaman Khan Shipu**, **Mr Md Salim Reza**, **Mr Md Tahidul Haque**, **Mr Md Abdur Razzak**, **Ms Naureen M Rahman**, and **Ms Meherun Nahar Lipi**, ex- and present fellows of Physics Deptt, BUET; **Mr A N M Omar Faruque Milon**, and **Mr Mafizur Rahman Khokan**, both are fellows of Chemistry Deptt, BUET; and **Mr Shubho**, MURP student, BUET; for their instant encouragement and cooperation. A special thanks is also due to **Ms Jahanara Begum Ruby**, M Phil student, Physics Deptt, BUET; for her sincere cooperation, advice, and guidance during the research work.

At last but not least, I would like to offer my deepest sense of gratitude to all of my venerable **brothers**, **sisters**, and **parents** because of their relentless support and encouragement by providing me all maximum possible corroboration in continuing this research. Without their active cooperation, it would be impossible for me to crown the conclusion of this research with success.

Department of Physics
BUET, Dhaka – 1000.
May 12, 1999.

Shyamal Ranjan Chakraborty

ABSTRACT

The indoor-outdoor radiation dose levels, and radioactivity levels of natural radionuclides in soil and water samples of 56 locations of Bangladesh were measured. The radiation dose levels at the sea-beaches of Bangladesh and the concentrations of naturally occurring radionuclides in the sand samples of Cox's Bazar sea-beach and Kuakata sea-beach were also measured. The radiation dose levels were measured by a calibrated portable radiation dose rate survey-meter PDR 1Sv. The assessment of radioactivity levels in soil, sand, and water samples were performed by a high-resolution low background HPGe detector. Radiation dose due to radioactivity in soil samples and intake of water samples were also assessed.

The average indoor dose levels at kutchahouses, new-buildings, and old-buildings were found to be $0.23 \pm 0.04 \mu\text{Sv.hr}^{-1}$, $0.25 \pm 0.04 \mu\text{Sv.hr}^{-1}$, and $0.27 \pm 0.04 \mu\text{Sv.hr}^{-1}$ respectively. The weighted average indoor dose levels in all kinds of houses was found to be $0.24 \pm 0.04 \mu\text{Sv.hr}^{-1}$. The average outdoor dose level was found to be $0.20 \pm 0.07 \mu\text{Sv.hr}^{-1}$. The ratio of average indoor dose level to average outdoor dose level was found to be 1.2. The total average effective dose equivalent due to external natural radiation was estimated to be $\sim 2 \text{ mSv.y}^{-1}$. The average concentrations of ^{232}Th , ^{238}U , ^{40}K , and ^{137}Cs in soil samples were found to be $83.56 \pm 17.96 \text{ Bq.kg}^{-1}$, $44.35 \pm 12.65 \text{ Bq.kg}^{-1}$, $630.89 \pm 173.85 \text{ Bq.kg}^{-1}$, and $5.37 \pm 4.87 \text{ Bq.kg}^{-1}$ respectively. The average activities of the mentioned radionuclides in water samples were found to be $249.59 \pm 51.67 \text{ mBq.L}^{-1}$, $156.77 \pm 30.46 \text{ mBq.L}^{-1}$, $9.08 \pm 3.36 \text{ Bq.L}^{-1}$, and $1.17 \pm 1.80 \text{ Bq.L}^{-1}$ respectively. The average annual effective dose equivalent due to ingestion of water was found to be $74.01 \pm 21.41 \mu\text{Sv}$ ranging between $24.20 \pm 5.57 \mu\text{Sv}$ and $134.04 \pm 16.10 \mu\text{Sv}$. The average annual effective dose equivalent due to terrestrial radiation was found to be $1.26 \pm 0.27 \text{ mSv}$ with a range from 0.56 ± 0.08 to $1.88 \pm 0.09 \text{ mSv}$. The average dose level in the shining-brown coloured sandy areas in Cox's Bazar sea-beach was found to be $8.94 \pm 3.15 \text{ mSv.y}^{-1}$ ranging between $6.39 \pm 2.28 \text{ mSv.y}^{-1}$ and $11.91 \pm 4.29 \text{ mSv.y}^{-1}$ while the average dose level in shining-brown coloured sandy areas of Kuakata sea-beach was found to be $4.20 \pm 0.88 \text{ mSv.y}^{-1}$ ranging from $2.98 \pm 0.70 \text{ mSv.y}^{-1}$ to $5.87 \pm 0.18 \text{ mSv.y}^{-1}$. The average radiation dose levels in public areas of Cox's Bazar sea-beach, Potenga sea-beach, and Kuakata sea-beach were found to be $1.49 \pm 0.18 \text{ mSv.y}^{-1}$, $1.58 \pm 0.26 \text{ mSv.y}^{-1}$, and $1.58 \pm 0.35 \text{ mSv.y}^{-1}$ respectively.

By plotting the cumulative frequency plots for the average concentrations of radionuclides and average radiation dose levels, the geometric mean and geometric standard deviation for each type of data were estimated and compared with the corresponding arithmetic mean and standard deviation. Except the ^{137}Cs concentration in water samples, all data were found to be distributed normally. A good correlation between the corresponding concentrations of radionuclides in soil and water samples of the same place was found.

The average fatal cancer risk was found to be 101 per 10^6 people with a range from 78 to 144 cases per million people, based on the measured average dose level.

TABLE OF CONTENTS

CHAPTER	TITLE/SUB-TITLE	PAGE
CHAPTER 1: INTRODUCTION		1
1.1	General	2
1.2	Biological effects of radiation	11
1.2.1	Role of free radicals in radiation damage	14
1.2.2	DNA damage by ionizing radiation	14
1.2.3	Effects of ionizing radiation on human body	15
1.2.4	Effects of ionizing radiation on embryo	17
1.2.5	Health effects of low-level radiation	17
1.3	Objectives of the research	18
CHAPTER 2: REVIEW		28
2.1	Introduction	29
2.1	Review of previous works	29
CHAPTER 3: EXPERIMENTAL		54
3.1	Introduction	55
3.1.1	Gas filled detectors	56
3.1.2	Solid-state detectors	56
3.1.2.1	Semiconductor detectors	57
3.1.2.2	Scintillation detectors	57
3.1.2.3	Thermoluminescence dosimeter	58
3.1.3	Film badge dosimeter	58
3.2	Gas filled radiation detectors	59
3.2.1	Geiger-Müller counter	61
3.3	High purity germanium (HPGe) detector	63
3.4	Equipment setup	66
3.4.1	Portable survey meter PDR 1Sv	66
3.4.2	The high purity germanium detector 'Silena'	68
3.4.2.1	Shielding arrangement of the detector	74
3.5	Experimental details	76
3.5.1	Measurements of dose levels	78
3.5.2	Sample collection	79

CHAPTER	TITLE/SUB-TITLE	PAGE
	3.5.3 Sample preparation	80
	3.5.4 Sample readout	80
	3.5.5 Radioactivity calculation	87
	3.5.6 Radiation dose due to radioactivity in soil and cosmic radiation	88
	3.5.7 Radiation dose due to intake of water	88
	3.5.8 Determination of annual collective dose equivalent	88
	3.6 Statistical errors in counting	88
	3.7 Cumulative frequency plot	90
	3.8 Calculation of population risk factor	91
CHAPTER 4: RESULTS AND DISCUSSION		92
4.1 Introduction		93
4.1.1 Energy calibration and resolution		93
4.1.2 Efficiency calibration		93
4.1.3 Lower limit of detection		93
4.2 Radiation dose level throughout Bangladesh		94
4.3 Radioactivity levels in soil samples		94
4.3.1 Radiation dose due to radioactivity in soil		94
4.4 Radioactivity levels in water samples		94
4.4.1 Radiation dose due to intake of water		94
4.5 Radiation dose due to cosmic radiation		95
4.6 Discussion		95
4.6.1 Indoor dose level		95
4.6.2 Outdoor dose level		96
4.6.3 Average annual effective dose equivalent and annual collective dose equivalent		97
4.6.4 Radiation dose levels in sea-beaches of Bangladesh		97
4.6.5 Radioactivity in soil samples		98
4.6.6 Radioactivity in beach sand samples		100
4.6.7 Radioactivity in water samples		100
4.6.8 Correlation between the activities of radionuclides found in soil and water samples		102
4.6.9 Radiation dose due to terrestrial radiation		103
4.6.10 Radiation dose due to cosmic radiation		103
4.6.11 Radiation dose due to intake of water		103

CHAPTER	TITLE/SUB-TITLE	PAGE
	4.6.12 Total radiation dose received by people living in Bangladesh	104
	4.6.13 Risk of Bangladeshi people in radiation induced diseases	104
4.7	Conclusion	106
4.8	Scope of future studies	107
	REFERENCES	160
	ANNEXURE	173

LIST OF FIGURES

FIGURE No.	TITLE	PAGE
Figure 1.1:	Uranium-238 decay Series.	22
Figure 1.2:	Thorium-232 decay Series.	23
Figure 1.3:	Actinium decay Series.	24
Figure 1.4:	Major pathways of radionuclides to man in the event of an uncontrolled release of radioactivity.	25
Figure 1.5:	Schematic diagram illustrating the absorption of energy from radiation resulting in biological damage.	26
Figure 1.6:	Development of cell injury.	27
Figure 3.1:	The curve showing the relation between the applied voltage and the number of counts in a gas filled radiation detector.	60
Figure 3.2:	A Geiger-Müller Counter.	62
Figure 3.3:	The configuration of an intrinsic Ge detector.	65
Figure 3.4:	Block diagram of circuit layout PDR 1Sv.	68
Figure 3.5:	A block diagram of HPGe detector system.	69
Figure 3.6:	Photograph of PDR 1Sv Surveymeter.	70
Figure 3.7:	Photographic profile of HPGe detector system.	70
Figure 3.8:	Map of Bangladesh showing the locations of dose measurement and sample collection.	77
Figure 4.1:	Efficiency curve for HPGe detector with 1 kg soil in Marinelli beaker geometry.	143
Figure 4.2:	Efficiency curve for HPGe detector with 1 L water in Marinelli beaker geometry.	144
Figure 4.3:	Cumulative frequency plot (probability plot) for average dose levels in kutcha-houses.	145
Figure 4.4:	Cumulative frequency plot (probability plot) for average dose levels in new-buildings.	146
Figure 4.5:	Cumulative frequency plot (probability plot) for average dose levels in old-buildings.	147
Figure 4.6:	Cumulative frequency plot (probability plot) for average dose levels in free-spaces.	148
Figure 4.7:	Probability plot (cumulative frequency plot) for Th-232 concentrations in soil samples.	149
Figure 4.8:	Probability plot (cumulative frequency plot) for U-238 concentrations in soil samples.	150
Figure 4.9:	Probability plot (cumulative frequency plot) for K-40 concentrations in soil samples.	151

FIGURE No.	TITLE	PAGE
Figure 4.10:	Probability plot (cumulative frequency plot) for Cs-137 concentrations in soil samples.	152
Figure 4.11:	Probability plot (cumulative frequency plot) for Th-232 concentrations in water samples.	153
Figure 4.12:	Probability plot (cumulative frequency plot) for U-238 concentrations in water samples.	154
Figure 4.13:	Probability plot (cumulative frequency plot) for K-40 concentrations in water samples.	155
Figure 4.14:	Probability plot (cumulative frequency plot) for Cs-137 concentrations in water samples.	156
Figure 4.15:	Cumulative frequency plot for terrestrial radiation dose throughout Bangladesh.	157
Figure 4.16:	Cumulative frequency plot for average radiation dose received due to intake of 1 L water.	158
Figure 4.17:	Cumulative frequency plot for average annual radiation dose due to the intake of water throughout Bangladesh.	159

LIST OF TABLES

TABLE No.	TITLE	PAGE
Table 1.1:	Annual effective doses to adults from natural sources.	3
Table 1.2:	Average annual exposures to cosmic rays.	4
Table 1.3:	National estimates of the average annual effective dose from terrestrial γ -rays.	5
Table 1.4:	Principal birth defects due to radiation exposure in uterine life.	17
Table 1.5:	Lifetime mortality in a population of all ages from specific fatal cancer exposure to low radiation.	18
Table 3.1:	Properties of intrinsic germanium.	64
Table 3.2:	Specification of PDR 1Sv Survey Meter.	67
Table 3.3:	Silena HPGe detector specification.	71
Table 3.4:	Summary of the experimental HPGe detector set up and equipment.	76
Table 3.5:	Dose conversion factors for ingestion of radionuclides.	88
Table 4.1:	Efficiency of HPGe detector for Marinelli beaker geometry.	108
Table 4.2:	Lower limit of detection of the HPGe detector (Counting time 10,000 sec.).	108
Table 4.3:	Dose levels at different locations of Bangladesh.	109
Table 4.4:	Activity of radionuclides in soil samples collected from different locations in Bangladesh.	118
Table 4.5:	Average outdoor radiation dose level throughout Bangladesh.	121
Table 4.6:	Activity of radionuclides in water samples collected from different locations in Bangladesh.	123
Table 4.7:	Average effective dose equivalent (H_E) based on ingestion of radionuclides ^{232}Th , ^{238}U , ^{40}K , and ^{137}Cs in 1 litre drinking water.	126
Table 4.8:	Average annual effective dose equivalent (H_E) based on ingestion of radionuclides ^{232}Th , ^{238}U , ^{40}K , and ^{137}Cs through drinking water.	127
Table 4.9:	data exhibiting the range and average values of minimum dose rates, maximum dose rates, and trend dose rates; found in kutcha-houses, new-buildings, old-buildings, and free-spaces; in different locations of Bangladesh.	128
Table 4.10:	Mean dose levels found from average dose rates in kutcha-houses, new-buildings, old-buildings, and free-spaces throughout Bangladesh.	129

TABLE No.	TITLE	PAGE
Table 4.11:	Comparison of average environmental radiation dose level in some of the countries of the world.	130
Table 4.12:	Average annual effective dose equivalent and annual collective dose equivalent due to environmental radiation in different locations of Bangladesh.	131
Table 4.13:	Comparison of radiation dose levels in some of the sea-beaches of the world.	133
Table 4.14:	The range and average activities of radionuclides found in soil and water samples collected from 56 locations throughout Bangladesh.	134
Table 4.15:	Average concentrations of radionuclides in soil and water samples.	134
Table 4.16:	Comparison of data on average radioactivity in surface soil in different countries of the world.	135
Table 4.17:	Radioactivity levels (Bq.kg^{-1}) of the radionuclides ^{232}Th , ^{238}U , ^{40}K , and ^{137}Cs in beach sand samples of Kuakata, Cox's Bazar, and Mangalore (Karnataka, India) sea-beaches.	137
Table 4.18:	Comparison of data on average radioactivity (Bq.L^{-1}) in drinking water in different countries of the world.	138
Table 4.19:	The correlation coefficients between the concentrations of radionuclides found in soil and water samples collected from different locations in Bangladesh.	139
Table 4.20:	Annual range and average radiation dose received ($\mu\text{Sv.y}^{-1}$) due to intake of radionuclides ^{232}Th , ^{238}U , ^{40}K , and ^{137}Cs through water in different locations of Bangladesh.	140
Table 4.21:	Average annual radiation dose received ($\mu\text{Sv.y}^{-1}$) due to intake of drinking water throughout Bangladesh.	140
Table 4.22:	Estimated total annual effective dose equivalent and corresponding fatal cancer risk in different locations of Bangladesh.	141
Table A1:	Radiation weighting factors	179
Table A2:	Tissue weighting factors	180
Table A3:	Recommended dose limits	181

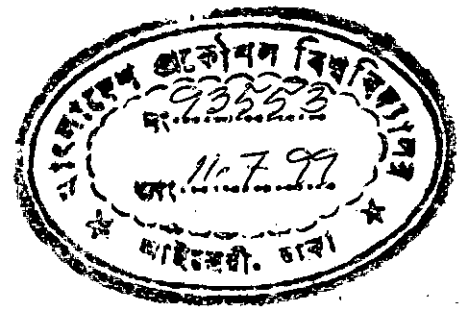
CHAPTER 1



INTRODUCTION

CHAPTER 1

INTRODUCTION



1.1 General

Man is always exposed to natural background radiation as well as artificial radiation sources. The sources of natural background radiation are the naturally occurring radionuclides in the ground (^{232}Th and ^{238}U and their decay products; ^{40}K etc.), gaseous radioactive elements in the atmosphere (radon, thoron), cosmic radiation, and the radioactivity in the body (^{14}C , ^{40}K , ^{232}Th , etc.). In addition to this, man is also exposed to artificial sources of radiation such as from diagnostic radiology, radiotherapy; uses of radioisotopes in medicine, in agriculture, and in industry; nuclear fallout, radioactive waste disposal, reactor accident etc. The average annual effective dose to adults from natural sources of ionizing radiation is $2.4 \text{ mSv}^{[1]}$.

There are certain amounts of ionizing radiations around us and everything in the environment are continuously exposed to those ionizing radiations. High external radiation levels have been found in Austria, Brazil, China, France, India, Italy, and other countries^[2]. Brazil has areas with abnormally high natural radiation. Among primordial radionuclides, ^{232}Th , ^{238}U , and ^{40}K mainly contribute to the total dose from natural background. Natural radiation is the main source of exposure to humans and the major contribution to the average annual dose received by mankind still comes from the natural sources. Also the distinctive features of natural radiation are that it involves the whole population of the world and that it has been radiated since the creation of the earth. Until 1945, Man was exposed to natural radiation only. Since 1945, man has been exposed to other artificial sources of radiation exposure like radioactive fallout from nuclear tests, radioactive waste disposal, and reactor operation and accident, uses of radioisotopes and ionizing radiation in industry, in agriculture, and in medicine. Moreover, enhanced radioactivity due to natural oil and gas production was observed in a North German oil field^[3].

Sources of natural radiation are the terrestrial and extraterrestrial radionuclides which are the members of well known three natural radioactive series namely: Thorium, Uranium and Actinium series associated with their progeny. In addition, there is another series called Neptunium (^{237}Np , $T_{1/2} 2.2 \times 10^6$ years) series with 15 daughters arising from the artificial

radionuclide ^{241}Pu ($T_{1/2}$ 13.2 years) as the parent. The long lived radionuclides ^{232}Th , having a half life of 1.39×10^{10} years represents as parent of 11 members Thorium decay series; ^{238}U having half life 4.5×10^9 years is the parent of uranium series with daughters and Actinium decay series on the other hand starts from ^{235}U ($T_{1/2}$ 8.25×10^8 years) having 11 members. The total number of radionuclides in the above mentioned four decay series may be about fifty and shown in Figures 1.1–1.3. In addition, there are certain other non-series natural radionuclides, ^{87}Rb , ^{40}K , ^{14}C , and ^3H ; the last two arises from cosmic ray interactions in the atmosphere. The natural radioactivity generates from three distinct sources viz.: (i) cosmic, (ii) terrestrial, and, (iii) radioactivity in the body. Terrestrial radiations are emitted mostly from natural radionuclides present in varying amounts in all types of sands, soil, rocks, air, water, and grass in the form of α , β , γ , even neutron or X-ray. About $460 \mu\text{Sv.y}^{-1}$ originate from the upper few feet of the crust, and a dose of $230 \mu\text{Sv.y}^{-1}$ results from natural body radioactivity. The average radiation dose received by the population from these three distinct sources is given in Table 1.1. The average indoor absorbed dose rate in air from terrestrial source of radioactivity is estimated to be 70 nGy.h^{-1} ⁽⁴⁾.

Table 1.1: Annual Effective Doses to Adults from Natural Sources⁽¹⁾.

Source of Exposure	Annual Effective Dose (mSv)	
	Typical	Elevated*
Cosmic rays	0.39	2.0
Terrestrial gamma-rays	0.46	4.3
Radionuclides in the body (except radon)	0.23	0.6
Radon and its decay products	1.30	10
Total (rounded)	2.40	—

* The elevated values are representative of large regions. Even higher values occur locally.

Galactic (cosmic) radiation consists of a low flux ($\sim 4 \text{ particles.cm}^{-2}.\text{sec}^{-1}$) of energetic (10^2 – 10^{14} MeV) bare nuclei which appear to fill our galaxy isotopically. The primary cosmic-rays are high energy particles like protons ($\sim 87\%$), α -particles ($\sim 11\%$), and a trace of heavier nuclei ($\sim 1\%$) from 10 MeV to 10^{14} MeV and higher that fill the space. Most of the cosmic rays originate from remote interstellar space far beyond our galaxy, from initial explosion of the expanding universe and from within the solar system itself. The geomagnetic effects on cosmic rays and the meson formation in the upper atmosphere confirm that the cosmic-rays originating

from outer space is mainly proton. The earth's atmosphere acts as a filter and absorbs much of the energy of the cosmic rays. That is why the intensity of the cosmic rays varies with altitude and the ionization decreases with the decrease of altitude. The dose contribution from cosmic rays depends greatly on altitude. It is about $26 \text{ nGy}\cdot\text{h}^{-1}$ at sea level in Taiwan and becomes twice that at 2000 m altitude^[5]. When interacting with earth's atmosphere, they produce "air showers" of energetic secondaries (nucleons, mesons, photons, electrons, and so on), many of which produce secondaries of their own, which in turn propagate. A total number of twenty radionuclides produced by cosmic rays in the earth atmosphere or in the earth itself (^{14}C , ^7Be , ^3H , ^{22}Na , ^{129}I) have so far been detected. The production rate of the cosmogenic radionuclides increases with both latitude and altitude due to flux variations. Average annual exposures to cosmic rays in some of the high altitude cities in the world are given in Table 1.2.

Table 1.2: Average Annual Exposures to Cosmic Rays^[1].

Location	Altitude (m)	Annual Effective Dose (μSv)
High Altitude Cities		
La Paz, Bolivia	3900	2020
Leas, China	3600	1710
Quito, Ecuador	2840	1130
Mexico City, Mexico	2240	820
Nairobi, Kenya	1660	580
Denver, United States	1610	570
Tehran, Iran	1180	440
Sea Level	—	270
World Average	—	380

The terrestrial radiations are emitted due to the presence of four radioactive decay series namely: uranium, thorium, actinium, and neptunium series and some other non-series single radioisotopes, such as: ^{87}Rb , ^{40}K , ^{14}C , ^3H , in nature. Of these, the major contributions are from ^{232}Th , ^{238}U , and, ^{40}K . Soil, sand, and rock; and consequently, the ground water contain a small quantity of these elements. They are producing over 50 radionuclides emitting α , β , and γ -radiations of varying intensities and energies. The radiation exposure to man due to terrestrial radiation in different countries of the world are listed in Table 1.3.

Table 1.3: National Estimates of the Average Annual Effective Dose from Terrestrial γ -Rays⁽¹⁾

Country	Effective Dose (mSv)
Bulgaria	0.45
Canada	0.23
China	0.55
Denmark	0.36
Finland	0.49
Germany	0.41
Japan	0.32
Norway	0.48
Spain	0.40
Sweden	0.65
United Kingdom	0.35
United States	0.28
USSR	0.32
Population-weighted world average	0.45

Before the invention and application of the fissioning of radionuclides, radioactivity was a natural phenomenon. In 1945, when man succeeded in fissioning of uranium and other nuclides; uranium fission product and other radioactive isotopes emerged on the earth as the source of man-made environmental radioactivity. This man-made radioactivity quickly exceeded that of natural radioactivity, contaminating the greater part of this planet. Now, there is not a single area in the lithosphere or biosphere, where man-made radioactivity is not present. Therefore environmental radioactivity is not only a natural phenomenon, but it is also an artificial phenomenon at present. The living beings of the earth are getting vulnerable to the increased radioactivity level and consequently in many cases suffering adversely at the hand of this evil state. The sources of artificial radioactivity to the environment are nuclear explosion tests, re-processing of nuclear fuels, uses of radioisotopes in medicine, sea bed disposal (Kara sea, Russian lake, Estonia etc.), accidents in nuclear facilities (Windscale 1957, Kystym 1957,

Three Mile Island 1979, Chernobyl 1986 etc.), radioactive laboratories, and test of nuclear weapons.

Manufactured (artificial) radioactive isotopes of caesium if introduced into the environment, will eventually reach humans via the food chain. Thus, artificial radioactive isotopes of caesium may contribute to the radiation dose that human receive from all sources. Nuclear weapons testing has been the most significant source of radiocaesium in the global environment. Above-ground nuclear testing has introduced about 1.3×10^9 GBq of ^{137}Cs into the atmosphere, much of which has been deposited on the earth as fallout, both on a regional and global scale^[6]. The Chernobyl accident in the former USSR released about 3.7×10^7 GBq of ^{137}Cs to the environment^[7]. Over the 35 years operating history of Savannah River Site (SRS), about 2.2×10^4 GBq of ^{137}Cs and 22 GBq of ^{134}Cs has been reported as releases to the atmosphere and streams^[7]. Caesium-137 in air is associated with suspended particles. Sources of ^{137}Cs in the air include the following: (i) direct fallout from nuclear weapons testing which occurred from 1945 until the end of atmospheric testing in 1980, (ii) ^{137}Cs releases from other nuclear facilities, (iii) resuspension of ^{137}Cs particles deposited in the soil from past weapon tests, and, (iv) SRS ^{137}Cs releases. It is often assumed that the concentrations of naturally occurring radionuclides in soil are roughly constant with depth, whereas surface induced materials, such as fallout ^{137}Cs , decrease rapidly with depth^[8]. The latter is certainly true for ^{137}Cs in undisturbed, clay containing soils.

The nature of environmental contamination is changing from the highly-concentrated, locally restricted, and, acute effect type to the lowly-concentrated, widely dispersed, and, chronic effect type. This evolution causes many difficulties in determining the environmental fate of trace concentrations of hazardous material, validation of mathematical models, and determination of exposure conditions^[9]. However, if we use radioactive fallout as indicator contaminants, these difficulties could easily be solved. A portion of the artificial radionuclides released from atmospheric nuclear tests is transported to the troposphere and the stratosphere with the ascending current caused by the nuclear detonation and globally dispersed with the general circulation of the atmosphere.

The total amount of radioactive material released into the environment since the advent of the atomic era originated mainly from a great number of atmospheric nuclear weapon tests

during 1945–1962 and continued individual tests occurring between 1964–1980^[10]. In 1963, after signing of the Moscow Treaty Banning Nuclear Tests in the atmosphere, on the ground, underground, in sea water; the contribution from nuclear weapons tests had decreased dramatically, but this act failed to stab off the nuclear danger. Because, firstly not all the nuclear empowered countries (such as France and China) signed the treaty and as such individual nuclear weapon tests occurring between 1964 and 1980 also made contribution^[10]. Besides this, many countries are becoming nuclear power day by day. The nuclear weapons contains enriched uranium and plutonium and when exploded produced over 200 different fission products and isotopes having different energy and half-lives contaminating the planet. Between 1945 and 1980 many (423) nuclear explosions tests were conducted in the atmosphere, of which 53 (12.5%) tests were made in the southern hemisphere and 370 (87.5%) in the northern hemisphere^[10]. Secondly, the inputs from other powerful sources of environmental contamination (nuclear fuel processing industry, nuclear reactors, nuclear power stations etc.) dramatically increased as atomic energy is increasingly utilized throughout the world for various purposes. By the year 1987, 433 nuclear reactors for generating electric power are either in operation or under construction in 30 countries and all of them depend on the energy derived from the fission of uranium^[11]. The whole process generates excess heat and needs a coolant which may be light or heavy water, CO₂, or molten sodium. These used coolants get enriched with radioactivity derived from the whole process and ultimately contaminate the environment. There are many reports on the nuclear power plant accident in developed countries such as a total failure of the cooling system, as occurred at the Three Mile Island, near Pittsburgh, USA in 1979; in the UK at Windscale in 1957. It was estimated that 20 kCi of ¹³¹I and about 0.7 kCi of caesium and strontium were released from Windscale accident. But the Chernobyl accident on 26 April 1986 became an unprecedented source of radionuclides input to the environment. The amount of radioactive materials released into the atmosphere by the damaged reactor during the first few hours following the accident was the largest in the entire nuclear history of the world. The amount of discharged radionuclides was ~3.6 EBq (100 MCi)^[12]. Aerosol particles and gases that escaped the active zone contained more than 30 varieties of hazardous radionuclides and subsequently contaminated our home planet by wind. Dumping of radioactive solid wastes into the sea has been regular practice since 1946. The 1972 London dumping convention, now ratified by 91 states regulates all dumping at sea and this agreement prohibits all dumping of high level radioactive wastes. But intermediate and low level radioactive wastes continued to be

dumped at sea until 1982. High level waste was defined as that containing per ton of material; 3.7 TBq of ^{90}Sr and ^{137}Cs or 0.037 TBq α -emitters, 38,000 TBq β -/ γ -emitters and 15,000 TBq Tritium, respectively^[11]. For disposal, it is packed in concrete-lined steel drums to ensure that the container reaches the sea bed intact without imploding under the great pressures. But unfortunately, in the course of time the container will erode and leach their contents out into the surrounding water. Since the oceans cover 71% of the earth surface, it would be expected that about 71% of the world-wide fallout would fall into the oceans. Because of the global pattern of atmospheric circulation, most of the fallout has occurred between latitudes 45°N and 45°S ^[11], with higher levels in the northern hemisphere of which 61% is covered with oceans. Besides, some of the fallout on land is leached from land and carried by rivers to the oceans along with the wastes from nuclear installations.

The natural radiation levels varies from place to place due to different geographical condition; different condition of soil and environment. The environmental radiation levels further depends on the use of radioactivity and ionizing radiation, nuclear waste disposal, and nuclear fallout. The background radiation levels have registered a significant rise after the Chernobyl nuclear accident in 1986^[13]. This natural radioactive background of the earth varies from place to place, subject to human alteration and their interference with the natural environment such as mining, milling, nuclear fuel fabrication, and various industrial set ups. Obviously, at the time of planet's genesis the variety of its radioactive elements was considerably larger. In the course of time short-lived radionuclides have virtually vanished owing to radioactive decay. Now the earth is mainly associated with natural radionuclides whose half life equals millions or tens of millions of years.

The radiation dose may be imparted to body both internally (when the source is inside the body) and externally (when the radioactive source is outside the body). Radionuclides enter the human body mainly through ingestion of contaminated food and drinks, and inhalation of contaminated air. Principal transfer routes for radionuclides through which these may enter into the body are shown in the Figure 1.4. Different radionuclides present different health hazards depending on (i) the nature of radionuclides, (ii) the nature of emitted radiation, (iii) it's half life, (iv) it's decay scheme, (v) the chemical form in which the radionuclide is encountered, (vi) the fraction that is assimilated, (vii) the organ in which it may accumulate, and, (viii) the concentration that may be reached. The internal dose from world-wide fallout is due to fission

products which enter the human body through plants and other food stuffs. Plants absorb fission products deposited in the surface soils through their roots, depending upon the metabolism of the particular isotopes. The fission products can also enter the plant by direct deposition on the leaves, i.e., by foliar uptake. The fission products enter the human system through vegetables, milk, meat, etc. and accumulate in specific organs. The two important fission products from the point of view of internal dose due to world-wide fallout are ^{90}Sr and ^{137}Cs . As both have long half-lives and are produced in abundant quantities in the fission of ^{235}U and ^{239}Pu , they form a large percentage of world-wide fallout. ^{137}Cs which has chemical properties similar to potassium distributes itself within the living cells in the same way as potassium and is found mostly in the muscle. Being a γ -emitter, it delivers a dose to the whole body including the gonads and is mainly significant as genetic hazard^[14].

Uranium, an element with the highest atomic number of the naturally occurring element, is found in the earth's crust. Its concentration in a few ores is in the range from 40% to 60%. About 100 mineral species contain 1% or more and the average concentration of uranium in the earth's crust is $4 \times 10^{-4}\%$. It is found in granites, metamorphic rocks, lignite, monazite sands and phosphate deposits as well as minerals such as uraninite, caroninite, and pitchblende. Natural uranium is commonly found in the uranyl ion (UO_2). All natural compounds of uranium contain oxygen. The best known use of uranium is as a fuel in nuclear power reactors and nuclear weapons. Uranium (U), atomic number 92, occurs only in radioactive form. Natural uranium is a mixture of ^{238}U (99.27%), ^{235}U (0.72%), and ^{234}U (0.006%); and for this combination, 1 mg of uranium has an activity of 0.67 pCi. Uranium-238 is the head of the uranium/radium series and ^{235}U starts the actinium series. Uranium isotopes are also found in other series of transuranic elements. The radioactive decay of ^{238}U as shown in Figure 1.1 is complex and passes through 14-steps, each with characteristic disintegration and daughter products before it reaches the final stable end product ^{206}Pb .

Thorium-232 is the principal isotope of natural thorium and has a complex decay process before reaching the stable end ^{208}Pb as shown in the Figure 1.2. Thorium is very widespread in the earth's crust. The mean content of ^{232}Th in the uppermost layers of the earth's crust is about $1.2 \times 10^{-5}\%$. The thorium content in the earth's crust is approximately three times that of uranium. Uranium and thorium are abundant in acidic than in basic rock. Thorium-232 constitutes upto 10% of monazite, which is particularly abundant in certain areas of the oceanic

coastal belt like Brazil, Kerala state in India, and, Cox's Bazar and off-shore islands in Bangladesh.

Potassium has a very simple form of decay scheme. 89% of ^{40}K decays into $^{40}\text{Ca} + \beta^-$, and, only 11% of ^{40}K decays into $^{40}\text{Ar} + \gamma$ (electron capture). Both $^{40}_{20}\text{Ca}$ and $^{40}_{18}\text{Ar}$ are stable elements. Only one $^{40}_{19}\text{K}$ of the natural isotopes of ^{40}K is radioactive. It's natural abundance is only 0.012%^[6]. No significant fractionation of the potassium isotopes takes place in nature and so the radioactivity of ^{40}K is constant under all conditions. Because of the simple decay scheme, it is characterized by a single γ -energy 1460.75 keV. The potassium has a specific activity of 3.3 γ -emission per sec per gm^[15].

Caesium is an alkaline metal, a congener of potassium which is very abundant in earth's crust, 2.59%. Because of its exchange capability it can substitute from potassium where there is a lack or deficiency of the latter. So, ^{137}Cs presence in plants may be caused by its uptake through soil as well as potassium uptake. Caesium and potassium have similar chemical and biochemical behaviour including distribution and metabolism in the body^[16]. Caesium-137 ($^{137}_{55}\text{Cs}$) has twenty one radioactive isotopes. The two isotopes of Cs with the longest physical half-lives, ~30 years for ^{137}Cs , and ~2.1 years for ^{134}Cs , are most likely to present contamination problems. Caesium-137 decays into $^{137}_{56}\text{Ba}$ (5.4%; stable) and $^{137m}_{56}\text{Ba}$ (94.6%; metastable) by emitting β^- particles. The $^{137m}_{56}\text{Ba}$ ($T_{1/2}$ 2.55 min.) reaches to ground state by emitting γ -photon. Caesium-137 decay scheme emitting γ -photon of energy 661.66 keV is more likely to be encountered because it is an important fission fragment produced during fissioning of either ^{238}U or ^{235}U . It has been subject to many radiobiological and metabolic effects studies, because it is one of the long-lived fission products associated with atmospheric weapon test.

Radon-222 is the only gaseous decay product of the ^{238}U series. Although it is soluble in adipose tissue; radon, as a noble gas, is chemically inert and does not easily form compounds. Therefore, the major part of the inhaled radon is exhaled again. The decay products of radon are short lived radioactive isotopes, a proportion of which are attached to the aerosol atmospheric particles. A small percentage of radon decay products inhaled are deposited on the respiratory tract, where the emitted α -particles may cause lung cancer^[17]. The major health risk in relation with residential radon exposure is thought to be lung cancer^[18]. Well-water can be a significant source of ^{222}Rn in room air. Ground water carries radon from its ^{226}Ra precursor in soil and rock

into the home, where radon gas escapes into the air, especially when the water is heated, sprayed, or agitated. Examination of exposure pathways indicates that the radiation dose to the lungs due to inhaling ^{222}Rn that escaped from the water used in a home generally is much higher than the dose to the gastro-intestinal (GI) tract due to drinking the radon-containing water^[19]. Lung exposure to radon and its decay products contribute approximately half of the average total effective dose of 2.4 mSv.y^{-1} received by the general population from naturally occurring radionuclides^[1]. Most of these radon decay product exposures occur indoors, and the time-averaged exposure to these decay products varies. This variability is mainly caused by variation in the indoor radon concentration, which, in turn, depends on the differences in the rate at which radon enters the indoor atmosphere. The ^{222}Rn concentrations are lower in summer than in winter time^[17]. The annual equivalent dose for the general public due to the inhalation of ^{222}Rn is equal to $0.81 \text{ mSv}^{[17]}$.

All ionizing radiation however small it is, carries a probability to induce radiation injury to man and living beings^[20]. The probability of radiation injury increases with the increase in radiation dose^[21]. The maximum permissible effective dose (whole body) to man is 1 mSv.y^{-1} ^[22].

1.2. Biological Effects of Radiation

Ionizing radiation normally causes ionization in a matter through which it passes and can cause extensive damage to the molecular structure of the substance either as a result of the direct transfer of energy to its atoms or molecules or as a result of the secondary electrons released by ionization. In biological tissue, the effect of ionizing radiation can be very serious, usually as a consequence of the ejection of an electron from a water molecule and the oxidizing or reducing effects of the highly reactive species. As a result, ionizing radiation can cause harmful somatic and genetic effects on living beings.

We live in an environment of low level ionizing radiation. Ionizing radiation has been present in the earth since the beginning of its formation and the animate (also inanimate) beings are continuously being exposed to such radiation. Ionizing radiation may be of nuclear and extra-nuclear origin. There are directly ionizing radiation e.g., α , β , ^1H (P), ^2H (D), etc. and indirectly ionizing radiation e.g., X-ray, γ -ray, neutron, etc. The range of α -particle is very short though its ability to do biological harm is twenty times that of β or γ -ray. The range of β -

particles is longer than that of α -particles but much more shorter than that of γ -rays. Since γ -photons have no charge, it does not suffer any influence of electric and magnetic field generally. Further, γ -rays does not suffer any common obstruction as it has no rest mass. Consequently, γ -rays have longer range and it may cause ionization in any point of human body. In the present study, the radiation dose to the people of Bangladesh, due to the γ -emitting radionuclides in the environment is mainly considered.

The interaction of ionizing radiation with matter is mainly described by three processes viz.: (i) photo-electric effect, (ii) Compton effect, and, (iii) pair production. The photo electric effect is predominant for photons in the low energy range, below 115 keV. An approximate relation for the photo electric absorption coefficient $\mu_{\tau}(E)$ is^[23]:

$$\mu_{\tau}(E) \approx 10^{-33} NZ^5 E^{-3.5} \text{ cm}^{-1}$$

where N is the atom density of the interacting atom, Z is the atomic number, and E is the energy of the γ -ray in MeV. The Compton process is predominant for photons with energies between 150 keV and 2.5 MeV. The Compton absorption coefficient $\mu_{\sigma}(E)$ is approximately given by^[23]:

$$\mu_{\sigma}(E) \approx (1.25 \times 10^{-25}) \frac{NZ}{E \cdot \log_e(2\alpha + 0.5)} \text{ cm}^{-1}$$

where $\alpha = \frac{h\nu}{0.511}$ ($h\nu$ is the energy of the incident photon in MeV), and the other terms are as said just before. The pair production process is predominant for photons of energy equal to or greater than the threshold value 1.022 MeV. The dependence of pair production absorption coefficient $\mu_{\kappa}(E)$ on energy is approximately linear near the threshold^[23], i.e.,

$$\mu_{\kappa}(E) \propto NZ^2 (E - 1.02) \text{ cm}^{-1}$$

where E is in MeV units; and logarithmic at higher energies^[23], i.e.,

$$\mu_{\kappa}(E) \propto NZ^2 \log_e E \text{ cm}^{-1}.$$

The transfer of energy of the incident photon (γ -ray) into the interacting medium occurs typically in a series of these interactions in which the energy is transferred to electrons, and, usually secondary photons of progressively less energy. The product of each interaction are secondary photons and high energy electrons. The high energy electrons ultimately are responsible for the deposition of energy in matter. Since μ_{σ} is nearly independent of Z while μ_{τ} and μ_{κ} are proportional to Z , we find that the lower the atomic number (Z) of the interacting medium, the wider the energy range over which the Compton effect is dominant. In practice, the most

commonly encountered γ -rays are between 100 keV and a few MeV, and consequently, Compton effect is dominant in common practice.

When a beam of photons passes through an absorbing medium such as body tissue, some of the energy carried by the beam is transferred to the medium where it may produce biological damage^[24]. The energy deposited per unit mass of the medium is known as the absorbed dose. The events that result in this absorbed dose and subsequent biological damage are quite complicated. These are illustrated in a simplified way in Figure 1.5.

Biological effects of radiation are the manifestations of the interaction between radiation and biological cells; which are the results of a chain of reactions initiated by their interactions with the atoms of low atomic number (C, H, O, N) which constitute organic matter^[20]. All living creatures and organisms consists of tiny structures known as cells. Cell is the basic unit of life. It is estimated that adult human body consists of about 10^{14} cells. Biological tissues comprise of 70% water, the remaining composition being special macromolecules and other elements. The basic components of a cell are the nucleus, a surrounding liquid known as the cytoplasm, and a membrane which forms the cell membrane. A typical cell is a sac of fluid, or cytoplasm, enclosed by a membrane which embeds a nucleus containing chromosomes which includes the more essential compound of life deoxyribonucleic acid or DNA; that carry life sustaining informations^[25]. The chromosomes hold the genes, a segment of DNA that codes the informations, and allows the transmission from a cell to its descendants. Since the role of DNA in life is dominant, thus the action of radiation on DNA is particularly important.

Molecules in the biological tissue are most often held by covalent bond. When an ionizing radiation passes through biological molecules, the covalent bonds, specially those of water are split to form free ions, free radicals, and finally H_2O_2 and consequently, biochemical changes occur in the body; which may later show up in the form of clinical symptoms^[26]. Interactions of radiation with cell material may occur at random at any moment during the dynamic process of reproduction of stem cells^[25]. At low radiation doses (e.g., 1 mSv per annum), there may be a great deal of incident radiation per cell but the frequency of interactions is extremely low^[25], about one interaction per cell in a year.

1.2.1. Role of Free Radicals in Radiation Damage

Free radicals are chemical species that have a single unpaired electron in an outer orbital. In such a state, the radical is extremely reactive and unstable and enters into reactions with inorganic or organic chemicals- proteins, lipids, carbohydrates; particularly with key molecules in membranes and nucleic acids^[27]. Moreover, free radicals initiate autocatalytic reactions thereby converting the molecules with which they react into free radicals and thus propagate the chain of damage. The main effects of the reactive species are on membrane, lipid, sulfhydryl bonds of proteins and nucleotides. In the presence of oxygen, they may cause preoxidation of lipids within cellular and organellar membranes and cause damage to endoplasmic reticulum, mitochondria, and other microsomal components. Cross linking of proteins by the formation of disulphide bonds may also occur and raise havoc through the cell, in particular inactivating enzymes, especially with sulfhydryl enzymes. The interaction of free radicals depends on^[20]- (i) the nature of radiation (on LET), and, (ii) presence of dissolved oxygen in the water. The process of the development of radiation injury is illustrated in Figure 1.6.

1.2.2. DNA Damage by Ionizing Radiation

The gene component, DNA, is a pair of linear long chain-like molecules called polynucleotides wrapped around one another as a spiral ladder-shaped double-helix complex molecule composed of two strands, wound around each other. The DNA is found in the eukaryotic cells and in mitochondria. This complex molecule comprises numerous individual units or nucleotides. Each nucleotide is composed of a nitrogenous base, a sugar molecule (deoxyribose), and a phosphate molecule. The nitrogenous bases in DNA are: adenine (A), guanine (G), thymine (T), and cytosine (C). The sequences of the bases express the genetic code^[25]. The A and G are called purine, and the T and C are called pyrimidine bases. A purine in one chain always pairs with a pyrimidine on the other chain by following the specific base pairing. The chains are bound together by disulphide bonding between the bases, with adenine bonding to thymine and guanine to cytosine. At nuclear division, the two strands of the DNA molecule separate and as a result of specific base pairing, each chain then builds its complement. In this way, when a cell divides, genetic information is conserved and transmitted to each daughter cells. An indication of the complexity of the DNA molecule is the fact that the DNA in the human haploid genome is made up of 3×10^9 base pairs^[28]. DNA is the component of the chromosomes that carries the "genetic message", the blueprint for all the heritable characteristics

of the cell and its descendants. Each chromosome contains a segment of the DNA double helix. The genetic message is encoded by the sequence of purine and pyrimidine bases in the nucleotide chains. The text of the message is the order in which the amino acids are lined up in the proteins manufactured by the cell. The message is transferred to the sites of protein synthesis in the cytoplasm by RNA. The proteins formed include all the enzymes, and these in turn control the metabolism of the cell. A gene has been defined as the amount of information necessary to specify a single peptide molecule. However, this protein may be the precursor of several different physiologically active proteins. Genes also contain promoters, DNA sequences that facilitate the formation of RNA. Mutations occur when the base sequence in the DNA is altered by ionizing radiation or other mutagenic agents. There are estimated to be 50,000 – 100,000 genes in the 3 billion base pairs that make up the human genome^[28]. By the action of chemical radicals, ionizing radiation can directly or indirectly induce changes in the sequences of the bases and therefore alter the genetic code. This process is known as mutation or DNA damage, which if not repaired, induce cellular derangements as well as inhibition of DNA replication and can alter the information that passes from a cell to its progeny^[27]. DNA mutation is subject to efficient repair mechanisms, but the repair is not error free. Most of the damage is repaired, but some damage remains or is badly repaired, and this has consequences for the cell and its progeny. Both chains of the molecule can be broken and this may lead to chromosomal breaks. If only one helix (strand) of the double helix is broken, the lesion can be repaired by a process called unscheduled DNA synthesis^[29]. A defect in this repair mechanism occurs in xerodermapigmentosum and is related to the development of cancer.

1.2.3. Effects of Ionizing Radiation on Human Body

The effects of ionizing radiation on human body are the result of damage to the individual cells. These effects may be conveniently divided into two classes, namely somatic and genetic^[30]. These effects may arise by acute or/and chronic exposures. However, the effects of radiation on biological matter are dependent on^[21]: (i) the energy and the type of radiation, (ii) the dose rate, (iii) the volume irradiated, and, (iv) the sensitivity of the tissue.

Somatic Effects: The somatic effects arise from damage to the ordinary cells of the body and affect only the radio-exposed individual^[30]. The somatic effects are dependent on whether the irradiation is acute or chronic. These effects are also dependent on^[23]: (i) the degree of oxygenation, and hence temperature of the exposed part of the body, (ii) the metabolic state,

and hence the diet, (iii) the irradiated person's sex; and, (iv) the body colour. The somatic effects are (a) inhibition of mitosis, (b) chromosome aberration and breakage, and, (c) death of cell.

Genetic Effects: The genetic or hereditary effects are due to the damage or mutation or alteration in the chromosome structure and sperm or ovum i.e., germ cells of irradiated individual and affect his/her descendants. These may be passed through generation to generation^[30]. A genetic mutation may result by natural radiation. Any unrepaired DNA mutations in germinal cells that are non-lethal for the cell could in principle be transmitted to subsequent generations and becomes manifest as hereditary disorders in the descendants of the radio exposed individual^[25]. Ionizing radiations can act directly on genetic materials. The effect is proportional to the dose and the dose rate; the relationship is generally linear. Thus, there is no threshold and a radio-exposed individual has a definite probability of producing a mutagenic effect^[20]. However, the natural background radiation is responsible for from 4 to 10% of all naturally occurring genetic mutations^[15].

Immediate or Short Term Effects: These effects are due to an acute exposure (above 1 Gy delivered between a few minutes to a few hours) and manifest within a few weeks of exposure^[20]. These are somatic effects and inevitable. The immediate effects manifest as: chromosome aberration, blood changes, nausea, vomiting, diarrhoea (NVD), loss of appetite, fatigue, epilation, skin erythema, sterility, etc. and death^[31]. There is no well defined threshold dose below which there is no risk of death due to acute doses and no well defined point above which death is certain, but the chances of surviving an acute dose of about 8 Gy would be very low^[30].

Delayed Effects: These effects are due to acute or/and chronic radio-exposure and generally manifest after a few years of exposure. These effects are: various types of cancer, leukaemia, cataract, hereditary effects etc. There exist no threshold doses below which no probability of cancer induction and hereditary effects occur; but for cataract formation, the threshold dose is 15 Sv over the whole working life time^[30]. Depending on the threshold dose and the probability of effects upon dose, the effects of radiation on human body are classified into two types, viz.: (i) stochastic effects, and, (ii) non-stochastic effects.

Stochastic Effects: For the manifestation of certain biological effects, no threshold dose can be defined. These effects are called stochastic effects. These effects may occur at any dose, the probability of manifestation increases with absorbed dose^[31]. On the basis of data obtained

on occupational exposure, radio-therapy experience, etc., the following probability values (risk factors) are accepted for these stochastic effects^[31]:

All cancers - 1 to 1.5% per Sv

Hereditary effects - 0.4% per Sv

Non-Stochastic Effects: The effects of ionizing radiation on human body for which a threshold dose for occurrence can be defined are called non-stochastic effects^[31]. The severity of the effect increases with dose. All early effects of radiation (say, Nausea, Vomiting, and Diarrhoea) and cataract formation are the examples of non-stochastic effects.

1.2.4 Effects of Ionizing Radiation on Embryo

Effects of ionizing radiation in utero are generally referred to as effects on the embryo. Radio-exposure has a harmful effect on the development of embryo. Its severity is explained by the fact that the cells of foetal tissues are immature, undifferentiated and rapidly dividing, and consequently are extremely sensitive to radiation, so that the death or mutation of only a few of these can bring about irreparable damage^[25]. The effects can occur at all stages of embryonic development, from zygote to foetus, and may include lethal effects, malformation, mental retardation and cancer induction and malignancies^[25]. The first three may be the possible outcome of deterministic effects during embryonic development, particularly at the period of formation of organs (from second to twelfth weeks of gestation). The birth defects commonly observed in the children who have been radio-exposed (0.1 to 0.2 Gy) during the uterine life are given in Table 1.4.

Table 1.4: Principal Birth Defects Due to Radiation Exposure in Uterine Life^[20]

Organ	Kind of birth defect
Brain	Anencephaly, Hydrocephaly, Cerebral Atrophy, Mental Retardation
Eye	Anophthalmia, Microphthalmia, Retinoblastoma
Skeleton	Dwarfism, Craniostenosis, Spina Bifida, Malformations of the Extremities.

1.2.5 Health Effects of Low Level Radiation Exposure

Since there is no threshold dose for the induction of various types of cancer, leukaemia, life shortening and hereditary effects; there exists a certain probability for the occurrence of these effects by a low level radiation exposure. Thus an individual have some risk although the

probability is very low. However, the radiobiological estimates for low (chronic) radiation doses around 1 mSv per year are cited below^[25] :

- (i) Probability of an excess malignancy: 10^{-4} per year.
- (ii) Lifetime probability: 0.5%.
- (iii) Proportion of fatal cancers in the population that may be attributed to radiation: approximately 1 in 40.

The lifetime mortalities in a population of all ages from specific fatal cancers after exposure to low doses are given in Table 1.5.

Table 1.5: Lifetime Mortality in a Population of All Ages from Specific Fatal Cancer After Exposure to Low Doses^[22].

Organ	Fatal Probability Coefficient (10^{-4} Sv^{-1})
Bladder	30
Bone Marrow	50
Bone Surface	5
Breast	20
Colon	85
Liver	15
Lung	85
Oesophagus	30
Ovary	10
Skin	2
Stomach	110
Thyroid	8
Remainder	50
Total	500*

* General public only. The total fatal cancer risk for a working population is taken to be $400 \times 10^{-4} \text{ Sv}^{-1}$.

1.3 Objectives of the Research

Although Bangladesh is not a nuclear powered country, nevertheless, it may be vulnerable to atmospheric fallout of technogenic radionuclides and waste disposal to the Indian ocean by neighbouring countries or by other developed countries, since no surveillance activity in this regard exists here. Beside this, Bangladesh is subjected to natural radioactivity through the draining of heavy silt-laden water by the Ganges-Jamuna-Brahmaputra-Meghna river system. The assessment of the radiation doses in human from natural sources is of special importance because natural radiation is by far the largest contribution to the collective dose received by the population, and any amount of radiation exposure bears a probability to cause harm to men and

environment. Even low doses of radiation may cause genetic effects and may be important in somatic consideration. Hence, general public should not be exposed to any radiation unless unavoidable.

In Bangladesh, the external background radiation levels lie between 1.0 and 3.9 mSv.y⁻¹ with an average value of 2 mSv.y⁻¹ excluding Cox's Bazar sea beach sand areas where an average value of 13 mSv.y⁻¹ with a range of 2.6–44.0 mSv.y⁻¹ was observed^[32]. The average of the total radiation exposure (both external and internal) all over the world is 2.4 mSv.y⁻¹[1]. Of this dose, about two third is due to internal radiation and one third results from external exposure giving a ratio of about 2:1 for internal to external exposures. If the same ratio of internal to external exposures is maintained in the dose pattern of public in Bangladesh, the total public dose equivalent would be around of 6 mSv.y⁻¹ from both internal and external sources of background radiation. This is a noteworthy very high dose from background sources (in Bangladesh). Therefore, the population of Bangladesh should not be exposed to any additional dose from artificial radioactivity if not ineluctable.

The most probable radioactive materials present in the samples of soil and natural water are tritium, carbon, iodine, potassium, strontium, radium, uranium, thorium, etc., which emit nuclear radiations. Living beings are exposed to these radiations through environmental exposure, ingestion of food and drinking water. Although in general, radiation is hazardous to living beings, there is a certain level of radiation dose which a living being can withstand called the "tolerance level". If the radiation dose exceeds this tolerance limit, it may cause harm to living beings, and may cause short-term or/and long-term effect. Since the internal radiation doses received by a living being through foodstuff and drinking liquids are more dangerous than external ones and since water is a drinking liquid and we live in an environment of low-level radioactivity, the knowledge of the level of natural radioactivity in soil and water samples, and the dose contribution due to these is of prime importance.

In the environment, the contents of radioactive elements increases due to continuous generation of radioactive isotopes by: (i) the reaction of cosmic radiation with the atoms of the atmospheric elements, (ii) the operations of nuclear reactors and their fuel processing plants, (iii) nuclear test's fallout, and, (iv) the other world-wide nuclear activities. In addition to the developed countries, some developed countries in Asia have started nuclear programmes to

achieve nuclear power recently. By this time, some successful nuclear explosions have already been carried out by our neighbouring countries- India, Pakistan, and China. Also South Korea is reported to be on the way to become a nuclear power. Therefore, the probability of contaminating the environment of Bangladesh may further be increased.

As an aftermath of Chernobyl accident, the radioactivity and background radiation levels have been measured in different countries of the world^[13]. In Bangladesh, no systematic data are available on radioactivity and radiation level to estimate the radiation exposure to population at large. In 1990, ICRP had recommended to reduce the existing MPD from 50 mSv.y^{-1} to 20 mSv.y^{-1} for occupational personnel and from 5 mSv.y^{-1} to 1 mSv.y^{-1} ^[22] for general public. It is therefore necessary to know the present level of population exposure in Bangladesh.

Different projects all over the world on the natural radioactivity level measurement had been undertaken by different countries for drawing up map of natural radiation levels of the respective countries. But no such systematic work have been reported regarding the assessment of natural radioactivity level and population dose due to environmental radioactivity, in our country, after the Chernobyl accident of 1986. To avoid radiation hazards, radiation levels due to natural sources as well as man made sources should be evaluated so that proper guideline could be developed to keep radiation exposure as low as reasonably achievable (ALARA). In this context, it was proposed to undertake a programme to measure the radioactivity and radiation levels in different locations in Bangladesh in order to estimate the exposure to population at large. The data obtained will be utilized for evaluation of collective dose equivalent to the population at large in Bangladesh in order to formulate the radiation protection guidelines. Therefore a research programme for the measurement of radioactivity level in soil and water, and measurement of radiation dose level all over Bangladesh was taken in order to fulfill the above mentioned goal. Under this research programme, the following studies were carried out: (i) measurement of indoor and outdoor radiation level, (ii) measurement of radioactivity in soil, (iii) measurement of radioactivity in drinking water, (iv) evaluation of radiation level by mathematical model (RESRAD & GENII) based on the measured radioactivity in soil samples, (v) determination of the correlation coefficients between the activities of radionuclides found in soil and water samples, (vi) evaluation of whole body dose equivalent due to drinking water by an established formula, (vii) estimation of cosmic-ray contribution,

(viii) estimation of effective dose equivalent of the population of Bangladesh, (ix) estimation of collective dose equivalent, and, (x) estimation of population risk factor.

This work would help to create a public awareness about the environmental radiation level. Also the result of the present study will help to develop a reference data on this important issue to show the condition of Bangladesh environment and shall stand as a bench mark for further changes in this regard.

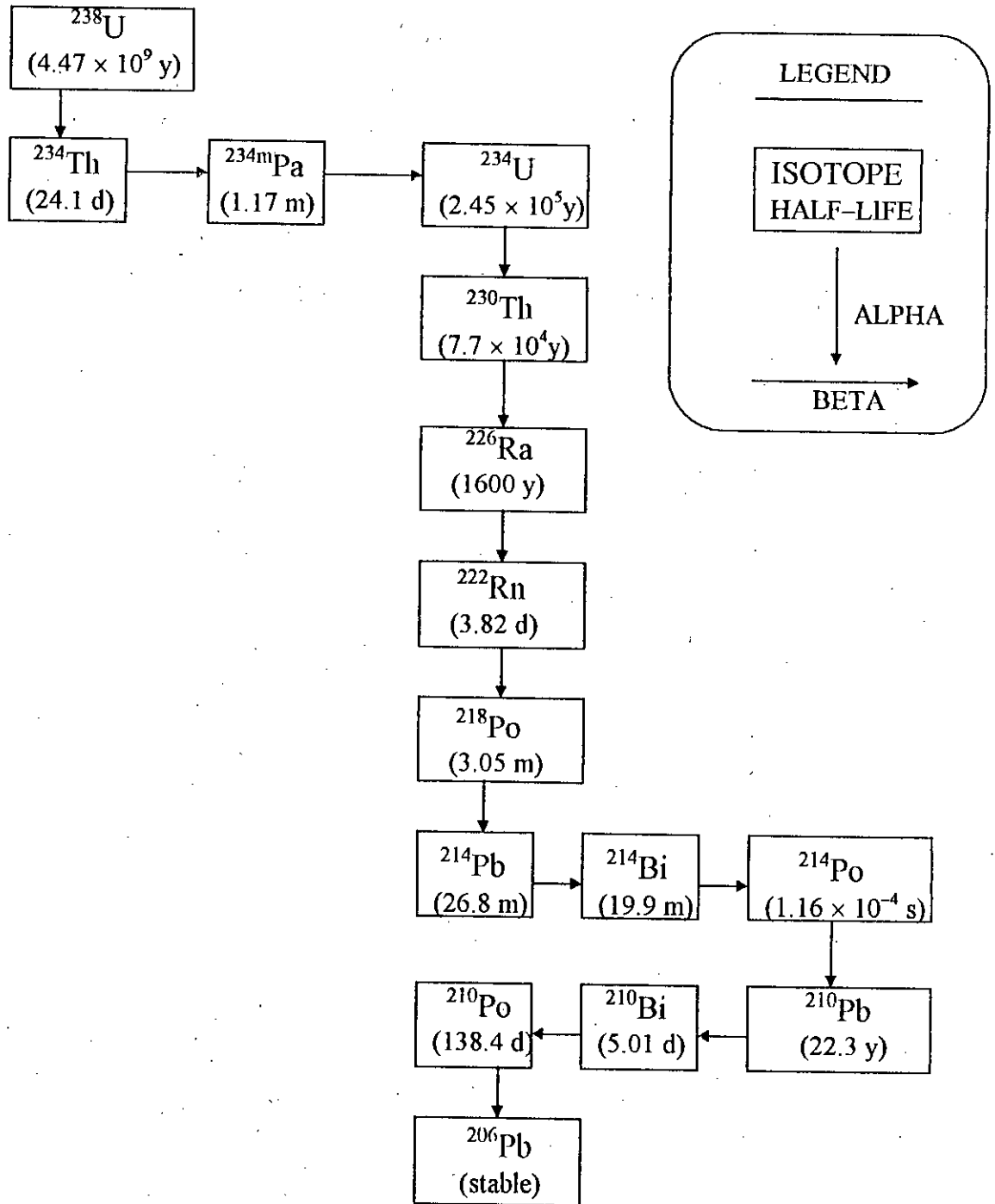


Figure 1.1: Uranium-238 Decay Series.

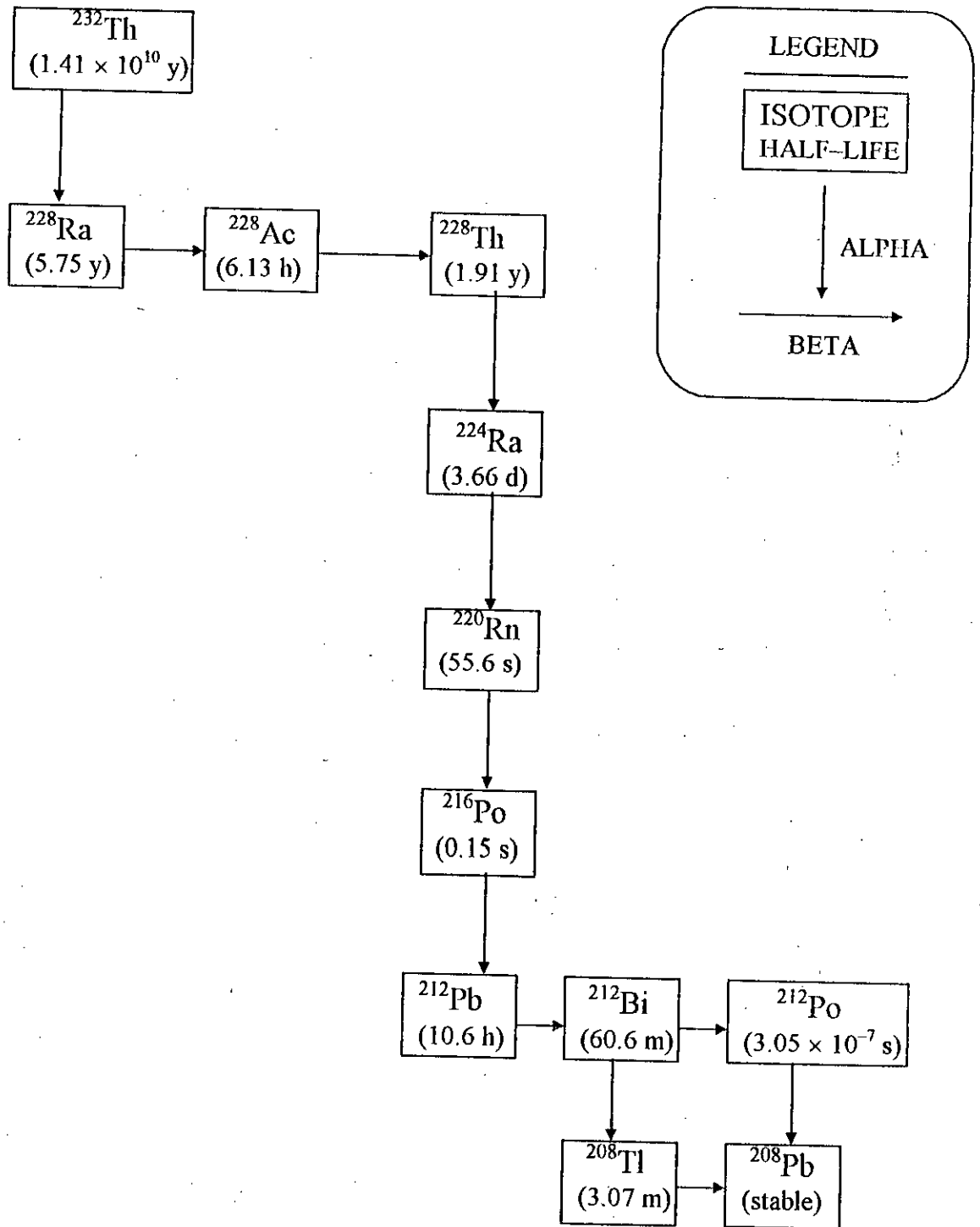


Figure 1.2: Thorium-232 Decay Series.

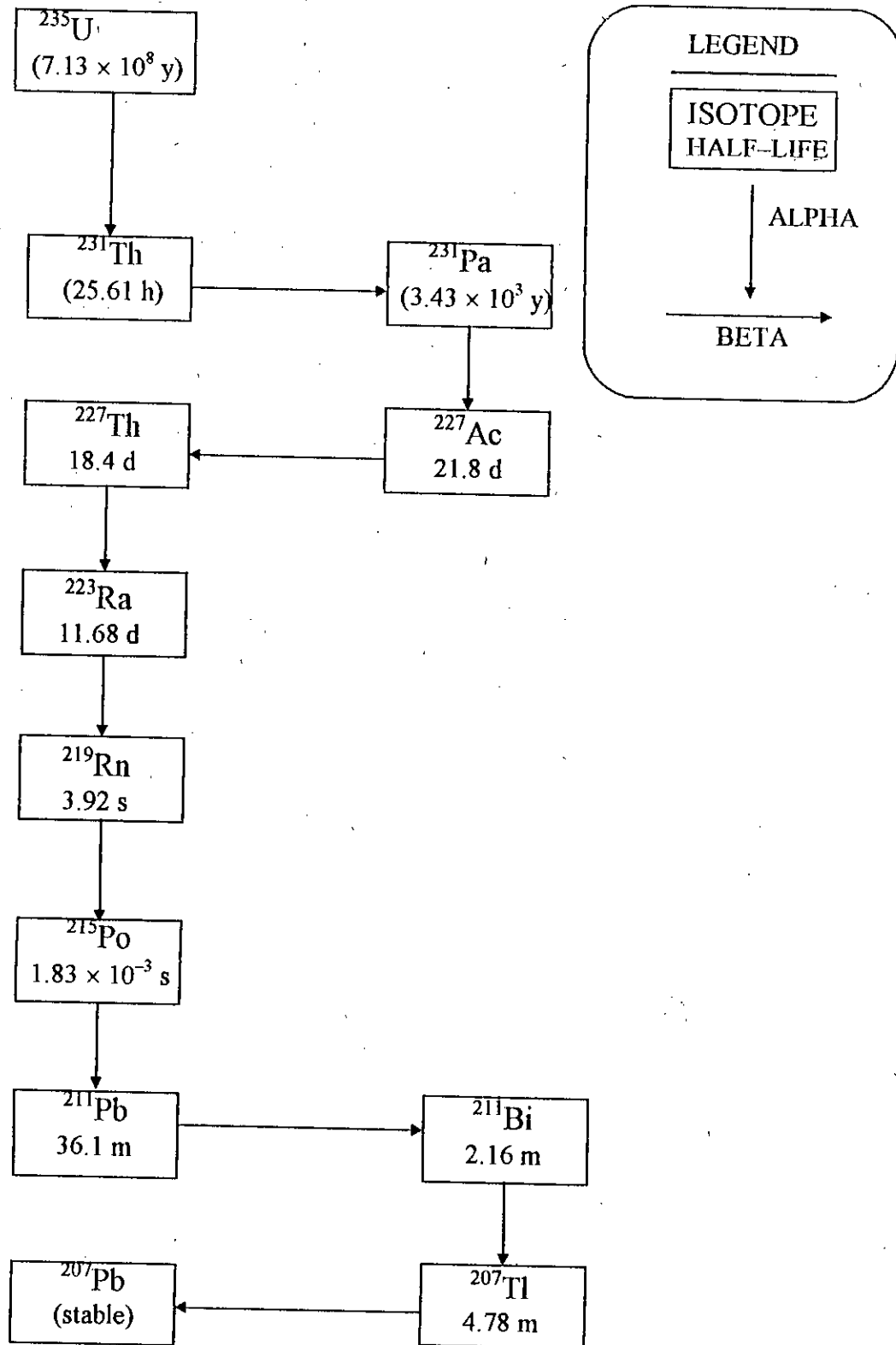


Figure 1.3: Actinium Decay Series.

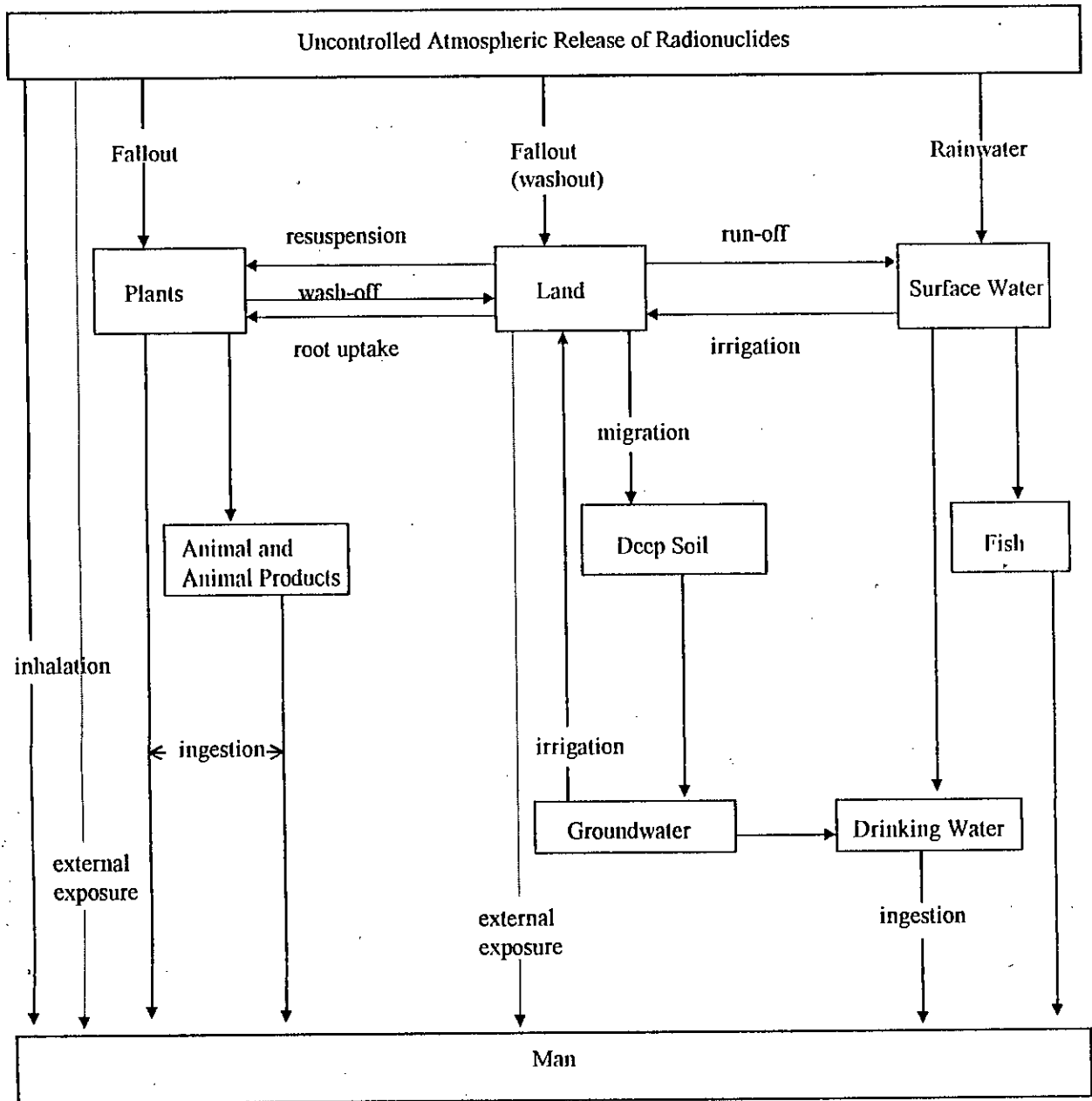


Figure 1.4: Major Pathways of Radionuclides to Man in the Event of an Uncontrolled Release of Radioactivity^[33].

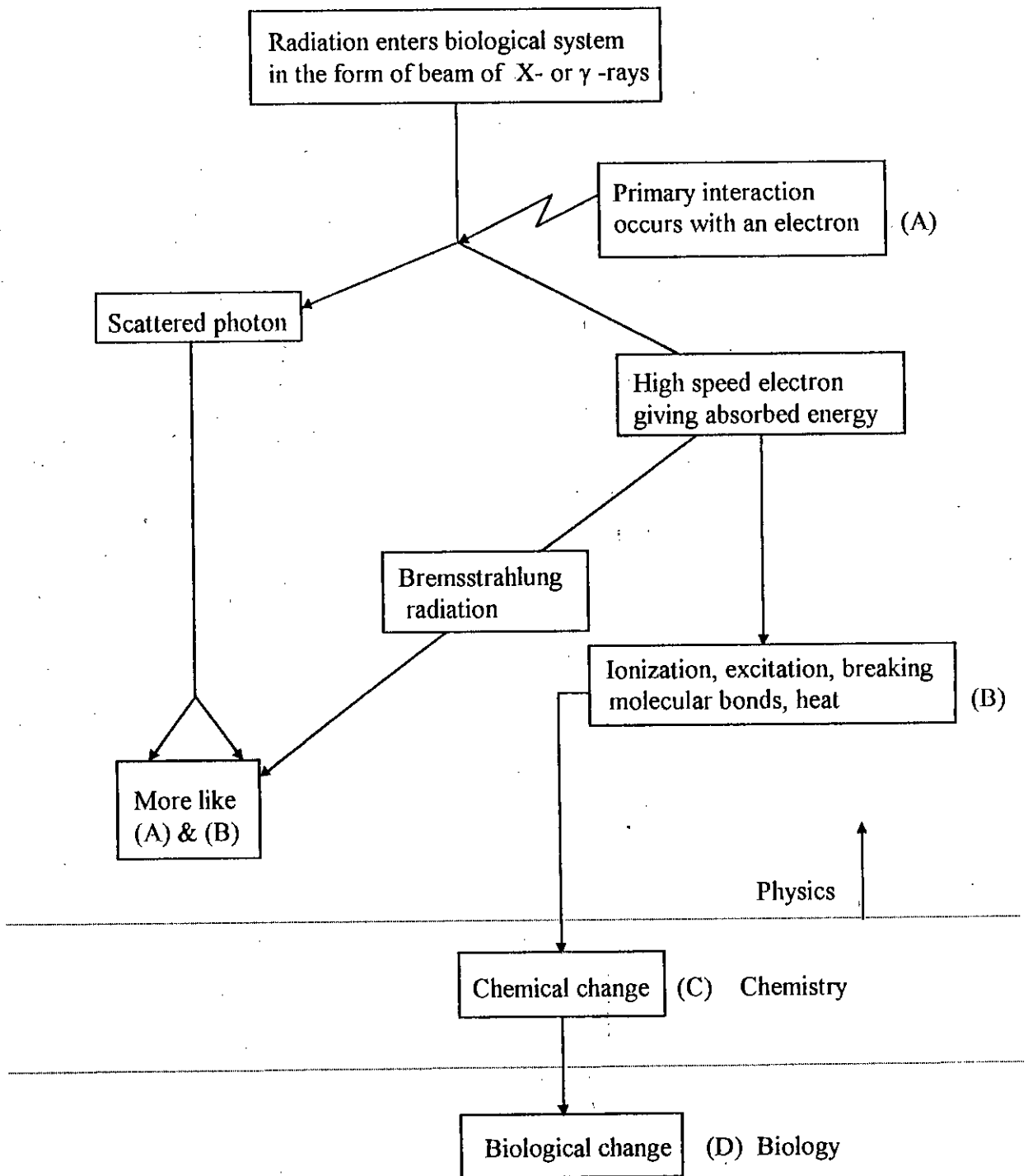


Figure 1.5: Schematic Diagram Illustrating the Absorption of Energy from Radiation Resulting in Biological Damage^[24].

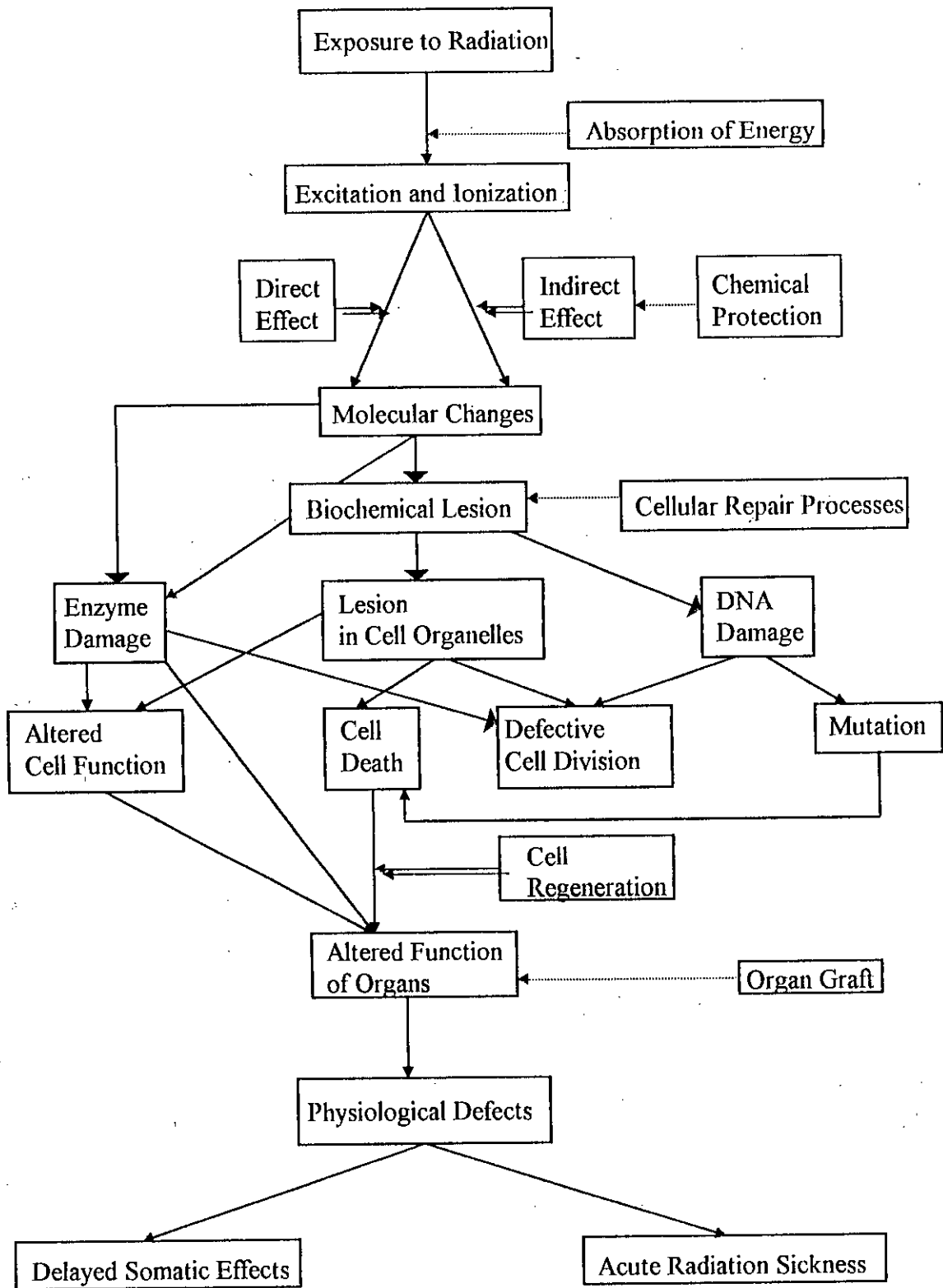


Figure 1.6: Development of Cell Injury^[26].

CHAPTER 2



REVIEW

CHAPTER 2

REVIEW

2.1 Introduction

Radioactivity is present in the environment since the formation of the earth. The level of this radioactivity is now increasing day by day due to the proper and improper use of radioisotopes and nuclear energy. As the deleterious effects of radiation became known, scientists all over the world measured the radioactivity level in different environmental samples. As there was no sensor to measure and detect radiation naturally, these measurements were done by different methods using different instruments. Methods and results of some of the recent works which are most relevant to the present work, are described below in brief.

2.2 Review of Previous Works

During the period of 1975 to 1979, Bangladesh Atomic Energy Commission had carried out a countrywide environmental radioactivity monitoring programme^[32]. It was found that the external background radiation levels lie between 1.0 and 3.9 mSv.y⁻¹ with an average value of 2 mSv.y⁻¹ excluding Cox's Bazar sea beach sand areas where an average value of 13 mSv.y⁻¹ with a range of 2.6 - 44.0 mSv.y⁻¹ was observed.

M. A. Rab Molla and A. F. M. Salahuddin Chowdhury^[34] studied the environmental radioactivity of ¹³⁷Cs in some soil samples of Bangladesh in 1975 by γ -spectrometry. They found that the range of the concentration of ¹³⁷Cs in the studied soil samples varied from 0.02 pCi.g⁻¹ (1.32 mCi.km⁻²) to 2.03 pCi.g⁻¹ (134.06 mCi.km⁻²). The lowest concentration of ¹³⁷Cs was found in the soil sample of Rangamati collected from a depth of 11"-13" and the highest concentration was found in the sample collected from Cox's Bazar at a depth of 0"-2". In most of the analyzed samples, they found that there was a random variation of ¹³⁷Cs activity with depth of the soil from where the samples were collected.

M. A. Rab Molla et al.^[35] made a study on the activity of ¹³⁷Cs in soil samples collected from different depths of 29 different sampling stations at Cox's Bazar, Chuandi, and Rangamati. They found that the activity level ranged from 5.17 to 479.93 mCi.km⁻². In most of the analyzed

samples, they found a definite indication of decreasing ^{137}Cs activity with increasing soil depth, having higher activity in the surface soil.

In Finland, M. Asikainen and H. Kahlos^[36] measured the natural radioactivity in drinking water with the help of scintillation detectors. They analyzed the water samples for ^{222}Rn , ^{226}Ra , gross α - and gross β - activity. They found that the mean concentrations were 670 pCi.L^{-1} for ^{222}Rn and 0.1 pCi.L^{-1} for ^{226}Ra in the drinking water distributed by water supply plants, and 17,000 pCi.L^{-1} for ^{222}Rn and 2.9 pCi.L^{-1} for ^{226}Ra in the water samples of drilled wells. They found the radioactivity to be very high in the water samples of drilled wells. Some of the drilled wells also had abnormally high concentrations of uranium, up to 2100 $\mu\text{g.L}^{-1}$ and even higher in some wells in the Helsinki region.

David E. McCurdy and Russel A. Mellor^[37] measured the concentrations of ^{226}Ra and ^{228}Ra in domestic and imported bottled water samples in the US in 1979. They found the ranges of the activities of ^{226}Ra in imported and domestic bottled water as from -0.02 ± 0.02 (origin- France) to 13.5 ± 0.8 pCi.kg^{-1} (origin- France) and from -0.04 ± 0.03 (origin- Massachusetts) to 2.2 ± 0.3 pCi.kg^{-1} (origin- New York) respectively; and the ranges of the activities of ^{228}Ra in imported and domestic bottled water samples as from -0.4 ± 0.2 (origin- Italy) to 12.8 ± 0.8 pCi.kg^{-1} (origin- France) and from -0.08 ± 0.06 (origin- New Hampshire and Maine) to 0.6 ± 0.2 pCi.kg^{-1} (origin- New York).

S. Abe et al^[38] made an extensive field survey of natural radiation in Japan. They estimated the exposure rate due to natural radiation composed of terrestrial radiation, cosmic ray, as well as a slight contribution from nuclear tests at 1,115 sites by an ionization chamber and NaI scintillation survey-meters. The distribution of the exposure rates along with the population-weighted annual collective dose in each area were obtained. The mean exposure rate over entire Japan was calculated to be $9.0 \mu\text{R.h}^{-1}$. The population-weighted mean dose for an individual person was 0.69 mGy.y^{-1} . There was a general trend that south-west Japan had higher level than north-east Japan. It was also revealed that the population size was a more important factor than the radiation level in determining the distribution of the population-weighted mean dose in Japan.

K. Fujitaka et al^[39] found a correlation between distribution of natural radiation and geologic properties, in Japan. An ionization chamber and three kinds of NaI scintillation surveymeters were used for this purpose. The measurements were done almost uniformly all over Japan where most cities were included. With a hope to find a relation between the distribution of geology and the natural radiation, Japan was divided into 376 pieces of 30 km meshes and a mean exposure rate of each mesh was obtained by averaging all values in it. Results were arranged on the basis of administrative section. Every analysis was brought about a consistency in that the higher radiation level area (south-west Japan) corresponds to the old weathered region of granite rocks. On the other hand, the lower radiation level area (north-east Japan) would correspond to Cenozoic volcanic belts.

Using gamma spectrometry technique, C. S. Chong and G. U. Ahmad^[40] measured the gamma activity of ^{40}K , ^{226}Ra , and ^{232}Th in building materials in Penang, Malaysia. In sand samples, they found the average activities of ^{40}K , ^{226}Ra , and ^{232}Th to be 11.5 pCi.g^{-1} , 1.9 pCi.g^{-1} , and 0.9 pCi.g^{-1} respectively.

Louis B. Kriege and Rolf M. A. Hahne^[41] measured the ^{226}Ra and ^{228}Ra in Iowa drinking water samples. Over a period of ~20 years (sampling preparation from 13-03-'63 to 06-01-'81), they used the "university hygienic laboratory" facilities of The University of Iowa, Iowa city, and found that the activity of ^{226}Ra ranged between 0.1 and 61.0 pCi.L^{-1} .

William Cline et al.^[42] explored the radium and uranium level in Georgia community water system and found that a significant number of water samples exceeded the maximum contamination level (MCL), [MCL is 5 pCi.L^{-1} for radium]. They followed the analysis pattern as- initial screening for gross α -particle activity, followed by measuring ^{226}Ra if the gross α -particle activity was above 5 pCi.L^{-1} , and then measuring ^{228}Ra if the ^{226}Ra concentration was above 3 pCi.L^{-1} ; and uranium analysis if the gross α -particle activity exceed 15 pCi.L^{-1} .

C. Richard Cothorn and William L. Lappenbusch^[43] analyzed the occurrence of uranium in drinking water in the US. Of the 59,812 community water supplies in the US, it was estimated that between 25 and 650 exceed 20 pCi.L^{-1} , 10 - 2,000 exceed 10 pCi.L^{-1} , and 2500 - 5000 exceed a uranium concentration of 5 pCi.L^{-1} .

T. E. Myrick et al.^[44] made a study to determine the concentrations of selected radionuclides viz. ^{226}Ra , ^{232}Th , and ^{238}U in surface soil in the US. The sampling programme provided background information at 356 locations in 33 states. The nationwide average concentrations of ^{226}Ra , ^{232}Th , and ^{238}U in surface soil were found to be $1.1 \pm 0.48 \text{ pCi.g}^{-1}$ (range- 0.23 - 4.2 pCi.g^{-1}), $0.98 \pm 1.46 \text{ pCi.g}^{-1}$ (range- 0.10 - 3.4 pCi.g^{-1}), and $1.0 \pm 0.83 \text{ pCi.g}^{-1}$ (range- 0.12 - 3.8 pCi.g^{-1}) respectively.

Malcolm E. Cox and Barry L. Fankhauser^[45] determined the concentration of ^{137}Cs in soils and surface-deposited volcanic sublimes from various climatic locations on the islands of Hawaii, Oahu and Maui by gamma spectrometry. Samples of undisturbed soil were taken from approximately $5(\pm 0.5)$ cm in depth and from locations where vegetation did not form an overhanging canopy. Gamma-ray detection was performed with a 7.6×7.6 cm Bicron well - type NaI(Tl) crystal detector. In the soil samples, the range of the concentrations of ^{137}Cs measured varied from 0.04 - 1.93 pCi.g^{-1} ; with an average for windward samples of 0.87 pCi.g^{-1} and 0.17 pCi.g^{-1} for leeward samples.

C. Richard Cothorn and William L. Lappenbusch^[46] measured the radium and gross α -particle activity in 50,000 water samples in the US. By using radiochemical method, they found that 500 samples exceeded the Maximum Contamination Level (MCL) of 5 pCi.L^{-1} . Almost all the violations occurred for ground water supplies.

Philippe Martin^[47] collected potable water samples in Saudi Arabia during August 1982 for assessment of gamma activity. The γ -ray spectra were obtained using a Ge(Li) detector coupled to a MCA. He found that the ^{226}Ra concentration ranged from 4.4 to 18.9 pCi.L^{-1} , the raw water had the highest one. Most of the ^{228}Ra concentrations were above quantitative determination level, and varied between 4.7 and 7.1 pCi.L^{-1} . ^{226}Ra and ^{228}Ra concentration ratios, which were usually close to one, did vary, as had been found in similar studies by other scientists.

C. Papastefanou et al.^[48] estimated the exposure from radioactivity in building materials. They found the average gamma-ray exposure rate in brick buildings, concrete buildings, and old buildings (built earlier than 1920) were 10.0 $\mu\text{R.h}^{-1}$, 6.5 $\mu\text{R.h}^{-1}$, and 4.3 $\mu\text{R.h}^{-1}$ respectively. In open air, they found the average dose rate level as 3.8 $\mu\text{R.h}^{-1}$.

W. A. Kolb and M. Wojick^[3] made a research on enhanced radioactivity due to natural oil and gas production and related radiological problems. They detected increased gamma radiation incidentally in a north German oil field traceable to radioactive scale. Dose equivalents rate of upto $50 \mu\text{Sv}\cdot\text{h}^{-1}$ was measured at the external surface of storage tanks for brines, but 73% of 160 sites investigated did not show an increase above the natural background. Brines from gas fields contained ^{226}Ra of upto $286 \text{ Bq}\cdot\text{L}^{-1}$ and scale of upto $1 \text{ Bq}\cdot\text{g}^{-1}$. In brines and scales from oil fields ^{228}Ra was usually the predominant radionuclide. Some samples contained "unsupported" ^{210}Pb and even ^{227}Ac , too, but practically no uranium or thorium. The ^{222}Rn concentrations in natural gas samples varied between 0.004 and $4 \text{ Bq}\cdot\text{L}^{-1}$ with a mean value of $0.6 \text{ Bq}\cdot\text{L}^{-1}$. It was shown that the radiation exposure due to natural gas consumption was negligible but some other problems of radiological relevance were recognized.

Concentration levels of natural radionuclides in mineral waters in several European countries were studied by I. Gans^[49]. In that research, the health risk from drinking mineral water for adults was found to be comparable to the risk from terrestrial radiation. The ranges of the concentrations of ^{226}Ra and ^{238}U in analyzed bottled mineral water samples were found to be $<1 - 1800 \text{ mBq}\cdot\text{L}^{-1}$ (264 samples) and $<1 - 140 \text{ mBq}\cdot\text{L}^{-1}$ (21 samples) respectively.

J. G. Ackers et al.^[50] analyzed about 140 samples of building materials in the Netherlands in the period 1982 - 1984 by gamma spectrometry for their ^{226}Ra , ^{232}Th , and ^{40}K concentrations. They also measured the radon exhalation rate from concrete slabs of different composition including fly ash components. They found that the mean activities of ^{226}Ra , ^{232}Th , and ^{40}K in sand samples respectively as- $8.1 \text{ Bq}\cdot\text{kg}^{-1}$, $10.6 \text{ Bq}\cdot\text{kg}^{-1}$, and $200 \text{ Bq}\cdot\text{kg}^{-1}$.

G. Keller and H. Muth^[51] estimated the radiation exposure in German dwellings. They found that in indoors, the median ^{222}Rn concentration was approximately four times higher than that of outdoors. A correlation analysis of the data obtained showed that in indoors the equilibrium factor F is almost independent of ventilation, ^{222}Rn concentration, and other parameters. The mean effective dose equivalent by residence in dwelling amounted to $0.2 - 0.8 \text{ mSv}\cdot\text{y}^{-1}$ for ^{222}Rn daughters, and approximately $0.1 \text{ mSv}\cdot\text{y}^{-1}$ for ^{220}Rn daughters.

H. Schimier and A. Wicke^[52] carried out a large scale radon survey in the then Federal Republic of Germany. As a result of measurements in almost 600 homes, the mean value of

^{222}Rn concentration was found to be 49 Bq.m^{-3} and the mean value of annual contribution to the effective dose equivalent was found to be 1.2 mSv .

I. R. McAulay and J. P. McLaughlin^[53] made a study on indoor radiation levels in Ireland. During the period 1983 - 1984, measurements were made over 250 houses. Most measurements were done using passive devices: TLD's for penetrating radiation and CR-39 alpha track plastic detectors for radon measurements. The median value of the penetrating radiation doses was 0.78 mGy.y^{-1} where a maximum value of 1.47 mGy.y^{-1} was detected. The radon concentrations showed a large degree of variability with a median value of 43 Bq.m^{-3} . About 10% of the houses had radon air concentrations in excess of 100 Bq.m^{-3} with a maximum value of 700 Bq.m^{-3} .

A pilot study was carried out by A. Sørensen et al.^[54] to establish techniques and procedures for the measurement of indoor radiation in Denmark. A passive cup dosimeter was designed containing CR-39 track detectors and TLD's to measure radon and external radiation respectively. A total of 82 dwellings was selected covering most regions of the country. The dwellings were monitored in two three-months periods, one in winter and the other in summer. The average dose rate in air due to external radiation was $0.09 \mu\text{Gy.h}^{-1}$. In the winter the average radon concentrations were 88 Bq.m^{-3} and 24 Bq.m^{-3} for single-family houses and flats, respectively; and in the summer the corresponding values were 52 Bq.m^{-3} and 19 Bq.m^{-3} .

A. Battaglia et al.^[55] used CISE low level γ -ray spectrometry equipment with high resolution Ge(Li) detectors for analysis of 110 various building material samples, and TLD data in order to assess the indoor dose level in Milano, Italy. They found that the new buildings (built in 1980's) expose lower dose rate ($13.2 \mu\text{R.h}^{-1}$ maximum) than that of the older (built in 1960 - 1971, dose rate $17.0 \mu\text{R.h}^{-1}$ maximum). They also found that the maximum dose rate is higher for multi-floor buildings ($17.0 \mu\text{R.h}^{-1}$) while the maximum dose rate is lower for cottages ($14.6 \mu\text{R.h}^{-1}$). They showed that the average dose rate is the highest for buildings formed in 1900 - 1919 ($12.27 \mu\text{R.h}^{-1}$) and the lowest for buildings made in 1880's ($10.82 \mu\text{R.h}^{-1}$). The average specific activities of ^{40}K , U, and Th in sand samples was found as 539 ± 48 , 17.5 ± 4.5 , and 24.2 ± 6.3 respectively; and in concrete samples, the corresponding values were 457 ± 68 , 19.0 ± 3.1 , and 24.2 ± 3.4 respectively.

R. Van Dongen and J. R. D. Stoute^[56] measured the outdoor natural background radiation with the help of an ionization detector at more than 1000 locations evenly distributed throughout the country (Netherlands). They showed that the gamma radiation originating from the soil in the Netherlands varies between 1.1 and 1.2 $\mu\text{R}\cdot\text{h}^{-1}$. They also found that, 'high' values of exposure rates correspond to areas with silty deposits and the 'low' exposure rates correspond to areas with sandy deposits. Gamma spectrometric analysis of the radiation at some location showed that the terrestrial radiation is mainly caused by natural radionuclides.

H. W. Julius and R. Van Dongen^[57] made an estimation of gamma doses to the population in the Netherlands, caused by natural radiation sources encountered in the environment. The data were derived from two independent types of measurement- (i) exposure/dose rate measurements in living environment (private houses as well as work places), using a high pressure ionization chamber and thermoluminescent dosimeters (TLD) respectively, and (ii) individual monitoring, using TLD. They found that the average levels of indoor exposure rate was 9.5 $\mu\text{R}\cdot\text{h}^{-1}$ and a dose rate of 95 $\text{nGy}\cdot\text{h}^{-1}$ for individuals; both with a standard deviation of 15 - 20%.

A representative sample of over 2000 UK dwellings was monitored for a year using thermoluminescent and etchable plastic dosimeters to measure gamma-ray dose rates and radon concentrations by B. M. R. Green et al.^[58]. The mean gamma-ray dose rates were 0.062 and 0.057 $\mu\text{Gy}\cdot\text{h}^{-1}$ in air for living areas and bedrooms respectively. They also conducted more detailed surveys in areas where the local geology indicated that elevated exposure to natural radiation might occur. They visited over 800 dwellings and made measurements of several parameters. The mean gamma-ray dose rates varied from 0.05 to 0.10 $\mu\text{Gy}\cdot\text{h}^{-1}$ in air. The gamma-ray dose rates and radon gas concentrations were measured in over 2000 dwellings with LiF TLD-100 and diethylene glycol bis(allyl carbonate) polymer (CR-39) etched-track dosimeters respectively.

A. Rannou et al.^[59] conducted a survey of natural radiation in France since 1981 with the assessment of the components resulting from external sources (ground and building materials) using thermoluminescent dosimeters. Moreover, the internal exposure to ^{222}Rn and the potential alpha energy due to radon daughters were estimated by passive track detectors in the first case and the active dosimeters in the second case. In order to estimate the terrestrial component and

the one due to building materials, each chosen location had two detectors: an indoor TLD and an outdoor TLD, the second one being used only in case of natural soil. The arithmetic mean values obtained after subtraction of the component due to cosmic rays (assumed to be $0.032 \mu\text{Gy}\cdot\text{h}^{-1}$) were as follows- Indoors (5798 measurements): $0.075 \mu\text{Gy}\cdot\text{h}^{-1}$ and Outdoors (5142 measurements): $0.068 \mu\text{Gy}\cdot\text{h}^{-1}$.

C. Richard Cothorn et al.^[60] measured the concentration of naturally occurring radionuclides in drinking water samples in the US and estimated the contribution to annual effective dose equivalent. They found that the resulting contribution from drinking water sources to the annual effective dose equivalent in the range of 0.002 to $0.05 \text{ mSv}\cdot\text{y}^{-1}$ (0.2 to $5 \text{ mrem}\cdot\text{y}^{-1}$) for those using community drinking water supplies. The contribution to the annual effective dose equivalent from ^{222}Rn dissolved in water was in the range of $0.8 - 30 \mu\text{Sv}\cdot\text{y}^{-1}$ ($0.08 - 3 \text{ mrem}\cdot\text{y}^{-1}$) based on the inhalation pathway following the release of ^{222}Rn from drinking water.

C. Papastefanou et al.^[61] measured the radiation level in Petralona cave (Chalkidiki, Northern Greece) using $3'' \times 3''$ NaI(Tl) detector and TLD- 200 ($\text{CaF}_2\text{-Dy}$), and found that the dose level varied from $27.8 \text{ mrad}\cdot\text{y}^{-1}$ (measured by NaI(Tl) detector) to $95.3 \text{ mrad}\cdot\text{y}^{-1}$ (measured by TLD - 200).

A. S. Mollah et al.^[62] measured the natural radioactivity level of some building materials in Bangladesh. All samples were ground to powder and then oven-dried at 110°C for 24h. 1 kg of each sample was placed in a Marinelli beaker (1-L capacity) which was sealed and stored for 4 week before counting to allow time for ^{238}U and ^{232}Th to reach equilibrium with their respective daughters. For activity measurements, they used semiconductor detector technique. In soil samples they found the average activity concentrations of ^{238}U , ^{232}Th , and ^{40}K respectively as $88.1 \pm 4.8 \text{ Bq}\cdot\text{Kg}^{-1}$, $68.2 \pm 5.2 \text{ Bq}\cdot\text{Kg}^{-1}$, and $256.4 \pm 16.3 \text{ Bq}\cdot\text{Kg}^{-1}$. For sand samples the corresponding values were $248.2 \pm 17.8 \text{ Bq}\cdot\text{Kg}^{-1}$, $219.0 \pm 19.2 \text{ Bq}\cdot\text{Kg}^{-1}$, and $389.2 \pm 22.8 \text{ Bq}\cdot\text{Kg}^{-1}$ respectively.

Thirty-seven soil samples representing the major soil types were collected from various sites around the Louisiana state, for estimation of radionuclide concentrations, by R. D. Delaune et al.^[63] For this purpose, they used a Ge(Li) detector which was connected to a multi-channel analyzer. The averages of the mean concentrations of ^{228}Ac (^{232}Th), ^{214}Pb (^{238}U), ^{137}Cs , and ^{40}K in

the analyzed samples were found respectively as- $36 \pm 4 \text{ Bq.kg}^{-1}$, $14 \pm 2 \text{ Bq.kg}^{-1}$, $23 \pm 1 \text{ Bq.kg}^{-1}$, and $472 \pm 13 \text{ Bq.kg}^{-1}$.

By using radiochemical separation technique and scintillation detector, James E. Watson, Jr., and Barry F. Mitsch^[64] measured the concentrations of ^{226}Ra and ^{222}Rn in 123 ground water samples collected from North Carolina Phosphate Lands. They found the ranges of ^{226}Ra and ^{222}Rn as $0.12 - 2.99 \text{ pCi.L}^{-1}$ (average 0.43 pCi.L^{-1}) and $6 - 5733 \text{ pCi.L}^{-1}$ respectively (average 198 pCi.L^{-1}) in the assessed water samples.

K. S. V. Nambi and S. D. Soman^[65] analyzed the available data of environmental radiation in India and concluded that the cancer risk is reduced with increase of external natural radiation doses to the population, which is consistent with the hormesis hypothesis. The reduction occurs at the rate of $0.3 \text{ per } \mu\text{Sv.y}^{-1}$ in the Indian population from a cancer incidence level of 79 per 100,000 population corresponding to a hypothetical, zero environmental radiation level.

Yu - Ming Lin et al.^[66] studied Taiwan's natural background radiation for a period of 3 years (1981 - 1983) which included the ambient exposure rate and radionuclides in soil and rock samples. They also compared the observed exposure rate and the exposure rate calculated from the concentrations of radioactive elements mainly ^{238}U , ^{232}Th , and ^{40}K in soil and rock samples and found a good correlation exists. For this purpose, they used a survey meter equipped with a 2.5 cm diameter by 2.5 cm long cylindrical NaI(Tl) detector, and a Ge(Li) detector of 23.5% relative efficiency for measuring the activities of soil and rock samples. They found that the exposure rate ranged from 2×10^{-8} to $9 \times 10^{-8} \text{ Gy.h}^{-1}$ with an average of $5.4 \times 10^{-8} \text{ Gy.h}^{-1}$. Taking into account the cosmic-ray contribution of $2.8 \times 10^{-8} \text{ Gy.h}^{-1}$, the average absorbed dose rate in Taiwan due to terrestrial γ -rays and cosmic-rays was $8.2 \times 10^{-8} \text{ Gy.h}^{-1}$. The K content ranged from 265 - 607 Bq.kg^{-1} , Th content ranged from 30 - 71 Bq.kg^{-1} , and U content ranged from 22 - 45 Bq.kg^{-1} . The average specific activities of K, Th, and U were 431 Bq.kg^{-1} , 44 Bq.kg^{-1} , and 30 Bq.kg^{-1} .

P. Corvisiero et al.^[67] measured the radioactivity in food and environment in Italy immediately after the Chernobyl reactor accident of 1986. They used a 3" \times 3" NaI detector for this purpose. They also estimated the internal dose from inhalation (assuming an average

inhalation rate of about $20 \text{ m}^3 \cdot \text{d}^{-1}$) external irradiation and ingestion as follows:- (i). Inhalation-dose equivalents in the target organs thyroid, lungs, and gonads were $120 \text{ } \mu\text{Sv}$, $2.5 \text{ } \mu\text{Sv}$ and $2.2 \text{ } \mu\text{Sv}$ respectively; (ii). External irradiation- estimated total body dose equivalent was $8.8 \text{ } \mu\text{Sv}$; (iii). Ingestion- dose equivalent in the target organs thyroid, lungs and gonads were $1000 \text{ } \mu\text{Sv}$, $20 \text{ } \mu\text{Sv}$ and $20 \text{ } \mu\text{Sv}$ respectively.

Isabel M. Fisenne et al.^[68] estimated the daily intake of long-lived α -emitting members of the U, Th, and Ac series by New York city residents from measurements of diet, water, and air samples. The total intakes from inhalation, food, and water consumption in mBq were $18(^{234}\text{U})$, $0.7(^{235}\text{U})$, $16(^{238}\text{U})$, $6(^{230}\text{Th})$, $4(^{232}\text{Th})$, and $52(^{226}\text{Ra})$. From this data, they inferred that the total daily intakes of ^{228}Th and ^{228}Ra were 4 and 35 mBq, respectively. They also found the activities of ^{238}U , ^{232}Th , and ^{226}Ra in New York city tap water samples respectively as $0.87 \pm 0.18 \text{ mBq} \cdot \text{L}^{-1}$, $0.050 \pm 0.023 \text{ mBq} \cdot \text{L}^{-1}$, and $0.41 \pm 0.09 \text{ mBq} \cdot \text{L}^{-1}$.

C. Papastefanou et al.^[69] measured the ^{137}Cs and ^{40}K content in soil samples immediately after the Chernobyl explosion, in Thessaloniki, North Greece. They used high resolution (1.9 - 2.0 keV at 1.33 MeV of ^{60}Co) and high efficiency (42%) spectrometers consisting of a Ge-Li and a high purity Ge detector for ^{137}Cs and ^{40}K measurements (total 56 samples). The concentration of ^{137}Cs in soils ranged between $290 \text{ Bq} \cdot \text{kg}^{-1}$ and $7670 \text{ Bq} \cdot \text{kg}^{-1}$, while the ^{40}K specific activity ranged between $226 \text{ Bq} \cdot \text{kg}^{-1}$ and $1604 \text{ Bq} \cdot \text{kg}^{-1}$. The ^{137}Cs concentrations was inversely proportional with ^{40}K concentration of K content of soils.

Tieh - Chi Chu et al.^[70] worked on the changes in per capita and collective dose equivalent in Taiwan in three decades (1950-1983) based on the measured terrestrial and cosmic radiation levels and the population distribution as well. The population had increased 2.5 times in that 33 years and reached to 1.9×10^7 person, yet the migration of population had been from the rural areas where the natural radiation was usually high to the urban areas where the natural radiation was usually low. The resulting collective dose equivalent had been increasing, yet the per capita dose equivalent, on the contrary, had been decreasing. In 1983, over 50% of the population in Taiwan was living in a radiation level interval of 50 - 60 $\text{nGy} \cdot \text{h}^{-1}$. Another 30% was living in the interval of 60 - 70 $\text{nGy} \cdot \text{h}^{-1}$. The rest was living either above or below the radiation intervals mentioned above. The population fraction in the radiation intervals of 50 - 60 $\text{nGy} \cdot \text{h}^{-1}$ was 51.7 % in 1950 and increased to 58.7% in 1980. On the contrary, the population

fraction in the radiation interval of 60 - 70 nGy.h⁻¹ was 31.1% in 1950 and decreased to 28.8% in 1980. Similarly, the population fraction in the radiation interval of 70 - 80 nGy.h⁻¹ was 0.45% in 1960 and decreased to 0.37% in 1980. The female per capita dose equivalent had been about 0.15% higher than that for males. This might account for the females who stay in the countryside while the males were working in the urban areas.

Chien Chung^[71] measured the concentrations of fission products immediately after the Chernobyl accident (beginning 12 day after the accident and lasting for the next 7 weeks) in the environmental samples and calculated its dose commitment to human in Taiwan. The individual effective dose equivalent committed by the first year of exposure and intake following the accident was evaluated. Average individual dose for the population in Taiwan was estimated to be 0.9 μSv due to global fallout from Chernobyl accident. That value was lower than those reported in neighbouring countries in the Far-East and poses no increased health impact to the population in Taiwan. The individual effective dose equivalents committed from the first year of exposure and intake following the accident was 0.8 μSv for adults, 1.2 μSv for children, and 2.1 μSv for infants in Taiwan. The collective dose for citizens in Taiwan was 18 man-Sv, less than 0.05% of annual background collective doses caused by natural radiation.

Olafur Arnalds et al.^[72] measured the fallout of ¹³⁷Cs levels in soil samples of 11 diverse sites throughout Montana, US. Soil samples were collected from 11 undisturbed native vegetation sites in the state. The sampling were performed during the summer of 1982. Most of the samples were taken in 10 cm depth increments, although sampling-depth increments differed at some sites. For the radioactivity measurements, they used Li- drifted Ge or intrinsic Ge γ-ray detectors coupled to a nuclear data 6620 analyzer system. Concentrations of ¹³⁷Cs in near-surface samples ranged from 20–200 mBq.g⁻¹ (0.51–5.41 pCi.g⁻¹). Most of the ¹³⁷Cs was found in the top 10 cm of soil. Deeper occurrences were attributed to disturbances by animals and to interstitial flow of small sediment particles within saturated soils. The areal concentrations ranged from 130–748 mBq.cm⁻² (3.6–20.2 pCi.cm⁻²) and was highly correlated with annual precipitation.

T. Yesin and N. Cakir^[73] used gamma-ray scintillation spectrometry in order to measure the ¹³⁷Cs and ¹³⁴Cs levels and depth distributions in soil of a tea plantation in the eastern black sea region in Turkey. Soil samples were collected in November 1987. The depth distribution was

found to be exponential with $\alpha = 0.16 \text{ cm}^{-1}$ and the exposure rate arising therefrom was calculated as $17.46 \mu\text{R}\cdot\text{h}^{-1}$ over the ground surface.

S. E. Simopoulos^[74] collected a total of 1242 soil samples, over Greece, during the period May-Nov. 1986 for ^{137}Cs analysis of the Chernobyl fallout in Greece. These samples were analyzed for ^{137}Cs and the counting was performed using a NaI detector on-line to a microcomputer; moreover, 252 of the samples were also analyzed by using Ge detectors, for inter-comparison and also for the assessment of other long-lived isotopes in the fallout. The results showed that ^{137}Cs fallout from Chernobyl present a remarkable geographical variability. The evaluated ground activity due to ^{137}Cs depositions ranged between 0.01 and $137 \text{ kBq}\cdot\text{m}^{-2}$.

R. J. de Meijer et al.^[75] measured the concentrations of radionuclides originating from the Chernobyl reactor accident as a function of time in air, rainwater, grass, cow's milk, vegetables, and dust by means of high-resolution γ -ray spectroscopy and found the high level of concentrations of fission product elements. They also found the concentrations of ^{137}Cs in rainwater samples (collected total 31 samples of different stations and mixed samples, from May 03 to July 01, 1986), ranged between $0.8 \text{ Bq}\cdot\text{L}^{-1}$ and $210 \text{ Bq}\cdot\text{L}^{-1}$.

Narayani P. Singh et al.^[76] estimated the U intake in Utah population by taking U measurements in urine and faeces of 12 human subjects of Utah, Salt Lake City, USA. They found that the daily U intake in the salt-lake city population, which comprises half the population in Utah, was $4.4 \pm 0.6 \mu\text{g}$ (higher value than other). In the salt lake city's drinking water samples the average activity of ^{238}U was found to be $17.8 \pm 3.33 \text{ mBq}\cdot\text{L}^{-1}$. Drinking water in Utah might contribute significantly higher amounts of U intake compared to others. They found that the dietary U intake in the Utah population was higher in comparison with other relevant reports.

H. Florou and P. Kritidis^[77] analyzed the environmental samples viz. soil, sediment, ores, and marine organisms collected from Milos island ($36^{\circ}42'\text{N}$, $24^{\circ}27'\text{E}$) located in the Volcanic arc of the Cyclades Archipelago in the south-eastern Aegean sea, Greece for estimating the natural radioactivity levels in the island. They used an HPGe detector and a car-borne scintillometry for this purpose. The results of radiometry indicated that the existence of some areas in Milos where the exposure rate exceeds $20 \mu\text{R}\cdot\text{h}^{-1}$, which corresponded to dose rate of

123 nSv.h⁻¹. In soil samples, the average concentrations of ²²⁶Ra, ²³²Th, and ⁴⁰K were found to be 50 ± 21 Bq.kg⁻¹, 57 ± 21 Bq.kg⁻¹, and 877 ± 332 Bq.kg⁻¹ respectively.

In 1990-91, Man-Yin W. Tso and Chung-Chuen Li^[78] measured the terrestrial gamma radiation dose rates in the 18 areas of Hong Kong. They used an energy-compensated GM dosimeter (MC-71) for the extensive terrestrial gamma dose rates measurements. A total of 194 indoor measurements and 76 outdoor measurements were made over 1,067 km², covering the 18 areas in Hong Kong island, Kowloon Peninsula, and the new Territories. They found the overall mean outdoor and indoor dose rates to be 0.163 µGy.h⁻¹ and 0.186 µGy.h⁻¹, respectively; while the corresponding population - weighted mean dose rates were 0.161 µGy.h⁻¹ and 0.189 µGy.h⁻¹. The mean annual dose equivalent from terrestrial gamma radiation for Hong Kong population was 1.11 mSv, and the collective dose equivalent was 5,919 man - Sv.

V. Bansal et al.^[79] analyzed the uranium concentrations in drinking water samples in India by using the dry fission-track registration method. They collected the drinking water samples from various sources in some cities of India. They found the range of the concentrations of uranium to be 0.67 - 20.26 µg.L⁻¹; depending on the type and site of the water source.

The exposure rates due to external gamma radiation in 11 Iraqi governorates were measured by B. A. Marouf et al.^[80] in 1990 - '91. They performed the measurements with a "Reuter Stokes Environmental Monitoring System (RSS-111)", which was a high-pressure ionization chamber with an electrometer specially designed for environmental measurements, in open air 1m above the ground. The average absorbed dose rate for the entire area studied was 6.3 × 10⁻² µGy.h⁻¹. The lowest absorbed dose rate was 4.3 × 10⁻² µGy.h⁻¹ and the highest absorbed dose rate was 11.3 × 10⁻² µGy.h⁻¹. The effective collective dose for all the governorates studied was 3570 person-Sievert.

M. Brai et al.^[81] estimated the population exposure to those living on the island of Pantelleria, Italy, by measuring the natural gamma background. They analyzed the gamma spectra of natural rocks and measurements of absorbed dose in air. They used a HPGe detector for gamma spectrometric measurements and thermoluminescent dosimeters LiF(Mg, Cu, P) for measurements of absorbed dose due to natural gamma terrestrial radiation. They found a correlation between the gamma exposure rate and the mean values of natural radionuclide

concentrations in the investigated rocks. They found the ranges of specific activities of ^{232}Th , ^{238}U , and ^{40}K in different rock samples respectively as 11.6 to 165.5 Bq.kg^{-1} , 12.1 to 168.5 Bq.kg^{-1} , and 27.7 to 1295 Bq.kg^{-1} . The minimum activity had been found for Basalts and the minimum for Pumice (Rhyolitic rocks). They further estimated the population absorbed dose to be 1.4 mGy.y^{-1} .

L. Zikovsky and G. Kennedy^[82] measured the concentrations of ^{232}Th , ^{226}Ra , and ^{40}K in 47 samples of seven different building materials available in Canada in 1990-'91, by semiconductor detector Ge(Li). Their estimation of the annual gonadal doses due to those building materials had been varied from 0.01 - 1.4 mSv .

T. Ren et al.^[83] measured the population doses from terrestrial gamma exposure in China by using High Pressure Ionization Chamber (HPIC) and TLD. The average dose levels for that country were found to be 81.5 nGy.h^{-1} and 69.0 nGy.h^{-1} respectively for HPIC and TLD.

Ching - Jiang Chen et al.^[84] investigated the natural radiation in houses built with black schist slabs located at an altitude of 1 km in the mountainous southern part of Taiwan by studying the naturally occurring radionuclides present in the black schist. In the mountainous area of southern Taiwan, houses owned by aborigines, such as the Lukai tribe, are commonly built with locally produced black schist slabs. Gamma-ray spectroscopy was performed using an HPGe detector coupled to a multichannel analyzer. In-situ measurements were carried out using a survey meter coupled to a sodium iodide detector. Cellulose nitrate films, ZnS(Ag) scintillation cells, and alpha spectroscopy were used to study radon and radon-daughters. They furthermore calculated the radiation doses due to all natural sources. In the black schist, concrete and soil samples, they found the ranges of ^{40}K , ^{232}Th , and ^{238}U are 432 - 911 Bq.kg^{-1} , 33.2 - 59.2 Bq.kg^{-1} and 26.8 - 57.0 Bq.kg^{-1} . ^{137}Cs was found only in soil samples and its level was 0.48 Bq.kg^{-1} . The total natural radiation doses received by the Lukai tribe was 1.50 mSv.y^{-1} ; while the corresponding value for average Taiwanese was 1.47 mSv.y^{-1} .

P. Schuller et al.^[85] collected soil, prairie plants, and milk samples from 39 dairy farms in southern Chile ($38^{\circ}44'$ - $41^{\circ}08'$ S) during the green-feed periods (September to March) between 1982 and 1990. They analyzed the samples with the help of a Ge(Li) detector and an HPGe detector for ^{137}Cs assay. In soil samples, the concentration of ^{137}Cs was found to range from 3.8

± 0.2 to $17.1 \pm 0.7 \text{ Bq.kg}^{-1}$. The reason for the increment of ^{137}Cs in soil samples was explained as due to higher average rainfall, latitudinal positions (which corresponds to the maximal radionuclide deposit bands of the southern hemisphere, according to UNSCEAR-1982^[10]); and the long term influence of radioactive fallout caused by the French and British atmospheric nuclear weapons testing had been undertaken within the southern hemisphere.

Using a hyperfine germanium spectrometer, N. M. Ibrahim et al.^[86] measured the concentrations of radionuclides ^{40}K , ^{137}Cs , ^{232}Th , and ^{238}U in surface soil across the Nile Delta, the north coast of Egypt. They collected the samples by either the template or core method. In the template method, a 25-cm \times 25-cm area sample was cut out using a template for guidance to a depth of 10 cm. In the core method, core of either 10.5 cm or 7.35 cm diameter and 7 cm of 25 cm in depth was used to take soil samples. They found the activities of ^{40}K , ^{238}U series, ^{232}Th series, and ^{137}Cs ranged from 29 ± 1.3 to $653 \pm 12.9 \text{ Bq.kg}^{-1}$, 5.2 ± 2.1 to $63.7 \pm 6.2 \text{ Bq.kg}^{-1}$, 1.1 ± 0.3 to $95.6 \pm 26 \text{ Bq.kg}^{-1}$, and below detectable limit to 2644 Bq.m^{-2} respectively for dry weight of 162 soil samples. They also calculated the absorbed dose rate for a height of 1m above the ground surface for each location from the wet weight concentrations of natural radionuclides measured; by using the standard conversion factors. The average value of the total dose rate at 1 m above the ground - due to ^{40}K , the ^{238}U series, and the ^{232}Th series in soil - was 31.5 nGy.h^{-1} (excluding cosmic radiation and ^{137}Cs Contribution); the range of which was 7.6 to 93.2 nGy.h^{-1} .

In 1991, Alberto Malanca et al.^[87] collected a total of 51 undisturbed soil samples each of $\sim 2\text{kg}$; to a depth of 30 cm in the central and eastern region of the Brazilian state Rio Grande do Norte. Concentrations of background radionuclides in soil samples were determined by gamma ray spectrometry with an HPGe detector. The average concentrations of ^{226}Ra , ^{232}Th , and ^{40}K in the surveyed soils were $29.0 \pm 19.4 \text{ Bq.kg}^{-1}$ (range- 10.3-137.6 Bq.kg^{-1}), $46.6 \pm 36.2 \text{ Bq.kg}^{-1}$ (range- 12.0-191.0 Bq.kg^{-1}), and $677.8 \pm 434.9 \text{ Bq.kg}^{-1}$ (range- 56.4-1972.0 Bq.kg^{-1}), respectively for dry weight of soil samples. The bedrock of Santana do Matos (Rio Grande do Norte) showed fairly high radioactivity (90 Bq.kg^{-1} of ^{226}Ra , 285.6 Bq.kg^{-1} of ^{232}Th , and 1414 Bq.kg^{-1} of ^{40}K). Radiological measurements carried out in Santana do Matos with a hand held scintillometer revealed external gamma radiation ranging from 200 - 330 nGy.h^{-1} in the down town area; the kerma rates in air due to the radionuclides found in soil samples was also estimated. The value of air kerma (corrected for moisture content) was found to be ranged between 18 - 205 nGy.h^{-1} with an average value of $81 \pm 43 \text{ nGy.h}^{-1}$.

A. P. Radhakrishna et al.^[88] made a systematic study on the background radiation and the distribution of radionuclides in the environment of coastal Karnataka, South India; an industrialized area endowed with nuclear and thermal power plants in addition to others. They measured the ambient gamma radiation dose in the environment by using a 5 cm × 5 cm NaI(Tl) scintillometer and by using TLD (CaF₂); and measured the concentrations of radionuclides in soil and sand samples by employing an HPGe detector coupled with MCA. Mangalore, a major industrial city of coastal Karnataka, revealed significantly high gamma dose in air. The measured gamma dose in air in high background area was in the range 44–2102 nGy.h⁻¹. The average activities of ²³²Th, ²³⁸U, and ⁴⁰K in soil samples (collected from the Bhagawathi temple area of Ullal beach, the area of highest radiation dose level) were found to be 2,971 Bq.kg⁻¹, 546 Bq.kg⁻¹, and 268 Bq.kg⁻¹, respectively.

During the period of 1989–1992, L. S. Quindós et al.^[89] collected soil samples nationwide from 952 sampling sites for assessment of natural radioactivity in the 17 autonomous regions of Spain. They made gamma spectrometry measurements of ²²⁶Ra, ²³²Th, and ⁴⁰K activities in soil samples by using a high-purity germanium co-axial detector with an efficiency of 20%, a resolution of 1.86 keV, and surrounded with shielding material to reduce the background counting rate. The detector was calibrated using standard solutions of ²²⁶Ra, ²³²Th, and ⁴⁰K in the same geometry as the measured soil samples. The ranges of concentrations of radionuclides ²²⁶Ra, ²³²Th, and ⁴⁰K were found over the 952 samples as 8 - 310 Bq.kg⁻¹ (average 39 Bq.kg⁻¹), 5–258 Bq.kg⁻¹ (average 41 Bq.kg⁻¹), and 31–2040 Bq.kg⁻¹ (average 578 Bq.kg⁻¹) respectively for dry weight of samples. For the whole Spain, an overall population-weighted mean outdoor terrestrial gamma dose rate of 53.3 nGy.h⁻¹ was also calculated from the measurements of the ²²⁶Ra, ²³²Th, and ⁴⁰K concentrations in soil. This value was comparable with that of 47.1 nGy.h⁻¹ derived from absorbed dose rates in air measured experimentally outdoors throughout the country (correlation co-efficient $r = 0.979$) and was also similar to the world average value of 55 nGy.h⁻¹ reported in UNSCEAR-1988^[4].

To estimate the level and distribution of fallout attributable to the Chernobyl nuclear power station accident (April 26, 1986) in the Ukraine which was estimated to released radioactivity of ~3.6 EBq (100 MCi) five years after the accident (in 1991); Masaharu Hoshi et al.^[12] sampled several kinds of substances at Korosten, Zhitomir, and at Katyuzhanka,

Vishgorod, Kiev in the Ukraine. The substances they investigated were soil, dry milk, wheat, rye, drinking water, and mushrooms; and measured the radioactivity levels of ^{137}Cs , ^{134}Cs , ^{90}Sr , ^{129}I , ^{238}Pu , $^{239,240}\text{Pu}$, and the density of ^{127}I (stable). Measurements of $^{137,134}\text{Cs}$ was performed with a germanium detector. In soil samples, which were air dried for ~2 months at room temperature, the concentration of ^{137}Cs and ^{134}Cs was found to ranged from 960 ± 70 to $1210 \pm 90 \text{ Bq.kg}^{-1}$ and 150 ± 11 to $177 \pm 12 \text{ Bq.kg}^{-1}$. The concentrations of both ^{137}Cs and ^{134}Cs in water samples were found to below 0.8 Bq.kg^{-1} .

W. H. Carlton et al.^[7] estimated the impact of ^{137}Cs released into the environment from the Savannah River Site Nuclear Installations of the US, on man. During the period 1955 - 1989, 130 GBq of ^{137}Cs was released into the atmosphere and 2.2×10^4 GBq of ^{137}Cs was released into the side streams and ponds. Approximately 65% of the latter remained on the site. The maximum individual effective dose equivalent at the site boundary was estimated to be 3.3 μSv from atmospheric releases and 600 μSv from liquid releases. The 80-km population dose was estimated to be 1.6 person-Sv.

Man-yin W. Tso et al.^[90] measured the concentrations of radionuclides of ^{226}Ra , ^{232}Th , and ^{40}K in building materials in Hong Kong. They also estimated the indoor ^{222}Rn level released from the building materials simultaneously. They further calculated the emanation coefficients and ^{222}Rn diffusion coefficients. The effect of surface coating on ^{222}Rn exhalation rate was also studied. The radionuclides contents of typical building materials used locally in Hong Kong was determined by γ -spectrometry method using an HPGe detector with MCA, and the results indicated that the average contents of ^{226}Ra , ^{232}Th , and ^{40}K in Hong Kong concrete were the highest known in the world. The average concentration of the mentioned radionuclides was the highest for granite chip. The average activities of ^{226}Ra , ^{232}Th , and ^{40}K in granite chips were $180 \pm 31 \text{ Bq.kg}^{-1}$, $122 \pm 5 \text{ Bq.kg}^{-1}$ and $1248 \pm 15 \text{ Bq.kg}^{-1}$ respectively; having Radium Equivalent (Ra-eq) of 451 Bq.kg^{-1} . The sea sand, river sand, aggregate, and concrete blocks had average Ra-eq as 38 Bq.kg^{-1} , 162 Bq.kg^{-1} , 395 , and 293 Bq.kg^{-1} respectively.

External γ -ray dose rates in air were measured by Y. Narayana et al.^[91], by using a sensitive plastic scintillometer in the environment of coastal Karnataka, on the south-west coast of India, where intensive industrial activities including a nuclear power plant, a super thermal power station, and a petrochemical complex were envisaged. The gamma dose rates in air were

found to be ranged from 26 to 174 nGy.h⁻¹ with a geometric mean of 74 nGy.h⁻¹ and a geometric standard deviation of 1.4. The activity of primordial radionuclides in soil samples of the region were measured by using an HPGe gamma-ray spectrometer and the resulting doses in air were calculated. The mean absorbed dose rate due to primordial radionuclides was 41.4 nGy.h⁻¹ with a geometric standard deviation of 1.4. A correlation was found between doses measured using scintillometer and doses estimated from the measured activity of primordial radionuclides when the cosmic-ray component was taken into account. The concentration of primordial radionuclides in soil and sand showed considerable variation in their vertical depth distribution in the high background area of the region.

A. S. Mollah et al.^[92] studied the radioactivity in soil samples at AERE, Savar, Dhaka, using an HPGe detector of volume 53 cc and of resolution 2.1 keV at 1332 keV line of ⁶⁰Co source. The samples were collected from a circular area having a radius of 10 km with the research reactor TRIGA- MARK-II of AERE as the centre; from two different depths, namely:- 2.5-5.0 cm, and 15-18 cm, at each sampling spot. They analyzed the samples for assessment of the concentrations of ²⁰⁸Tl, ²¹⁴Bi, ⁴⁰K, and ¹³⁷Cs. In the superficial (2.5-5.0 cm) soil samples, they found the ranges of the concentrations of the mentioned radionuclides as- 21.55 - 25.98 Bq.kg⁻¹, 32.43 - 48.73 Bq.kg⁻¹, 322.10 - 526.51 Bq.kg⁻¹, and from below detectable limit to 3.17 Bq.kg⁻¹ respectively.

K. E. Holbert et al.^[93] radiochemically analyzed 667 water samples of Arizona in US, collected over 5-y period 1989 to 1993. They found the average activities of ²²⁶Ra, and ²³⁸U as 76.2 ± 2.06 mBq.L⁻¹ and 346.0 ± 9.34 mBq.L⁻¹ respectively. The ranges of these two radionuclides were found to be 15.5 ± 0.04 to 1170 ± 31.5 mBq.L⁻¹ and 5.9 ± 0.16 to 2500 ± 67 mBq.L⁻¹ respectively.

John R. Meriwether et al.^[94] developed a new protocol for soil sampling named "Pedologically Based Sampling Technique" and applied successfully in determining the concentration of radionuclides in Louisiana, US. For determining the concentrations of naturally occurring radionuclides in Louisiana's soil samples, they used an HPGe detector associated with necessary electronics and a computer based MCA. The ranges of the concentrations of ²²⁶Ra(²¹⁴Bi), and ²³²Th(²²⁸Ac) was found to be from 14.4 ± 1.44 to 53.6 ± 5.36 Bq.kg⁻¹ and from 10.8 ± 1.08 to 61.6 ± 6.16 Bq.kg⁻¹ respectively. They also showed that the concentration levels

of primordial radionuclides are dependent on the depth from where the samples had been collected; the activity levels differs significantly with the variation of the depth of soil samples of same place.

^{222}Rn levels in dwellings and soil gas was investigated by H. J. Albering et al.^[18] in the Eijsden-Visé region, located at the Dutch - Belgian border, in order to analyze the relationship between domestic radon levels and soil gas radon levels. During February 1992, charcoal detectors were exposed for 24h in 116 dwellings in the township of Visé, a radon prone area in Belgium and found an average indoor air radon level of 116 Bq.m^{-3} . In the nearby township of Eijsden, the Netherlands, an area with a lower radiation level, similar measurements by means of charcoal detectors in 42 dwellings during March 1993, was resulted in an averaged indoor ^{222}Rn concentration of 46 Bq.m^{-3} . Furthermore, in the same region time-integrated radon measurements were performed in 15 dwellings on different floors. Those results indicated that a gradient in indoor air radon concentration exists from basement to upper floor level. In addition, a significant positive correlation was found between radon gas levels of soils surrounding 26 houses and indoor air radon levels. Soil gas ^{222}Rn levels was measured using a soil gas extraction method as described by T. K. Ball et al.^[95] in 1991.

Ilya Likhtariov et al.^[96] developed a model for the external exposure of the Ukrainian population after the Chernobyl accident. It was based on extensive measurements of external gamma exposure rates in air and measurement of external effective doses to members of five population groups (children younger than seven years, the age group from eight to seventeen years, employees, agricultural workers, and pensioners). In order to estimate the population dose for the six years period- May 1986 to April 1991, they used the Occupancy time & Behaviour factor of people, TLD technique, γ -spectrometry in determining ^{137}Cs concentration, and questionnaire data. During the six year period after the Chernobyl accident, they found that the agricultural workers had received the highest radiation dose $44 \mu\text{Sv per kBq.m}^{-2}$ and the children below 7 years had received the lowest radiation dose $17 \mu\text{Sv per kBq.m}^{-2}$, due to external radiation.

Y. Shimada et al.^[9] developed a numerical model for the analysis and evaluation of global ^{137}Cs fallout by analyzing the available data of the fallout of ^{137}Cs from atmospheric nuclear detonation tests that had been monitored worldwide since the late 1950's. Some of the

conclusions of their research are:- the deposition pattern of ^{137}Cs depends on the latitude but not on the longitude; the amount of ^{137}Cs deposition depends largely on the latitude where the nuclear detonation tests were made; the ^{137}Cs is accumulated much more in the surface and deep ocean waters of the North Pacific and the North Atlantic oceans than those of other oceans; and the peaks of ^{137}Cs accumulation in the surface ocean water occur earlier than those in the deep ocean water.

J. Manuel Pérez et al.^[171] carried out a survey of the ^{222}Rn concentrations in 106 homes in the four main towns of the central Austria's region, over four years. A total of 1014 measurements were obtained using passive radon charcoal canisters. The ^{222}Rn concentration was fitted a lognormal distribution law, with a geometric mean of 23 Bq.m^{-3} . There was a marked difference between the ^{222}Rn concentration for the ground inhabitant floors. For the other floors, the ^{222}Rn concentrations remained practically constant. The annual equivalent dose for general public due to the inhalation of ^{222}Rn was equal to 0.81 mSv .

Masayoshi Yamamoto et al.^[97] made a survey on the residual radioactivity in the soil at the "Semipalatinsk Nuclear Test Site (SNTS)" and at off-site areas in Kazakhstan. The soil was sampled in October 1994 from four locations in SNTS and the cities of Kurchatov and Almaty. The concentrations of different fission product radionuclides were assessed by using non-destructive γ - spectrometric analysis on ordinary Ge detector. During soil sampling, they also measured the radiation dose level above 1m from the ground surface by portable type survey meters PDR-101 & PDR-102. The radiation dose level was found to be ranged between $0.1 \mu\text{Sv.h}^{-1}$ (headquarters and research centre for SNTS) to $30 \mu\text{Sv.h}^{-1}$ (near hypocentre where the first Soviet nuclear explosion was tested on 29 August, 1949).

Kiyoshi Shizuma et al.^[98] performed low background gamma-ray measurement to determine the ^{137}Cs content in soil samples collected in a very early survey of Hiroshima atomic bomb. Those soil samples had been collected just 3 day after the explosion within 5 km from the hypocentre and had not been exposed to the global fallout from nuclear weapon tests. In their research work, soil samples were repackaged in plastic containers instead of glass vials to eliminate the ^{40}K gamma-ray background from the vial itself. Out of 22 samples, ^{137}Cs was detected in 11 samples, and their activities found to be ranged from 0.16 to 10.6 mBq.g^{-1} at the time of the measurement (1994–1995). Cumulative exposure by the fallout was estimated to be

0.12 ± 0.02 R (0.031 ± 0.004 mCi.kg⁻¹) in Hiroshima city except for the heavy fallout area and at most 4.0 ± 0.4 R (1.03 ± 0.11 mCi.kg⁻¹) in the heavy fallout area.

Shu-Ying Lai et al.^[99] measured the fallout of ¹³⁷Cs activities in soils and trees from samples taken in mountainous areas and along three-cross island highways in Taiwan. Typical concentration in near surface samples was about 5 Bq.kg⁻¹ depending on soil density. No correlation was found between the concentrations of ¹³⁷Cs and stable elements in soils. Mechanical disturbance and soil density were identified as major causes for redistribution of ¹³⁷Cs in both forest soils and trees. The transfer coefficient of ¹³⁷Cs from soil to *Bastard banian* estimated as 0.23. Each sample was counted by a Ge(Li) detector of 23.5% relative efficiency which was housed with a heavy shield to reduce background activity. The detector had a resolution of 1.86 keV full width at half maximum (FWHM) 1.33 MeV, MCA 4096, PCA coupled.

Z. Pietrzak-Flis et al.^[100] measured the intake of ²²⁶Ra, ²¹⁰Pb, and ²¹⁰Po with food and water in Poland. They found that the average activity of ²²⁶Ra in water was 4.46 ± 0.20 mBq.kg⁻¹, and the annual effective dose to man due to the intake of ²²⁶Ra was 4 μSv.y⁻¹.

By means of in-situ gamma-spectrometry with semiconductor detectors, J. Uyttenhove et al.^[101] measured the residual radiocaesium concentration, nearly 10 years after the Chernobyl accident at different sites on the Belgian territory. They also investigated a possible link between the rainfall at the beginning of May 1986 and the actual cesium concentration. The concentration of ¹³⁷Cs in Belgian surface soil samples was found to be ranged between 400 and 5600 Bq.m⁻². The measured radiocaesium activity was the sum of the Chernobyl accident contribution and the residual activity from previous contamination. The radiological impact of that contamination, even in the most affected regions in the Ardennes, was very small (5.6 μSv.y⁻¹).

S. Bellia et al.^[102] performed gamma-ray spectrometric measurements on rocks and soils of the island of Ustica (Southern Italy) to quantify the concentrations of the natural radionuclides. The ranges of the concentrations of ²³⁸U, ²³²Th, and ⁴⁰K were found to be 15–164 Bq.kg⁻¹, 16–174 Bq.kg⁻¹, and 201–1350 Bq.kg⁻¹ respectively. They also measured indoor and outdoor environmental air kerma using TLD. The outdoor values were generally found very low (less than 700 μGy.y⁻¹) while the indoor values of air kerma, measured in different dwellings

were found to be ranged between 1.9 and 4.0 $\mu\text{Gy.d}^{-1}$ and were, generally, higher than the world population-weighted average (1.92 $\mu\text{Gy.d}^{-1}$) reported in UNSCEAR-'93^[1] but lower than the indoor values measured on the island of Vulcano (4.4 – 6.6 $\mu\text{Gy.d}^{-1}$).

G. Manjon et al.^[103] separated the radium isotopes from water samples by precipitation method (Ra is coprecipitated with Ba as sulphate) and measured the activities with a low background scintillation counting system. In the drinking water samples, they found the activity of ^{226}Ra ranged from <0.7 to $267 \pm 3 \text{ mBq.L}^{-1}$ and the activity of ^{224}Ra ranged from <0.5 to $11 \pm 2 \text{ mBq.L}^{-1}$.

E. Gomez et al.^[104] studied the radioactive concentrations of the man-made radionuclides ^{137}Cs , ^{89}Sr , and ^{90}Sr ; in Calcareous soils of the island of Majorca (Spain), by analyzing the top 5 cm of the surface layer. The activity of ^{137}Cs was determined by γ -ray spectrometry and found to be ranged between 10 to 60 Bq.kg^{-1} .

Yen-Chuan Kuo et al.^[105] measured the concentrations of ^{226}Ra in drinking water samples in Taiwan by liquid scintillation counter. They found the ^{226}Ra content in ground-water was 12.0 mBq.L^{-1} and dose contribution to man was 1.8 $\mu\text{Sv.y}^{-1}$.

By using gamma-spectrometry technique with an HPGe, F. K. Miah et al.^[106] measured the concentrations of natural radionuclides of the uranium and thorium series, and ^{40}K and a fission product ^{137}Cs in soil samples collected from Dhaka city and its neighbouring environs. Activities of the radionuclides present in the soil samples were greatly influenced by the geomorphologic conditions in the area from where samples were collected. In their study, the average concentrations of the radionuclides ^{226}Ra , ^{228}Ra (^{228}Ac), ^{228}Th (^{208}Tl), ^{40}K , and ^{137}Cs were found to be $33 \pm 7 \text{ Bq.kg}^{-1}$ (range- 21 ± 6 to $43 \pm 7 \text{ Bq.kg}^{-1}$), $55 \pm 14 \text{ Bq.kg}^{-1}$ (range- 34 ± 12 to $81 \pm 15 \text{ Bq.kg}^{-1}$), $16 \pm 4 \text{ Bq.kg}^{-1}$ (range- 9 ± 2 to $22 \pm 2 \text{ Bq.kg}^{-1}$), $574 \pm 111 \text{ Bq.kg}^{-1}$ (range- 402 ± 78 to $750 \pm 82 \text{ Bq.kg}^{-1}$), and $7 \pm 2 \text{ Bq.kg}^{-1}$ (range- 3 ± 1 to $10 \pm 1 \text{ Bq.kg}^{-1}$) respectively.

John Jagger^[107] found a negative correlation of Natural Background Radiation (NBR) with overall cancer death. He made calculations and analyses based on data from the NCRP and from the American Cancer Society. Data from the NCRP reports showed that the average level of NBR in Rocky Mountain states was 3.2 times that in Gulf Coast states. On the other hand,

data from the American Cancer Society showed that the age-adjusted overall cancer death in Gulf Coast states was actually 1.26 times higher than that in Rocky Mountain states. The difference from proportionality was a factor of 4.0. This is a clear negative correlation of NBR with overall cancer death. It was also shown that, comparing 3 Rocky Mountain states and 3 Gulf Coast states, there was a strong negative correlation of estimated lung cancer mortality with natural radon levels (factors of 5.7 to 7.5).

N. N. Jibiri and I. P. Farai^[108] determined the average annual effective dose equivalent and the collective effective dose equivalent from measurements of the concentrations of ^{40}K , ^{238}U , and ^{232}Th in the top soil in and around the city of Lagos using in-situ γ -spectrometry. The average outdoor absorbed dose rate was $0.041 \pm 0.012 \mu\text{Gy}\cdot\text{h}^{-1}$ resulting in an annual average effective dose equivalent of $50 \mu\text{Sv}\cdot\text{y}^{-1}$. The collective effective dose equivalent to the populations in the city was $2.84 \times 10^2 \text{ man}\cdot\text{Sv}\cdot\text{y}^{-1}$.

B. Baggoura et al^[109] carried out a national environmental sampling programme during 1993 to determine natural and artificial radionuclide content in the (0-15 cm) upper layer of the soil, in Algeria. Soil samples were analyzed with the help of direct counting by gamma-ray spectrometry (an HPGe detector associated with necessary accessories). In addition, terrestrial gamma-ray dose rates in air had been measured out of doors throughout Algeria at the time of sample collection, at each of the sampling locations, by means of a pressurized argon ionization chamber; type RSS-112, at 1m above the top soil. In each of the 48 administrative divisions of the country, selected sites were chosen to collect soil samples and to measure gamma-ray dose rates simultaneously. Radioactivity concentrations in $\text{Bq}\cdot\text{kg}^{-1}$ dry mass in soil samples of ^{226}Ra , ^{214}Pb , ^{214}Bi , ^{212}Pb , ^{228}Ac , ^{40}K , and ^{137}Cs were found to be range between (5-176), (2-107), (3-65), (2-97), (3-144), (36-1405), and (0.3-0.41) respectively. The dose rates in air measured over the whole country were found to be range between 20 and 133 $\text{nGy}\cdot\text{h}^{-1}$.

R. H. Higgy and M. Pimpl^[110] measured the specific radioactivities of U-series, ^{232}Th , ^{137}Cs , and ^{40}K in soil samples around the Inshass reactor in Cairo (Egypt), using a γ -ray spectrometer with an HPGe detector. The specific activities of ^{238}U , ^{232}Th , ^{40}K , and ^{137}Cs obtained from direct γ -spectrometric measurements for soil samples were found to be range between 5.3 and 7.7 (average 6.3), 10.7 and 17.0 (average 13.3), 152 and 202 (average 163), and from 1.6 to 19.1 (average 5.5) respectively in $\text{Bq}\cdot\text{kg}^{-1}$ dry weight.

Using an HPGe γ -ray detector, M. M. Rahman^[111] analyzed soil (sand) samples collected from the sea-beaches of Cox's Bazar, Potenga, Fauzdarhat (Chittagong), and Harinbaria (Borguna); and rock samples collected from Fultala (Sylhet) for determining the concentrations of ^{208}Tl , ^{214}Bi , ^{228}Ac , ^{40}K , and ^{137}Cs . He collected the sand samples at a depth of 20-25 cm from each of the beaches. The average concentrations of the mentioned radionuclides in sand samples were respectively found to be $31.31 \pm 12.98 \text{ Bq.kg}^{-1}$, $29.55 \pm 11.43 \text{ Bq.kg}^{-1}$, $39.95 \pm 13.26 \text{ Bq.kg}^{-1}$, $454.08 \pm 96.59 \text{ Bq.kg}^{-1}$, and $2.28 \pm 0.59 \text{ Bq.kg}^{-1}$.

Muhammad Anwar Uddin^[112] measured the concentrations of primordial and anthropogenic radionuclides in drinking water samples collected from Chittagong City. He used an HPGe detector for this purpose. In his research, he analyzed the samples for finding out the activities of ^{222}Rn , ^{238}U , ^{226}Ra , ^{232}Th , ^{40}K , and ^{137}Cs . He found the ranges of the concentrations of the mentioned radionuclides as between $1.23 \pm 0.002 \text{ Bq.L}^{-1}$ and $20.42 \pm 0.048 \text{ Bq.L}^{-1}$ (average- $7.90 \pm 0.018 \text{ Bq.L}^{-1}$), $11.72 \pm 0.045 \text{ mBq.L}^{-1}$ and $120.00 \pm 0.463 \text{ mBq.L}^{-1}$ (average- $45.67 \pm 0.176 \text{ mBq.L}^{-1}$), $11.16 \pm 0.076 \text{ mBq.L}^{-1}$ and $139.52 \pm 0.096 \text{ mBq.L}^{-1}$ (average- $52.62 \pm 0.36 \text{ mBq.L}^{-1}$), $24.55 \pm 0.094 \text{ mBq.L}^{-1}$ and $289.65 \pm 1.12 \text{ mBq.L}^{-1}$ (average- $170.96 \pm 0.661 \text{ mBq.L}^{-1}$), and $2.04 \pm 0.009 \text{ Bq.L}^{-1}$ and $12.41 \pm 0.052 \text{ Bq.L}^{-1}$ (average- $4.54 \pm 0.02 \text{ Bq.L}^{-1}$) respectively. No ^{137}Cs was detected at any of the samples in the whole study area. By considering a person drinks 1.2 litre of water per day, he further calculated the population dose from all of these source due to consumption of drinking water; and it was 0.06 mSv.y^{-1} .

The outdoor environmental background radiation were measured by thermoluminescence dosimetry, gamma spectrometry of soil samples, and ionization chamber (β - γ survey meter); by Tutul Kanti Saha^[113]. The study was carried out for 2 and 4 months periods in the region of Chittagong City prefecture of Bangladesh. The average environmental dose rate during the monitoring period was found to be $1321.93 \pm 223.20 \mu\text{Sv.y}^{-1}$ with TL dosimeters and $1847.35 \pm 171.33 \mu\text{Sv.y}^{-1}$ with a β - γ survey meter. The average environmental radiation dose rate due to natural ^{238}U , ^{232}Th , and ^{40}K radionuclides in surface soil of Chittagong obtained by the measurement with an HPGe detector was $559.34 \pm 115.04 \mu\text{Sv.y}^{-1}$. The variation in these three dose levels was explained as the β - γ survey meter measured the β & γ radiation of all energies, the TL dosimeters measured only γ -radiation (the perspex holder of TL-chips absorbed β -

radiation), and the last one was only due to ^{238}U series, ^{232}Th series, and ^{40}K radionuclides without considering the impact of other (cosmic and natural) sources of radiation.

CHAPTER 3



EXPERIMENTAL

CHAPTER 3

EXPERIMENTAL

3.1 Introduction

Human sensors are unable to measure or even detect the presence of ionizing radiation. Hence, to detect and measure the ionizing radiation, we need some instruments based on the principle of interaction of radiation with matter. There are different types of radiation detectors characterized by nature of the interaction of radiations with the detecting materials. The common types of interaction of ionizing radiation with matter are: (i) photo electric effect (consequence of which may be Bremsstrahlung and/or Auger effect), (ii) Compton scattering, (iii) pair production (triplet production may also occur), (iv) photo-nuclear reaction (photo-disintegration), (v) Thomson scattering, and (vi) Rayleigh scattering. Among these, first three are most important as they play significant roles in interaction of ionizing radiations of low to moderate energies with either biological or inanimate matter^[114]. There are mainly two types of radiation detecting devices, viz.- (i) devices to detect and measure the level of radioactivity, and, (ii) devices to measure the radiation dose rate or accumulated dose.

Several types of instruments have been developed for measurement of radioactivity and radiation dose. Different types of operation are involved by virtue of ionization which is produced in detectors by radiation. For measuring radioactivity, there are: (i) gas filled radiation detectors [which include ionization chamber, proportional counter, and Geiger-Müller counter etc.], (ii) scintillation detectors [solid and liquid; NaI(Tl), CsI(Tl), KI(Tl), LiI(Tl), ZnS(Ag), p-terphenyl, 2-phenyl-5-(4-biphenyl)-oxazole (PBO), 2-phenyl-5-(4-biphenyl)-1,3,4-oxadiazole (PBD) etc.], (iii) semiconductor radiation detectors [Si-Li, Ge-Li, Cd-Te, Cd-S, HPGe etc.], and, (iv) Cerenkov detector [high density glasses whose refractive index is 1.6 to 1.7 for sodium D-lines, and some liquids of high refractive index^[15]]. For measuring radiation dose rate or accumulated dose over a certain time period, there are: (i) gas filled chamber [which include GM tube based survey meters, pocket dosimeter, thimble chamber, electret ionization chamber (EIC)^[115], ion current chamber^[15] etc.], (ii) measurement of absorbed dose by measuring chemical change in certain radiation-sensitive matter [FeSO_4 ^[116], alanine or a mixture of alanine and paraffin^[117]], (iii) measurement of absorbed dose by calorimeters^[24], (iv) measurement of absorbed dose by photographic techniques [film badge], (v) measurement of absorbed dose by

autoradiographic techniques [transparent detectors^[20]], (vi) radioluminescent detectors [glass doped by silver phosphate^[20]], and, (vii) thermoluminescent dosimeter(TLD) [LiF, Li₂B₄O₇:Mn, Li₂B₄O₇:Cu, LiF(Mg,Cu,P), BeO:Li, BeO:Na, NaCl:Ba(T), CaF₂, CaF₂:Dy, CaSO₄:Mn, CaSO₄:Dy, CaSO₄:Tm, etc.].

Gamma-ray spectrometry is one of the most important non-destructive techniques to determine the presence and amount of radionuclides in the environment^[6]. In the past, scintillation detectors were used for gamma spectrometry but nowadays, these are quite obsolete in complex gamma-ray spectrometry where high resolution and precision are required. Gamma-ray spectrometry allows both qualitative identification and quantitative determination of the radionuclide in the sample.

Principle, operation, and merit & demerit of some commonly employed radiation detectors are described below in brief.

3.1.1 Gas Filled Detectors

The gas filled radiation detectors are operated on the principle of ionization of gases during passage of ionizing radiation through it. These consists of a tube filled with a mixture of an inert gas and an quenching organic gas at a reduced pressure with a central electrode well insulated from the chamber walls. Radiation passing through the gas filled closed chamber produces ion-pairs which flow towards respective electrodes where the central wire is maintained at a high positive potential with respect to the walls of the chamber. Details about the gas filled radiation detectors are described latter.

3.1.2 Solid-State Detectors

There exist certain classes of crystalline substances which exhibit measurable effects when exposed to ionizing radiation. In such substances, electrons exist in definite energy bands separated by forbidden bands. The highest energy band in which electrons normally exist is the valence band. When ionizing radiation passes through such substances, the kinetic energy of the radiant particles is transferred into the valence electrons which cause them to rise into exciton or conduction band^[30] through the forbidden band or may be trapped within the forbidden band. The vacancy left by the electron is known as hole. These effects is measured individually in different types of detectors, viz., (i) semiconductor detectors, (ii) scintillation detectors, and, (iii) thermoluminescence detectors.

3.1.2.1 Semiconductor Detectors: Semiconductors are those substances whose electrical conductivity or resistivity (10^{-4} to $0.5 \Omega\text{m}^{[118]}$) lies in between conductors and insulators. In such substances, the valence band is almost filled and the conduction band is almost empty. The energy gap between the valence band and the conduction band is <1 eV. Semiconductors exhibit negative temperature coefficient of resistance and in those substances, the atoms are bound to one another by covalent bond. Examples of semiconductors are: Ge, Si, Se, C etc. When ionizing radiation passes through a semiconductor, a large number of electron-hole pairs are produced. The electrons are generally lifted to the conduction band; the electrons and holes are independently mobile and in the presence of an electric potential, are attracted oppositely. Consequently, contributing to electrical conduction in the crystal. In a semiconductor detector, the charges are collected by applying a high voltage across the sensitive region of the detector. The resultant collected charge is integrated by a charge sensitive preamplifier and converted into a voltage pulse with an amplitude proportional to photon energy. Semiconductor detectors can be used for complex gamma spectrometry. Scintillation NaI(Tl) spectrometers were exclusively used in the past for the estimation of gamma-activities in different environmental samples. However, their poor energy resolution has made them unsuitable for the purpose. The high resolution counting systems such as Si(Li), Ge(Li), and HPGe detectors are now widely used for the analysis of environmental and biological samples. The gamma-ray peaks obtained with NaI(Tl) detectors are very broad, for which two adjacent gamma-ray peaks cannot be resolved. The Si(Li) detector cannot detect and measure the high energy gamma-rays. Though the Ge(Li) detector has high resolving power, it has several drawbacks. For example, to make accurate measurement, it must always be kept at liquid nitrogen temperature 77 °K. To overcome this disadvantage and limitation, HPGe detectors are presently used. The HPGe detectors have good efficiency and excellent energy resolution. The chief advantage of HPGe detector is its ability to measure gamma-emitters in the sample directly without the need of chemical separation. The detail about HPGe is discussed latter.

3.1.2.2 Scintillation Detector: In certain crystalline materials, the ionizing radiation causes the valence band's electrons to raise into exciton band. In this case, the electron is still bound to the hole by electrical forces and so they cannot contribute to conduction. The excited electrons, during return to their ground state, emit light photon or scintillation. This light is picked up by photomultiplier (PM) tube and is analyzed to determine the nature of radioactivity or radiation

dose. Detectors operating in this mode are called scintillation detectors. The absorption of a 1 MeV gamma photon in a scintillation detector results in about 10,000 excitations and the same number of photons of light^[30]. Certain liquids (which may later be a polymer or a thin film) also exhibit scintillation property and can be used for radiation monitoring e.g., PBO, PBD etc. The scintillator detectors have excellent efficiency but poor resolution. Hence, now-a-days, the scintillator detector is rarely used in complex gamma-ray spectrometry.

3.1.2.3 Thermoluminescence Dosimeters: The third process which can occur in certain crystals due to passage of ionizing radiation through them is electron trapping. Traps are imperfections or impurity atoms in the crystal structure which cause electrons to be caught in the forbidden band and may exist there at room temperature for a longer period. If the irradiated crystal is subsequently heated at $\sim 200^\circ\text{C}$, the trapped electrons firstly rise into exciton band and then return into the valence band with the emission of light photon. This process is called thermoluminescence^[119] and the detector/dosimeter operated in this mode is called thermoluminescence dosimeter (TLD). TLD is the best for personnel monitoring and environmental accumulated dose measurement because of its wide dose range, linearity in dose response, approximately no angular dependence, negligible fading, smaller in size etc. But TLD cannot measure instantaneous dose rate.

3.1.3 Film Badge Dosimeter

Another popular personnel dosimeter is the film badge. A film badge dosimeter consists of a packet of two or three pieces of dental-sized photographic film wrapped in light-tight paper mounted within a suitable plastic or metallic film-holder called badge which clips to the wearer's clothing. The holder acts as a filter for low energy γ or X- radiation and for β -radiation. A photographic film consists of an emulsion of crystals (grains) of silver halide (generally bromide) on a transparent cellulose acetate base. When ionizing radiation is exposed to the film, a small cluster of metallic silver is formed. This cluster is known as latent image^[120]. After completion of the development procedure of the film, the unconverted silver bromide grains are removed from the base and a dark image (of Ag) is obtained. The degree of darkening (optical density) of the film can be precisely measured by a photoelectric densitometer whose reading is expressed as the logarithm of the intensity of the radiation transmitted through the film. The optical density of the exposed film is quantitatively related to the amount of exposure and consequently the radiation dose exposure of an individual who wore the badge in a radiation field can be found.

Personnel dosimeter film badge suffers a number of demerits in the opposite of a number of merits. Its use is only limited to occupational personnel dosimetry.

In the present study, gas filled radiation dosemeter (survey meter PDR 1Sv) and the semiconductor radiation detector (HPGe) were employed. A brief description of gas filled chamber and HPGe detector are given below.

3.2 Gas Filled Radiation Detectors

The ionizing radiation causes ionization in gaseous medium while passing through it. If the ionizing radiations are allowed to pass through a gaseous medium (kept at low pressure) between two electrodes (one is kept constant at positive potential and the other at negative potential) within a closed chamber, then at moderate electrode potential, the electrons move towards the +ve electrode and the +vely charged atoms towards the -ve electrode. Consequently, electric conducting property arises within the gas and current flows. Then by the help of RC-circuit, this current can be converted into voltage pulses which can be recorded by an external pulse recording circuit. On the basis of operating conditions, the gas filled radiation detectors are classified into three categories, viz.: (i) ionization chamber, (ii) proportional counter, and, (iii) Geiger-Müller counter.

In a gas filled radiation detector as shown in the Figure 3.2, A voltage V is applied between the wall and central electrode through a resistor R shunted by a capacitor C . When radiation passes through the detector, N number of ion pair is produced. The negative and positive ions move towards the anode and cathode respectively. Under this condition, the time constant RC is much greater than the time required for the collection of charge, the charge Q appearing on the capacitor C per particular interaction as a function of V is shown in the Figure 3.1.

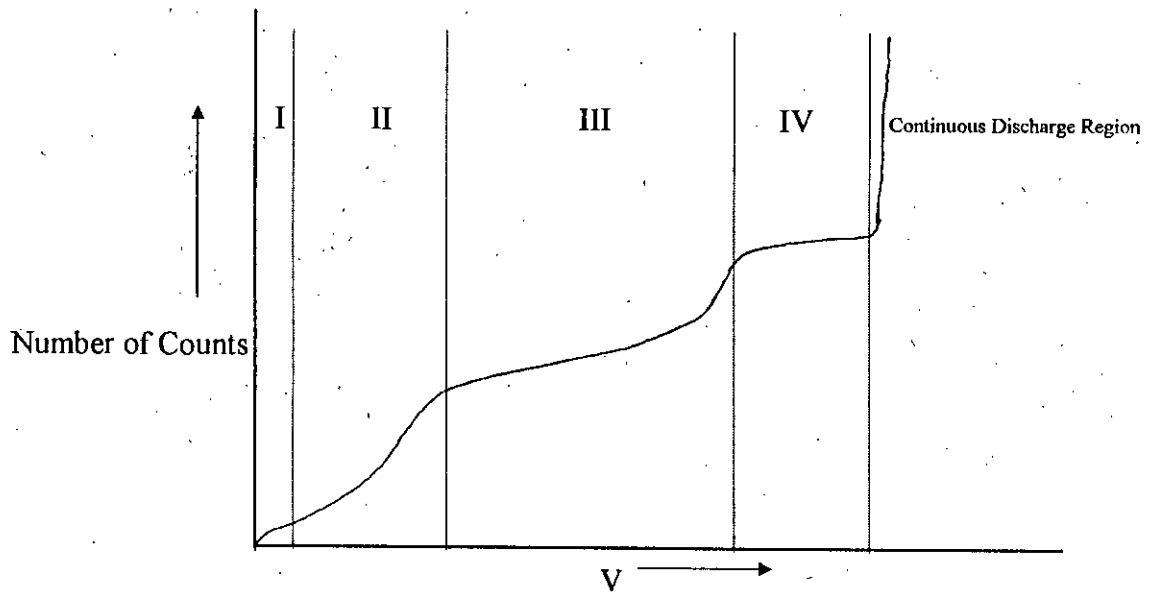


Figure 3.1: The Curve Showing the Relation Between the Applied Voltage and the Number of Counts in a Gas-Filled Radiation Detector.

This curve can be divided into four regions^[121]. In region-I, there is a competition between the loss of ion pairs by recombination and the removal of the charges by collection on anode. With the increase in voltage i.e., electric field intensity, the drift velocity of the ions increases. So the time for recombination decreases and the fraction of charge collection on anode becomes larger. In region-II, the recombination loss is negligible and the charge collection on two electrodes is $Q = Ne$ (where, 'e' is the charge of an electron). The change in voltage across C is:

$$\Delta V = \frac{Ne}{C} \quad \left(\because C = \frac{Q}{V} \right)$$

This region is known as saturation region or ionization chamber region. In region-III, the collected charge is increased by a factor of 'M' through the phenomenon of gas-multiplication, the electrons which are released by primary ionization are accelerated sufficiently to produce additional ionization and thus add to the collected charge. The collected charge is increased with the applied voltage (directly proportional). At the onset of region III, the multiplication M for a given applied voltage is independent of the initial ionization, thus preserving the proportionality of pulse sizes. This strict proportionality breaks down with increase in applied voltage until, at the upper limit of region III, the pulse size is independent of the initial ionization. This region, in which gas multiplication is employed while at the same time a dependence of the collected

charge of the initial ionization remains, is called proportional region. The detector operated in this region is called proportional counter/chamber. With the help of proportional chamber one can differentiate the nature of detected radiation i.e., α , β , or γ . In region-IV, the charge collection is independent of the ionization initiating it. Consequently, in this region one cannot differentiate the nature of radiation whether it is α , β , or γ . Rather, the gas-multiplication increases the charge to a value that is limited by the characteristics of the tube or chamber and external circuit^[121]. This region is called Geiger-Müller region. The detector operated in this region is called Geiger-Müller (GM) detector/counter. GM detectors can be used to measure all types of nuclear and extra-nuclear radiant particles which will produce ionization within the tube, no matter how small the amount of ionization.

3.2.1 Geiger Müller (GM) Counter

A GM counter is a gas-filled detector designed for maximum gas multiplication effect. The GM tube consists of a metallic (having good conducting property) cylinder with a thin axial wire of tungsten (generally) enclosed in a glass envelope in which usually a mixture of 90% argon and 10% quenching gas such as organic vapour (ethyl alcohol gas) or halogen gases (chlorine) is filled at a pressure of 2 to 10 cm of Hg. A potential difference of about 800 to 2000 Volts is applied to make the tube negative with respect to the central wire^[120, 121]. In the complete counter assembly, an RC circuit, a discriminator, and a counter is employed. Since the output pulse of the GM tube is generally large enough for evaluation, no preamplifier or amplifier is normally required. In the Figure 3.2, an 'end-window' type GM tube and necessary electronics for counting/detection is shown. The series resistance R between the high voltage supply and the anode of the tube is the load resistance across which the signal voltage is developed. The parallel combination of R with the capacitance of the tube and associated wiring C determines the time constant of the charge collection circuit. This time constant is normally chosen to be a few microseconds so that only the fast-rising components of the pulse are preserved^[120].

When a beam of radiations enters into the chamber through the thin window of mica of the tube chamber, it produces a large number of ion pairs in the enclosed gas along its path. The GM tube is widely used for counting electrons, beta particles, γ -rays and x-rays. The gas-filled radiation detectors specially GM tubes are used for measuring both the radioactivity level and the dose rate (in survey meters) & accumulated dose (pocket dosimeter).

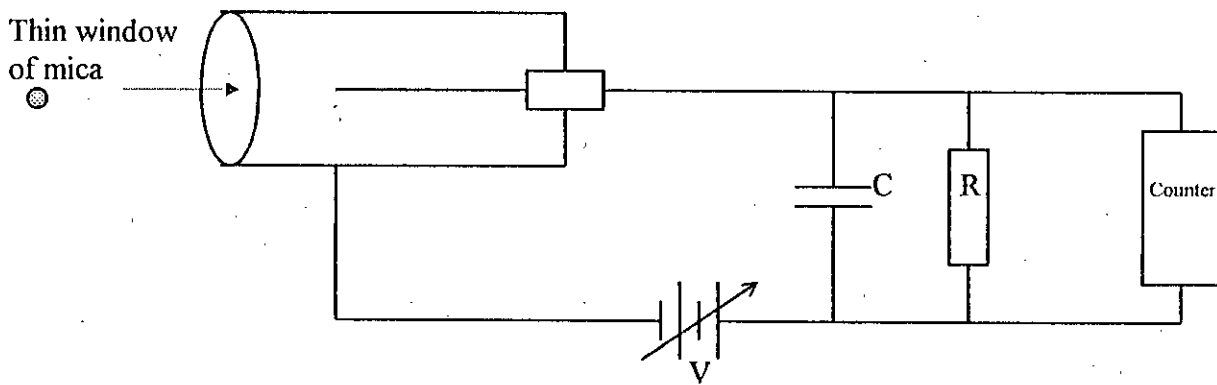


Figure 3.2: A Geiger-Müller Counter.

Because the pulse sizes in GM tubes are independent of the primary ionization, this instrument cannot be used as a measure of particle energy, nor it is possible to discriminate between different types of particles by means of the sensitivity of the electronic circuit. All pulses from a GM tube are of the same amplitude regardless of the number of original ion pairs that initiated the process^[120]. A GM tube can therefore function only as a simple counter of radiation-induced events, and cannot be applied in direct radiation spectroscopy because all information on the amount of energy deposited by the incident radiation is lost. Since GM tubes have comparatively large dead-time, these detectors are therefore limited to relatively low counting rates.

The GM counter tube has been a widely used detector of nuclear radiation for many years. The great utility of the GM tube is a result of several of its characteristics. Some of the more important of these are: high sensitivity, versatility for use with different types of radiation, wide variety of shapes and windows, large size of the output signal, ease of operation and reasonable cost. The large sensitivity of these devices arises from the characteristic that the nuclear radiation serves only to trigger a discharge. Any particle that produces ionization in the tube will produce a discharge, even though the ionization may consist of only one ion pair. Thus any types of particles which can release charge within GM tubes can be counted by them^[121]. This includes X and γ -rays, which produce ionization by secondary processes, as well as all types of charged radiant particles.

Therefore, a Geiger-Müller counter or a GM tube based survey meter is often the best choice when a simple and economical low level counting system is needed; for example, in case of measuring the environmental radiation level.

GM tubes may be of different size and shape. Tubes have been built and operated successfully with diameters from around 2 mm to several centimetres and with lengths from about 1 cm to several feet. Further, there is no apparent limitation at either extreme. Few of the several shapes & forms in which GM tubes are available are: (i) cylindrical type, (ii) bell type, (iii) needle counter, (iv) jacketed counter, and, (v) flow-type detector. The most common design of GM tubes is the 'end-window' type, as shown in the Figure 3.2.

3.3 High Purity Germanium (HPGe) Detectors

935523
HPGe detector is a solid analogue of a gaseous ionization chamber where high-purity germanium is used instead of usual gas. It is a high quality precision instrument and is used in gamma-ray spectrometry above about 100 keV for its high efficiency and good resolution. The basic component of an HPGe detector is a single crystal of germanium with p-n diode structure as shown in Figure 3.3. If the impurity concentration in germanium can be reduced to about 10^{10} atoms/cm³ (i.e., 1 impurity atom per 10^{13} atoms), a depletion depth of about 10 mm can be obtained. These large-volume germanium diode detectors are usually called 'intrinsic' or "high purity" germanium detectors. The reliability of the detector depends on its depletion depth. The depletion depth at a given voltage increases in proportion to the square-root of the material resistivity and inversely proportional to the net impurity concentration in the detector material^[120]. The bulk of the high purity material is generally p-type, due either to residual acceptor impurities (such as aluminum) or to acceptor centres associated with lattice defects within the germanium itself. The configuration is sometimes referred as to n⁺-p-p⁺ diode structure. The n⁺ is usually formed by lithium evaporation onto a lapped surface of the germanium followed by a short period of diffusion at elevated temperature. The detector depletion region is formed by reverse biasing this n⁺-p junction. The p⁺ contact at the opposite face is a typically diffused gold surface barrier junction. The outer n-type diffused Li contact is about 300 nm thick. The inner surface barrier contact is about 40 mg/cm² of evaporated gold. The intrinsic region is sensitive to electromagnetic ionizing radiation. Under reverse bias, an electric field extends across the intrinsic or depleted region.

In an HPGe detector, gamma-rays are detected by their (radiation) ionizing properties i.e., by the creation of primary and secondary electron-hole pair(s) when they enter into the detector. When photon interact with the material within the depleted volume of a detector, ion-pairs (electron-hole pairs) are produced and are swept by the electric field to the p and n

electrodes. All the electron-hole pairs thus produced when are collected under the influence of an applied electric field, result in a voltage pulse height proportional to the gamma-ray energy absorbed^[122], by an integral charge sensitive preamplifier. The ionization is produced when gamma-rays are interacted in the detecting material (crystal) generally by any one of the following three processes, viz.- (i) photo-electric effect, (ii) Compton scattering, and, (iii) pair production. At low energies, the predominant mode of absorption are photo-electric effect and Compton scattering^[23, 24]. But at energies ≥ 1.022 MeV, pair production is dominant. A spectrum of mono-energetic gamma-rays consists of a full absorption peak, a Compton continuum, and for energies ≥ 1.022 MeV, pair production peaks. The relative intensity with which each of them contributes to the resulting spectrum depends on the energy of the primary gamma-ray, the material of the detector, and the size of the detector^[123].

Few important physical characteristics of intrinsic germanium are summarized in the Table 3.1.

Table 3.1: Properties of Intrinsic Germanium^[120].

Atomic number	:	32
Atomic weight	:	72.60
Density	:	5.33 gm/cm ³ (300 °K)
Atomic density	:	4.41 × 10 ²² atoms / cm ³
Dielectric constant	:	16
Forbidden energy gap	:	0.665 eV (300 °K) 0.746 eV (0 °K)
Intrinsic carrier density	:	2.4 × 10 ³ / cm ³ (300 °K)
Intrinsic resistivity	:	47 Ωcm (300 °K)
Electron drift mobility	:	3900 cm ² / V-s (300 °K) 3.6 × 10 ⁴ cm ² / V-s (77 °K)
Hole drift mobility	:	1900 cm ² / V-s (300 °K) 4.2 × 10 ⁴ cm ² / V-s (77 °K)
Energy per hole-electron pair	:	2.96 eV / (77 °K)
Fano-factor	:	from 0.057 to 0.129 (77 °K)

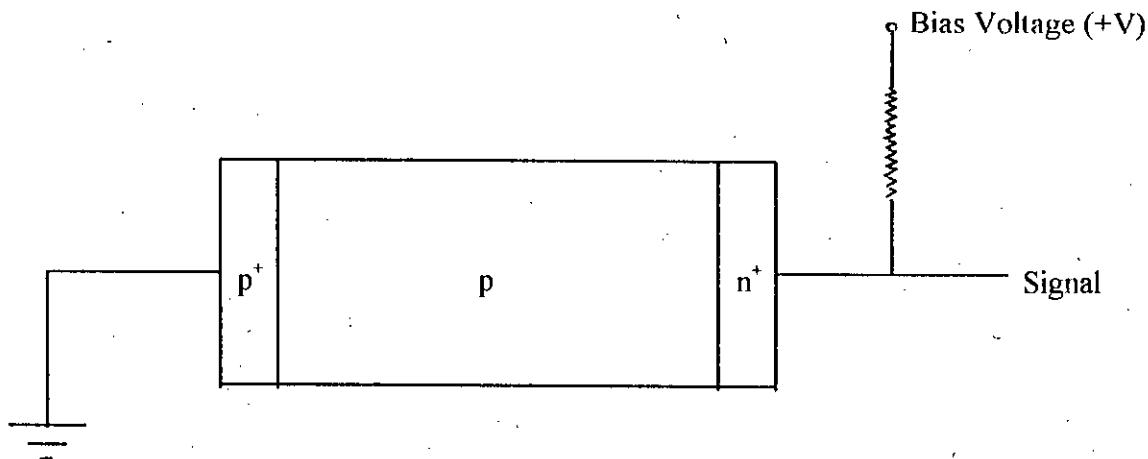


Figure 3.3: The Configuration of an Intrinsic Ge Detector. The p-type Central Region is Made of Germanium of the Highest Available Purity, and the n^+ -p Junction is Reverse Biased.

The HPGe detectors are available in two relatively simple geometry: the planer detector, in which the electric field is fairly uniform; and the coaxial configuration, in which the electric field varies inversely with the radial distance from the detector axis. The gamma-ray detection efficiency and corresponding function of an HPGe detector are identical to those in a Ge(Li) detector of same size and shape.

Since germanium has relatively low band gap and high temperature sensitivity, these detectors must be cooled in order to reduce the thermal generation of charge carriers (thus reduce leakage current) to acceptable level. Otherwise, leakage current induced noise destroys the energy resolution of the detector. Liquid Nitrogen, which has a temperature of 77°K is the common cooling medium for such detector. The detector is mounted in a vacuum chamber which is attached to or inserted into a liquid nitrogen dewar. The sensitive detector surfaces are thus protected from moisture and condensable contaminants.

The performances of an HPGe are usually specified in terms of energy resolution, relative efficiency, lower limit of detection (LLD), and peak-to-Compton ratio etc. The detector manufacturer commonly specify the energy resolutions of their germanium detectors in terms of full width at half maximum (FWHM) at the $1332\text{ keV }^{60}\text{Co}$ peak. The coaxial HPGe detector can be used in detecting the photon of energies between 50 keV and 10 MeV or more.

Advantages: The worldwide popularity of germanium as a semiconductor radiation detector is attributable to the excellent charge transport properties, which allows the use of large crystals without excessive carrier losses due to trapping or recombination. The greater efficiency, larger photofraction, and lower cost of sodium iodide may well tip the balance in its favour when only a few gamma-ray energies are involved. Germanium detectors are clearly preferred for the analysis of complex gamma-ray spectra involving many energies and peaks. It also aids in detection of weak sources of discrete energies when superimposed on a broad continuum. Germanium must always be operated at low temperatures (77°K) to reduce thermally generated leakage current. The reason behind the attractiveness of the semiconductor detectors lies in the improved energy resolution compared to scintillation detectors (NaI, CsI, ZnS, etc.) and in the increased stopping power of a solid material instead of a gas. In case of germanium, about 3 eV energy is needed for the production of one electron-hole pair, whereas 100 eV in a solid state scintillation detector and 34 eV in a gaseous ionization detector are needed to form an ion-pair. So the number of carriers produced for a given energy absorption is large in the case of semiconductor, and the statistical fluctuations in that number are small when expressed as a percentage of the total number^[124].

3.4 Equipment Setup

The present research was carried out by employing a survey meter- PDR 1SV (supplied by NE Technology Limited, England) for extensive field survey and an HPGe detector- Intrinsic Germanium p-Type Coaxial (supplied by SILENA Detektor Systeme GmbH, Germany) for measuring the radioactivity levels in soil and water samples collected from different locations in Bangladesh.

3.4.1 Portable Survey Meter PDR 1Sv

The Portable Dose Ratemeter type PDR 1Sv is a low gamma field survey meter with an internal Geiger. The PDR 1Sv displays dose equivalent in $\mu\text{Sv/h}$ on the basis that $1 \mu\text{Sv/h} = 100 \mu\text{R/h}$ over the range $0.05 \mu\text{Sv/h}$ to $100 \mu\text{Sv/h}$. The PDR 1Sv survey meter have a safety construction, easily carriable, and a little bit malleable. It has no remarkable sensitivity on temperature upto 45°C . It has an ability of measuring a dose range which is wide enough in respect to environmental world wide dose level. So, it is most suitable for extensive field survey in Bangladesh. The photograph and the block circuit diagram of PDR 1Sv survey meter is

shown in Figure 3.6 and Figure 3.4 respectively. Detail specification of the survey meter is given in Table 3.2 in the next page.

Table 3.2: Specification of PDR 1Sv Survey Meter^[125]:

Range	:	0.05 $\mu\text{Sv/h}$ to 100 $\mu\text{Sv/h}$, 3½ decades on a 70 mm scale
Doserate Accuracy (662 keV)	:	$\pm 20\%$ at 20 °C $\pm 20\%$ between -10 °C and +45 °C
Overload Protection	:	Indicates > full-scale deflection upto at least 10 Sv/h
Detector	:	Internal compensated GM tube
Energy response	:	$\pm 15\%$ from 40 keV to 6 MeV
Beta response	:	Indicates < 1% of doserate due to $^{90}\text{Sr}/^{90}\text{Y}$ (measured as absorbed doserate to air in air)
Neutron response	:	Indicates < 2% of neutron dose equivalent rate
Meter Response Time (time to reach 90% of a factor of 10 change in doserate)		
0.1 $\mu\text{Sv/h}$ to 1 $\mu\text{Sv/h}$:	30 s
1 $\mu\text{Sv/h}$ to 10 $\mu\text{Sv/h}$:	10 s
10 $\mu\text{Sv/h}$ to 100 $\mu\text{Sv/h}$:	5 s
100 $\mu\text{Sv/h}$ to 10 $\mu\text{Sv/h}$:	6 s
10 $\mu\text{Sv/h}$ to 1 $\mu\text{Sv/h}$:	12 s
1 $\mu\text{Sv/h}$ to 0.1 $\mu\text{Sv/h}$:	40 s
Batteries		
Type	:	Two IEC R20
Life	:	> 100 h (4 h continuous use every 24 h)
Control	:	A three position rotary switch OFF – BATT . CHECK – ON
Construction	:	The tough ABS white case and black moulded handle provide a light weight construction which is resistant to abrasion and easy to decontaminate and clean.
Temperature Range	:	- 10 °C to + 45 °C
Dimensions	:	Length 241 mm Width 120 mm Height 146 mm (including handle)
Weight	:	1.6 kg

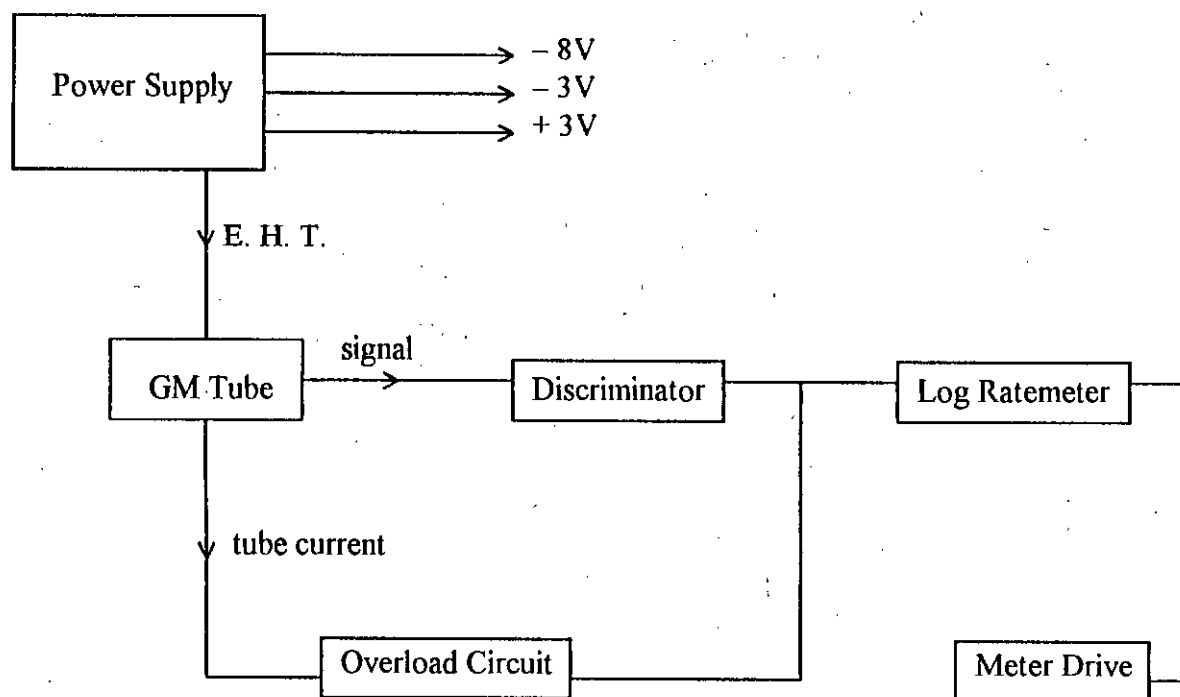


Figure 3.4: Block Diagram of Circuit Layout PDR 1Sv.

3.4.2 The High purity Germanium Detector ‘Silena’

The high purity germanium “closed-end-coaxial p-type dipstick” radiation detector ‘Silena’ was employed in the present research for measurement of γ -activity in soil and water samples collected from different locations in Bangladesh. The high resolution of the detector and its reliability alongwith a charge sensitive preamplifier, an amplifier, and a pulse height analyzer made it possible to use exclusively in the analysis of complex gamma-ray spectra. The main electric components associated with the counting system and HPGe detector coupled with the personal computer analyzer (PCA) consist of the following units: (i) liquid nitrogen dewar with cryostat, (ii) preamplifier, (iii) spectroscopy amplifier, (iv) high voltage detector power supply (5 kV), (v) PC based multichannel analyzer (MCA), and, (vi) shielding arrangement of the detector. A photographic profile of the HPGe detector and associated electronics is shown in the Figure 3.7, and a block diagram of the detection system is shown in the Figure 3.5. The detector was mounted in a common vacuum chamber attached to a liquid nitrogen dewar to protect the sensitive detector surface from moisture and condensable contaminants. The prevailing characteristics of the used ‘Silena’ HPGe detector are high atomic number, low impurity concentration i.e., large depletion depth, higher conductivity, compact in size, fast time

response, high resolution, and relative simplicity in operation at room temperature. A brief description of the equipment is given in the following sections.

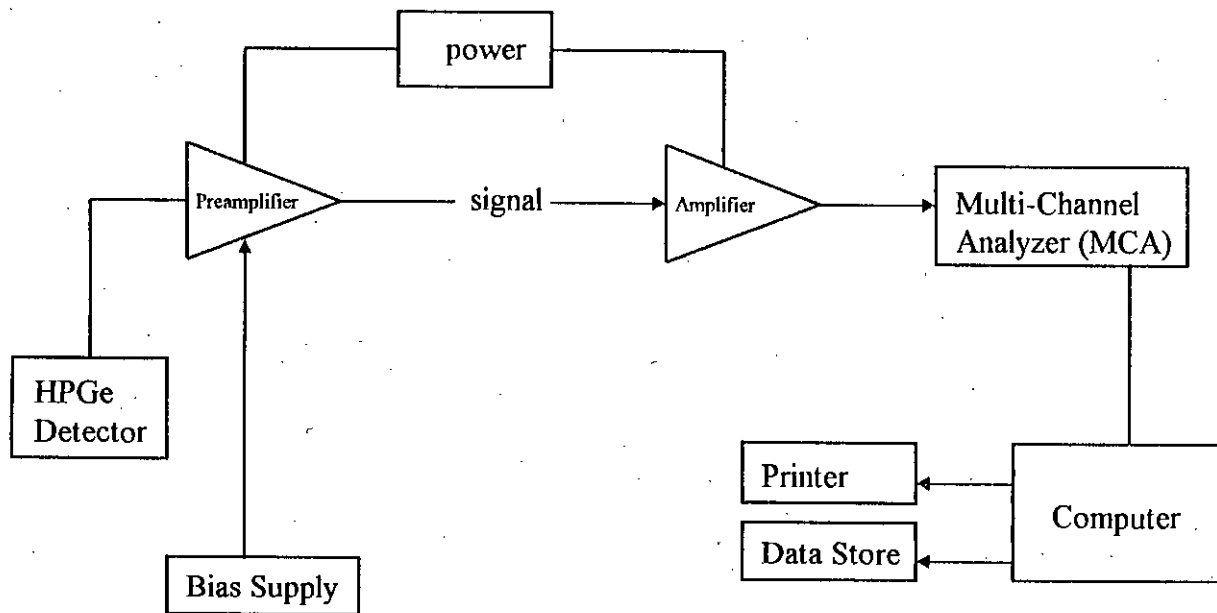


Figure 3.5: A Block Diagram of HPGe Detector System.

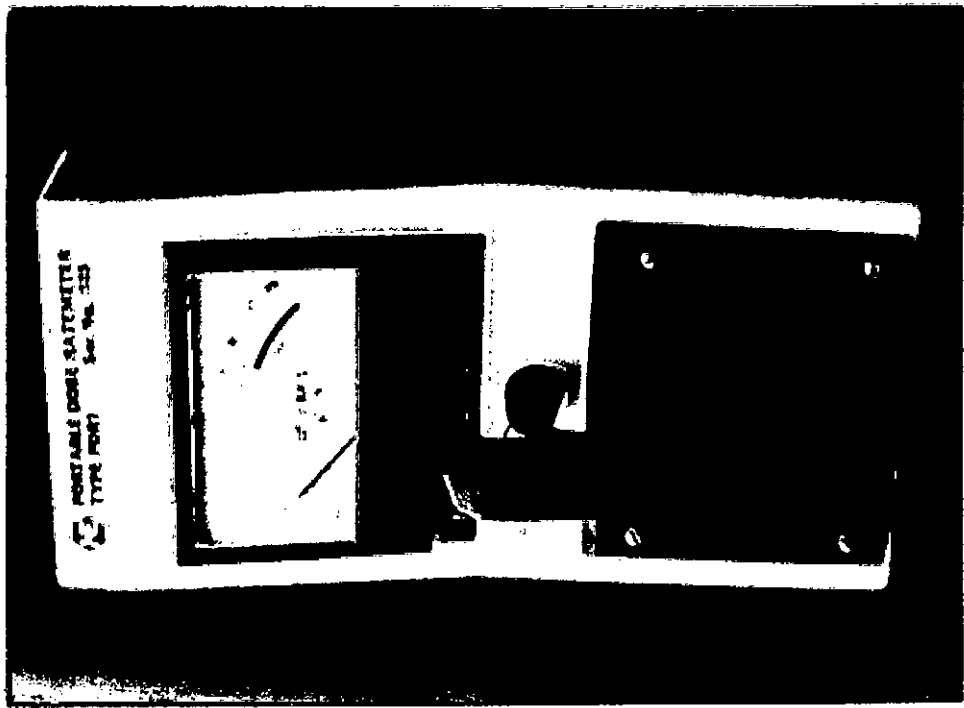


Figure 3.6: Photograph of PDR 1Sv Survey-meter.

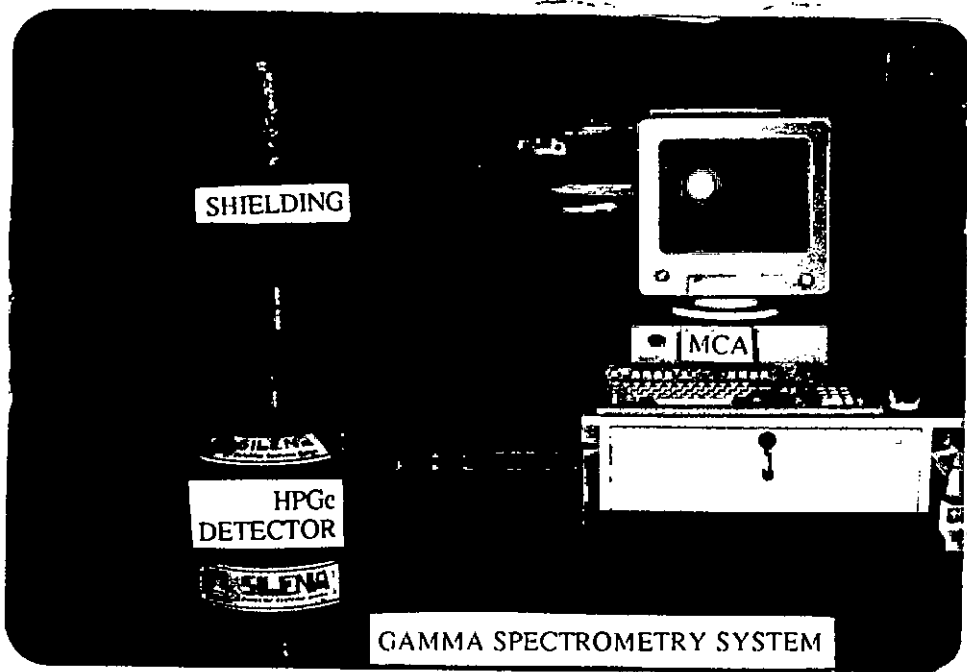


Figure 3.7: Photograph of Gamma Spectrometry System.

HPGe detector 'Silena' specification: The basic configuration of HPGe detector 'Silena' are given in the Table 3.3: below.

Table 3.3: Silena HPGe detector specification^[126].

Detector	:	High Purity Germanium (HPGe)
Characteristics	:	intrinsic p-type coaxial Ge crystal geometry
Crystal-		
	Diameter	: 5.49 cm
	Length	: 4.33 cm
	Volume	: 98 cm ³
Detector - window distance	:	0.5 cm
Face dead-layer thickness	:	0.05 cm
Core	:	0.9 cm
Liquid nitrogen dewar volume	:	30 litre, Silena
Preamplifier	:	Resistive feedback RFP 11
Operating ranges-		
	Operating bias	: + 2300 Volts DC
	Polarity	: Positive
	Shaping time	: 6 μ sec.
	Leakage current	: < 50 pA
	Testpoint	: - 0.70 Volts at operating bias
	Cooldown time	: 6 hours
Resolution FWHM for ⁶⁰ Co	:	1.70
Relative efficiency	:	18.8 %
Peak to Compton ratio	:	49 : 1

Liquid Nitrogen Dewar with Cryostat: In order to reduce the thermally generated charge carriers to an acceptable level, the detector must be cooled sufficiently. Otherwise, the noise due to leakage current would destroy the energy resolution of the detector. The liquid nitrogen which has a temperature 77°K, is the common cooling medium for the detector. The liquid nitrogen dewar serves as a reservoir of liquid nitrogen, while the cryostat provides a path via the copper stem for heat transfer from the detector to liquid nitrogen reservoir.

High Voltage Power Supply: Nucleus Model- ORTEC 495^[127]: Most radiation detectors produce electrical signals which must be processed to get meaningful information about the radiation being detected. For proper operation and optimum performance of most

radiation detectors, an external high voltage power supply is required. This voltage is called "detector bias" and high voltage power supply used for this purpose are often called detector bias supplies. This high voltage output is regulated and filtered and can be varied from 0V to 5000V by the front panel controls. This bias produces the maximum (and minimum) voltage level and its polarity. The maximum current available against long term drifts due to change in temperature or power line voltage and the degree of filtering provided to eliminate ripple at power line frequency or other low frequency noise. The high voltage polarity is manufacturer preset to be positive by switching the power switch polarity card which is located inside the instrument. The bias applied to the used HPGe detector in the present research was +2300 Volts. An LED on the front panel of the power supply unit serves as a monitor of the polarity that is being furnished.

Detector Preamplifier: Model- RFP 11¹¹²⁶¹: The preamplifier associated with radiation detectors performs three essential functions, viz.: (i) conversion of electric charges into voltage pulses, (ii) signal amplification, and, (iii) Pulse shaping.

Only two basic types of preamplifiers are used in HPGe detectors, viz.: (i) resistive feedback, and (ii) pulsed-optical feedback. In the present study, 'RFP 11' preamplifier which is charge sensitive that employed dynamic charge restoration (resistive feedback) for discharging the integrator. Absorption of photons by detector produce ionization within the detector and produces a current pulse at the preamplifier input. These pulses are too small to measure without amplification into a measurable electrical signal. Therefore, the first element in a signal processing chain is a preamplifier which provides an interference between the detector and pulse processing & analyzing electronics. It is directly coupled to the output of the detector. The preamplifier produces a voltage pulse $V(t)$ by passing the electrical charge $q(t)$ from the detector to the capacitor C , i.e.,

$$V(t) = \frac{q(t)}{C}$$

The basic function of this amplification stage is to provide a voltage pulse whose height must be proportional to the total charge collected. The rise time of this pulse must be equal to the charge collection time. The preamplifier was located as close as possible to the detector to minimize the signal from noise ratio and capacitive loading. It also serves as an impedance matcher, presenting a high impedance to detector to minimize loading, while providing a low

impedance output to drive succeeding components. It changes the shape of the detector signal to allow the circuits in the amplifier to operate properly and amplifies the detector signal to make the signal to cable noise ratio as high as possible when entering into the amplifier. It is designed primarily for high resolution gamma-spectroscopy using cooled Ge(Li) detectors. Now-a-days it is widely used within the HPGe detector assembly.

Spectroscopy Amplifier: Nucleus Model- ORTEC 570^[128]: The spectroscopy amplifier is a key unit in the gamma-ray spectrometer. The function of the amplifier is to further amplify the signal from the preamplifier and change its shape and size. The purpose of this additional amplification and shaping is two-fold: First, further amplification improves the signal-to-cable noise ratio. Second, further shaping acts to prevent pulse pile up. Since pulses from the radiation detector occur randomly, one pulse from the detector may begin before the preceding detector pulse has terminated. A good amplifier should have low input noise and high amplification or gain factor. For the present work, "ORTEC 570" spectroscopy amplifier was used which has all the characteristics necessary to make itself useful in present HPGe detector.

The ORTEC 570 spectroscopy amplifier is a single width NIM module that features a versatile combination of switch-selectable pulse shaping characteristics. The amplifier has extremely low noise, a wide gain range, and excellent overload response for universal application in high resolution spectroscopy. The 570 has an input impedance of approximately 1000 Ω and accepts either positive or negative input pulses with rise times < 650 ns and fall times > 40 μ s. The output is unipolar and is used for spectroscopy systems where DC coupling can be maintained from the 570 to the analyzer. The 570 can be used for constant fraction timing when operated in conjunction with an OTREC 551, 552, or 553 Timing Single-Channel Analyzer. The 570 has complete provisions, including power distribution for operating any ORTEC solid state preamplifier.

Multichannel Analyzer (MCA): EMCAPLUS EMULSION Software^[129]: A computerized multichannel pulse height analyzer is used to measure rapidly the spectrum of pulse heights emerging from the spectroscopy amplifier. It is capable of analyzing pulses simultaneously within many different intervals or channels. In fact, MCAs are the heart of most modern gamma- spectrometry arrangements. It performs the essential functions of collecting the

data providing a visual monitor and producing output either in the form of final results or as raw data for further analysis.

The MCA consists of an analog-to-digital converter (ADC), MCA buffer, and a display. The main component of the MCA is an ADC which converts the incoming analog amplifier signal to a group of standard-shaped pulses. The pulses are digitized by a 'Wilkinson' type ADC and the output is stored in a memory like a computer. The channel number is the memory address and is proportional to the input signal voltage. Therefore, pulses of constant amplitude is always stored in a single channel. Each pulse is digitized and the count is added to the appropriate memory location. So the ADC is the key element in determining the performance characteristics of the analyzer. All MCA buffers include a microprocessor and a memory. The MCA buffer microprocessor normally supports data acquisition and input-output (I/O) functions including display controlled via the host computer. The standard software includes the MCA emulsion programme enabling control of MCA and traditional operations like display, I/O, overlap, smooth, strip, transfer, energy calibration, ROI, and peak information like centroid, FWHM, gross and net area with ROI, optionally available are peak search, nuclide identification, etc.

A printer was coupled with the PC based MCA. The necessary print out of data and graphics could be taken from it.

3.4.2.1 Shielding Arrangement of the Detector: Shielding of the detector from the environmental radiations is the utmost requirement in low level radioactivity measurement, but it is also advantageous and recommended for other measurements. The shielding not only reduces the background resulting from cosmic radiation and from natural radionuclides in the building materials or in the surface of the earth, but also from nearby nuclear facilities and other radiation sources like the ambient air, which presumably contains trace of radioactive gases, radon ^{222}Rn and thoron ^{220}Th etc.

Because of high density (11.4 gm/cm^3) and large atomic number ($Z=82$) and comparatively low cost, lead is the most widely used material for construction of shields. High energetic gamma-rays from external sources such as 1.46 MeV from ^{40}K can be absorbed efficiently by lead. Moreover, it is reasonably effective for removing many of the cosmic ray components of the background radiation. X-ray photons, generated by interaction(s) of cosmic and natural gamma radiation with the shielding assembly are relatively energetic and penetrate a

significant thickness of intervening materials are shielded by covering the lead shielding by steel sheet and copper sheet which has much lower atomic numbers compared to that of lead. Further for avoiding the effect of scattered radiation, the distance between the detector and shielding arrangement was made sufficiently large. In the present experiment, the shielding arrangement was made by using lead, copper, and steel materials.

For a good geometry condition, the shielding effectiveness of a material is expressed as:

$$I = I_0 e^{-\mu t}$$

Where, I is the beam intensity after penetrating a thickness ' t ' of the material, μ is the linear attenuation coefficient of absorbing material (depends on the atomic number of the material). Alternatively, μ can be replaced by μ/ρ and t by $t.\rho$ where μ/ρ is called the mass attenuation coefficient and $t.\rho$ is the mass per unit area. Thus the reduction of initial gamma flux can be calculated as^[130]:

$$\frac{I_0 - I_0 e^{-\mu t}}{I_0} \times 100$$

This equation was used for the verification of effectiveness of shield. Theoretically, the shielding arrangement found to attenuate 95% – 99.99% of unwanted gamma flux of energy ranging from 303 keV to 1332 keV. The shielding effectiveness in reducing the interfering background radiation was experimentally verified, where most of the gamma lines from background radiation (thorium, uranium and actinium series) were found to decrease by 74% – 96%.

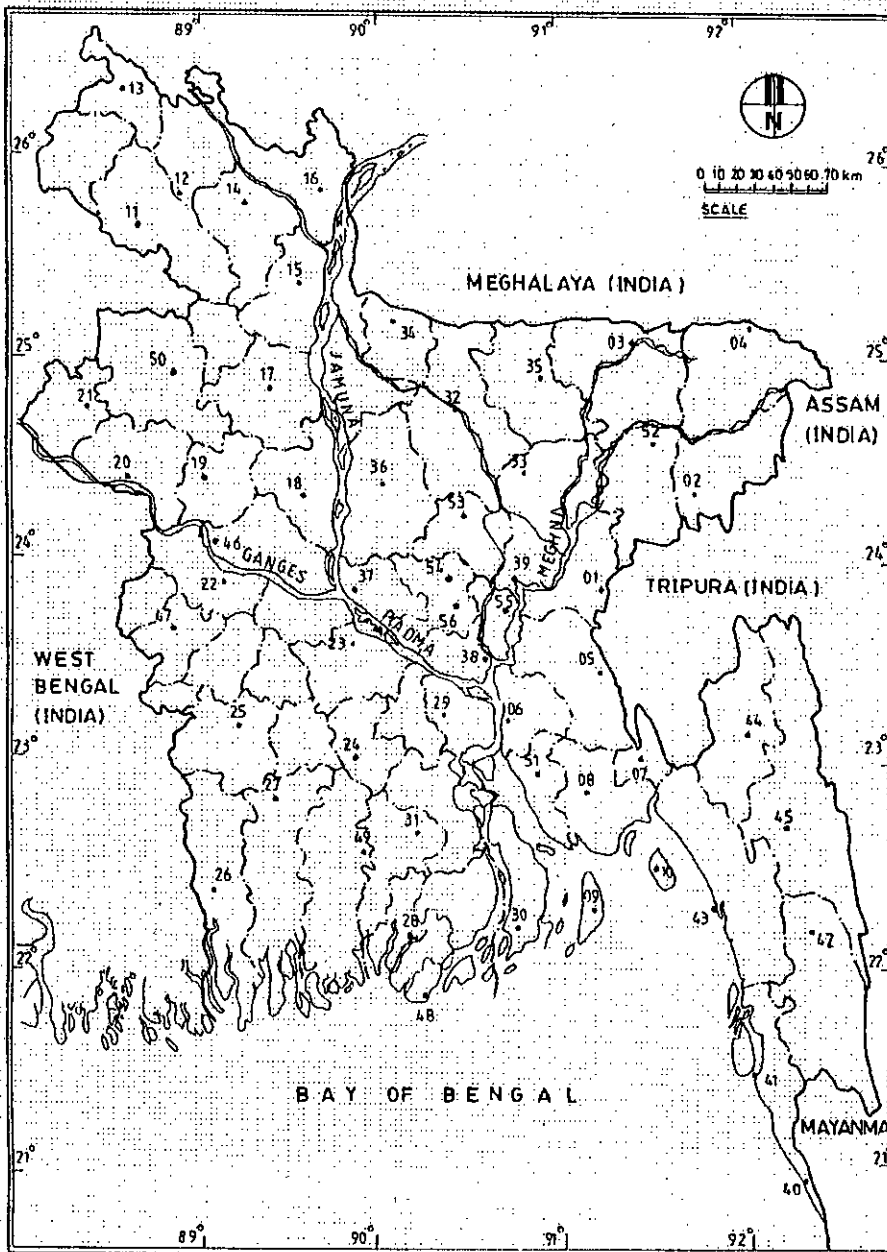
The summary of the experimental HPGe detector set up and equipment is given in the Table 3.4 in the next page.

Table 3.4: Summary of the Experimental HPGe Detector Set-up and Equipment.

Detector	HPGe	: Closed and coaxial p-type
	Bias	: + 2300 Volts
	FWHM	: 1.70 keV (at 1332 keV ⁶⁰ Co γ -ray)
	Crystal type	: Vertical dipstick
	Polarity	: Positive
High voltage supply		: Nucleus model – 495
	Typical efficiency	: 70%
	Noise and ripple	: Less than 15 mV peak-to-peak, 20 MHz bandwidth
	Operating temperature range	: 0 to 60 °C (32 to 140 °F)
Preamplifier	DC coupled, resistive feedback type	: Model RFP 11, charge sensitive
Amplifier	Spectroscopy amplifier	: Nucleus model – 570
	Noise	: < 8 μ V referred to the input using 2 μ s shaping and gain \geq 100.
	Temperature stability	: Gain, \leq 0.0075 % / °C, 0 to 50 °C. Level < \pm 50 μ V / °C, 0 to 50 °C.
Low- background shielding	Lead, Copper and Steel	: Cylindrical shape
Multichannel Analyzer	Emcaplus MCA emulsion software	: 4096 channels.

3.5 Experimental Details

In order to assess the environmental radioactivity level and radiation dose level in Bangladesh, 56 dose measuring and sample collecting spot as shown in Figure 3.8, was selected all over Bangladesh by considering the population density, area, and the communication system(s). These 56 locations covered the entire geographical area of Bangladesh. In each of the spot, indoor-outdoor radiation dose level was measured by a portable survey meter PDR 1Sv. Further, from each of the survey stations, undisturbed soil and community-based drinking water samples were collected for radioactive assessment. In addition to 56 stations, radiation dose levels were measured at few other places. The radiation dose level at sea-beaches of Bangladesh were also measured and the sand samples from Cox's Bazar sea beach and Kuakata sea beach were also collected for radioactive evaluation. All of the field works were performed during the period January 1998 – June 1998.



- 01 Akhaura (Brahminbaria)
- 02 Srimangal (Maulavibazar)
- 03 Sunamgonj
- 04 Jafiong (Goainghat, Sylhet)
- 05 Comilla
- 06 Chandpur
- 07 Feni
- 08 Noakhali
- 09 Hatiya (Noakhali)
- 10 Sandweep (Chittagong)
- 11 Dinajpur
- 12 Syedpur (Nilphamari)
- 13 Panchagarh
- 14 Rangpur
- 15 Gaibandha
- 16 Kurigram
- 17 Bogra
- 18 Ullapara (Sirajgonj)
- 19 Natore
- 20 Rajshahi
- 21 Nachole (Chapai Nawabgonj)
- 22 Kushtia
- 23 Faridpur
- 24 Gopalganj
- 25 Jessore
- 26 Shyamnagar (satkhira)
- 27 Khulna
- 28 Borguna
- 29 Shariatpur
- 30 Chorfashion (Bhola)
- 31 Barisal
- 32 Mymensingh
- 33 Kishoregonj
- 34 Jhenagati (Sherpur)
- 35 Barhalta (Netrakona)
- 36 Kalihati (Tangail)
- 37 Aricha (Shibalaya, Manikgonj)
- 38 Munsigonj
- 39 Narsingdi
- 40 Teknaf (Cox's Bazar)
- 41 Cox's Bazar
- 42 Roangchheri (Bandarban)
- 43 Chittagong
- 44 Khagrachheri
- 45 Rangamati
- 46 Roop Pur (Ishwardi, Pabna)
- 47 Chuadanga
- 48 Kuakata (Khepupara, Potuakhali)
- 49 Pirojpur
- 50 Badalgachhi (Naogaon)
- 51 Lakshimpur
- 52 Nabigonj (Habigonj)
- 53 Sripur (Gazipur)
- 54 Ashulia (Savar, Dhaka)
- 55 Sonargaon (Narayangonj)
- 56 BUET (Dhaka)

Figure 3.8: Map of Bangladesh Showing the Locations of Dose Measurement and Sample Collection

3.5.1 Measurement of Dose Levels

Radiation dose levels in 56 stations covering entire area of Bangladesh were measured by a low level portable radiation dose rate survey meter 'PDR 1Sv'. Details of this survey meter is described earlier. In each of the dose measuring stations, indoor-outdoor radiation dose level was monitored. The radiation dose levels within the kutcha-houses, pucca(building)-houses, and old-buildings (where available) were measured. The dose level at outdoor viz.- front & back yard of homes from the houses of which dose level was monitored, free space, play ground, road (kutcha & pucca), bus stand, and market place; was also measured many times at each of the dose measuring stations. In each time of dose measurement, survey meter was checked up and placed on the ground by a piece of paper (to save the survey meter from dirty ground surface) at first. The survey meter switch was then made 'ON'. One minute was allowed to reach the survey meter voltage in plateau region of the internal Geiger tube (of the survey meter). Then, the dose level for at least two minutes was observed in the display-scale of the PDR 1Sv. For each of the measurement within the mentioned time span, the minimum dose level, the maximum dose level, and the trend (average) dose level were noted down. After recording these information, the dose level at one metre above the ground (gonad level) was measured by the same method and for about the same time span. In each of the spot, several pairs of readings were taken from each variety of dose measuring surrounding-place i.e., kutcha-house, pucca-house, old-building, and free-space by considering the "time occupancy factor"^[84] and "behaviour factor"^[96]. In UNSCEAR-1988^[4] report, the time occupancy factor is 20% outdoors and 80% indoors for daily activities. Since most of the people of Bangladesh are peasants, day-labourers, and work at outdoors, this time occupancy factor was changed for the present study to 33.33% outdoors and 66.67% indoors. In each of the 56 sampling stations, radiation dose level was measured in at least 6 kutcha houses, 5 new buildings (buildings which were built after 1975), and 3 old buildings (the buildings which were built before 1947) (if available), by random sampling method with the cooperation of local public (it is somewhat difficult to measure indoor dose level in Bangladeshi dwellings due to religious-social reality). Since most of the peoples of Bangladesh live in kutcha-houses and houses like that in slum, emphasize was given in taking readings from kutcha-houses and from free space in each of the dose measuring location. In addition to the 56 spot from where soil and water samples were further collected for radioassay, several sets of readings were also taken from different places where the congenial atmosphere was found for dose measurement during the research trip, e.g., at launch ghat, ferry ghat, bus terminal, bus

stopper, and at different places of staying stations. The average $\pm 1\sigma$ (standard deviation) of minimum, maximum, and trend value of each category of data were calculated and noted separately. The PDR 1Sv survey meter used in this research, was calibrated routinely at the Secondary Standard Dosimetry Laboratory (SSDL) of Radiation Control and Waste Management Division (RCWMD), Institute of Nuclear Science and Technology (INST), Atomic Energy Research Establishment (AERE), Bangladesh Atomic Energy Commission (BAEC), Ganakbari, Saver, Dhaka.

3.5.2 Sample Collection

From each of the pre-selected 56 sampling stations, soil and drinking water samples were collected. In each of the spot, $\sim 1\frac{1}{2}$ kg of soil sample from an area of 20 cm \times 20 cm and upto a depth of ~ 3 cm from the surface, of undisturbed land (the land which is kept naturally i.e., the land which was not ploughed, cultivated, digged, fertilized, or filled-up during the last 20 years period, ignoring the natural flow/drainage of rain water and normal land erosion; so that the land may be considered as the representative land of the sampling station). The soil samples were packaged in polythene bags tightly in such a way that no fraction of the collected soil can normally escape the polythene bag. Individual identification marks were given on each of the soil sample packets by marker pens. Drinking water samples were also collected from each of the sampling stations. In each of the spot, a community-tubewell or any other community based water supply system like municipality water supply, was selected from where most of the people faces the need for drinking water. In the spot Jaflong (Sylhet) where many of the people uses the Jaflong-river water, two samples were collected; one from a tubewell and the other from Jaflong-river. In Rangamati town and in the residential areas nearby and upward the Kaptai lake, most of the people use lake-water as drinking water. Consequently, the water from the Kaptai lake nearby Rangamati town was collected as it represents the drinking water of Rangamati's people. In all cases, 1.02 litre of water was collected and packed within plastic bottles air-tightly to avoid any leakage and spillage. An individual identification mark was given on each of the water sample bottle by non-erasable markers. In addition to 56 sampling spot, sand samples were also collected from Cox's Bazar sea beach and Kuakata sea beach points where the dose levels were exactly highest for individual beaches as measured instantaneously on specific point by PDR 1Sv.

3.5.3 Sample Preparation

The soil samples were crushed to powder individually and then sieved by a 1.0 mm sieve. All of the samples were in dry condition as these were collected during the dry season. Then 1 kg of pure soil from each of the crushed and sieved sample were measured individually by a sensitive balance. The powdered 1 kg samples were then poured into marinelli beakers carefully and sealed air-tightly. Water samples were measured by measuring flask and 1 litre of water from each of the collected sample were poured into the marinelli beakers and sealed air-tightly. The sealed soil and water samples were allowed to attain the radioactive secular equilibrium between the gaseous (^{222}Rn and ^{220}Rn) and non-gaseous radioactive decay products (of the natural radioactive serieses) with their respective parents and daughters by preserving them in an air-tight condition individually for 28 days. All sample preparation was done and HPGe detector reading out was taken in the Health Physics laboratory of RCWMD, INST, AERE, BAEC, Ganakbari, Savar, Dhaka.

3.5.4 Sample Readout

After establishment of the secular equilibrium and after completion of necessary quality assurance of the HPGe detector 'Silena', the samples were read out. The experimental procedure followed to perform measurements on each of the samples is as follows.

The liquid nitrogen dewar of the HPGe detector was filled with liquid nitrogen at least 6 hours before the measurements were started. This allowed the sufficient time for cooling of the detector. Before the first measurement of each day, the detector system was turned ON and a 15 minute warm-up period was allowed. The high voltage bias supply to the detector was gradually raised to the operating voltage (+2300 Volt.), the amplifier coarse gain, fine gain, and peak shaping time was also adjusted to the desired values. The counting time in the MCA was adjusted to 10,000 second to obtain a reasonable counting reliability. After all these settings had done, a period of about half an hour was allowed for the stabilization of the system. Then the energy calibration of the detector was checked by placing successively a ^{137}Cs point source and a ^{60}Co point source at the detector axis with a source-to-detector distance of ~10 cm for a few minutes and was found that 661.66 keV peak, 1332 keV peak, and 1170 keV peak appeared in the appropriate channels. Then a background spectrum was obtained by placing an empty marinelli beaker at the top of the well-shielded detector head for 10,000 sec. After completion of taking background reading, each of the sample-filled marinelli beakers were placed on the top of

the detector head and then the sample entrance door of shielding arrangement was closed. The samples were read out for 10,000 sec and the spectrum were preserved in floppy and hard disk of interfaced computer. When the samples read out time was elapsed, an analysis of the spectrum was printed by the printer interfaced with the computer. The analysis contained the energy and corresponding counts per second of emitted gamma photons including the statistical error, FWHM, etc. In the present study, the counts per second corresponding to the energies of the emitted photons 238.63 keV, 583.19 KeV, and, 911.07 keV of the radionuclides ^{212}Pb (44.60%), ^{208}Tl (85.77%), and, ^{228}Ac (27.70%) respectively within the decay chain of ^{232}Th ; the counts per second corresponding to the energies of the emitted photons 351.92 keV, 609.31 keV, and, 1120.29 keV of the radionuclides ^{214}Pb (38.90%), ^{214}Bi (43.30%), and ^{214}Bi (15.70%) respectively within the decay chain of ^{238}U ; counts per second corresponding to the energy of 1460.75 keV emitted from ^{40}K (10.70%); and counts per second corresponding to the energy 661.66 keV emitted from ^{137}Cs (85.21%) were considered. Then by different calculations, the activity of the radionuclides ^{212}Pb , ^{208}Tl , ^{228}Ac , ^{214}Pb , ^{214}Bi , ^{40}K , and, ^{137}Cs ; and ultimately, the activities of ^{232}Th , ^{238}U , ^{40}K , and ^{137}Cs in each of the soil and water sample were evaluated. The ^{232}Th activity was found by averaging the activity of ^{212}Pb , $3 \times$ activity of ^{208}Tl , and, the activity of ^{228}Ac . The activity of ^{238}U in each sample was found out by averaging the activity of ^{214}Pb , the activity of ^{214}Bi calculated from 609.31 keV, and the activity of ^{214}Bi calculated from 1120.29 keV. The activities of ^{40}K and ^{137}Cs were obtained by direct measurement from single channel energy counts. The specific activities of the individual samples for specific radionuclide were then calculated by employing the equation given in section 3.5.5.

Before and after a set of readout of samples, background reading of the detector was taken by placing an empty marinelli beaker^[131] on the detector head as described earlier for the same time period as that for soil and water samples. The mean background reading from a set of measurement was subtracted from each of the sample reading.

Before and within the read out procedure, a number of operations of HPGe detector had to be done. These are: (i) energy calibration, (ii) energy resolution, (iii) efficiency calibration, and, (iv) finding of lower limit of detection for each of the detecting radionuclides. During the readout period, the dewar was filled by liquid nitrogen weekly.

Energy Calibration of HPGe Detector: An essential requirement for the measurement of gamma-rays is the exact identification of photopeaks present in a spectrum produced by the detector system for a sample. In gamma-ray spectrometry, the spectrum accumulated on the MCA provide data on both count rate and the location of each peak depending on gamma energy. For identifying the radionuclides and their activity in the samples, it is necessary to calibrate the observed gamma energy spectrum against the channel number of MCA. The displayed spectrum from an HPGe detector is usually a series of photopeaks superimposed on a more or less varying background. The peak location indicate gamma-ray energy. The value of the base line, i.e., channel number has no real significance until it is calibrated proportionally to read in terms of energy. In case of an HPGe detector, the relation between gamma-ray energy and output pulse height is approximately linear. Therefore, two or more peaks of sufficiently different energy will serve to establish the energy calibration. If E_1 and E_2 are the known energies of two peaks then S_1 and S_2 are the respective peak locations, as measured in the pulse height spectrum. Thus, energy for any channel number S can be calculated by:

$$E = cS + b$$

$$c = \frac{E_2 - E_1}{S_2 - S_1}$$

$$b = E_1 - cS_1$$

$$\text{Thus, } S = \frac{E - b}{c}$$

where, b & c are constants. The calibration of MCA should be done by employing good geometry point sources of known radionuclides with well-defined energies within the energy range of interest, usually 60 keV to 2 MeV^[33].

In the present study, calibration of the MCA was carried out by using good geometry point sources placed close to the detector inside the shield. The gamma spectra obtained on the PCA monitor after the equipment set up of live time, high voltage power supply, amplification gain, lower level discriminator, adjustment of spectroscopy amplifier such as course gain, fine gain, and, shaping time. The energies of gamma photons emitted from these point sources are known and the position of full energy peaks (FEP) on the baseline of the spectrum in the MCA were adjusted to suitable channel numbers by entering the energies of the calibration sources in keV into the MCA to convert all 4096 channels to respective energies.

Energy Resolution of HPGe detector: The resolving power of a detector is called the energy resolution of the detector to separate two adjacent peaks in a gamma-ray spectrum. In general, the resolution is a measure of the detector's ability to distinguish between two closely spaced gamma energy peaks in a gamma-ray spectrum. The resolution of a coaxial detector is given for 1.33 MeV ^{60}Co line and is defined as the Full Width at Half Maximum (FWHM) of the full energy peak and expressed in keV. The factors that influence the resolving power of the detector are^[123]: (i) statistics of charge creation process, (ii) properties particular to the individual detector, (iii) completeness of charge collection process, and, (iv) electronic noise. The width of the differential pulse height distribution of a detector with poor resolution is much larger than that of a detector with good resolution. Resolution is calculated as:

$$\text{Resolution} = \frac{E_2 - E_1}{S_2 - S_1} \times \Delta S$$

where, $(E_2 - E_1)$ is the energy difference between 1332 keV and 1173 keV lines, $(S_2 - S_1)$ is the channel difference of the two photo peaks, and, ΔS is the number of channel under FWHM in the 1332 peak, of ^{60}Co source.

In the present study, the energy resolution of the detector was obtained for different radionuclides. The detector resolution (FWHM) obtained in this research to be 1.82 keV for the 1332 keV of ^{60}Co source.

Efficiency Calibration of HPGe Detector: The most important parameters that characterizing a radiation detector are: efficiency and energy resolution. The efficiency calibration should be performed with great care because the accuracy of experimental results depends on it. Efficiency changes with physical changes of counting system and the environment surrounding to it. For low level activity of environmental samples, it is desirable to increase the efficiency as much as possible to increase the minimum level of detection.

The efficiency of a detector is a measure of the number of gamma-rays detected out of a total number of gamma-rays that are actually emitted by the source. The full energy peak (FEP) efficiency is defined as:

$$\varepsilon(E) = \frac{N(E)}{R(E)}$$

where, $N(E)$ = Count rate (total number of counts in the peak divided by the measuring time) in the peak corresponding to the energy E and $R(E)$ = Rate at which photon of energy E are emitted from the source (i.e., activity).

This efficiency is related to a specific source-detector geometry and particular peak analysis procedure. It varies with the detector size and types of counting geometry, height and weight of the standard sample and the environment surrounding the detector system^[123]. The counting efficiencies are measured with standard or reference samples in which the activities of radionuclides are exactly known. Sometimes it may not be possible to obtain all the desired samples. In such a situation, the best way is to plot an efficiency calibration curve from the available standard sources and extrapolate the curve.

There are three types of efficiencies, viz., - (i) intrinsic photopeak efficiency, (ii) absolute efficiency, and, (iii) relative efficiency. The intrinsic photopeak efficiency is defined as the fraction of mono-energetic gamma-rays which on striking the detector will produce counts in the corresponding photopeak. This efficiency can be obtained by using the following expression:

$$\epsilon_p = 1 - e^{-\mu t}$$

where, ϵ_p is the photopeak efficiency, μ is the linear attenuation coefficient of the detector material at energy of interest, and t is the thickness of the detector. The absolute (or total) efficiency ϵ_t of a counting system is the probability that a gamma-ray emitted from a point source at a particular source-to-detector distance will produce a count in the corresponding photopeak.

$$\epsilon_t = \frac{\text{photopeak count rate}}{\text{gamma - ray emission rate}}$$

The absolute efficiency is the product of the probability that a gamma-ray will strike the detector and the probability that it will interact and will produce an event in the photopeak. In general, it depends on the source to detector distance. The above equation can therefore be restated as:

$$\epsilon_t = \epsilon_g \cdot \epsilon_p$$

where, ϵ_g is the probability of gamma-ray striking the detector of area A positioned at a distance r from a point gamma source i.e., geometric efficiency. The absolute efficiency can be re-expressed as:

$$\epsilon_t = \frac{A \cdot \epsilon_p}{4\pi r^2}$$

In general, the absolute efficiency or simply the efficiency is expressed as follows:

$$\text{Efficiency } \varepsilon(E) = \frac{CPS}{DPS \times I_\gamma}$$

where, I_γ is the γ -ray intensity of the source at a specific energy, CPS is the observed counts per second at the particular energy of interest, and, DPS is the disintegration per second (activity) of the radionuclide. A generally accepted and simple expression for efficiency determination is as follows^[33].

$$\ln \varepsilon = a_1 + a_2 \ln E$$

where, \ln is the natural logarithm, ε is the absolute full energy peak (FEP) efficiency, a_1 & a_2 are fit parameters, and E is the energy (keV) of corresponding gamma line. This expression is adequate for determining efficiency of gamma energies from 100 keV to 2 MeV. The relative efficiency of a detector is the ratio of the absolute efficiency of the that detector for counting the 1332 keV gamma-rays from the ^{60}Co source at 25 cm distance to the absolute efficiency of a standard 3" \times 3" NaI(Tl) crystal for the same source at the same source to detector distance.

$$\text{The Relative Efficiency of an HPGe Detector} = \frac{R_1}{R_2} \times 100\%$$

where R_1 is the count rate in Bq in the 1.33 MeV photopeak for HPGe, and, R_2 is the product of gamma activity of the source in Bq and efficiency of the standard NaI detector (i.e., 1.2×10^{-3}).

Measurements of environmental radioactivity usually involves a large volume of sample. When a large volume of sample is used for the radioactivity measurement, self absorption and counting geometry are of major importance in data processing. So it is necessary to choose a detector-to-sample geometry to maximize the counting efficiency and to minimize the self absorption for that specific geometry. Hence, for a large volume of sample (soil or water) analysis, the marinelli beaker is preferred. This design should be nearly optimum in terms of placing the sample materials as close as possible to the detector active volume. In the present study, the efficiencies of the detector for evaluating soil and water sample for marinelli beaker geometry were obtained.

In the present study, the absolute and relative efficiency of the used HPGe detector were found out. Using ^{60}Co standard point source, the relative efficiency of the detector was found to be 18%. In determining the efficiencies for measuring soil samples, 1 kg fresh soil in a marinelli beaker was read-out for 10,000 sec by the HPGe detector (background plus soil reading). Then

400 Bq of ^{226}Ra liquid source was well-amalgamated with the soil (1 kg) just measured and then read-out for 10,000 sec in the same geometry and other operating conditions. The “background plus soil readings” were subtracted from the “ ^{226}Ra plus soil plus background readings”, and the net counts were noted. The efficiencies at different energies were then calculated by using formula described earlier. A graph (Figure 4.1) was then plotted with energy (keV) as abscissa and corresponding efficiency (%) as ordinate. A smooth trend line of the plotted points was drawn using “Excel-97” computer software and the efficiencies at energies of interest were found out and recorded which are shown in Table 4.1. The efficiencies for assessment of water samples were made by the same procedure that for soil samples except the activity of solute (^{226}Ra) which was 100 Bq. A graph (Figure 4.2) was also drawn by the same method and aid and the efficiencies at energies of interest were found out and recorded which are shown in Table 4.1.

Lower Limit of Detection of Radionuclides: The detection limit, as it is known as the minimum detectable emission rate or lower limit of detection (LLD), is a term used to express the detection ability of a measurement system under certain conditions. The limit depends^[33] on the sample geometry, the energy of radiation, the source-to-detector distance, the detector efficiency, the background, the available time for measurements, and the quantity of samples (mass and volume). In order to obtain lower detection limits, the efficiency of the detector should be high, the sample should be as large as practicable, the counting time should be as long as practicable and the background should be as low as attainable. Pasternack^[132] et al defined LLD as:

$$LLD = 1.645 \cdot (2\sqrt{2}) \cdot S_b$$

where, S_b is the standard deviation of background count. A generally accepted expression for the estimation of LLD can be expressed as^[33]:

$$LLD = \frac{4.66 \cdot S_b}{\epsilon \cdot I_\gamma}$$

where, S_b is the estimated standard error of the net count rate, ϵ is the counting efficiency at the desired energy of the nuclides, and I_γ is the absolute transition probability by γ -decay through the selected energy as for ϵ . When a sample is introduced into the gamma measurement(s), the term usually associated with detection limits is the minimum detectable concentration (MDC) which is expressed by:

$$MDC = \frac{4.66 \cdot S_b}{\epsilon \cdot I_\gamma \cdot W}$$

where, W is the mass of the sample (kg).

3.5.5 Radioactivity Calculation

After completion of necessary pre-measurements of HPGe detector, the radioactive evaluation of processed and sampled soil and water samples were done. At first, an empty marinelli beaker was placed on the top of the detector head and counted for 10,000 seconds to obtain background counts. Then the sealed 1 kg soil samples and 1 litre water samples were counted for the same period one by one. The background count was subtracted from the gross spectrum obtained with the sample. In each day of measurement, background reading was taken, and the other parameters of the detector such as energy calibration and efficiency were checked occasionally.

The most gamma energy peaks at 238.63 keV, 351.92 keV, 583.19 keV, 609.31 keV, 911.07 keV, 1120.29 keV, and 1460.75 keV were clearly identified for soil and water samples. For most of the soil samples and few of the water samples, a gamma energy peak at 661.66 keV were also identified. These energy peaks were used for the estimation of the corresponding radionuclides. After determination of the integral counts under the gamma energy peaks of interest, the gamma activity was calculated according to the equations^[33].

$$A = \frac{C}{\epsilon(E) \times I_\gamma \times W} \quad \text{- for measuring soil samples}$$

$$\text{and, } A = \frac{C}{\epsilon(E) \times I_\gamma \times V} \quad \text{- for measuring water samples}$$

where, A is the activity of the sample in Bq.kg⁻¹ (for soil samples) or Bq.l⁻¹ (for water samples), C is the peak area counts in CPS, $\epsilon(E)$ is the efficiency of the detector at energy E (keV), I_γ is the photon emission probability at energy E (keV), W is the mass of the solid (soil) samples in kg, and V is the volume of liquid (water) samples in litre.

3.5.6 Radiation Dose Due to Radioactivity in Soil and Cosmic Radiation

The radiation dose due to radioactivity in soil i.e., terrestrial radiation dose in different locations of Bangladesh were estimated by using computer software "RESRAD & GENII". Some parameters such as the individual activities of the radionuclides, the area of sample collection etc. for each sample were entered into the computer in the definite way and the

corresponding resulting radiation dose was found from the computer. The cosmic radiation dose at each location was estimated by subtracting the terrestrial radiation dose from the average outdoor dose level at that location.

3.5.7 Radiation Dose Due to Intake of Water

The effective dose equivalents due to intake of radionuclides through water for each of the sampling location were calculated by using the conversion factors given in Table 3.5. The detailed of the results are shown in Table 4.7 and in Table 4.8.

Table 3.5: Dose Conversion Factors for Ingestion of Radionuclides^[133].

SL. No.	Radionuclide	Conversion Factor (Sv/Bq)
1	²³⁸ U	4.4×10^{-8}
2	²³² Th	9.2×10^{-8}
3	⁴⁰ K	6.2×10^{-9}
4	¹³⁷ Cs	1.3×10^{-8}

3.5.8 Determination of Annual Collective Dose Equivalent

Annual collective dose equivalent for an area is the product of annual effective dose equivalent (in Sv) and the total population of that area. It shows the total amount of radiation dose received by a population and consequently it is a measure of burden of that population group. Its unit is person-Sievert. In the present study, the annual collective dose equivalents for different locations of Bangladesh were determined which are shown in Table 4.12. The areas (in sq. km) covering the corresponding locations and population in 1998 in individual areas estimated from "Statistical Pocket Book of Bangladesh 1997"^[134] are also shown in Table 4.12 alongwith the annual effective dose equivalent and annual collective dose equivalent.

3.6 Statistical Errors in Counting

The disintegration of radionuclide is a statistical phenomenon. Nuclei undergoing radioactive transformation in a sample is a random event. Radioactive decay is random in time and so the number of particles or photons counted in a given time by a detector will fluctuate about an average value. The standard deviation ' σ ' is a measure of the scatter of a set of observations about their average value. The most common method of analyzing gamma-ray spectrum of radioactive samples containing a mixture of nuclides is to use the full energy peak counts of various isotopes for estimating their activities because the full energy peak is a

characteristic of the isotopes and it is in this energy region, a better sample to background counts is obtained. Sometimes the constituent nuclides emit gamma-rays of closely spaced energies, from which a small portion of the full energy peak of each of them are selected. This reduces the region of mutual overlap of adjacent peaks, thereby improving source counts to background counts ratio for each of the radionuclides. If a radioisotope emits more than one gamma-ray, the most abundant gamma energy should be taken for analysis in order to minimize the statistical error. If there are several gamma energies with comparable abundance, the highest energy that is likely to have least Compton contribution from other nuclides should be selected. In gamma-ray spectrometry, counting error can be reduced by increasing the number of counts by increasing- (i) counting efficiency, (ii) volume of the sample to be evaluated, and, (iii) counting time. Additionally, reduction in background counts of the detector by employing appropriate shielding, will also increase the sample counting accuracy.

In gamma-ray spectrometry, the quantities of interest like the activity of a source or the energy of a gamma-ray are derived from other measured quantities by a mathematical relationship. In the present research, used "EMCAPLUS EMULSION" software of the MCA provides information about the counting error in percent. Since percent of error is defined as:

$$\text{Percent of Error} = \frac{\sigma}{A}$$

where, σ is the standard deviation, and A is the observed activity (CPS); the standard deviation of any count rate was obtained by multiplying the percent of error and the observed CPS. In the other hand, since the corresponding background CPS including standard deviation should be subtracted from the sample's CPS including the standard error/deviation, and other arithmetic operations involving the standard deviation had to be done, special mathematical formulae were used for this purpose.

If x, y, z, are directly measured counts or related variables for which we know σ_x , σ_y , σ_z , are corresponding standard deviations, then the standard deviation for any quantity u derived from these counts can be calculated from^[120]:

$$\sigma_u^2 = \left(\frac{\partial u}{\partial x}\right)^2 \sigma_x^2 + \left(\frac{\partial u}{\partial y}\right)^2 \sigma_y^2 + \left(\frac{\partial u}{\partial z}\right)^2 \sigma_z^2 + \dots\dots\dots$$

where $u = u(x, y, z, \dots\dots)$ represents the derived quantity. The above equation is generally known as the error propagation formula and is applicable to almost all situations in nuclear measurements. The variables x, y, z, however, must be chosen so that they are truly

independent in order to avoid the effects of correlation. By using the above equation, we get the following formulae:

$$\text{If } u = x + y, \quad \sigma_u = \sqrt{\sigma_x^2 + \sigma_y^2}$$

$$u = x - y, \quad \sigma_u = \sqrt{\sigma_x^2 + \sigma_y^2}$$

$$u = x \cdot y, \quad \sigma_u = u \sqrt{\left(\frac{\sigma_x}{x}\right)^2 + \left(\frac{\sigma_y}{y}\right)^2}$$

$$u = \frac{x}{y}, \quad \sigma_u = u \sqrt{\left(\frac{\sigma_x}{x}\right)^2 + \left(\frac{\sigma_y}{y}\right)^2}$$

In the present study, $\pm 1\sigma$ of all the measurements were considered as it cover 68.27% of most probable values.

3.7 Cumulative Frequency Plot:

The cumulative frequency plot or simply the probability plot of a series of entries in a data is the tool for determining its geometric mean (GM) and geometric standard deviation (GSD). For a series of entries or datas, the GM is the corresponding value of 50% cumulative percent, and the GSD is the ratio of the corresponding values of 84.1% and 50% Cumulative Percents^[135]. These measures the deviation of a data from normal distribution. For severely skewed data or data having either higher-positive or higher-negative skewness, the arithmetic mean (AM) and standard deviation (SD) can not represent the actual data. In that case, The GM and GSD which are measured by considering the geometric distribution of data; can represent the actual situation. Moreover, GM and GSD are also a measure of the degree of variation of entries in a data. With the help of cumulative frequency plot, the average activity for a specific radionuclide in an amount of samples; for most of which the activity is below the detectable range at a certain detector, can be determined^[135]. To draw the cumulative frequency plot (probability plot) for a data containing a number of entries, the entries were ranked at first by arranging them in ascending order and then the cumulative percents were calculated by using the formula^[135]:

$$\text{Cumulative Percent} = \frac{100(i - 0.5)}{n}$$

where, 'i' is the serial position and 'n' is the total number of entries. In the present study, cumulative frequency plots were drawn for average concentrations of radionuclides ²³²Th, ²³⁸U, ⁴⁰K, and, ¹³⁷Cs both in soil and water samples; average radiation dose levels in kutcha-houses,

new-buildings, old-buildings, and in free-spaces; radiation dose due to terrestrial radioactivity; and radiation dose due to intake of water; at different locations of Bangladesh. These are shown in Figures 4.3–4.17 in chapter 4. From each of the plot, corresponding GM and GSD were determined and noted, and finally compared with their respective AM and SD.

3.8 Calculation of Population Risk Factor

The risk of the population at different locations of Bangladesh in radiation induced cancer incidence and death were calculated by using the fatal cancer risk given in ICRP-60^[22]. For general people which is: $500 \times 10^{-4} \text{ Sv}^{-1}$ i.e., 50 cases per million population per milli-Sievert annual effective dose equivalent ($50 \times 10^{-6} \text{ mSv}^{-1}$). The detailed results are shown in Table 4.22.

CHAPTER 4



RESULTS AND DISCUSSION

CHAPTER 4

RESULTS AND DISCUSSION

4.1 Introduction

In the present work, the radioactivity levels in soil and water samples collected from 56 different locations throughout Bangladesh were measured. Indoor and outdoor radiation dose levels in these 56 locations and few other locations were also measured. Moreover, the radiation dose levels at the sea-beaches of Bangladesh were measured and the concentrations of radionuclides in the Cox's Bazar and Kuakata sea beach's sand samples were also investigated. Before the inception of sample measurement procedure, a number of quality assurance of HPGe detector viz., energy calibration, energy resolution, efficiency calibration, determination of LLD (and consequently MDC), were made. These are described briefly in the following sections (4.1.1 – 4.1.3).

4.1.1 Energy Calibration and Resolution

The energy calibration of HPGe detector was made by using standard point sources ^{22}Na , ^{57}Co , ^{60}Co , ^{137}Cs , and ^{241}Am . The detector resolution at full width at half maximum (FWHM) obtained in this measurement was found to be 1.82 keV for 1332 keV of ^{60}Co source.

4.1.2 Efficiency Calibration

The most important characteristic of a detector is its efficiency and as such, it is indispensable to measure efficiency of a detector before starting the sample measurement. In the present study, the efficiency calibration of the HPGe detector for Marinelli-beaker geometry for assessment of soil and water samples were done individually by employing standard ^{226}Ra sources. The results of the efficiency calibration for assessment of the radionuclides in soil and water samples obtained from the corresponding graphs (Figure 4.1 and Figure 4.2 respectively) are shown in Table 4.1.

4.1.3 Lower Limit of Detection (LLD)

The lower limit of detection at a certain energy of a radioactivity measuring system is its ability to measure the lowest level of radioactivity at that energy with 95% confidence level at specified measurement time, measuring geometry, source to detector distance, and background shielding arrangement. In the present study, LLD for the HPGe detector was measured by a 1 L

water sample for Marinelli-beaker geometry for 10,000 sec and the results are shown in Table 4.2. The lowest LLD was found to be 35.74×10^{-3} Bq for ^{208}Tl (583.19 keV) and the highest LLD was found to be 1.95 Bq for ^{40}K (1460.75 keV). Since the LLD of a specific radionuclide at a specific energy is greatly influenced by the efficiency of the detector at that energy, the LLD for ^{40}K was found higher.

4.2 Radiation Dose Level Throughout Bangladesh

The indoor and outdoor radiation dose levels throughout Bangladesh were measured by a sensitive portable survey-meter PDR 1Sv. The dose levels at the points of soil sample collection were also recorded. The radiation dose levels at the Cox's Bazar sea-beach, Kuakata sea-beach, and Potenga sea-beach were also measured in the present study. The detailed result of this radiation survey is given in Table 4.3.

4.3 Radioactivity Levels in Soil samples

The specific activities of the radionuclides ^{232}Th , ^{238}U , ^{40}K , and ^{137}Cs in soil samples were determined by following the standard procedure as described in Chapter 3. The detailed results are given in the Table 4.4.

4.3.1 Radiation Dose Due to Radioactivity in Soil

The effective dose equivalent due to presence of radionuclides in soil samples were calculated by employing the computer software "RESRAD & GENII". The results of the calculation alongwith the average dose level (of the area) and the average dose rate at each point of soil sample collection are given in Table 4.5.

4.4 Radioactivity Levels in Water Samples

The radioactivity in water samples were found out by the same methodology that for soil samples. The detailed results of the specific activities of the radionuclides ^{232}Th , ^{238}U , ^{40}K , and ^{137}Cs in water samples are given in the Table 4.6.

4.4.1 Radiation Dose Due to Intake of Water

The effective dose equivalents due to intake of radionuclides through water for each of the sampling location were calculated by using the conversion factors given in Table 3.5 (in chapter 3). The results are shown in Tables 4.7 and 4.8.

4.5 Radiation Dose Due to Cosmic Radiation

The radiation doses due to cosmic radiation in each of the 56 locations were estimated by subtracting the corresponding terrestrial radiation dose calculated from the soil radioactivities (by REARAD & GENII computer software) from the average dose level in that particular location measured by PDR 1Sv. The results of cosmic radiation are shown in Table 4.5.

4.6 Discussion

The findings of the present work are discussed in the following paragraphs.

4.6.1 Indoor Dose Level

The indoor radiation dose levels were measured in kutcha-houses, new buildings, and old buildings. More than half of the people of Bangladesh are peasant and destitute, they live in kutcha-houses and houses in slum. On the whole, about 75% people live in kutcha houses, and the rest 25% in pucca-houses (buildings); about 0.01% of the total houses are old buildings. Most of the old buildings were found in district and division level towns. In the greater districts of Mymensingh and Kushtia, in entire north-bengal except Gaibandha and Sirajgonj, and in districts of Gazipur, Narsingdi, Tangail, Habigonj, Brahminbaria, Comilla, Chittagong, Rangamati, Khagrachheri, Jessore, Jhenidah, Satkhira, and Faridpur; kutcha houses owned by well-to-do people; are generally built with walls made of processed soil having 12"-18" thickness. These houses have poor ventilation system. On the other hand, most of the kutcha houses of Bangladesh are made of soil, bamboo, cane, reed and another aquatic plant, dried straw, thatched roof, wood, corrugated iron sheet (CI sheet) and plane sheet, and brick tiles (very limited cases in north-bengal); which have well ventilation compared to those for buildings and kutcha-houses with surrounding thick walls of clay and mud. Therefore, more emphasize was given in determining the indoor dose level of kutcha-houses. In each of the locations, at least 6 set of readings (ground level and gonad level) were taken from different kutcha houses, 5 set of readings were taken from different new-buildings, and 3 set of readings (wherever available) were taken from different old buildings by random sampling method. No remarkable variation was seen in the dose levels of ground and gonad levels and therefore average of these two levels in each set of readings was noted. Moreover, no significant variation in dose level was observed in each location at the same variety of houses. In each case of measurement, minimum dose level, maximum dose level, and the trend dose level was noted. In kutcha houses, the average of the average dose (trend) rate was found to be $0.23 \pm 0.04 \mu\text{Sv}\cdot\text{hr}^{-1}$, and the range

was from 0.17 ± 0.01 to $0.38 \pm 0.02 \mu\text{Sv}\cdot\text{hr}^{-1}$. In new-buildings, the average of the trend (average) dose rates was found to be $0.25 \pm 0.04 \mu\text{Sv}\cdot\text{hr}^{-1}$, the range of which was from 0.18 ± 0.02 to $0.33 \pm 0.02 \mu\text{Sv}\cdot\text{hr}^{-1}$. In old-buildings, the average dose level was found to be $0.27 \pm 0.04 \mu\text{Sv}\cdot\text{hr}^{-1}$ having the range from 0.19 ± 0.01 to $0.36 \pm 0.02 \mu\text{Sv}\cdot\text{hr}^{-1}$. In old-buildings and in kutcha houses having thicker wall of mud and clay, the dose levels were found to be higher than those in other houses and in free spaces. This may be explained as due to the dense environs and build-up of gaseous decay products (^{222}Rn and ^{220}Rn) on account of poor ventilation. The detailed analysis of the results are shown in Table 4.9. Weighted-average of the indoor dose rate of all kinds of houses was found to be $0.24 \pm 0.04 \mu\text{Sv}\cdot\text{hr}^{-1}$ by assuming that 75% people spend their time in kutcha houses, 24% people spend their time in new-buildings, and 1% people spend their time in old-buildings. In individual measurements, the lowest and highest dose rates for kutcha-houses was found to be $0.05 \mu\text{Sv}\cdot\text{hr}^{-1}$ in a kutcha house of Srimangal and $0.70 \mu\text{Sv}\cdot\text{hr}^{-1}$ in a kutcha house (having thicker wall of processed soil) of Badalgachhi respectively. The lowest and highest dose rates in new buildings in individual measurements were found to be $0.10 \mu\text{Sv}\cdot\text{hr}^{-1}$ (in one new-buildings each of Sylhet, Maulavibazar, Srimangal, and Comilla) and $0.56 \mu\text{Sv}\cdot\text{hr}^{-1}$ (in a new building of Madhabpasha, Barisal) respectively. The individual measurements of the indoor dose levels in old-buildings revealed the lowest dose rate $0.13 \mu\text{Sv}\cdot\text{hr}^{-1}$ in an old building of Chittagong and the highest dose rate $0.65 \mu\text{Sv}\cdot\text{hr}^{-1}$ in an old-building of Barisal town. However, the trend dose rate in these points of measurement are very different from the said values. These variation may be explained as due to the statistical fluctuation of natural and cosmic radioactivity.

4.6.2 Outdoor Dose Level

By following the same procedure as that for indoors, the outdoor dose measurements were done in yards of houses, kutcha and pucca-roads, play grounds, market places, and relatively free spaces throughout Bangladesh. There was no noteworthy variation in outdoor dose levels in each of the location. The average of the trend (average) outdoor (free space) dose rates was found to be $0.20 \pm 0.07 \mu\text{Sv}\cdot\text{hr}^{-1}$, the minimum being $0.16 \pm 0.02 \mu\text{Sv}\cdot\text{hr}^{-1}$ in Sylhet, Srimangal, and Sitakundo; while the maximum being $0.28 \pm 0.04 \mu\text{Sv}\cdot\text{hr}^{-1}$ in Nachole. The detail analysis of the outdoor dose rates are given in Table 4.9.

By considering the time occupancy factor of 66.67% indoors and 33.33% outdoors for Bangladeshi people, we get the average environmental dose rate is $\sim 2.0 \text{ mSv.y}^{-1}$. This dose level is somewhat higher than that of the other countries but comparable with the results obtained during 1975–1979 in Bangladesh, as shown in Table 4.11. The ratio of average indoor dose rate to the average outdoor dose was found to be 1.2, which is comparable to the world average indoor outdoor dose ratio 1.27 reported elsewhere^[4] and the average indoor-outdoor dose ratios 1.15 and 1.12 for Hongkong and Shenzhen respectively^[78].

All of the outdoor and indoor dose levels were further investigated by cumulative frequency plot (probability plot) to find out the geometric means and geometric standard deviations. These plots are shown in Figures 4.3–4.6 and the geometric means and geometric standard deviations calculated from these graphs are shown in Table 4.10. It was found that there was no variation in the arithmetic and geometric mean values for all types of measurement, which indicates that the data were normally distributed.

4.6.3 Average Annual Effective Dose Equivalent and Annual Collective Dose Equivalent

Average annual effective dose equivalent in different locations of Bangladesh were calculated by assuming that: (i) 75% people in each of the locations of Bangladesh live in kutcha-houses, 24% people live in new-buildings, and 1% people live in old-buildings; (ii) in the locations where old-buildings are not available, 25% people live in new-buildings; (iii) on an average, people spend 66.67% of their time in indoors and the rest 33.33% in outdoors. In calculating the annual collective dose equivalent, data for population and area of Bangladesh were used from “Statistical Pocketbook Bangladesh 97”^[134]. Estimations of population in the year 1998 from the data for population in the years 1997 and 1996; were made by assuming the population growth rate 1.7%^[137]. The detailed results of annual effective dose equivalent and collective dose equivalent are given in Table 4.12. Since both the radiation dose level and population density in Bangladesh are higher, the annual collective dose equivalents for different locations were found to be higher than those of reported values of different countries.

4.6.4 Radiation Dose Levels in Sea-Beaches of Bangladesh

Bangladesh has two world renowned sea-beaches, one is the longest beach in the world named Cox’s Bazar sea beach, and the other- the Kuakata sea-beach is endowed with the opportunity to observe both the sunrise and sunset. Both the beaches have shining-brown

coloured sandy areas exhibiting high radiation dose level. In Cox's Bazar sea-beach, the average dose level in shining-brown coloured sandy areas (off shore) was found to be 8.94 ± 3.15 mSv.y^{-1} ranging from 6.39 ± 2.28 to 11.91 ± 4.29 mSv.y^{-1} . The average dose level is higher than that of highest dose level found in Brazil and Ullal sea-beach, Karnataka, India; though individual effective dose equivalent upto 20.02 mSv.y^{-1} in Ullal sea beach was reported. However, this dose level is somewhat lower than the dose level measured in 1975–1979 in Cox's Bazar sea beach. Then average value of dose level was ~ 13 mSv.y^{-1} with a range between 2.6 and 44 mSv.y^{-1} . In the public movement areas of Cox's Bazar sea-beach, the average dose level was found to be 1.49 ± 0.18 mSv.y^{-1} (range 0.96 ± 0.18 to 2.01 ± 0.35 mSv.y^{-1}), which is lower than the average outdoor radiation dose level throughout Bangladesh. In Kuakata sea beach, the higher dose levels were found in shining-brown coloured sandy areas, the average value of which was 4.20 ± 0.88 mSv.y^{-1} ranging between 2.98 ± 0.70 and 5.87 ± 0.18 mSv.y^{-1} . The average value is again higher than the maximum values found in Brazil and Ullal sea-beach. However, in public movement areas of Kuakata sea-beach, the average dose level was found to be 1.58 ± 0.35 mSv.y^{-1} having range 1.05 ± 0.26 to 2.19 ± 0.44 mSv.y^{-1} , which is slightly higher than that of Cox's Bazar sea-beach. The detail analysis of sea beach dose levels are shown in Table 4.13. In Potenga sea-beach, Chittagong; the average dose level was found to be 1.58 ± 0.26 mSv.y^{-1} having the range from 1.14 ± 0.26 to 2.10 ± 0.53 mSv.y^{-1} . This level is similar to the average outdoor dose level of Bangladesh.

4.6.5 Radioactivity in Soil samples

Thorium-232 in soil samples: The average concentration of ^{232}Th in soil samples was found to be 83.56 ± 17.96 Bq.kg^{-1} ranging from 39.27 ± 7.74 to 128.21 ± 7.83 Bq.kg^{-1} . The lowest activity was found in the soil sample collected from Nabigonj (in Habigonj district) and the highest activity was found in the soil sample of Nachole (Table 4.14). This level is comparable to the levels of ^{232}Th found in Italy, Egypt, China, and Brazil, but higher than other countries and locations as shown in Table 4.16. The cumulative frequency plot for the ^{232}Th concentrations in soil samples is shown in Figure 4.7. From this graph, it was found that the geometric mean of ^{232}Th in soil samples is 53.50 Bq.kg^{-1} which is approximately equal to the arithmetic mean value; indicating the normal distribution. The geometric means and geometric

standard deviations of the concentrations of radionuclides ^{232}Th , ^{238}U , ^{40}K , and ^{137}Cs in soil and water samples alongwith the arithmetic means and standard deviations are shown in Table 4.15.

Uranium-238 in Soil Samples: Average specific activity of ^{238}U in soil samples was found to be $44.35 \pm 12.65 \text{ Bq.kg}^{-1}$ with a range 17.84 ± 6.21 to $76.06 \pm 7.58 \text{ Bq.kg}^{-1}$. The lowest concentration of ^{238}U was found in the soil sample of Nabigonj while the highest concentration was found in the soil sample collected from Nachole. The average level of ^{238}U in soil samples is comparable to the levels found in the soil of US, China, Greece, Brazil, Spain; but higher than those levels of Egypt, Louisiana, and Dhaka, and lower than the levels found in Italy. The detailed analysis of the results are shown in Table 4.16. The geometric mean and geometric standard deviation of ^{238}U in soil samples were found from the cumulative frequency plot shown in Figure 4.8. The geometric mean was found to be 44.30 Bq.kg^{-1} and the geometric standard deviation was 1.32. The close proximity of arithmetic mean and geometric mean indicates the distribution of ^{238}U in soil samples is normal.

Potassium-40 in Soil Samples: The average concentration of radioactive potassium (^{40}K) in the soil samples collected from different locations of Bangladesh was found to be $630.89 \pm 173.85 \text{ Bq.kg}^{-1}$ ranging between 276.78 ± 61.47 and $923.79 \pm 69.02 \text{ Bq.kg}^{-1}$. The highest and lowest activities of ^{40}K found in the soil samples collected from Khulna and Nabigonj respectively. The geometric mean and geometric standard deviation of ^{40}K concentration in soil samples were found to be 632.0 Bq.kg^{-1} and 1.32 respectively from the corresponding cumulative frequency plot shown in Figure 4.9. The close proximity of average ^{40}K concentration in soil samples in arithmetic and geometric view indicates that the distribution is normal. The concentration level of ^{40}K in soil samples of Bangladesh is similar to those of China, Italy, Brazil, Spain and Dhaka; is higher than those of US, Taiwan, Egypt, and Algeria; and is lower than that of Greece; as shown in Table 4.16.

Caesium-137 in Soil Samples: The average specific activity of ^{137}Cs in soil samples of Bangladesh was found to be $5.37 \pm 4.87 \text{ Bq.kg}^{-1}$ with a range from 2.76 ± 1.51 to $26.79 \pm 2.23 \text{ Bq.kg}^{-1}$. The highest activity $26.79 \pm 2.23 \text{ Bq.kg}^{-1}$ was found in the soil sample of Jaflong while the lowest activity $2.76 \pm 1.51 \text{ Bq.kg}^{-1}$ was found in the soil samples of Natore. Out of 56 soil samples collected from 56 different locations of Bangladesh, no ^{137}Cs activity was detected in 14 samples (25%), e.g. Srimangal, Chandpur, Gopalganj, etc. The geometric mean and standard

deviation of ^{137}Cs concentration in soil samples were found to be 5.30 Bq.kg^{-1} and 1.96 respectively from the corresponding cumulative frequency plot of ^{137}Cs in soil samples shown in Figure 4.10. The approximately equal arithmetic and geometric average concentration values of ^{137}Cs in soil samples, reveals the normal distribution. The concentration level of ^{137}Cs in soil samples of Bangladesh is comparable to those of Taiwan, Chile, and Dhaka; higher than that of Algeria; and lower than those of Bangladesh (as measured in 1976^[34]), Hawaii, US, and Spain. The details of the ^{137}Cs concentration in soil samples in some of the countries of the world are shown in Table 4.16.

4.6.6 Radioactivity in Beach Sand Samples

The concentrations of ^{232}Th , ^{238}U , ^{40}K , and ^{137}Cs in beach sand samples of Cox's Bazar sea beach and Kuakata sea beach of Bangladesh in compared to the corresponding concentrations in the beach sand samples of Mangalore sea beach, Karnataka, India are given in Table 4.17. It was found that the average concentrations of ^{232}Th was higher in sand samples of Mangalore sea beach ($1842 \pm 6.6 \text{ Bq.kg}^{-1}$) while the average concentration of ^{238}U was found higher in the sand sample of Cox's Bazar ($455.99 \pm 16.35 \text{ Bq.kg}^{-1}$); which strongly suggests the existence of monazite in Cox's Bazar sea beach. The highest ^{40}K concentration was found in sand samples of Kuakata sea-beach ($266.00 \pm 24.80 \text{ Bq.kg}^{-1}$) while the lowest in Cox's Bazar sea beach. Though sand samples of Kuakata sea beach have lower activities of ^{232}Th and ^{238}U in comparison to those of Cox's Bazar sea beach; these activities are far higher than those of soil samples of Bangladesh and the colour of sand samples in some area of Kuakata sea beach is shining-brown as that in Cox's Bazar sea beach; which indicate the probability of existing of monazite in Kuakata sea beach sand. The radiation dose level in the shining-brown coloured sandy areas of Kuakata sea beach which is somewhat comparable to the dose levels of monazite-beaches of the world as described earlier, further enhances the probability of existence of monazite. No ^{137}Cs was detected in any of the sand samples of two sea-beaches of Bangladesh. The detail analysis of the radionuclide concentration in beach sand samples is shown in Table 4.17.

4.6.7 Radioactivity in Water Samples

Thorium-232 in Water Samples: The average concentration of ^{232}Th in water samples collected from 56 different locations was found to be $249.59 \pm 51.67 \text{ mBq.L}^{-1}$ ranging between

109.06 ± 29.92 and 365.36 ± 45.31 mBq.L⁻¹. The lowest and highest concentrations were found in water samples of Nabigonj and Kurigram respectively as shown in Table 4.14. This level is higher than the level found in New York and comparable to that of Chittagong. The Table 4.18 shows in detail the concentration of different radionuclides in some of the countries of the world. The geometric mean and geometric standard deviation were found to be 250.0 mBq.L⁻¹ and 1.23 respectively; from the corresponding cumulative frequency plot shown in Figure 4.11. The very close similarity of the arithmetic and geometric average specific activities of ²³²Th in water samples indicates statistical normal distribution.

Uranium-238 in Water Samples: The range of the concentration of ²³⁸U in water samples was found to be 82.91 ± 27.54 to 229.65 ± 33.16 mBq.L⁻¹ with an average 156.77 ± 30.46 mBq.L⁻¹. The highest and lowest concentrations of ²³⁸U in water samples were found in the water samples of Dinajpur and Jhenaigati respectively. This level is comparable to the corresponding level found in the water sample of India; higher than those of Finland and European countries, US, North Carolina, and Taiwan; and lower than those of Iowa and Saudi Arabia; as shown in Table 4.18. The geometric mean and geometric standard deviation of the ²³⁸U in water samples were found to be 157.0 mBq.L⁻¹ and 1.14 respectively from the corresponding cumulative frequency plot as shown in Figure 4.12. The close proximity of the arithmetic and geometric mean concentration (shown in Table 4.15) values indicate the normal distribution of ²³⁸U in water samples.

Potassium-40 in Water Samples: The average specific concentration of the single radioisotope of potassium ⁴⁰K in water samples was found to be 9.08 ± 3.36 Bq.L⁻¹. This average concentration was ranged between 3.12 ± 1.13 and 16.57 ± 1.22 Bq.L⁻¹. The highest concentration of ⁴⁰K was found in the water sample of Khulna and the lowest concentration of the same radionuclide was found in the water sample of Nabigonj. The geometric mean and the geometric standard deviation of the concentrations of the mentioned radionuclide in the assessed water samples were found to be 9.10 Bq.L⁻¹ and 1.42 respectively from the corresponding cumulative frequency plot as shown in Figure 4.13. The approximately equal arithmetic and geometric mean values of ⁴⁰K strongly suggests the normal distribution of the mentioned radionuclide.

Caesium-137 in Water Samples: Out of the 57 water samples collected from 56 different locations of Bangladesh, the ^{137}Cs radionuclide was detected only in 18 samples (32%). The range of the activity of the mentioned radionuclide in the said number of samples was found to be from 2.21 ± 1.41 to $5.47 \pm 1.55 \text{ Bq.L}^{-1}$. The lowest and the highest activities of ^{137}Cs were found in the water samples of Rangamati and Jaflong respectively. By considering the zero concentration of ^{137}Cs in 39 samples, the average concentration was found to be $1.17 \pm 1.80 \text{ Bq.L}^{-1}$. The geometric mean and the geometric standard deviation of the radionuclide in water samples were found to be 0.61 Bq.L^{-1} and 6.07 respectively as shown in Table 4.15 found from the corresponding cumulative frequency plot of ^{137}Cs in water samples shown in Figure 4.14. This marked difference between the arithmetic mean and geometric mean, and the larger value of geometric standard deviation indicates that the distribution is not normal. Since ^{137}Cs is an artificial nuclide, it is quite natural to find its distribution in drinking water is “not normal”.

4.6.8 Correlation Between the Activities of Radionuclides Found in Soil and Water Samples

The correlation coefficients between the concentrations of radionuclides ^{232}Th , ^{238}U , ^{40}K , and ^{137}Cs found in soil and water samples were calculated by computer software “Excel-97”. The correlation coefficients between the activities of same radionuclide in soil and water samples arranged in same order were also calculated by the same aid. The detail of the results are shown in Table 4.19. In soil samples, the highest correlation coefficient ($r = 0.88$) was found for ^{232}Th and ^{238}U concentration levels; and the lowest ($r = 0.13$) was found for ^{40}K and ^{137}Cs . A good correlation between ^{232}Th and ^{238}U in soil samples and a very poor correlation between ^{40}K and ^{137}Cs were observed. The highly significant correlation occurred between ^{232}Th and ^{238}U is consistent with the geochemical behaviour of their complexes, namely, the tendency of uranium and thorium to concentrate in the fluid phase during magmatic differentiation^[81]. In water samples, a good correlation was also found between ^{232}Th and ^{238}U ($r = 0.83$) concentration levels and very poor correlation between all other combinations having the poorest correlation ($r = 0.01$) between ^{232}Th and ^{137}Cs concentration levels. Good correlations between the corresponding concentration levels of the same radionuclides (found in soil and water samples) were also found. The highest $r = 0.94$ was found for ^{232}Th concentrations (of the soil and water samples of the same place), and the lowest (but not least) $r = 0.61$ was found between the ^{137}Cs concentration levels in soil and water samples. These good correlation coefficients indicate good mixing and precipitation of radionuclide from surface soil to ground water.

4.6.9 Radiation Dose Due to Terrestrial Radiation

The terrestrial radiation dose in different locations of Bangladesh were estimated from the concentration levels of ^{232}Th , ^{238}U , ^{40}K , and ^{137}Cs in the soil samples of the corresponding locations by using computer software "RESRAD & GENII". These are shown in Table 4.5. The average terrestrial radiation dose was found to be $1.26 \pm 0.27 \text{ mSv.y}^{-1}$ having a range from $0.56 \pm 0.08 \text{ mSv.y}^{-1}$ to $1.88 \pm 0.09 \text{ mSv.y}^{-1}$. The highest dose was found for the soil sample of Rangpur and the lowest for that of Nabigonj. The terrestrial radiation dose level in Bangladesh is comparable to that of Hongkong (1.11 mSv.y^{-1}) but higher than the reported values of different countries. These are shown in Table 4.11. The geometric mean and the geometric standard deviation of the terrestrial radiation dose value were estimated to be 1.26 mSv.y^{-1} and 1.24 respectively from the corresponding cumulative frequency plot as shown in Figure 4.15. The similar arithmetic and geometric mean values of terrestrial radiation dose levels indicate the normal distribution of terrestrial radiation throughout Bangladesh.

4.6.10 Radiation Dose Due to Cosmic Radiation

The radiation dose levels due to cosmic radiation in different locations of Bangladesh were estimated from the average outdoor dose level and terrestrial radiation dose level. The cosmic radiation in different locations of Bangladesh are shown in Table 4.5 alongwith average outdoor dose levels. The average cosmic radiation dose level was found to be 0.63 mSv.y^{-1} ranging between 0.04 and 1.30 mSv.y^{-1} . The world average level of cosmic radiation dose is 0.39 mSv.y^{-1} [1].

4.6.11 Radiation Dose Due to Intake of Water

Radiation doses received due to the intake of water throughout Bangladesh were calculated by employing the conversion coefficients given in ICRP-68^[133] (Table 3.5 in this manuscript). The average value of the annual radiation dose received by an adult in Bangladesh through water intake was found to be $74.01 \pm 21.41 \mu\text{Sv}$ by considering an adult intake of 730 L water per year; the range of which was from 24.20 ± 5.57 to $134.04 \pm 16.10 \mu\text{Sv.y}^{-1}$ (shown in Table 4.20). The lowest dose was found for the people of Nabigonj (covering the district Habigonj) while the highest dose was found for the people of Sunamgonj. This dose level is comparable to the dose level estimated in Chittagong (Table 4.18) but higher than the dose level estimated in US (range $2 - 50 \mu\text{Sv.y}^{-1}$)^[60]. The geometric mean and the geometric standard

deviation values of the radiation dose received due to intake of drinking water by the people throughout Bangladesh, as shown in Table 4.21, were found to be $74.00 \mu\text{Sv.y}^{-1}$ and 1.32 respectively. These were estimated from the corresponding cumulative frequency plots as shown in Figures 4.16 and 4.17. The proximity of the arithmetic and geometric mean dose levels indicates the normal distribution of dose levels and the distribution of radionuclides in a broad sense.

4.6.12 Total Radiation Dose Received By People Living in Bangladesh

The average value of environmental exposure dose (terrestrial plus cosmic) was found to be $\sim 2 \text{ mSv.y}^{-1}$. Since about one third of the total effective dose equivalent is received from terrestrial and cosmic radiation, (except radon and its decay products which contributes more than half of the total radiation received)^[1]; it may be estimated that the total radiation dose received by an adult of Bangladesh on an average is $\sim 6 \text{ mSv.y}^{-1}$. This level is exactly $2\frac{1}{2}$ times of the world average dose level (2.4 mSv.y^{-1}) reported in UNSCEAR-93 report^[1]. Though this level of radiation in Bangladesh is much higher, this level is far lower than the more elevated radiation dose level 16.9 mSv.y^{-1} in the world reported in elsewhere^[1].

4.6.13 Risk of Bangladeshi People in Radiation Induced Cancer

The risk to the population of the different locations of Bangladesh in inducing fatal cancer i.e., total fatal probability coefficients; were estimated which are shown in Table 4.22. These estimations were made only by considering the annual effective dose equivalent due to external exposure from natural background radiation (measured in the present work). The total risk will be somewhat higher. However, the average total fatal probability coefficient was found to be 101 cases per million people, the range of which was from 78 to 144 per million people. The lowest risk was found for the people of Srimangal (Maulavibazar) and Sandweep; while the risk was highest for the people of Nachole (Chapai Nawabgonj) and Badalgachhi (Naogaon), the two locations in Borendra region. The risk factors were found to be around average level for the people of Dhaka, Chittagong, and Rajshahi. Since a very significant portion of people of Bangladesh live in these areas, the calculated average risk factor become more meaningful. Moreover, since both the average effective dose equivalent and the population density in Bangladesh is higher than those of the countries given in Table 4.11; we are in more risk than those countries.

It was an established fact that the probability of radiation injury (and consequently the stochastic effects) increases with the increase in radiation dose. However, few recent publications show that, the risk of cancer incidence is reduced with the increase of external radiation dose, which is called 'hormesis'. A complete issue of the Journal of Health Physics [Health Physics; Vol. 52, No 5, May-1987] was published as the proceedings of an international symposium on radiation hormesis in 1987. A more recent publication, in the October-1998 issue of the Journal "Health Physics"^[107] showed a negative correlation between the Natural Background Radiation and Overall Cancer Death. So it is still a matter of research to define the maximum permissible dose below which there is no probability of cancer incidence and how the elevated natural radio-exposure reduces the probability of cancer incidence and mortality. It is also a matter of research to redefine the existing fatal cancer risk factor. On the other hand, there is no available data on the cancer incidence of the people of the different locations of Bangladesh and consequently, it was not possible to compare the rate of cancer incidence and the radiation dose level of the locations; and no comment could be made on the hormesis effect in Bangladesh. Moreover, the exact reason behind the cancer incidence is still a matter of further research and no acceptable unique solution had been made. Radiation injury of living cell is one of the causes of cancer incidence. Other causes of cancer incidence were claimed to be genetic, viral, and metabolic disorders (due to various causes) and pre-cancerous conditions. Further, It is very difficult to trace the exact reason behind the cancer incidence in a patient. So it is not prudent to make comment on the cancer incidence only by justifying the radiation dose level.

Hormesis may be explained as the survival of the fittest of cells since the formation of the earth. Radionuclides are present in the earth since just after the big bang and the living cells were exposed to this radiation since their formation. Some of the cells survived from this radiation exposure without any damage, some of the cells survived with few damage, some of the cells survived with mutation, and some of the cells died. The present beautiful universe is the consequence of many serieses of genetic mutation of cells and the renowned evolution theory of Charle's Darwin may also be explained as the manifestation of genetic mutation of primates. So there is a probability to kill the ill cells of living beings by elevated level of chronic exposure (i.e., environmental radiation) thereby saving the healthy cells from any unwanted mutation of reproductive genes; (as in the principle of radiotherapy to a great extent) the consequence of which is the reduction of the probability of cancer incidence. If we accept the hormesis effect in the context of Bangladesh, then we may make comment that the people of Bangladesh are in

lower risk of radiation induced diseases like cancer incidence and death (as in India^[65] and in USA^[107]) than the other countries having lower background radiation than that of us.

In the present work, the radiation dose received through inhalation and ingestion, and the radiation dose due to radioactivity in the body were not measured directly; which constitute approximately two-third of the total effective dose equivalent. On the other hand, the data about the cancer incidence in different locations of Bangladesh is not available. Consequently, the risk factors calculated here are only partial estimations indicating the probability of cancer incidence due to external natural radiation exposure. The actual probability of cancer risk of the people of Bangladesh could only be estimated when the total effective dose equivalents due to all sources and through all routes are measured accurately and the data relating the cancer incidence and mortality in different locations of Bangladesh are known. However, this study would provide baseline dose for the estimation of risk to the population at large in Bangladesh.

4.7 Conclusion

No significant difference in average radiation dose levels in the years 1975–1979 and in 1998 in Bangladesh was observed. So there is no radiation impact of Chernobyl accident on the environment of Bangladesh. It may be mentioned here that the work carried out between 1975 – 1979^[32] was random in nature involving only few locations of Bangladesh. But the present study was carried out in a much more detailed and reliable way covering the entire geographical area of Bangladesh.

The concentration levels of radionuclides in soil and water samples are somewhat higher than that of most reported values of the developed countries. This is due to the geological characteristics of the earth. No significant amount of ¹³⁷Cs in the soil and water samples were detected. So there is no obvious influence of nuclear explosions and accidents on the environment of Bangladesh.

Since the radiation dose received through ingestion of daily-foodstuffs is quite smaller than that through inhalation and external exposure, the dose level estimated in the present work may be considered as the total effective dose equivalent excluding that due to inhalation and radioactivity in body; and would help to formulate the radiation protection guideline for the people of Bangladesh.

4.8 Scope of Future Studies

From the present study, the average effective dose equivalent was found to be ~ 2 mSv.y⁻¹. However, the estimated annual effective dose equivalent (due to external and internal exposure) was found to be ~ 6 mSv. In order to confirm this value, further studies are needed. For this reason, the research programme may be extended to find out the radiation dose received due to radioactivity in body, inhalation of gaseous radionuclides, and intake of radionuclides through daily foodstuffs of different locations in Bangladesh. This would help to estimate the average radiation dose received by the people of Bangladesh from all sources through all possible routes and consequently the total radiation dose received by the general public of Bangladesh may be known. The total radiation dose level of the different locations of Bangladesh would help to investigate the hormesis in Bangladesh by knowing the data about the cancer incidence and death in different locations (of Bangladesh). So the fatal cancer risk factors with higher accuracy could be found out and the radiation protection guideline for the people of our country could be established properly.

Table 4.1: Efficiency of HPGe Detector for Marinelli Beaker Geometry.

Energy (keV)	Efficiency (%) for 1-L Marinelli Beaker Geometry with	
	Soil Samples	Water Samples
238.63	0.92	1.04
583.19	0.49	0.49
911.07	0.36	0.33
351.92	0.70	0.75
609.31	0.48	0.47
1120.29	0.31	0.28
1460.75	0.26	0.23
661.66	0.45	0.44

Table 4.2: Lower Limit of Detection of the HPGe Detector (Counting Time 10,000 sec).

Radionuclide		Energy (keV)	LLD (Bq)
²³² Th Series	²¹² Pb	238.63	78.56×10^{-3}
	²⁰⁸ Tl	583.19	35.74×10^{-3}
	²²⁸ Ac	911.07	89.64×10^{-3}
²³⁸ U Series	²¹⁴ Pb	351.92	61.58×10^{-3}
	²¹⁴ Bi	609.31	73.28×10^{-3}
	²¹⁴ Bi	1120.29	81.99×10^{-3}
-	⁴⁰ K	1460.75	1.95
-	¹³⁷ Cs	661.66	72.43×10^{-3}

Table 4.3: Dose Levels at Different Locations of Bangladesh.

Location	Surrounding	Dose Rate ($\mu\text{Sv/hr}$)			Date of Measurement
		Minimum	Maximum	Trend value	
Akhaura (Brahminbardia)	a. Free space	0.12 ± 0.02	0.21 ± 0.04	0.17 ± 0.03	27/01/98
	b. Kutcha house	0.17 ± 0.02	0.29 ± 0.02	0.21 ± 0.02	
	c. New building	0.13 ± 0.02	0.24 ± 0.04	0.19 ± 0.02	
	d. Old building	0.15 ± 0.01	0.27 ± 0.04	0.19 ± 0.01	
Maulavibazar	a. Free space	0.11 ± 0.02	0.22 ± 0.03	0.17 ± 0.02	28/01/98
	b. Kutcha house	0.14 ± 0.01	0.22 ± 0.02	0.17 ± 0.01	
	c. New building	0.12 ± 0.03	0.23 ± 0.03	0.18 ± 0.02	
	d. Old building	0.18 ± 0.03	0.39 ± 0.05	0.27 ± 0.03	
Srimangal (Maulavibazar)	a. Free space	0.12 ± 0.02	0.20 ± 0.03	0.16 ± 0.02	28/01/98
	b. Kutcha house	0.10 ± 0.03	0.24 ± 0.02	0.19 ± 0.02	
	c. New building	0.14 ± 0.02	0.22 ± 0.04	0.18 ± 0.02	
	d. Old building	0.16 ± 0.04	0.26 ± 0.05	0.22 ± 0.04	
Sunapur (Sunamgonj)	a. Free space	0.13 ± 0.02	0.22 ± 0.04	0.17 ± 0.03	29/01/98
	b. Kutcha house	0.16 ± 0.02	0.26 ± 0.02	0.21 ± 0.02	
	c. New building	0.16 ± 0.01	0.29 ± 0.02	0.23 ± 0.02	
	d. Old building	0.18 ± 0.02	0.38 ± 0.06	0.26 ± 0.04	
Sylhet	a. Free space	0.12 ± 0.02	0.19 ± 0.03	0.16 ± 0.02	30/01/98
	b. Kutcha house	0.14 ± 0.01	0.26 ± 0.02	0.19 ± 0.01	
	c. New building	0.14 ± 0.04	0.25 ± 0.06	0.19 ± 0.04	
	d. Old building	0.17 ± 0.02	0.31 ± 0.06	0.24 ± 0.02	
Jafiong (Sylhet)	a. Free space	0.14 ± 0.02	0.23 ± 0.03	0.18 ± 0.02	31/01/98
	b. Kutcha house	0.14 ± 0.02	0.29 ± 0.03	0.21 ± 0.03	
	c. New building	0.15 ± 0.01	0.29 ± 0.05	0.22 ± 0.03	
Comilla	a. Free space	0.12 ± 0.03	0.23 ± 0.04	0.18 ± 0.02	04/02/98
	b. Kutcha house	0.17 ± 0.01	0.26 ± 0.01	0.21 ± 0.01	
	c. New building	0.13 ± 0.03	0.27 ± 0.05	0.19 ± 0.03	
	d. Old building	0.15 ± 0.01	0.27 ± 0.05	0.20 ± 0.02	

Continued

Location	Surrounding	Dose Rate ($\mu\text{Sv/hr}$)			Date of Measurement
		Minimum	Maximum	Trend value	
Chandpur	a. Free space	0.15 ± 0.01	0.23 ± 0.03	0.18 ± 0.02	05/02/98
	b. Kutcha house	0.16 ± 0.01	0.22 ± 0.02	0.19 ± 0.02	
	c. New building	0.15 ± 0.01	0.24 ± 0.01	0.19 ± 0.02	
	d. Old building	0.16 ± 0.01	0.39 ± 0.05	0.23 ± 0.03	
Feni	a. Free space	0.13 ± 0.02	0.23 ± 0.03	0.17 ± 0.02	06/02/98
	b. Kutcha house	0.14 ± 0.01	0.28 ± 0.03	0.20 ± 0.02	
	c. New building	0.14 ± 0.02	0.24 ± 0.03	0.19 ± 0.02	
Noakhali	a. Free space	0.12 ± 0.02	0.21 ± 0.03	0.17 ± 0.02	07/02/98
	b. Kutcha house	0.12 ± 0.03	0.23 ± 0.03	0.18 ± 0.02	
	c. New building	0.14 ± 0.02	0.25 ± 0.04	0.19 ± 0.03	
	d. Old building	0.16 ± 0.02	0.27 ± 0.04	0.22 ± 0.04	
Hatiya (Noakhali)	a. Free space	0.14 ± 0.02	0.24 ± 0.06	0.18 ± 0.03	08/02/98
	b. Kutcha house	0.15 ± 0.01	0.26 ± 0.04	0.19 ± 0.01	
	c. New building	0.14 ± 0.01	0.29 ± 0.04	0.21 ± 0.04	
Sandweep (Chittagong)	a. Free space	0.13 ± 0.02	0.21 ± 0.03	0.17 ± 0.02	09/02/98
	b. Kutcha house	0.13 ± 0.02	0.20 ± 0.05	0.17 ± 0.02	
	c. New building	0.12 ± 0.02	0.23 ± 0.05	0.18 ± 0.03	
Sitakundo (Chittagong)	a. Free space	0.12 ± 0.01	0.20 ± 0.02	0.16 ± 0.01	10/02/98
	b. Kutcha house	0.14 ± 0.01	0.26 ± 0.01	0.19 ± 0.01	
	c. New building	0.15 ± 0.01	0.27 ± 0.03	0.20 ± 0.02	
Dinajpur	a. Free space	0.15 ± 0.04	0.25 ± 0.04	0.19 ± 0.03	26/02/98
	b. Kutcha house	0.20 ± 0.04	0.34 ± 0.09	0.25 ± 0.06	
	c. New building	0.17 ± 0.02	0.34 ± 0.07	0.26 ± 0.04	
	d. Old building	0.20 ± 0.02	0.32 ± 0.02	0.25 ± 0.01	

Continued

Location	Surrounding	Dose Rate ($\mu\text{Sv/hr}$)			Date of Measurement
		Minimum	Maximum	Trend value	
Syedpur (Nilphamari)	a. Free space	0.14 ± 0.02	0.26 ± 0.06	0.20 ± 0.04	26/02/98
	b. Kutcha house	0.22 ± 0.04	0.38 ± 0.04	0.29 ± 0.02	
	c. New building	0.18 ± 0.02	0.36 ± 0.05	0.26 ± 0.04	
	d. Old building	0.18 ± 0.02	0.36 ± 0.06	0.27 ± 0.04	
Panchagarh	a. Free space	0.14 ± 0.02	0.26 ± 0.02	0.20 ± 0.02	27/02/98
	b. Kutcha house	0.16 ± 0.02	0.31 ± 0.01	0.25 ± 0.01	
	c. New building	0.19 ± 0.01	0.32 ± 0.02	0.25 ± 0.02	
Rangpur	a. Free space	0.17 ± 0.03	0.33 ± 0.04	0.26 ± 0.04	28/02/98
	b. Kutcha house	0.16 ± 0.02	0.29 ± 0.03	0.21 ± 0.03	
	c. New building	0.20 ± 0.04	0.36 ± 0.07	0.29 ± 0.06	
	d. Old building	0.23 ± 0.05	0.46 ± 0.06	0.33 ± 0.04	
Gaibandha	a. Free space	0.14 ± 0.03	0.25 ± 0.03	0.19 ± 0.02	01/03/98
	b. Kutcha house	0.16 ± 0.02	0.29 ± 0.03	0.24 ± 0.01	
	c. New building	0.18 ± 0.02	0.36 ± 0.06	0.27 ± 0.04	
	d. Old building	0.20 ± 0.02	0.37 ± 0.02	0.30 ± 0.02	
Kurigram	a. Free space	0.13 ± 0.03	0.30 ± 0.04	0.22 ± 0.03	02/03/98
	b. Kutcha house	0.16 ± 0.03	0.31 ± 0.06	0.24 ± 0.04	
	c. New building	0.19 ± 0.03	0.37 ± 0.04	0.28 ± 0.03	
Bogra	a. Free space	0.15 ± 0.03	0.29 ± 0.06	0.21 ± 0.05	03/03/98
	b. Kutcha house	0.21 ± 0.04	0.42 ± 0.04	0.31 ± 0.02	
	c. New building	0.17 ± 0.03	0.37 ± 0.05	0.27 ± 0.03	
	d. Old building	0.19 ± 0.02	0.39 ± 0.02	0.30 ± 0.02	
Ullapara (Sirajgonj)	a. Free space	0.15 ± 0.03	0.26 ± 0.04	0.20 ± 0.03	04/03/98
	b. Kutcha house	0.14 ± 0.20	0.29 ± 0.06	0.21 ± 0.05	
	c. New building	0.17 ± 0.03	0.28 ± 0.03	0.22 ± 0.02	

Continued

Location	Surrounding	Dose Rate ($\mu\text{Sv/hr}$)			Date of Measurement
		Minimum	Maximum	Trend value	
Natore	a. Free space	0.13 ± 0.02	0.27 ± 0.04	0.18 ± 0.02	05/03/98
	b. Kutcha house	0.13 ± 0.03	0.32 ± 0.07	0.23 ± 0.05	
	c. New building	0.15 ± 0.03	0.36 ± 0.07	0.25 ± 0.04	
	d. Old building	0.19 ± 0.01	0.36 ± 0.03	0.27 ± 0.01	
Rajshahi	a. Free space	0.13 ± 0.02	0.27 ± 0.04	0.21 ± 0.02	06/03/98
	b. Kutcha house	0.18 ± 0.01	0.32 ± 0.06	0.24 ± 0.03	
	c. New building	0.16 ± 0.02	0.30 ± 0.05	0.23 ± 0.04	
	d. Old building	0.17 ± 0.02	0.33 ± 0.06	0.26 ± 0.05	
Nachole (Chapai Nawabgonj)	a. Free space	0.17 ± 0.03	0.37 ± 0.05	0.28 ± 0.04	07/03/98
	b. Kutcha house	0.28 ± 0.03	0.48 ± 0.06	0.37 ± 0.02	
	c. New building	0.19 ± 0.02	0.41 ± 0.06	0.30 ± 0.03	
Kushtia	a. Free space	0.12 ± 0.03	0.26 ± 0.05	0.19 ± 0.03	08/03/98
	b. Kutcha house	0.15 ± 0.03	0.29 ± 0.03	0.24 ± 0.02	
	c. New building	0.16 ± 0.01	0.31 ± 0.01	0.22 ± 0.02	
	d. Old building	0.19 ± 0.02	0.34 ± 0.04	0.27 ± 0.02	
Faridpur	a. Free space	0.14 ± 0.03	0.27 ± 0.04	0.19 ± 0.03	09/03/98
	b. Kutcha house	0.15 ± 0.01	0.32 ± 0.05	0.23 ± 0.03	
	c. New building	0.16 ± 0.02	0.34 ± 0.06	0.24 ± 0.03	
	d. Old building	0.18 ± 0.03	0.36 ± 0.05	0.27 ± 0.05	
Gopalganj	a. Free space	0.14 ± 0.02	0.27 ± 0.03	0.20 ± 0.02	11/03/98
	b. Kutcha house	0.11 ± 0.02	0.30 ± 0.04	0.21 ± 0.02	
	c. New building	0.17 ± 0.03	0.32 ± 0.04	0.25 ± 0.03	
	d. Old building	0.19 ± 0.02	0.40 ± 0.02	0.31 ± 0.01	
Jessore	a. Free space	0.13 ± 0.02	0.27 ± 0.05	0.20 ± 0.04	17/03/98
	b. Kutcha house	0.17 ± 0.03	0.32 ± 0.05	0.25 ± 0.04	
	c. New building	0.16 ± 0.02	0.35 ± 0.04	0.26 ± 0.03	
	d. Old building	0.17 ± 0.02	0.29 ± 0.02	0.22 ± 0.02	

Continued

Location	Surrounding	Dose Rate ($\mu\text{Sv/hr}$)			Date of Measurement
		Minimum	Maximum	Trend value	
Shyam Nagar (Satkhira)	a. Free space	0.15 ± 0.03	0.32 ± 0.05	0.24 ± 0.03	18/03/98
	b. Kutcha house	0.15 ± 0.01	0.30 ± 0.03	0.22 ± 0.02	
	c. New building	0.16 ± 0.03	0.39 ± 0.09	0.26 ± 0.04	
Khulna	a. Free space	0.13 ± 0.03	0.33 ± 0.06	0.22 ± 0.04	19/03/98
	b. Kutcha house	0.11 ± 0.01	0.25 ± 0.02	0.19 ± 0.01	
	c. New building	0.17 ± 0.03	0.34 ± 0.06	0.25 ± 0.05	
	d. Old building	0.18 ± 0.03	0.36 ± 0.05	0.26 ± 0.02	
Borguna	a. Free space	0.12 ± 0.03	0.25 ± 0.05	0.18 ± 0.03	20/03/98
	b. Kutcha house	0.13 ± 0.02	0.24 ± 0.03	0.19 ± 0.01	
	c. New building	0.16 ± 0.01	0.37 ± 0.07	0.27 ± 0.04	
	d. Old building	0.17 ± 0.02	0.36 ± 0.05	0.28 ± 0.02	
Shariatpur	a. Free space	0.12 ± 0.03	0.27 ± 0.08	0.19 ± 0.05	21/03/98
	b. Kutcha house	0.14 ± 0.02	0.30 ± 0.04	0.21 ± 0.03	
	c. New building	0.18 ± 0.02	0.38 ± 0.02	0.28 ± 0.03	
	d. Old building	0.18 ± 0.02	0.38 ± 0.02	0.28 ± 0.03	
Chorfashion (Bhola)	a. Free space	0.12 ± 0.02	0.29 ± 0.05	0.21 ± 0.03	22/03/98
	b. Kutcha house	0.10 ± 0.03	0.26 ± 0.04	0.18 ± 0.03	
	c. New building	0.17 ± 0.04	0.32 ± 0.06	0.23 ± 0.05	
	d. Old building	0.25 ± 0.03	0.47 ± 0.05	0.34 ± 0.02	
Barisal	a. Free space	0.14 ± 0.03	0.34 ± 0.07	0.24 ± 0.05	23/03/98
	b. Kutcha house	0.12 ± 0.04	0.29 ± 0.05	0.20 ± 0.05	
	c. New building	0.18 ± 0.03	0.45 ± 0.07	0.30 ± 0.02	
	d. Old building	0.19 ± 0.02	0.43 ± 0.12	0.28 ± 0.05	
Mymensingh	a. Free space	0.14 ± 0.03	0.30 ± 0.06	0.23 ± 0.04	26/03/98
	b. Kutcha house	0.16 ± 0.02	0.36 ± 0.10	0.24 ± 0.04	
	c. New building	0.16 ± 0.03	0.38 ± 0.10	0.26 ± 0.05	
	d. Old building	0.20 ± 0.02	0.45 ± 0.07	0.31 ± 0.01	

Continued

Location	Surrounding	Dose Rate ($\mu\text{Sv/hr}$)			Date of Measurement
		Minimum	Maximum	Trend value	
Kishoregonj	a. Free space	0.13 ± 0.02	0.32 ± 0.07	0.21 ± 0.04	27/03/98
	b. Kutcha house	0.14 ± 0.02	0.30 ± 0.04	0.22 ± 0.04	
	c. New building	0.17 ± 0.03	0.37 ± 0.11	0.25 ± 0.04	
	d. Old building	0.17 ± 0.02	0.34 ± 0.03	0.25 ± 0.05	
Jhenaigati (Sherpur)	a. Free space	0.12 ± 0.02	0.33 ± 0.05	0.23 ± 0.03	28/03/98
	b. Kutcha house	0.15 ± 0.04	0.35 ± 0.05	0.24 ± 0.04	
	c. New building	0.15 ± 0.03	0.35 ± 0.04	0.25 ± 0.02	
Barhatta (Netrokona)	a. Free space	0.13 ± 0.02	0.31 ± 0.04	0.21 ± 0.02	29/03/98
	b. Kutcha house	0.16 ± 0.04	0.33 ± 0.05	0.24 ± 0.04	
	c. New building	0.18 ± 0.02	0.35 ± 0.07	0.25 ± 0.03	
	d. Old building	0.18 ± 0.02	0.30 ± 0.01	0.26 ± 0.01	
Kalihati (Tangail)	a. Free space	0.14 ± 0.03	0.32 ± 0.08	0.23 ± 0.05	30/03/98
	b. Kutcha house	0.13 ± 0.02	0.29 ± 0.04	0.21 ± 0.03	
	c. New building	0.18 ± 0.03	0.42 ± 0.11	0.28 ± 0.05	
	d. Old building	0.16 ± 0.02	0.31 ± 0.02	0.25 ± 0.02	
Aricha (Shibalaya, Manikgonj)	a. Free space	0.13 ± 0.02	0.28 ± 0.05	0.20 ± 0.02	31/03/98
	b. Kutcha house	0.14 ± 0.03	0.32 ± 0.06	0.22 ± 0.04	
	c. New building	0.16 ± 0.02	0.40 ± 0.06	0.28 ± 0.03	
Munsigonj	a. Free space	0.13 ± 0.03	0.33 ± 0.07	0.23 ± 0.03	01/04/98
	b. Kutcha house	0.12 ± 0.03	0.28 ± 0.04	0.21 ± 0.03	
	c. New building	0.17 ± 0.03	0.43 ± 0.08	0.29 ± 0.02	
	d. Old building	0.23 ± 0.04	0.45 ± 0.07	0.31 ± 0.03	
Norsingdi	a. Free space	0.12 ± 0.02	0.31 ± 0.05	0.21 ± 0.03	04/04/98
	b. Kutcha house	0.13 ± 0.03	0.31 ± 0.05	0.22 ± 0.04	
	c. New building	0.16 ± 0.02	0.39 ± 0.07	0.26 ± 0.03	
	d. Old building	0.20 ± 0.02	0.36 ± 0.03	0.28 ± 0.01	

Continued

Location	Surrounding	Dose Rate ($\mu\text{Sv/hr}$)			Date of Measurement
		Minimum	Maximum	Trend value	
Teknaf (Cox's Bazar)	a. Free space	0.14 ± 0.02	0.25 ± 0.05	0.19 ± 0.03	12/04/98
	b. Kutcha house	0.14 ± 0.02	0.28 ± 0.04	0.21 ± 0.03	
	c. New building	0.14 ± 0.02	0.27 ± 0.06	0.19 ± 0.02	
Cox's Bazar Sea Beach	a. On the whole	0.55 ± 0.35	1.04 ± 0.66	0.78 ± 0.49	12-13/04/98
	b. Off shore	0.73 ± 0.26	1.36 ± 0.49	1.02 ± 0.36	
	c. On shore	0.11 ± 0.02	0.23 ± 0.04	0.17 ± 0.02	
Cox's Bazar	a. Free space	0.14 ± 0.02	0.27 ± 0.07	0.19 ± 0.03	13/04/98
	b. Kutcha house	0.16 ± 0.02	0.33 ± 0.06	0.24 ± 0.04	
	c. New building	0.14 ± 0.02	0.29 ± 0.05	0.20 ± 0.04	
Roangchheri (Bandarban)	a. Free space	0.12 ± 0.02	0.30 ± 0.05	0.19 ± 0.03	14/04/98
	b. Kutcha house	0.14 ± 0.04	0.28 ± 0.06	0.20 ± 0.03	
	c. New building	0.15 ± 0.03	0.31 ± 0.05	0.22 ± 0.04	
Chittagong	a. Free space	0.13 ± 0.02	0.27 ± 0.04	0.20 ± 0.03	15/04/98
	b. Kutcha house	0.17 ± 0.03	0.37 ± 0.07	0.27 ± 0.04	
	c. New building	0.18 ± 0.02	0.35 ± 0.04	0.25 ± 0.03	
	d. Old building	0.14 ± 0.04	0.39 ± 0.11	0.24 ± 0.03	
Potenga Sea Beach (Chittagong)	a. Free space	0.13 ± 0.03	0.24 ± 0.06	0.18 ± 0.03	15/04/98
Khagrachheri	a. Free space	0.11 ± 0.03	0.24 ± 0.07	0.17 ± 0.06	16/04/98
	b. Kutcha house	0.14 ± 0.04	0.30 ± 0.09	0.21 ± 0.05	
	c. New building	0.14 ± 0.03	0.32 ± 0.07	0.23 ± 0.04	
Rangamati	a. Free space	0.12 ± 0.02	0.26 ± 0.04	0.18 ± 0.02	17/04/98
	b. Kutcha house	0.14 ± 0.02	0.30 ± 0.04	0.22 ± 0.03	
	c. New building	0.14 ± 0.02	0.38 ± 0.08	0.27 ± 0.04	
Roop Pur (Ishwardi, Pabna)	a. Free space	0.12 ± 0.03	0.27 ± 0.05	0.19 ± 0.03	21/04/98
	b. Kutcha house	0.14 ± 0.02	0.34 ± 0.07	0.24 ± 0.04	
	c. New building	0.15 ± 0.02	0.32 ± 0.07	0.23 ± 0.04	

Continued

Location	Surrounding	Dose Rate ($\mu\text{Sv/hr}$)			Date of Measurement
		Minimum	Maximum	Trend value	
Chuadanga	a. Free space	0.15 ± 0.03	0.33 ± 0.08	0.23 ± 0.06	21/04/98
	b. Kutcha house	0.19 ± 0.03	0.40 ± 0.05	0.30 ± 0.03	
	c. New building	0.18 ± 0.02	0.39 ± 0.06	0.30 ± 0.04	
	d. Old building	0.21 ± 0.02	0.42 ± 0.10	0.30 ± 0.07	
Kuakata (Khepuparda, Patuakhali)	a. Free space	0.14 ± 0.02	0.29 ± 0.02	0.21 ± 0.01	26/04/98
	b. Kutcha house	0.14 ± 0.04	0.30 ± 0.05	0.22 ± 0.04	
	c. New building	0.19 ± 0.01	0.37 ± 0.02	0.27 ± 0.02	
Kuakata Sea Beach	a. On the whole	0.19 ± 0.12	0.40 ± 0.24	0.28 ± 0.16	26/04/98
	b. Off shore	0.34 ± 0.08	0.67 ± 0.20	0.48 ± 0.10	
	c. On shore	0.12 ± 0.03	0.25 ± 0.05	0.18 ± 0.04	
Pirojpur	a. Free space	0.13 ± 0.04	0.27 ± 0.06	0.20 ± 0.04	28/04/98
	b. Kutcha house	0.14 ± 0.01	0.28 ± 0.05	0.21 ± 0.03	
	c. New building	0.18 ± 0.03	0.39 ± 0.06	0.28 ± 0.04	
	d. Old building	0.23 ± 0.02	0.40 ± 0.04	0.30 ± 0.01	
Badalgachhi (Naogaon)	a. Free space	0.17 ± 0.04	0.35 ± 0.12	0.25 ± 0.05	02/05/98
	b. Kutcha house	0.26 ± 0.04	0.56 ± 0.07	0.38 ± 0.02	
	c. New building	0.21 ± 0.02	0.45 ± 0.04	0.33 ± 0.02	
	d. Old building	0.23 ± 0.03	0.52 ± 0.11	0.36 ± 0.02	
Lakshmipur	a. Free space	0.14 ± 0.02	0.33 ± 0.07	0.22 ± 0.03	04/05/98
	b. Kutcha house	0.12 ± 0.03	0.28 ± 0.09	0.18 ± 0.04	
	c. New building	0.17 ± 0.03	0.39 ± 0.08	0.27 ± 0.04	
	d. Old building	0.19 ± 0.02	0.45 ± 0.04	0.28 ± 0.02	
Nabigonj (Habigonj)	a. Free space	0.12 ± 0.03	0.24 ± 0.05	0.18 ± 0.02	07/05/98
	b. Kutcha house	0.13 ± 0.03	0.28 ± 0.08	0.19 ± 0.04	
	c. New building	0.14 ± 0.02	0.30 ± 0.06	0.20 ± 0.04	

Continued

Location	Surrounding	Dose Rate ($\mu\text{Sv/hr}$)			Date of Measurement
		Minimum	Maximum	Trend value	
Sripur (Gazipur)	a. Free space	0.14 ± 0.03	0.30 ± 0.08	0.22 ± 0.04	15/05/98
	b. Kutcha house	0.22 ± 0.03	0.44 ± 0.11	0.31 ± 0.03	
	c. New building	0.19 ± 0.03	0.39 ± 0.03	0.28 ± 0.03	
Ashulia (Savar, Dhaka)	a. Free space	0.15 ± 0.02	0.35 ± 0.06	0.24 ± 0.02	12/06/98
	b. Kutcha house	0.19 ± 0.02	0.39 ± 0.06	0.21 ± 0.03	
	c. New building	0.18 ± 0.02	0.36 ± 0.09	0.26 ± 0.04	
Sonargaon (Narayangonj)	a. Free space	0.15 ± 0.02	0.33 ± 0.08	0.23 ± 0.04	12/06/98
	b. Kutcha house	0.18 ± 0.02	0.38 ± 0.04	0.28 ± 0.04	
	c. New building	0.19 ± 0.02	0.45 ± 0.03	0.30 ± 0.04	
	d. Old building	0.20 ± 0.03	0.45 ± 0.05	0.32 ± 0.04	
Daulatdia Ghat (Rajbardi)	a. Free space	0.13 ± 0.03	0.28 ± 0.03	0.21 ± 0.01	12/03/98
Madaripur	a. Free space	0.14 ± 0.01	0.33 ± 0.04	0.22 ± 0.02	21/03/98
BUET (Dhaka City)	a. Free space	0.14 ± 0.02	0.34 ± 0.06	0.22 ± 0.02	13/06/98
	b. New building	0.20 ± 0.06	0.38 ± 0.13	0.29 ± 0.09	
	c. Old building	0.17 ± 0.02	0.39 ± 0.03	0.30 ± 0.02	

Table 4.4: Activity of Radionuclides in Soil Samples Collected From Different Locations in Bangladesh.

Sl. No.	Location	Activity (Bq/kg)			
		²³² Th	²³⁸ U	⁴⁰ K	¹³⁷ Cs
01	Akhaura	81.63 ± 7.92	49.11 ± 8.61	373.83 ± 61.83	4.04 ± 1.62
02	Srimangal	74.13 ± 6.03	35.61 ± 7.61	333.31 ± 56.53	*ND
03	Sunamgonj	104.82 ± 7.30	45.08 ± 9.04	915.66 ± 72.65	9.72 ± 1.98
04	Jajlong	83.34 ± 7.97	42.07 ± 7.80	480.36 ± 58.49	26.79 ± 2.23
05	Comilla	65.94 ± 6.46	34.99 ± 8.24	636.23 ± 65.42	4.67 ± 1.59
06	Chandpur	65.24 ± 6.45	29.73 ± 8.27	467.29 ± 63.26	ND
07	Feni	74.00 ± 9.27	46.20 ± 9.45	729.69 ± 72.97	10.56 ± 2.03
08	Noakhali	76.49 ± 6.80	37.48 ± 8.69	632.79 ± 67.77	7.61 ± 1.79
09	Hatiya	81.11 ± 8.65	37.36 ± 8.44	672.18 ± 67.22	4.98 ± 1.62
10	Sandweep	92.26 ± 9.56	46.23 ± 9.38	758.84 ± 73.49	6.03 ± 1.80
11	Dinajpur	104.98 ± 9.07	74.28 ± 9.19	848.31 ± 69.02	7.93 ± 1.83
12	Syedpur	96.51 ± 8.88	54.51 ± 8.67	564.34 ± 64.70	5.09 ± 1.67
13	Panchagarh	110.95 ± 9.08	73.52 ± 9.33	815.96 ± 67.94	3.44 ± 1.62
14	Rangpur	123.99 ± 8.72	64.51 ± 8.41	869.87 ± 64.34	12.31 ± 1.85
15	Gaibandha	81.20 ± 8.51	43.54 ± 8.60	718.91 ± 66.86	7.07 ± 1.72
16	Kurigram	124.59 ± 9.35	62.95 ± 9.13	740.47 ± 67.58	17.00 ± 2.03
17	Bogra	101.03 ± 8.94	55.88 ± 8.77	664.99 ± 66.50	5.66 ± 1.67
18	Ullapara	93.64 ± 8.91	61.10 ± 8.99	812.37 ± 67.94	16.74 ± 2.09
19	Natore	71.48 ± 8.41	43.47 ± 8.30	715.31 ± 66.50	2.76 ± 1.51
20	Rajshahi	92.85 ± 8.80	54.08 ± 8.85	657.80 ± 66.14	6.42 ± 1.67
21	Nachole	128.21 ± 7.83	76.06 ± 7.58	402.59 ± 53.56	5.97 ± 1.33
22	Kushtia	83.47 ± 9.39	56.23 ± 9.65	611.07 ± 71.17	3.81 ± 1.70
23	Faridpur	70.83 ± 8.31	40.54 ± 8.50	744.06 ± 66.86	5.58 ± 1.64
24	Gopalganj	76.08 ± 8.54	45.91 ± 8.56	553.56 ± 64.70	ND
25	Jessore	80.88 ± 8.59	50.35 ± 8.69	751.26 ± 67.22	4.38 ± 1.64

*ND → Not Detected.

Continued

Sl. No.	Location	Activity (Bq/kg)			
		²³² Th	²³⁸ U	⁴⁰ K	¹³⁷ Cs
26	Shyamnagar	81.33 ± 7.99	44.50 ± 7.90	747.66 ± 62.19	6.68 ± 1.41
27	Khulna	85.69 ± 8.62	48.92 ± 8.67	923.79 ± 69.02	3.49 ± 1.54
28	Borguna	80.80 ± 8.57	39.69 ± 8.22	736.87 ± 66.50	6.39 ± 1.72
29	Shariatpur	92.36 ± 8.83	46.12 ± 8.63	830.34 ± 68.30	ND
30	Chorfashion	87.49 ± 8.68	44.29 ± 8.59	693.75 ± 66.14	ND
31	Barisal	81.50 ± 8.62	43.87 ± 8.63	873.47 ± 69.02	4.36 ± 1.62
32	Mymensingh	93.35 ± 8.41	50.48 ± 8.31	704.53 ± 63.98	7.02 ± 1.64
33	Kishoregonj	85.62 ± 8.62	40.78 ± 8.24	733.29 ± 67.22	6.81 ± 1.67
34	Jhenaigati	58.55 ± 8.11	30.32 ± 8.14	355.86 ± 61.83	4.30 ± 1.56
35	Barhatta	80.27 ± 8.47	38.54 ± 8.33	603.88 ± 65.42	13.07 ± 1.96
36	Kalihati	85.18 ± 8.72	37.36 ± 8.14	470.88 ± 63.62	3.55 ± 1.59
37	Aricha	69.79 ± 8.34	36.50 ± 8.39	664.99 ± 65.78	4.04 ± 1.64
38	Munsigonj	86.89 ± 8.72	40.08 ± 8.70	744.07 ± 67.22	5.19 ± 1.64
39	Norsingdi	79.47 ± 8.53	37.07 ± 8.33	657.80 ± 65.78	8.24 ± 1.72
40	Teknaf	105.59 ± 9.02	45.01 ± 8.49	524.80 ± 64.34	8.58 ± 1.83
41	Cox's Bazar	56.04 ± 8.03	18.39 ± 7.76	434.94 ± 62.90	ND
42	Sea Beach	1085.99 ± 20.01	455.99 ± 16.35	25.16 ± 5.39	ND
43	Roangchheri	58.28 ± 7.73	23.71 ± 7.49	492.45 ± 60.39	3.34 ± 1.43
44	Chittagong	65.07 ± 8.32	32.00 ± 8.29	726.10 ± 66.86	6.26 ± 1.70
45	Khagrachheri	68.47 ± 8.36	30.20 ± 8.13	727.75 ± 62.90	ND
46	Rangamati	45.28 ± 7.86	22.23 ± 6.72	373.83 ± 62.54	3.86 ± 1.59
47	Roop Pur	74.20 ± 8.45	36.14 ± 8.41	636.23 ± 65.78	ND
48	Chuadanga	73.44 ± 8.42	40.16 ± 8.30	593.10 ± 65.06	4.15 ± 1.56
49	Kuakata	101.33 ± 9.01	58.75 ± 8.71	442.13 ± 63.26	4.04 ± 1.64
50	Sea Beach	269.04 ± 11.62	110.84 ± 10.22	266.00 ± 24.80	ND
51	Pirojpur	104.75 ± 9.07	49.88 ± 8.39	381.02 ± 62.19	ND
52	Badalgachhi	103.30 ± 9.07	59.05 ± 9.00	884.26 ± 69.02	4.49 ± 1.67

Continued

Sl. No.	Location	Activity (Bq/kg)			
		²³² Th	²³⁸ U	⁴⁰ K	¹³⁷ Cs
53	Lakshmipur	77.07 ± 8.53	34.97 ± 7.66	776.42 ± 67.22	ND
54	Nobigonj	39.27 ± 7.74	17.84 ± 6.21	276.78 ± 61.47	4.22 ± 1.59
55	Sripur	93.56 ± 8.87	56.17 ± 8.83	298.35 ± 61.47	4.88 ± 1.64
56	Ashulia	66.07 ± 8.24	38.19 ± 8.13	294.75 ± 61.47	ND
57	Sonargaon	77.98 ± 8.59	41.82 ± 8.46	740.47 ± 66.86	ND
58	BUET, Dhaka	81.94 ± 8.60	39.77 ± 8.23	514.01 ± 64.34	5.22 ± 1.70

Table 4.5: Average Outdoor Radiation Dose Level Throughout Bangladesh.

Sl. No.	Location	Average Dose Rate (mSv.y ⁻¹)			
		At the Point of Sample Collection	At the Area (Location) of sample Collection	Due to Radionuclides in Soil*	Due to Cosmic Radiation†
01	Akhaura	1.58	1.49	1.12	0.46
02	Srimangal	1.49	1.40	0.96	0.53
03	Sunamgonj	1.66	1.49	1.67	0.09
04	Jaflong	1.58	1.58	1.45	0.43
05	Comilla	1.84	1.58	1.05	0.79
06	Chandpur	1.66	1.58	0.93	0.73
07	Feni	1.50	1.49	1.32	0.26
08	Noakhali	1.31	1.49	1.15	0.16
09	Hatiya	1.66	1.58	1.21	0.45
10	Sandweep	1.58	1.49	1.39	0.18
11	Dinajpur	1.84	1.66	1.69	0.15
12	Syedpur	2.10	1.75	1.37	0.74
13	Panchagarh	1.75	1.75	1.72	0.04
14	Rangpur	2.54	2.28	1.88	0.74
15	Gaibandha	1.40	1.66	1.27	0.14
16	Kurigram	2.10	1.93	1.83	0.37
17	Bogra	1.66	1.84	1.46	0.20
18	Ullapara	1.75	1.75	1.65	0.24
19	Natore	1.58	1.58	1.19	0.39
20	Rajshahi	1.93	1.84	1.38	0.54
21	Nachole	2.19	2.45	1.65	0.54
22	Kushtia	1.84	1.66	1.29	0.54
23	Faridpur	1.75	1.66	1.18	0.57
24	Gopalganj	1.84	1.75	1.15	0.69
25	Jessore	1.75	1.75	1.32	0.44
26	Shyamnagar	2.10	2.10	1.29	0.81
27	Khulna	2.01	1.93	1.44	0.58
28	Borguna	2.10	1.58	1.25	0.85

* Calculated by employing computer software RESRAD & GENII.

† Estimated value

Continued

Sl. No.	Location	Average Dose Rate (mSv.y ⁻¹)			
		At the Point of Sample Collection	At the Area (Location) of sample Collection	Due to Radionuclides in Soil*	Due to Cosmic Radiation†
29	Shariatpur	2.28	1.66	1.43	0.85
30	Chorfashion	1.93	1.84	1.31	0.62
31	Barisal	2.01	2.10	1.35	0.66
32	Mymensingh	2.37	2.01	1.39	0.97
33	Kishoregonj	1.84	1.84	1.30	0.54
34	Jhenaigati	1.93	2.01	0.82	1.11
35	Barhatta	1.84	1.84	1.32	0.67
36	Kalihati	1.66	2.01	1.14	0.53
37	Aricha	1.75	1.75	1.11	0.64
38	Munsigonj	2.37	2.01	1.31	1.06
39	Norsingdi	2.01	1.84	1.19	0.83
40	Teknaf	1.93	1.66	1.37	0.56
41	Cox's Bazar	1.93	1.66	0.78	1.15
42	Roangchheri	1.84	1.66	0.86	0.98
43	Chittagong	1.84	1.75	1.08	0.76
44	Khagrachheri	1.58	1.49	1.10	0.48
45	Rangamati	1.66	1.58	0.68	0.98
46	Roop Pur	1.75	1.66	1.13	0.62
47	Chuadanga	2.01	2.01	1.12	0.90
48	Kuakata	1.84	1.84	1.36	0.48
49	Pirojpur	1.84	1.75	1.31	0.53
50	Badalgachhi	2.01	2.19	1.61	0.40
51	Lakshmipur	2.19	1.93	1.22	0.97
52	Nabigonj	1.49	1.58	0.56	0.93
53	Sripur	2.45	1.93	1.21	1.24
54	Ashulia	2.19	2.10	0.89	1.30
55	Sonargaon	2.19	2.01	1.24	0.95
56	BUET, Dhaka	1.84	1.93	1.14	0.70

* Calculated by employing computer software RESRAD & GENII.

† Estimated value

Table 4.6: Activity of Radionuclides in Water Samples Collected From Different Locations in Bangladesh.

Sl. No.	Location	Activity			
		mBq/L		Bq/L	
		²³² Th	²³⁸ U	⁴⁰ K	¹³⁷ Cs
01	Akhaura	241.51 ± 37.98	164.24 ± 32.29	5.19 ± 1.13	4.13 ± 1.52
02	Srimangal	216.12 ± 35.73	157.21 ± 31.16	5.28 ± 1.35	3.79 ± 1.49
03	Sunamgonj	319.43 ± 43.26	191.49 ± 32.28	15.13 ± 1.56	4.00 ± 1.49
04	Jaflong	247.33 ± 38.48	153.62 ± 31.94	6.50 ± 1.75	5.47 ± 1.55
05	Jaflong River	231.25 ± 36.80	142.73 ± 31.97	10.97 ± 1.97	*ND
06	Comilla	209.34 ± 35.04	139.47 ± 30.19	7.31 ± 1.56	4.67 ± 1.55
07	Chandpur	201.56 ± 34.31	171.86 ± 31.98	4.06 ± 1.94	ND
08	Feni	219.92 ± 36.50	175.07 ± 32.40	8.98 ± 1.12	ND
09	Noakhali	232.65 ± 37.10	158.25 ± 31.15	8.13 ± 1.44	ND
10	Hatiya	243.54 ± 38.09	165.35 ± 31.16	9.97 ± 1.56	ND
11	Sandweep	278.58 ± 39.01	169.47 ± 31.29	11.68 ± 1.13	ND
12	Dinajpur	336.07 ± 43.16	229.65 ± 33.16	13.28 ± 1.35	ND
13	Syedpur	295.76 ± 41.30	167.26 ± 31.31	7.68 ± 1.72	ND
14	Panchagarh	337.69 ± 43.55	170.33 ± 31.88	13.25 ± 2.06	ND
15	Rangpur	343.67 ± 44.13	189.48 ± 32.98	15.32 ± 1.35	ND
16	Gaibandha	253.14 ± 39.07	161.85 ± 31.56	11.51 ± 1.94	ND
17	Kurigram	365.36 ± 45.31	174.24 ± 31.70	12.01 ± 1.75	ND
18	Bogra	306.81 ± 43.11	171.85 ± 32.10	8.53 ± 1.85	ND
19	Ullapara	275.08 ± 40.21	163.07 ± 32.28	10.97 ± 1.56	ND
20	Natore	193.86 ± 34.27	104.85 ± 31.28	8.27 ± 1.56	3.71 ± 1.55
21	Rajshahi	271.75 ± 39.06	167.58 ± 32.17	7.95 ± 1.75	ND
22	Nachole	351.94 ± 45.15	228.49 ± 32.44	4.39 ± 1.75	ND
23	Kushtia	249.76 ± 39.00	159.65 ± 30.68	8.52 ± 1.56	ND
24	Faridpur	200.46 ± 35.13	142.14 ± 31.62	11.39 ± 1.56	ND

* Not Detected.

Continued

Sl. No.	Location	Activity			
		mBq/L		Bq/L	
		²³² Th	²³⁸ U	⁴⁰ K	¹³⁷ Cs
25	Gopalganj	224.32 ± 37.30	163.25 ± 32.30	10.77 ± 1.97	ND
26	Jessore	239.44 ± 38.14	146.45 ± 30.86	12.84 ± 1.97	ND
27	Shyamnagar	244.54 ± 38.01	165.06 ± 32.33	13.44 ± 1.32	ND
28	Khulna	233.69 ± 37.94	156.87 ± 31.95	16.57 ± 1.22	ND
29	Borguna	242.96 ± 38.03	161.37 ± 32.16	11.32 ± 1.24	ND
30	Shariatpur	270.71 ± 39.12	174.07 ± 32.23	14.82 ± 1.90	ND
31	Chorfashion	244.85 ± 38.98	168.37 ± 31.15	8.50 ± 1.34	ND
32	Barisal	247.91 ± 37.03	165.09 ± 32.15	12.38 ± 1.21	ND
33	Mymensingh	283.27 ± 41.04	173.66 ± 32.05	12.90 ± 2.19	3.04 ± 1.44
34	Kishoregonj	254.33 ± 38.16	152.44 ± 31.94	11.86 ± 1.35	ND
35	Jhenaigati	144.27 ± 30.16	82.91 ± 27.54	5.82 ± 1.35	3.12 ± 1.47
36	Barhatta	246.53 ± 39.27	148.93 ± 32.20	8.76 ± 1.94	ND
37	Kalihati	275.19 ± 38.33	157.76 ± 32.16	5.82 ± 1.94	ND
38	Aricha	186.98 ± 31.02	105.53 ± 32.31	8.38 ± 1.05	2.72 ± 1.44
39	Munsigonj	257.07 ± 37.06	171.98 ± 31.77	9.51 ± 1.34	3.73 ± 1.47
40	Norsingdi	218.91 ± 36.67	160.17 ± 31.44	8.39 ± 1.35	ND
41	Teknaf	329.98 ± 43.08	218.19 ± 32.86	6.27 ± 1.56	ND
42	Cox's Bazar	171.99 ± 28.23	98.22 ± 28.35	5.77 ± 1.56	ND
43	Roangchheri	177.24 ± 30.17	92.47 ± 28.10	6.33 ± 1.75	3.76 ± 1.44
44	Chittagong	208.46 ± 32.17	132.69 ± 31.89	11.08 ± 1.35	4.51 ± 1.55
45	Khagrachheri	210.79 ± 33.91	167.36 ± 31.23	12.51 ± 1.72	ND
46	Rangamati	228.08 ± 34.13	132.04 ± 30.26	4.63 ± 1.72	2.21 ± 1.41
47	Roop Pur	220.75 ± 35.13	165.17 ± 30.26	9.14 ± 1.75	2.59 ± 1.44
48	Chuadanga	223.74 ± 35.14	159.28 ± 30.08	7.38 ± 1.94	ND
49	Kuakata	299.35 ± 38.05	168.62 ± 31.60	3.51 ± 1.13	2.45 ± 1.44
50	Pirojpur	305.66 ± 43.36	172.31 ± 32.08	3.19 ± 1.88	ND

Continued

Sl. No.	Location	Activity			
		mBq/L		Bq/L	
		²³² Th	²³⁸ U	⁴⁰ K	¹³⁷ Cs
51	Badalgachhi	315.92 ± 44.23	197.36 ± 32.27	10.57 ± 1.13	3.87 ± 1.49
52	Lakshmipur	207.75 ± 35.50	116.84 ± 32.10	8.39 ± 1.56	ND
53	Nabigonj	109.63 ± 29.92	84.69 ± 28.20	3.12 ± 1.13	ND
54	Sripur	289.75 ± 42.60	173.25 ± 31.66	4.20 ± 1.28	ND
55	Ashulia	234.84 ± 35.33	139.08 ± 32.41	5.89 ± 1.75	4.48 ± 1.55
56	Sonargaon	209.51 ± 36.06	118.15 ± 32.08	10.58 ± 1.56	4.45 ± 1.47
57	BUET, Dhaka	245.68 ± 38.94	127.05 ± 32.13	6.76 ± 1.35	ND

Table 4.7: Average Effective Dose Equivalent (H_E) Based on Ingestion of Radionuclides ^{232}Th , ^{238}U , ^{40}K , and ^{137}Cs in 1 Litre Drinking Water.

SL. No.	Location	Radiation Dose ($\mu\text{Sv.L}^{-1}$)	SL. No.	Location	Radiation Dose ($\mu\text{Sv.L}^{-1}$)
01	Akhaura	0.1153 ± 0.0213	30	Shariatpur	0.1244 ± 0.0124
02	Srimangal	0.1088 ± 0.0214	31	Chorfashion	0.0826 ± 0.0092
03	Sunamgonj	0.1630 ± 0.0221	32	Barisal	0.1068 ± 0.0084
04	Jaflong	0.1409 ± 0.0232	33	Mymensingh	0.1532 ± 0.0235
05	Jaflong River	0.0956 ± 0.0128	34	Kishoregonj	0.1036 ± 0.0092
06	Comilla	0.1314 ± 0.0226	35	Jhenaigati	0.0936 ± 0.0211
07	Chandpur	0.0513 ± 0.0125	36	Barhatta	0.0835 ± 0.0126
08	Feni	0.0836 ± 0.0078	37	Kalihati	0.0683 ± 0.0126
09	Noakhali	0.0788 ± 0.0097	38	Aricha	0.1092 ± 0.0201
10	Hatiya	0.0915 ± 0.0104	39	Munsigonj	0.1387 ± 0.0212
11	Sandweep	0.1055 ± 0.0080	40	Norsingdi	0.0792 ± 0.0091
12	Dinajpur	0.1234 ± 0.0094	41	Teknaf	0.0788 ± 0.0106
13	Syedpur	0.0822 ± 0.0114	42	Cox's Bazar	0.0559 ± 0.0101
14	Panchagarh	0.1207 ± 0.0135	43	Roangchheri	0.1085 ± 0.0218
15	Rangpur	0.1349 ± 0.0094	44	Chittagong	0.1523 ± 0.0221
16	Gaibandha	0.1018 ± 0.0126	45	Khagrachheri	0.1043 ± 0.0112
17	Kurigram	0.1157 ± 0.0117	46	Rangamati	0.0842 ± 0.0215
18	Bogra	0.0887 ± 0.0122	47	Roop Pur	0.1179 ± 0.0219
19	Ullapara	0.1005 ± 0.0105	48	Chuadanga	0.0733 ± 0.0125
20	Natore	0.1220 ± 0.0226	49	Kuakata	0.0886 ± 0.0203
21	Rajshahi	0.0817 ± 0.0115	50	Pirojpur	0.0555 ± 0.0124
22	Nachole	0.0697 ± 0.0117	51	Badalgachhi	0.1536 ± 0.0210
23	Kushtia	0.0828 ± 0.0104	52	Lakshmipur	0.0763 ± 0.0103
24	Faridpur	0.0953 ± 0.0102	53	Nabigonj	0.0332 ± 0.0076
25	Gopalganj	0.0946 ± 0.0127	54	Sripur	0.0603 ± 0.0090
26	Jessore	0.1081 ± 0.0128	55	Ashulia	0.1224 ± 0.0232
27	Shyamnagar	0.1131 ± 0.0090	56	Sonargaon	0.1479 ± 0.0217
28	Khulna	0.1311 ± 0.0084	57	BUET, Dhaka	0.0701 ± 0.0092
29	Borguna	0.0996 ± 0.0086	—	—	—

Table 4.8: Average Annual Effective Dose Equivalent (H_E) Based on Ingestion of Radionuclides ^{232}Th , ^{238}U , ^{40}K , and ^{137}Cs through Drinking Water.

SL. No.	Location	*Radiation Dose ($\mu\text{Sv.y}^{-1}$)	SL. No.	Location	*Radiation Dose ($\mu\text{Sv.y}^{-1}$)
01	Akhaura	84.18 ± 15.55	30	Shariatpur	90.85 ± 9.05
02	Srimangal	79.43 ± 15.62	31	Chorfashion	60.32 ± 6.68
03	Sunamgonj	134.04 ± 16.10	32	Barisal	77.98 ± 6.10
04	Jaflong	102.87 ± 16.94	33	Mymensingh	111.84 ± 17.14
05	Jaflong River	69.77 ± 9.31	34	Kishoregonj	75.66 ± 6.70
06	Comilla	95.94 ± 16.51	35	Jhenaigati	68.30 ± 15.39
07	Chandpur	37.43 ± 9.14	36	Barhatta	60.99 ± 9.23
08	Feni	61.04 ± 5.73	37	Kalihati	49.89 ± 9.21
09	Noakhali	57.50 ± 7.05	38	Aricha	79.69 ± 14.65
10	Hatiya	66.79 ± 7.58	39	Munsigonj	101.23 ± 15.45
11	Sandweep	77.02 ± 5.83	40	Norsingdi	57.82 ± 6.66
12	Dinajpur	90.05 ± 6.85	41	Teknaf	57.55 ± 7.70
13	Syedpur	60.00 ± 8.33	42	Cox's Bazar	40.82 ± 7.37
14	Panchagarh	88.12 ± 9.83	43	Roangchheri	79.21 ± 15.95
15	Rangpur	98.51 ± 6.87	44	Chittagong	111.21 ± 16.11
16	Gaibandha	74.29 ± 9.22	45	Khagrachheri	76.15 ± 8.17
17	Kurigram	84.49 ± 8.55	46	Rangamati	61.49 ± 15.68
18	Bogra	64.73 ± 8.92	47	Roop Pur	86.08 ± 16.00
19	Ullapara	73.36 ± 7.63	48	Chuadanga	53.54 ± 9.14
20	Natore	89.03 ± 16.51	49	Kuakata	64.66 ± 14.85
21	Rajshahi	59.62 ± 8.41	50	Pirojpur	40.50 ± 9.05
22	Nachole	50.84 ± 8.54	51	Badalgachhi	112.12 ± 15.36
23	Kushtia	60.46 ± 7.59	52	Lakshmipur	55.68 ± 7.52
24	Faridpur	69.58 ± 7.51	53	Nabigonj	24.20 ± 5.57
25	Gopalganj	69.05 ± 9.32	54	Sripur	44.03 ± 6.54
26	Jessore	78.90 ± 9.33	55	Ashulia	89.41 ± 16.91
27	Shyamnagar	82.55 ± 6.58	56	Sonargaon	107.98 ± 15.86
28	Khulna	95.73 ± 6.17	57	BUET, Dhaka	51.18 ± 6.73
29	Borguna	72.73 ± 6.25	—	—	—

* Annual Effective Dose Equivalent is estimated on the assumption that an adult person of Bangladesh intake 2 L water per day in an average (730 L per year).

Table 4.9: Data Exhibiting the Range and Average Values of Minimum Dose Rates, Maximum Dose Rates, and Trend Dose Rates; Found in Kutcha-Houses, New-Buildings, Old-Buildings, and Free-Spaces; in Different Locations of Bangladesh.

Dose Level for-	Minimum \pm 1σ ($\mu\text{Sv/hr}$)	Location	Maximum \pm 1σ ($\mu\text{Sv/hr}$)	Location	Average \pm 1σ ($\mu\text{Sv/hr}$)
Kutcha Houses					
Minimum Dose Rate	0.10 ± 0.03	Srimangal, and, Chorfashion,	0.28 ± 0.03	Nachole	0.15 ± 0.03
Maximum Dose Rate	0.20 ± 0.05	Sandweep	0.56 ± 0.07	Badalgachhi	0.31 ± 0.06
Average (Trend) Dose Rate	0.17 ± 0.01	Maulavibazar, and, Sandweep	0.38 ± 0.02	Badalgachhi	0.23 ± 0.04
New Building					
Minimum Dose Rate	0.12 ± 0.03	Maulavibazar, and Sandweep	0.21 ± 0.02	Badalgachhi	0.16 ± 0.02
Maximum Dose Rate	0.22 ± 0.04	Srimangal	0.45 ± 0.04	Badalgachhi	0.34 ± 0.06
Average (Trend) Dose Rate	0.18 ± 0.02	Maulavibazar, Srimangal, and Sandweep	0.33 ± 0.02	Badalgachhi	0.25 ± 0.04
Old Building					
Minimum Dose Rate	0.14 ± 0.04	Chittagong	0.25 ± 0.03	Chorfashion	0.19 ± 0.03
Maximum Dose Rate	0.26 ± 0.05	Srimangal	0.52 ± 0.11	Badalgachhi	0.37 ± 0.06
Average (Trend) Dose Rate	0.19 ± 0.01	Akhaura	0.36 ± 0.02	Badalgachhi	0.27 ± 0.04
Free Space					
Minimum Dose Rate	0.11 ± 0.02	Maulavibazar, and, Khagrachheri	0.17 ± 0.03	Nachole, and, Badalgachhi	0.13 ± 0.01
Maximum Dose Rate	0.19 ± 0.03	Sylhet	0.37 ± 0.05	Nachole	0.27 ± 0.04
Average (Trend) Dose Rate	0.16 ± 0.02	Srimangal, Sylhet, and, Sitakundo	0.28 ± 0.04	Nachole	0.20 ± 0.07

* The average of the average dose levels in all types of houses i.e. average indoor dose level is $(0.24 \pm 0.04) \mu\text{Sv/hr}$.

** In every dose measuring points, the minimum dose level, the maximum dose level, and the trend dose levels were noted. The above table is an analysis of the findings of each type of data; viz., the minimum of minimum dose rates observed, the maximum of minimum dose rates observed, the minimum of maximum dose rates observed, the average of the average (trend) dose rates observed etc.

Table 4.10: Mean Dose Levels Found from Average Dose Rates in Kutcha-Houses, New-Buildings, Old-Buildings, and Free-Spaces Throughout Bangladesh.

Dose Level for-	Arithmetic		Geometric*	
	Mean ($\mu\text{Sv/hr}$)	Standard Deviation ($\mu\text{Sv/hr}$)	Mean ($\mu\text{Sv/hr}$)	Standard Deviation†
Kutcha Houses	0.23	0.04	0.23	1.24
New Buildings	0.25	0.04	0.25	1.19
Old Buildings	0.27	0.04	0.27	1.17
Free Spaces	0.20	0.07	0.20	1.17

* Geometric mean and standard deviations were estimated from the corresponding cumulative frequency plot (probability plot).

† The geometric standard deviation has no unit.

Table 4.11: Comparison of Average Environmental Radiation Dose Level in Some of the Countries of the World.

Sl. No.	Location	Dose Level (mSv.y ⁻¹)	Reference No. (year)
1	Bangladesh (outdoor)	2.0 (1.0 – 3.9)	32 (1975–1979)
2	Japan (outdoor)	0.48	38 (1981)
3	Ireland (indoor)	0.55	53 (1985)
4	Netherlands (individual monitoring)	0.58	57 (1985)
5	UK (indoor)	(0.31 – 0.61)	58 (1985)
6	Petalona Cave, Greece (natural)	(0.19 – 0.67)	61 (1986)
7	Taiwan (natural)	0.50	66 (1987)
8	Hongkong (terrestrial)	1.11	78 (1992)
9	Iraq (external gamma)	0.39	80 (1992)
10	China (environmental)	0.42	83 (1992)
11	India (external gamma)	0.42	89 (1993)
12	Spain (terrestrial)	0.29	89 (1994)
13	Karnataka, India (external gamma)	0.45 (0.16 – 1.07)	91 (1994)
14	Ustica, Italy : outdoor→ : indoor→	< 0.49 (0.49 – 1.02)	102 (1997)
15	Algeria (environmental)	(0.12 – 0.81)	109 (1998)
16	Aeolian Islands, Vulcano (indoor)	(1.12 – 1.69)	136(1995)
17	Chittagong, Bangladesh (natural)	1.32 ± 0.22	113 (1996)
18	Bangladesh : indoor→ : outdoor→	2.10 ± 0.35 (0.88 ± 0.26 to 4.91 ± 0.61) 1.75 ± 0.61 (0.96 ± 0.18 to 3.24 ± 0.44)	Present Study (1998)

† In developing the above table, it is assumed that 1 Gy = 0.7 Sv, 1R = 0.0096 Gy, and, 100 rad = 1 Gy.

* Data given in parenthesis indicates range.

☆ Average indoor to average outdoor dose ratio in Bangladesh is 1.2.

Table 4.12: Average Annual Effective Dose Equivalent and Annual Collective Dose Equivalent Due to Environmental Radition in Different Locations of Bangladesh.

Map Ref. Number	Location (District Covered)	Area (Sq. km)	Population in 1998†	Average Dose Rate (mSv.y ⁻¹)	Annual Collective Dose Equivalent (Person-Sv)
01	Akhaura (Brahminbaria)	1927	23,06,556	1.68	3875
02	Srimangal (Maulavibazar)	2799	14,78,718	1.55	2292
03	Sunamgonj	3670	18,32,634	1.75	3207
04	Jaflong (Sylhet)	3490	23,19,777	1.68	3897
05	Comilla	3085	43,35,471	1.72	7457
06	Chandpur	1704	21,85,533	1.64	3584
07	Feni	928	11,77,686	1.65	1943
08	Noakhali*	2093	20,36,275	1.56	3177
09	Hatiya	1508	3,50,624	1.65	579
10	Sandweep	762	3,39,247	1.55	509
11	Dinajpur	3438	24,11,307	2.03	4895
12	Syedpur (Nilphamari)	1641	14,40,072	2.23	3211
13	Panchagarh (Panchagarh & Thakurgaon)	3214	18,35,685	2.04	3745
14	Rangpur	2308	23,07,573	2.10	4846
15	Gaibandha	2179	20,75,697	2.00	4151
16	Kurigram (Kurigram & Lalmonirhat)	3538	27,25,560	2.10	5724
17	Bogra (Bogra & Joypurhat)	3885	36,62,217	2.37	8679
18	Ullapara (Sirajgonj)	2498	24,14,358	1.83	4418
19	Natore	1896	14,79,735	1.90	2811
20	Rajshahi	2407	20,21,796	2.00	4044
21	Nachole (Chapai Nawabgonj)	1702	12,52,944	2.88	3608
22	Kushtia (Kushtia & Jhenidah)	3582	30,33,711	1.93	5855
23	Faridpur (Faridpur & Rajbari)	3192	24,64,191	1.94	4781
24	Gopalganj (Gopalganj & Narail)	2480	18,09,243	1.87	3383
25	Jessore (Jessore & Magura)	3616	29,94,048	2.06	6168
26	Shyamnagar (Satkhira)	3858	16,88,220	2.04	3444
27	Khulna	4395	21,66,210	1.84	3986

* Excluding Hatiya.

† The population in 1998 in different locations were estimated by extrapolating the data of population in 1997 and 1996⁽¹³⁴⁾ by considering the population growth rate 1.7%⁽¹³⁷⁾ (overlooking the migration rate).

Continued

Map Ref. Number	Location (District Covered)	Area (Sq. km)	Population in 1998†	Average Dose Rate (mSv.y ⁻¹)	Annual Collective Dose Equivalent (Person-Sv)
28	Borguna	1832	8,18,685	1.75	1433
29	Shariatpur (Shariatpur & Madaripur)	2326	21,27,564	1.94	4127
30	Chorfashion (Bhola)	3403	15,58,044	1.74	2711
31	Barisal (Barisal & Jhalokathi)	3549	30,43,881	2.01	6118
32	Mymensingh	4363	41,65,632	2.11	8789
33	Kishoregonj	2689	24,28,596	1.94	4711
34	Jhenaigati (Sherpur & Jamalpur)	3396	31,74,057	2.09	6634
35	Barhatta (Netrakona)	2810	18,21,447	2.03	3698
36	Kalihati (Tangail)	3414	31,60,836	2.00	6322
37	Aricha (Manikgonj)	1379	12,37,689	1.96	2426
38	Munsigonj	955	12,49,893	2.02	2525
39	Norsingdi	1141	17,39,070	1.96	3409
40	Teknaf	389	1,83,069	1.75	320
41	Cox's Bazar*	2103	13,44,465	1.90	2554
42	Roangchheri (Bandarban)	4479	2,50,182	1.75	438
43	Chittagong**	4521	55,02,401	1.87	10289
44	Khagrachheri	2700	3,71,205	1.75	650
45	Rangamati	6116	4,37,310	1.88	822
46	Roop Pur (Pabna)	2371	20,50,272	1.94	3978
47	Chuadanga (Chuadanga & Meherpur)	1874	13,78,035	2.42	3335
48	Kuakata (Patuakhali)	3205	13,45,491	1.97	2651
49	Pirojpur (Pirojpur & Bagerhat)	5267	26,37,081	1.91	5037
50	Badalgachhi (Naogaon)	3436	22,89,267	2.88	6593
51	Lakshmipur	1456	14,14,647	1.82	2575
52	Nabigonj (Habigonj)	2637	16,38,387	1.65	2703
53	Sripur (Gazipur)	1741	17,11,611	2.41	4125
55	Sonargaon (Narayanganj)	759	18,49,923	2.34	4329
54 & 56	Ashulia & BUET (Dhaka)	1464	62,67,771	2.00	12536

* Excluding Teknaf. **Excluding Sandweep.

† The population in 1998 in different locations were estimated by extrapolating the data of population in 1997 and 1996⁽¹³⁴⁾ by considering the population growth rate 1.7%⁽¹³⁷⁾ (overlooking the migration rate).

Table 4.13: Comparison of Radiation Dose Levels in Some of the Sea Beaches of the World.

SL. No	Location	*Radiation Dose (mSv.y ⁻¹)	Reference No. (Year)
1	Brazil	3.07 – 3.68	89
2	Ullal sea beach, Karnataka, India.	**0.55 – 4.13	89 (1993)
3	Cox's Bazar sea beach, Bangladesh	13 (2.6 – 44)	32 (1975 – 1979)
4	Cox's Bazar sea beach, Bangladesh	8.94 ± 3.15 (6.39 ± 2.28 to 11.91 ± 4.29) [in shining brown-coloured sandy areas] 1.49 ± 0.18 (0.96 ± 0.18 to 2.01 ± 0.35) [in public movement areas]	Present Study (1998)
5	Kuakata sea beach, Bangladesh	4.20 ± 0.88 (2.98 ± 0.70 to 5.87 ± 0.18) [in shining brown-coloured sandy areas] 1.58 ± 0.35 mSv.y ⁻¹ (1.05 ± 0.26 to 2.19 ± 0.44 mSv.y ⁻¹) [in public movement areas]	Present Study (1998)

* In developing the above table, the conversion factor 1Gy = 0.7Sv, is employed.

** Individual dose equivalent upto 20.02 mSv.y⁻¹ was also reported.

† Data given in parenthesis indicates range.

Table 4.14: The Range and Average Activities of Radionuclides in Soil and Water Samples Collected from 56 Locations Throughout Bangladesh.

Name of Radionuclide	Minimum Activity $\pm 1\sigma$	Location	Maximum Activity $\pm 1\sigma$	Location	Average Activity $\pm 1\sigma$
For Soil Samples (Bq/kg)					
²³² Th	39.27 \pm 7.74	Nabigonj	128.21 \pm 7.83	Nachole	83.56 \pm 17.96
²³⁸ U	17.84 \pm 6.21	Nabigonj	76.06 \pm 7.58	Nachole	44.35 \pm 12.65
⁴⁰ K	276.78 \pm 61.47	Nabigonj	923.79 \pm 69.02	Khulna	630.89 \pm 173.85
¹³⁷ Cs	†2.76 \pm 1.51	Natore	26.79 \pm 2.23	Jaflong	5.37 \pm 4.87
For Water Samples (²³²Th & ²³⁸U are in mBq/L; ⁴⁰K & ¹³⁷Cs are in Bq/L)					
²³² Th	109.06 \pm 29.92	Nabigonj	365.36 \pm 45.31	Kurigram	249.59 \pm 51.67
²³⁸ U	82.91 \pm 27.54	Jhenaigati	229.65 \pm 33.16	Dinajpur	156.77 \pm 30.46
⁴⁰ K	3.12 \pm 1.13	Nabigonj	16.57 \pm 1.22	Khulna	9.08 \pm 3.36
¹³⁷ Cs	†2.21 \pm 1.41	Rangamati	5.47 \pm 1.55	Jaflong	1.17 \pm 1.80

Table 4.15: Average Concentrations of Radionuclides in Soil and Water Samples.

Name of the Radionuclide	Arithmetic		Geometric*	
	Mean	Standard Deviation	Mean	Standard Deviation**
For Soil Samples (Bq/kg)				
²³² Th	83.56	17.96	83.50	1.23
²³⁸ U	44.35	12.65	44.30	1.32
⁴⁰ K	630.89	173.85	632.0	1.32
¹³⁷ Cs	5.37	4.87	5.30	1.96
For Water Samples (²³²Th & ²³⁸U are in mBq/L; ⁴⁰K & ¹³⁷Cs are in Bq/L)				
²³² Th	249.59	51.67	250.0	1.23
²³⁸ U	156.77	30.46	157.0	1.14
⁴⁰ K	9.08	3.36	9.10	1.42
¹³⁷ Cs	1.17	1.80	0.61 (from extrapolated curve)	6.07

* Geometric Mean and Standard Deviation were found from the corresponding Cumulative Frequency Plot (Probability Plot).

** Geometric Standard Deviation has no unit as it is simply a ratio between the corresponding values of 50% and 84.1% cumulative frequency.

† These minimum activities are the corresponding minimum activities detected above the MDC (ignoring All ND activities). In calculating the average values, all ND values were assumed to zero.

Table 4.16: Comparison of Data on Average Radioactivity (Bq.kg^{-1}) in Surface Soil in Different Countries of the World.

SL. No.	Location	^{238}U	^{232}Th	^{40}K	^{137}Cs	Resulting dose rate due to soil radioactivity	Reference number (Year)
1	Bangladesh	*NA	NA	NA	(0.74 – 75.11)	NA	34 (1976)
2	US	37.00 ± 30.71 **(4.44 – 140.60)	36.26 ± 54.02 (3.70 – 125.80)	NA	NA	NA	44 (1983)
3	Hawaii	NA	NA	NA	(1.48 – 71.41)	NA	45 (1984)
4	Louisiana, US	14 ± 2	36 ± 4	472 ± 13	23 ± 1	NA	63 (1986)
5	Taiwan	30 (22 – 45)	44 (30 – 71)	431 (265 – 607)	NA	0.47 mGy.y^{-1}	66 (1987)
6	Montana, US	NA	NA	NA	(20 – 200)	NA	72 (1989)
7	Milos Island, Greece	50 ± 21 (^{226}Ra)	57 ± 21	877 ± 332	NA	NA	77 (1991)
8	Pantelleria, Italy	(12.1 – 168.5)	(11.6 – 165.5)	(27.7 – 1295.0)	NA	1.4 mGy.y^{-1}	81 (1992)
9	Southern Chile	NA	NA	NA	(3.8 ± 0.02 to 17.1 ± 0.07)	NA	85 (1993)
10	Nile Delta, Egypt	(5.2 ± 2.1 to 63.7 ± 6.2)	(1.1 ± 0.03 to 95.6 ± 26.0)	(29 ± 1.3 to 653 ± 12.9)	NA	0.27 mGy.y^{-1}	86 (1993)
11	Rio Grande do Norte, Brazil	29.0 ± 19.4 (^{226}Ra) (10.3 – 137.6)	46.6 ± 36.2 (12.0 – 191.0)	677.8 ± 434.9 (56.4 – 1972.0)	NA	$0.71 \pm 0.37 \text{ mGy.y}^{-1}$	87 (1993)
12	China	40 ± 34 (1.8 – 520)	49 ± 28 (1.5 – 440)	580 ± 200 (12 – 2190)	NA	0.63 mGy.y^{-1}	1 (1993)
13	US	35 (4 – 140)	35 (4 – 130)	370 (100 – 700)	NA	0.48 mGy.y^{-1}	1 (1993)

*NA \Rightarrow Not Available.

**Data given in parenthesis indicates range.

Continued

SL. No.	Location	^{238}U	^{232}Th	^{40}K	^{137}Cs	Resulting dose rate due to soil radioactivity	Reference number (Year)
14	Spain	39 (^{226}Ra) (8 - 310)	41 (5 - 258)	578 (31 - 2040)	NA	0.47 mGy.y ⁻¹	89 (1994)
15	Savar, Dhaka	(32.43 - 48.73) (^{214}Bi)	(21.55 - 25.98) (^{208}Tl)	(322.10 - 326.51)	(below MDC to 3.17)	NA	92 (1994)
16	Louisiana, US	14.4 ± 1.44 to 53.6 ± 5.36 ^{226}Ra (^{214}Bi)	10.8 ± 1.08 to 61.6 ± 6.16 (^{228}Ac)	NA	NA	NA	94 (1995)
17	Taiwan	NA	NA	NA	5	NA	99 (1996)
18	Ustica, Italy	15 - 164	16 - 174	201 - 1350	NA	NA	102 (1997)
19	Majorca, Spain	NA	NA	NA	10 - 60	NA	104 (1997)
20	Dhaka, Bangladesh	33 ± 7 (21 ± 6 to 43 ± 7)	16 ± 4 (9 ± 2 to 22 ± 2)	574 ± 111 (402 ± 78 to 750 ± 82)	7 ± 2 (3 ± 1 to 10 ± 1)	NA	106 (1998)
21	Algeria	5 - 176 (^{226}Ra)	3 - 144 (^{228}Ac)	36 - 1405	0.3 - 0.41	NA	109 (1998)
22	Bangladesh	44.35 ± 12.65 (17.84 ± 6.21 to 76.06 ± 7.58)	83.56 ± 17.96 (39.27 ± 7.74 to 128.21 ± 7.83)	630.89 ± 173.85 (276.78 ± 61.47 to 923.79 ± 69.02)	5.37 ± 4.87 (2.76 ± 1.51 to 26.79 ± 2.23)	1.26 ± 0.27 mSv.y ⁻¹ (0.56 ± 0.08 to 1.88 ± 0.09 mSv.y ⁻¹)	Present Study (1998)

*NA ⇒ Not Available.

**Data given in parenthesis indicates range.

Table 4.17: Radioactivity Levels (Bq.kg⁻¹) of the Radionuclides ²³²Th, ²³⁸U, ⁴⁰K, and ¹³⁷Cs in Beach Sand Samples of Kuakata, Cox's Bazar, and Mangalore (Karnataka, India) Sea Beaches.

SL. No	Location	²³² Th	²³⁸ U	⁴⁰ K	¹³⁷ Cs	Reference No. (Year)
1	Mangalore sea beach, Karnataka, India.	1842 ± 6.6	374 ± 2.6	158 ± 15.3	NA	89 (1993)
2	Cox's Bazar sea beach, Bangladesh	1085.99 ± 20.01	455.99 ± 16.35	25.16 ± 5.39	ND	Present Study (1998)
3	Kuakata sea beach, Bangladesh	269.04 ± 11.62	110.84 ± 10.22	266.00 ± 24.80	ND	Present Study (1998)

*NA ⇒ Not Available.

**ND ⇒ Not Detected.

Table 4.18: Comparison of Data on Average Radioactivity in Drinking Water in Different Countries of the World.

SL. No.	Location	²³⁸ U	²³² Th	⁴⁰ K	¹³⁷ Cs	Annual Dose Due to Intake of Water	Reference No. (Year)
		mBq.L ⁻¹		Bq.L ⁻¹			
1	Finland	107.3 (²²⁶ Ra)	NA	NA	NA	NA	36 (1980)
2	US	(-1.48 ± 1.11 to 81.4 ± 11.1) (²²⁶ Ra)	NA	NA	NA	NA	37 (1981)
3	Iowa	3.7 - 2257	NA	NA	NA	NA	41 (1982)
4	Saudi Arabia	(162.8 - 699.3) (²²⁶ Ra)	NA	NA	NA	NA	47 (1984)
5	European Countries	(<1 - 140)	NA	NA	NA	NA	49 (1985)
6	North Carolina	15.91 (²²⁶ Ra) (4.44 - 110.63)	NA	NA	NA	NA	64 (1987)
7	New York	0.87 ± 0.18	0.050 ± 0.023	NA	NA	NA	68 (1987)
8	Utah, Salt Lake City, USA	17.8 ± 3.33	NA	NA	NA	NA	76 (1990)
9	India	(8.35 - 252.40)	NA	NA	NA	NA	79 (1992)
10	Arizona, US	346.0 ± 9.34 (5.9 ± 0.16 to 2500 ± 67)	NA	NA	NA	NA	93 (1995)
11	Taiwan	12.0 (²²⁶ Ra)	NA	NA	NA	1.8 μSv.y ⁻¹	105 (1997)
12	Chittagong, Bangladesh	45.67 ± 0.18 (11.72 ± 0.05 to 120.00 ± 0.46)	170.96 ± 0.66 (24.55 ± 0.09 to 289.65 ± 1.12)	4.54 ± 0.02 (2.04 ± 0.01 to 12.41 ± 0.05)	Not Detected	60 μSv.y ⁻¹	112 (1996)
13	Bangladesh	156.77 ± 30.46 (82.91 ± 27.54 to 229.65 ± 33.16)	249.59 ± 51.67 (109.06 ± 29.92 to 365.36 ± 45.31)	9.08 ± 3.36 (3.12 ± 1.13 to 16.57 ± 1.22)	1.17 ± 1.80 (2.21 ± 1.41 to 5.47 ± 1.55)	74.01 ± 21.41 μSv.y ⁻¹ (24.20 ± 5.57 to 134.04 ± 16.10 μSv.y ⁻¹)	Present Study (1998)

*NA ⇒ Not Available.

**Data given in parenthesis indicates range.

Table 4.19: The Correlation Coefficients Between the Concentrations of Radionuclides Found in Soil and Water Samples Collected from Different Locations in Bangladesh.

Serial Number	Names of Radionuclides between which correlation coefficient is calculated	Correlation Coefficient (r)
Correlation coefficients between activities of radionuclides found in Soil Samples		
1	^{232}Th and ^{238}U	0.8817
2	^{232}Th and ^{40}K	0.3562
3	^{232}Th and ^{137}Cs	0.2929
4	^{238}U and ^{40}K	0.3411
5	^{238}U and ^{137}Cs	0.1744
6	^{40}K and ^{137}Cs	0.1254
Correlation coefficients between activities of radionuclides found in Water Samples		
1	^{232}Th and ^{238}U	0.8263
2	^{232}Th and ^{40}K	0.2730
3	^{232}Th and ^{137}Cs	0.0097
4	^{238}U and ^{40}K	0.2688
5	^{238}U and ^{137}Cs	0.0564
6	^{40}K and ^{137}Cs	0.1643
Correlation coefficients between the corresponding activities of radionuclides found in Soil & Water Samples		
1	^{232}Th	0.9410
2	^{238}U	0.7069
3	^{40}K	0.8978
4	^{137}Cs	0.6093

Table 4.20: Annual Range and Average Radiation Dose Received ($\mu\text{Sv.y}^{-1}$) Due to Intake of Radionuclides ^{232}Th , ^{238}U , ^{40}K , and ^{137}Cs Through Water in Different Locations of Bangladesh.

Minimum	Location	Maximum	Location	Average $\pm 1\sigma$
24.20 ± 5.57	Nabigonj	134.04 ± 16.10	Sunamgonj	74.01 ± 21.41

Table 4.21: Average Annual Radiation Dose Received ($\mu\text{Sv.y}^{-1}$) Due to Intake of Drinking Water Throughout Whole Bangladesh.

Arithmetic		Geometric*	
Mean	Standard Deviation	Mean	Standard Deviation**
74.01	21.41	74.00	1.32

* Geometric Mean and Standard Deviation were found from the corresponding Cumulative Frequency Plot (Probability Plot).

** Geometric Standard Deviation has no unit as it is simply a ratio between the corresponding values of 50% and 84.1% cumulative frequency.

Table 4.22: Estimated Fatal Cancer Risk in Different Locations of Bangladesh.

Map Ref. Number	Location (District Covered)	Average Dose Rate (mSv.y ⁻¹)	Fatal Cancer Probability Coefficient (Per Million People)†
01	Akhaura (Brahminbaria)	1.68	84
02	Srimangal (Maulavibazar)	1.55	78
03	Sunamgonj	1.75	88
04	Jaflong (Sylhet)	1.68	84
05	Comilla	1.72	86
06	Chandpur	1.64	82
07	Feni	1.65	83
08	Noakhali*	1.56	78
09	Hatiya	1.65	83
10	Sandweep	1.55	78
11	Dinajpur	2.03	102
12	Syedpur (Nilphamari)	2.23	112
13	Panchagarh (Panchagarh & Thakurgaon)	2.04	102
14	Rangpur	2.10	105
15	Gaibandha	2.00	100
16	Kurigram (Kurigram & Lalmonirhat)	2.10	105
17	Bogra (Bogra & Joypurhat)	2.37	119
18	Ullapara (Sirajgonj)	1.83	92
19	Natore	1.90	95
20	Rajshahi	2.00	100
21	Nachole (Chapai Nawabgonj)	2.88	144
22	Kushtia (Kushtia & Jhenidah)	1.93	97
23	Faridpur (Faridpur & Rajbari)	1.94	97
24	Gopalganj (Gopalganj & Narail)	1.87	94
25	Jessore (Jessore & Magura)	2.06	103
26	Shyamnagar (Satkhira)	2.04	102
27	Khulna	1.84	92

* Excluding Hatiya.

† The fatal cancer risk for general public is taken to be $500 \times 10^{-4} \text{ Sv}^{-1}$, i.e., 50 per mSv per million people ($50 \times 10^{-6} \text{ mSv}^{-1}$). The figures in this column are rounded.

Continued

Map Ref. Number	Location (District Covered)	Average Dose Rate (mSv.y ⁻¹)	Fatal Cancer Probability Coefficient (Per Million People)†
28	Borguna	1.75	88
29	Shariatpur (Shariatpur & Madaripur)	1.94	97
30	Chorfashion (Bhola)	1.74	87
31	Barisal (Barisal & Jhalokathi)	2.01	101
32	Mymensingh	2.11	106
33	Kishoregonj	1.94	97
34	Jhenaigati (Sherpur & Jamalpur)	2.09	105
35	Barhatta (Netrakona)	2.03	102
36	Kalihati (Tangail)	2.00	100
37	Aricha (Manikgonj)	1.96	98
38	Munsigonj	2.02	101
39	Norsingdi	1.96	98
40	Teknaf	1.75	88
41	Cox's Bazar*	1.90	95
42	Roangchheri (Bandarban)	1.75	88
43	Chittagong**	1.87	94
44	Khagrachheri	1.75	88
45	Rangamati	1.88	94
46	Roop Pur (Pabna)	1.94	97
47	Chuadanga (Chuadanga & Meherpur)	2.42	121
48	Kuakata (Patuakhali)	1.97	99
49	Pirojpur (Pirojpur & Bagerhat)	1.91	96
50	Badalgachhi (Naogaon)	2.88	144
51	Lakshmipur	1.82	91
52	Nabigonj (Habigonj)	1.65	83
53	Sripur (Gazipur)	2.41	121
55	Sonargaon (Narayangonj)	2.34	117
54 & 56	Ashulia & BUET (Dhaka)	2.00	100

* Excluding Teknaf. ** Excluding Sandweep.

† The fatal cancer risk for general public is taken to be $500 \times 10^{-4} \text{ Sv}^{-1}$; i.e., 50 per mSv per million people ($50 \times 10^{-6} \text{ mSv}^{-1}$). The figures in this column are rounded.

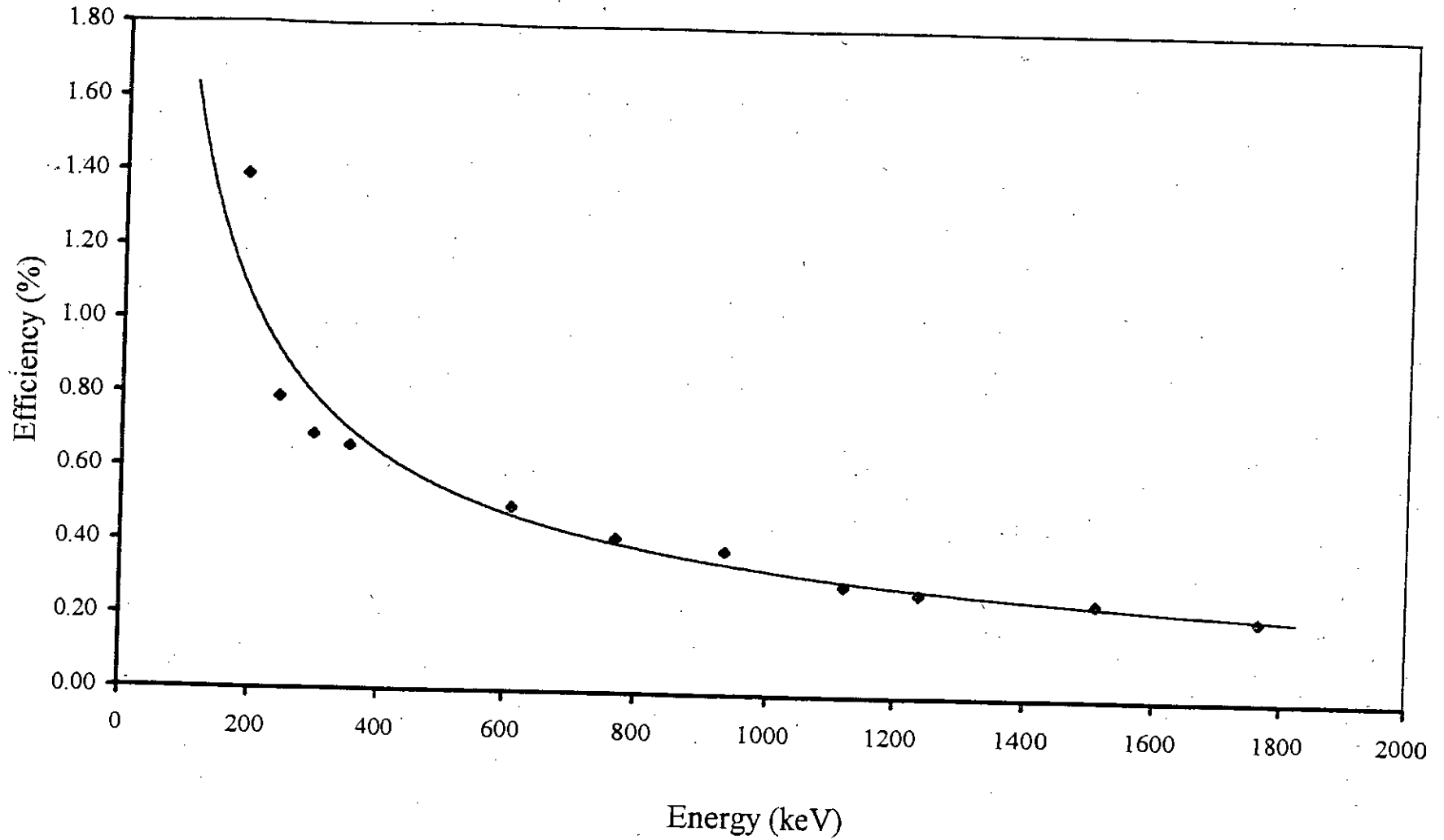


Figure 4.1: Efficiency Curve for the HPGe Detector with 1 kg Soil in Marinelli Beaker Geometry.

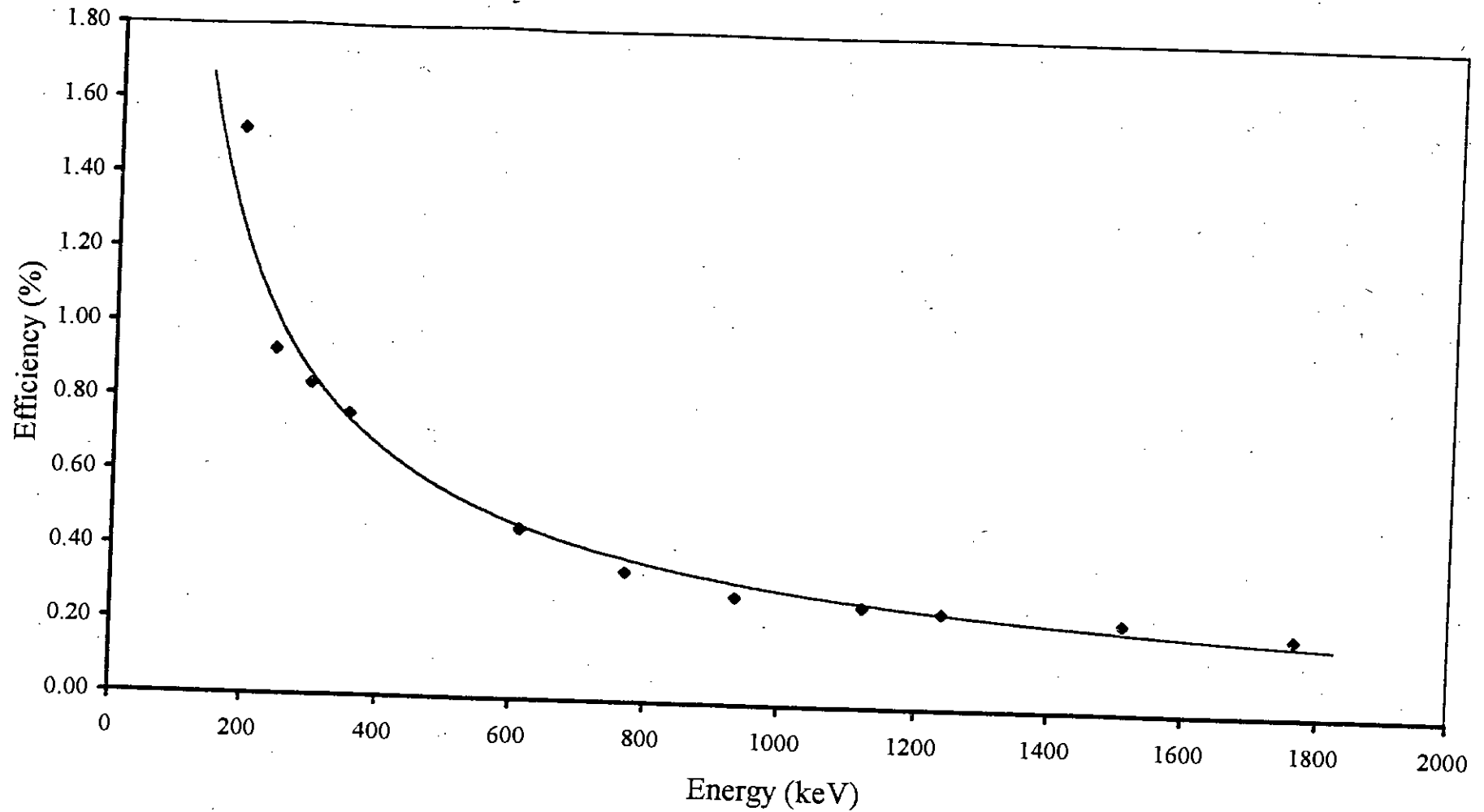


Figure 4.2: Efficiency Curve for the HPGe Detector with 1 L Water in Marinelli Beaker Geometry.

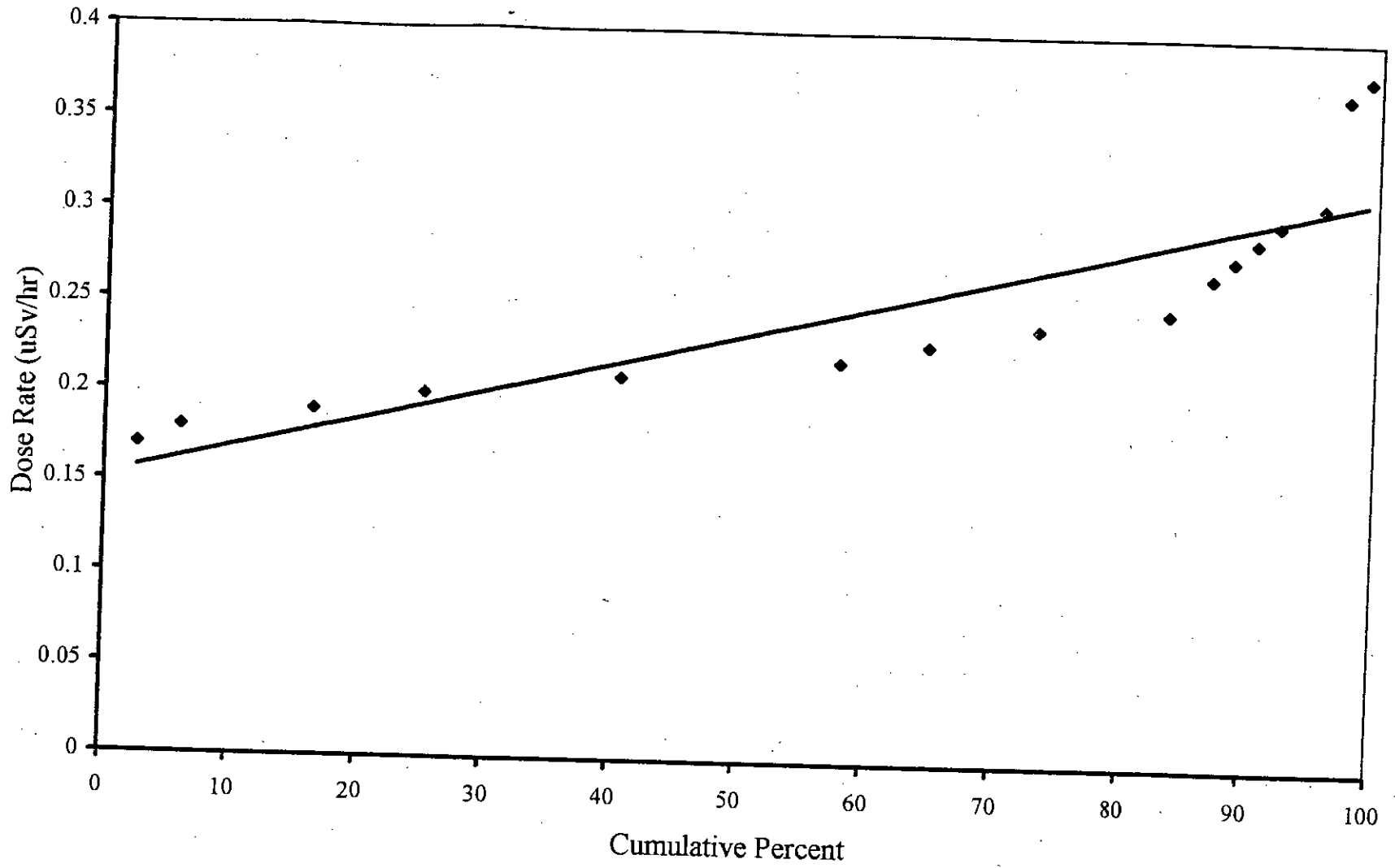


Figure 4.3: Cumulative Frequency Plot (Probability Plot) for Average Dose Levels in Kutcha Houses.

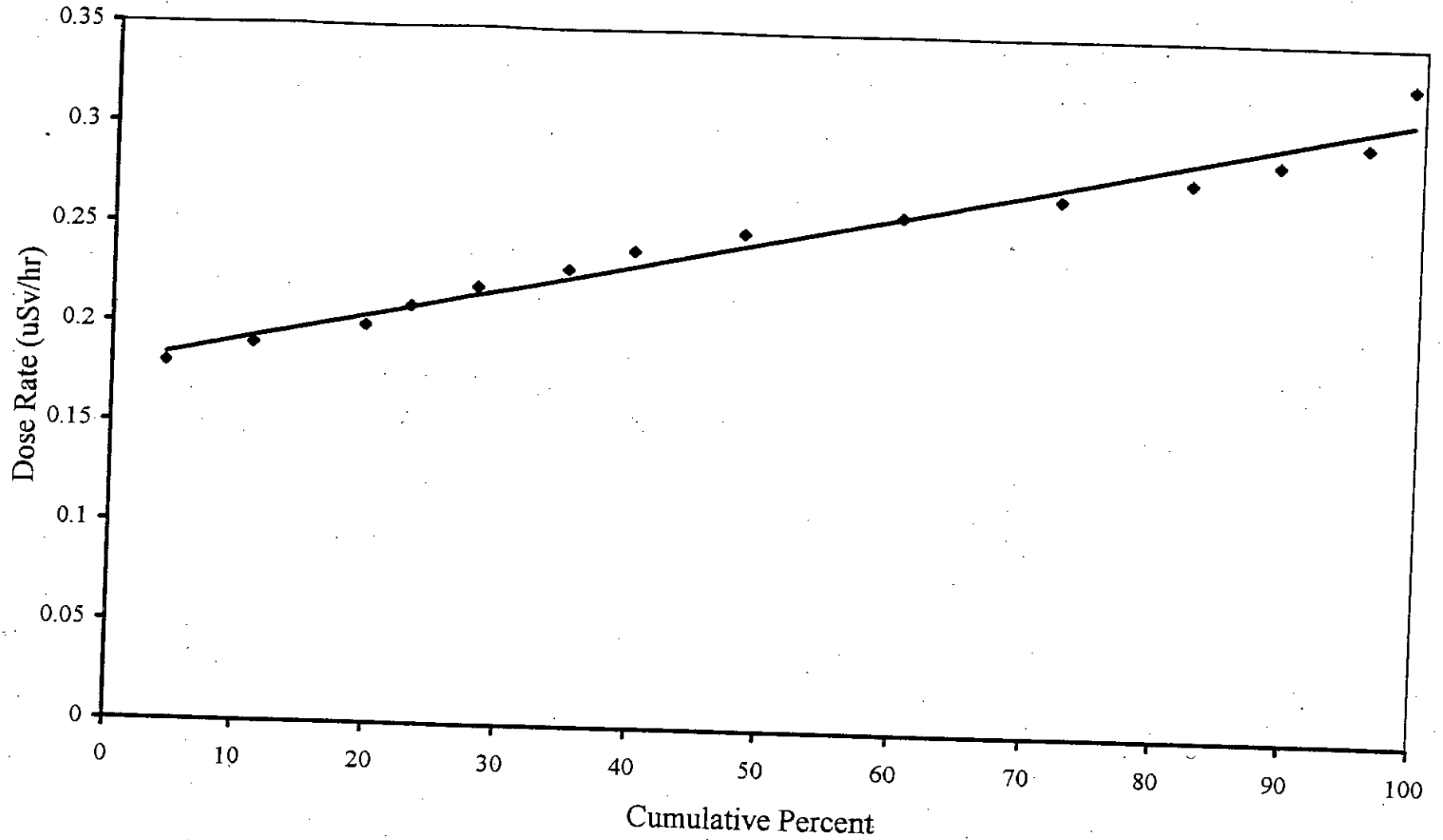


Figure 4.4: Cumulative Frequency Plot (Probability Plot) for Average Dose Levels in New-Buildings.

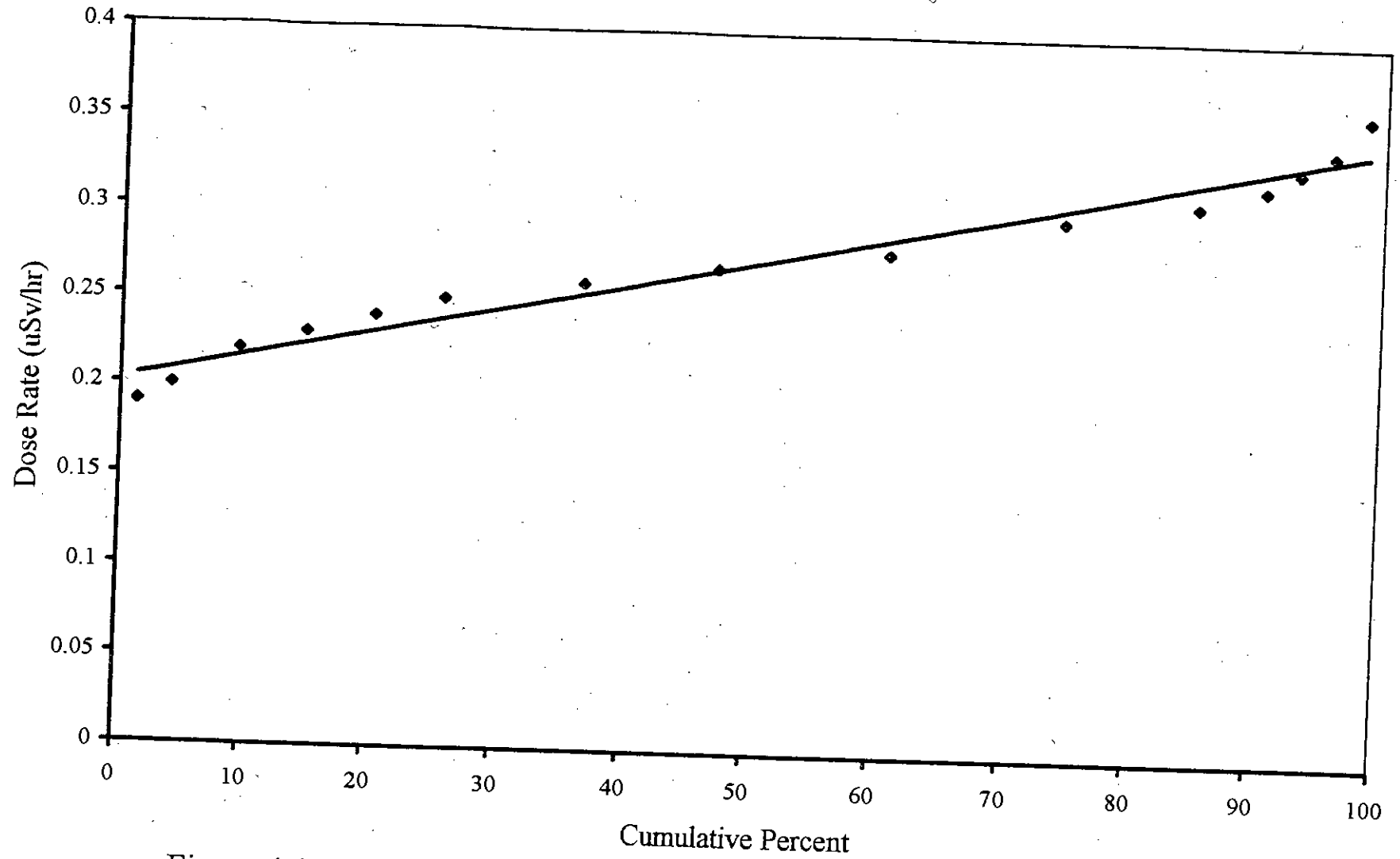


Figure 4.5: Cumulative Frequency Plot (Probability Plot) for Average Dose Levels in Old-Buildings.

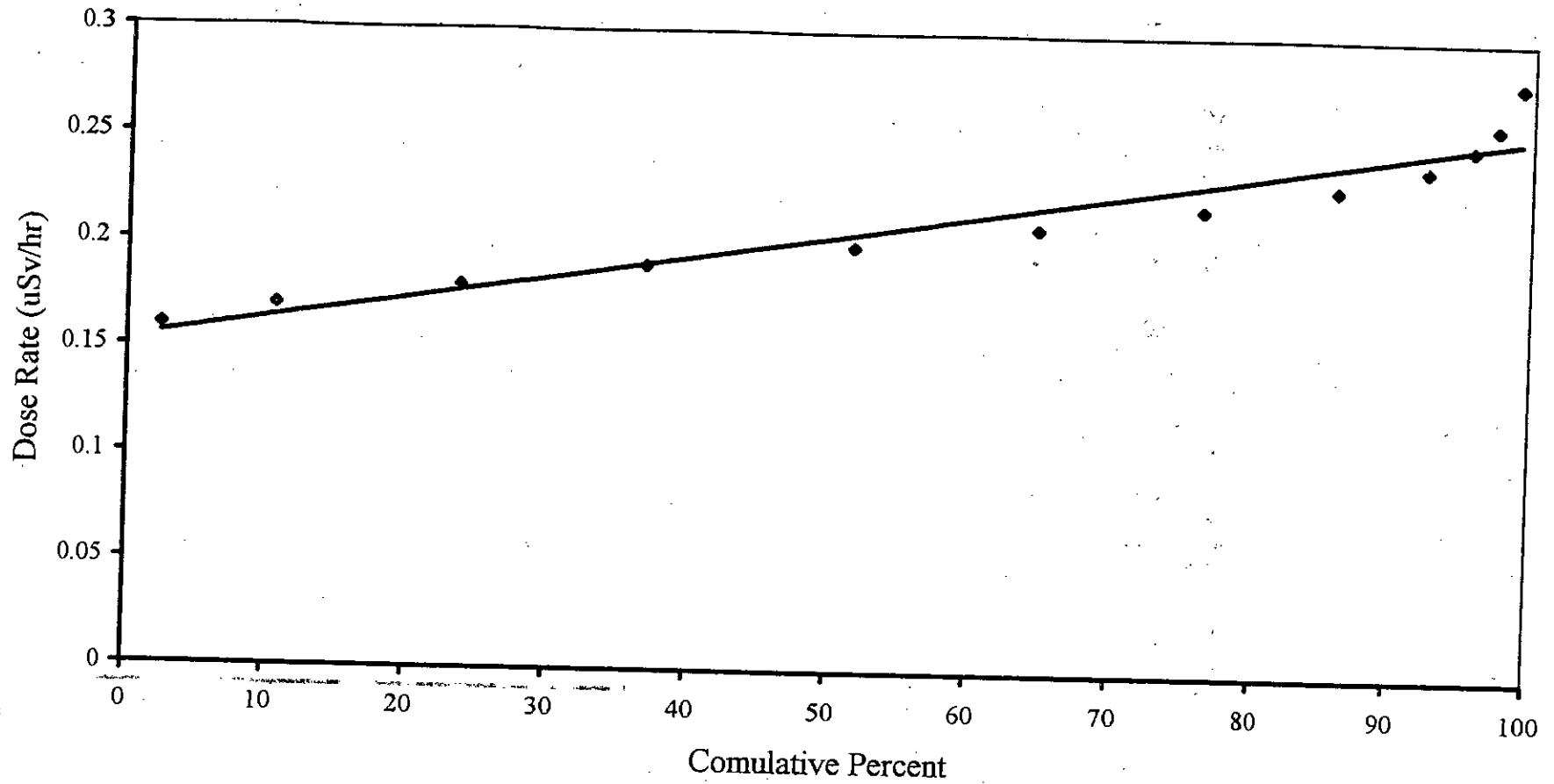


Figure 4.6: Cumulative Frequency Plot (Probability Plot) for Average Dose Levels in Free Spaces .

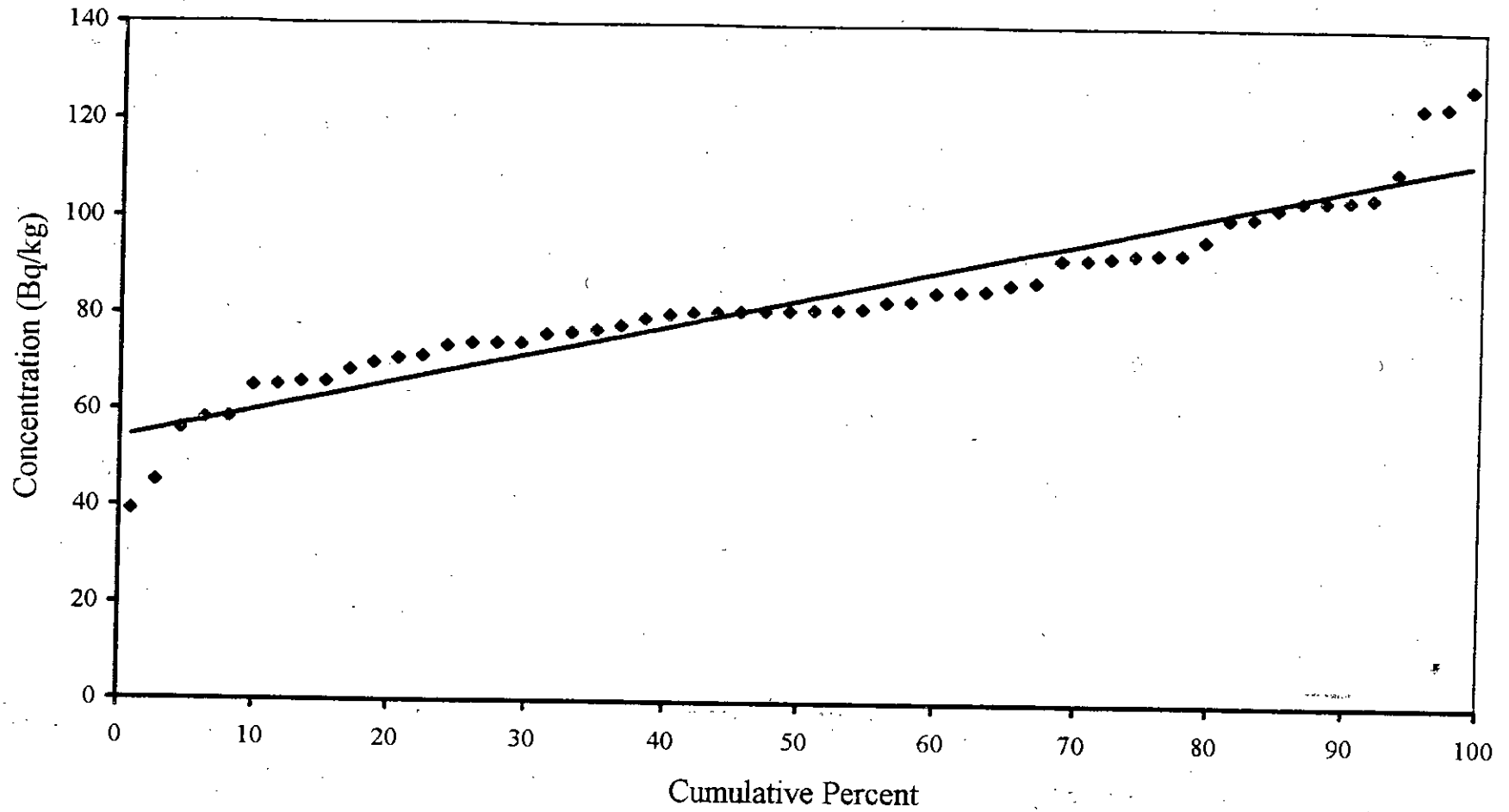


Figure 4.7: Probability Plot (cumulative frequency plot) of Th-232 in Soil Samples.

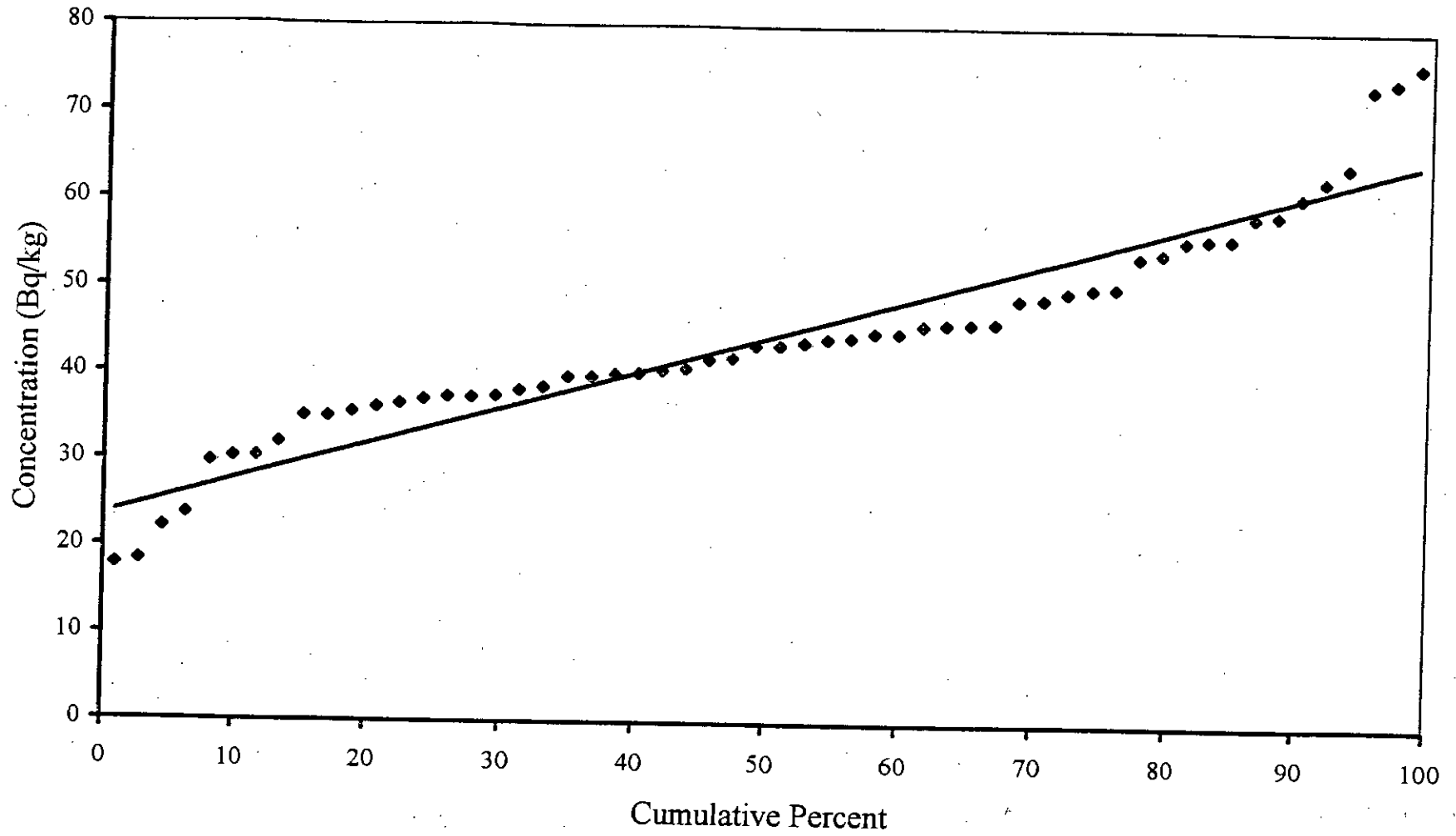


Figure 4.8: Probability Plot (cumulative frequency plot) of U-238 in Soil Samples.

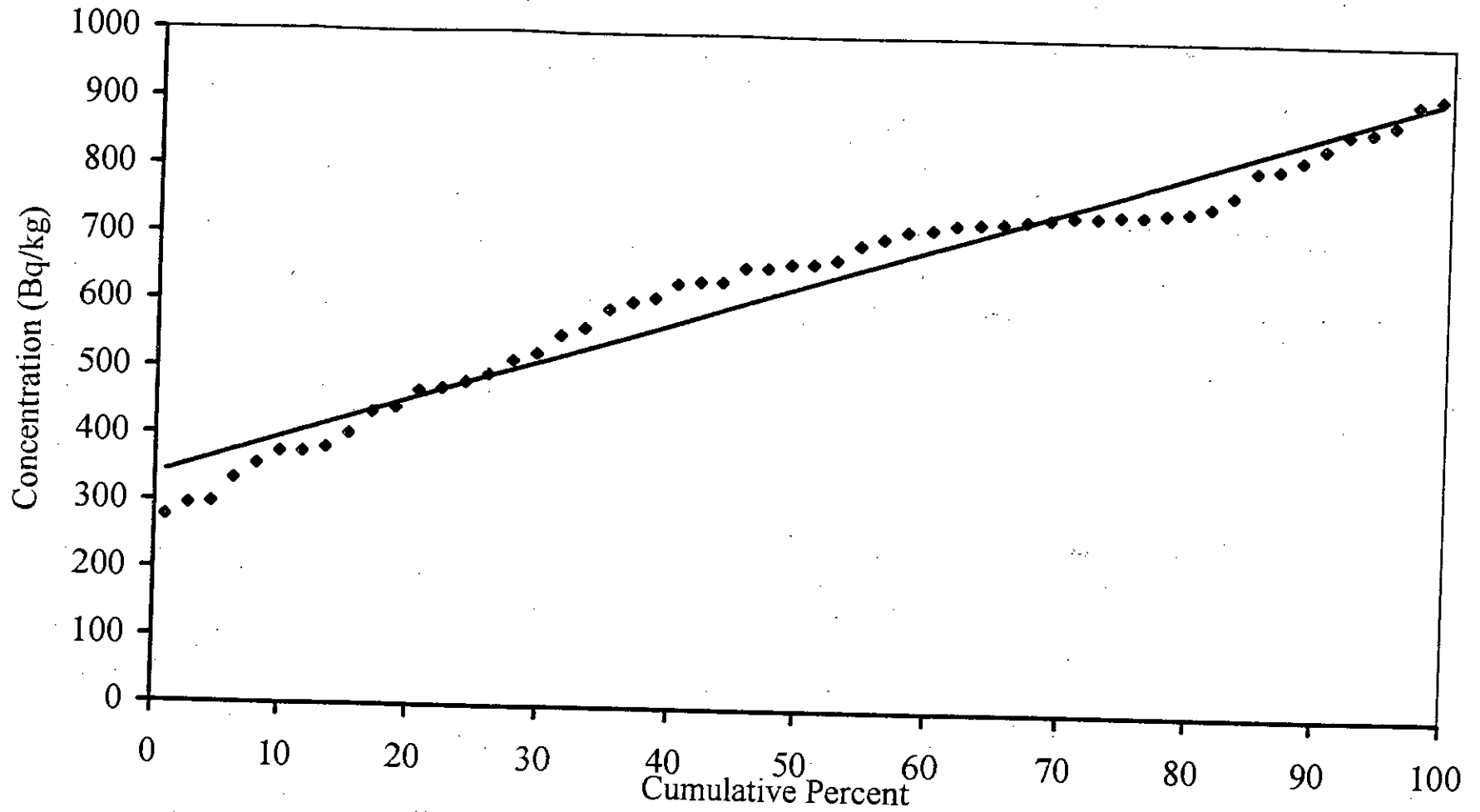


Figure 4.9: Probability Plot (cumulative frequency plot) of K-40 in Soil Samples.

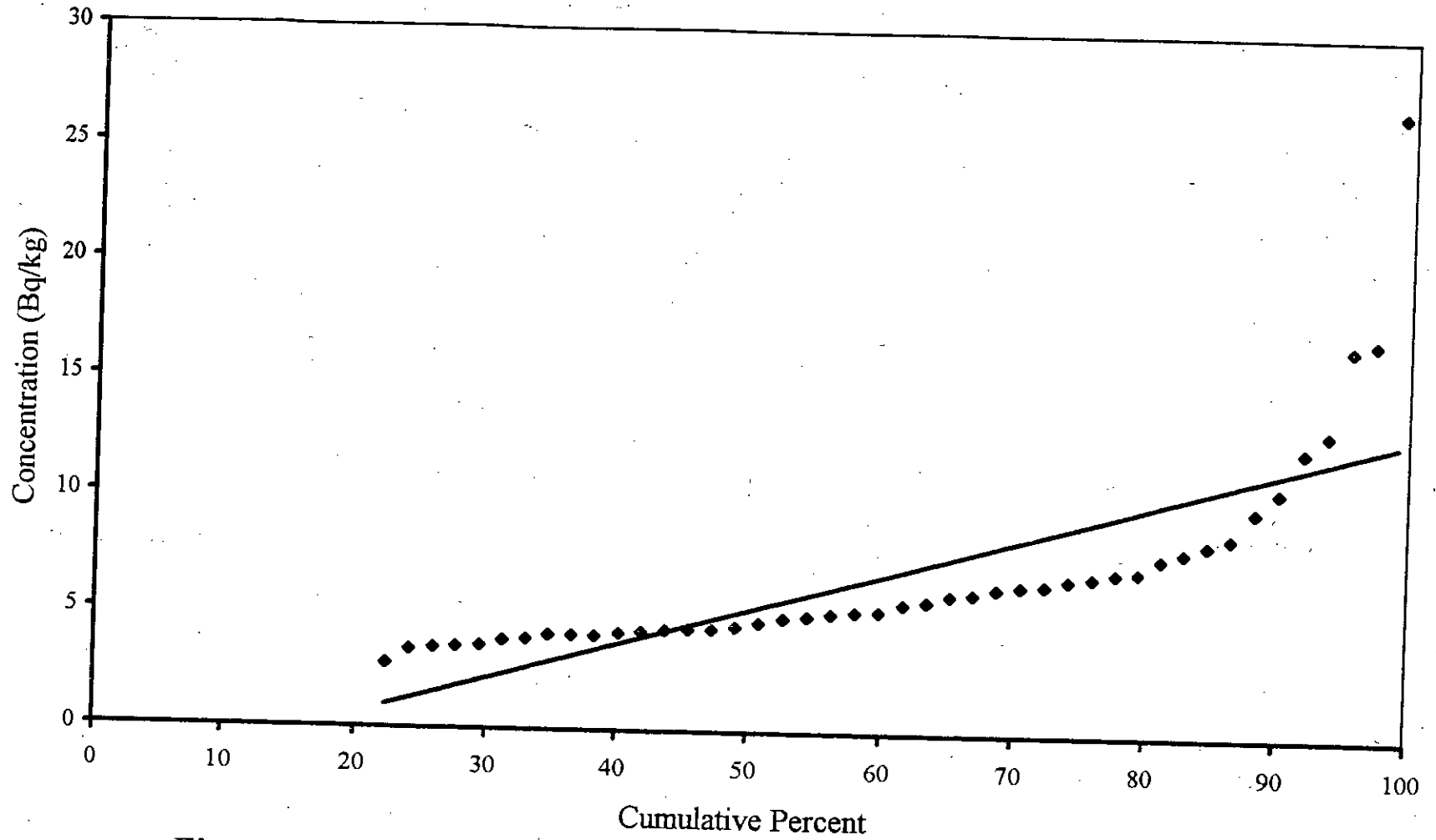


Figure 4.10: Probability Plot (cumulative frequency plot) of Cs-137 in Soil Samples.

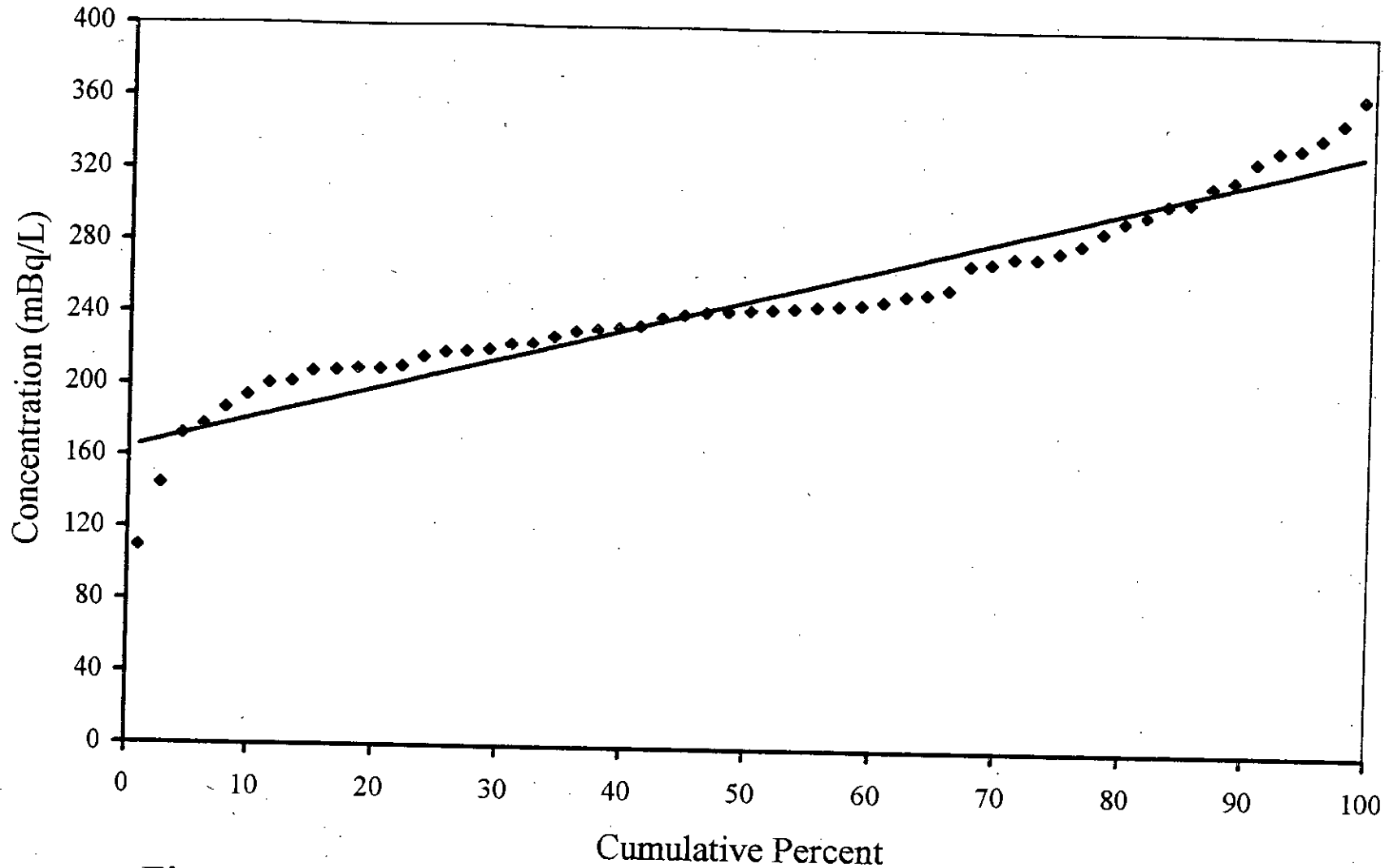


Figure 4.11: Probability Plot (cumulative frequency plot) for Th-232 in Water Samples.

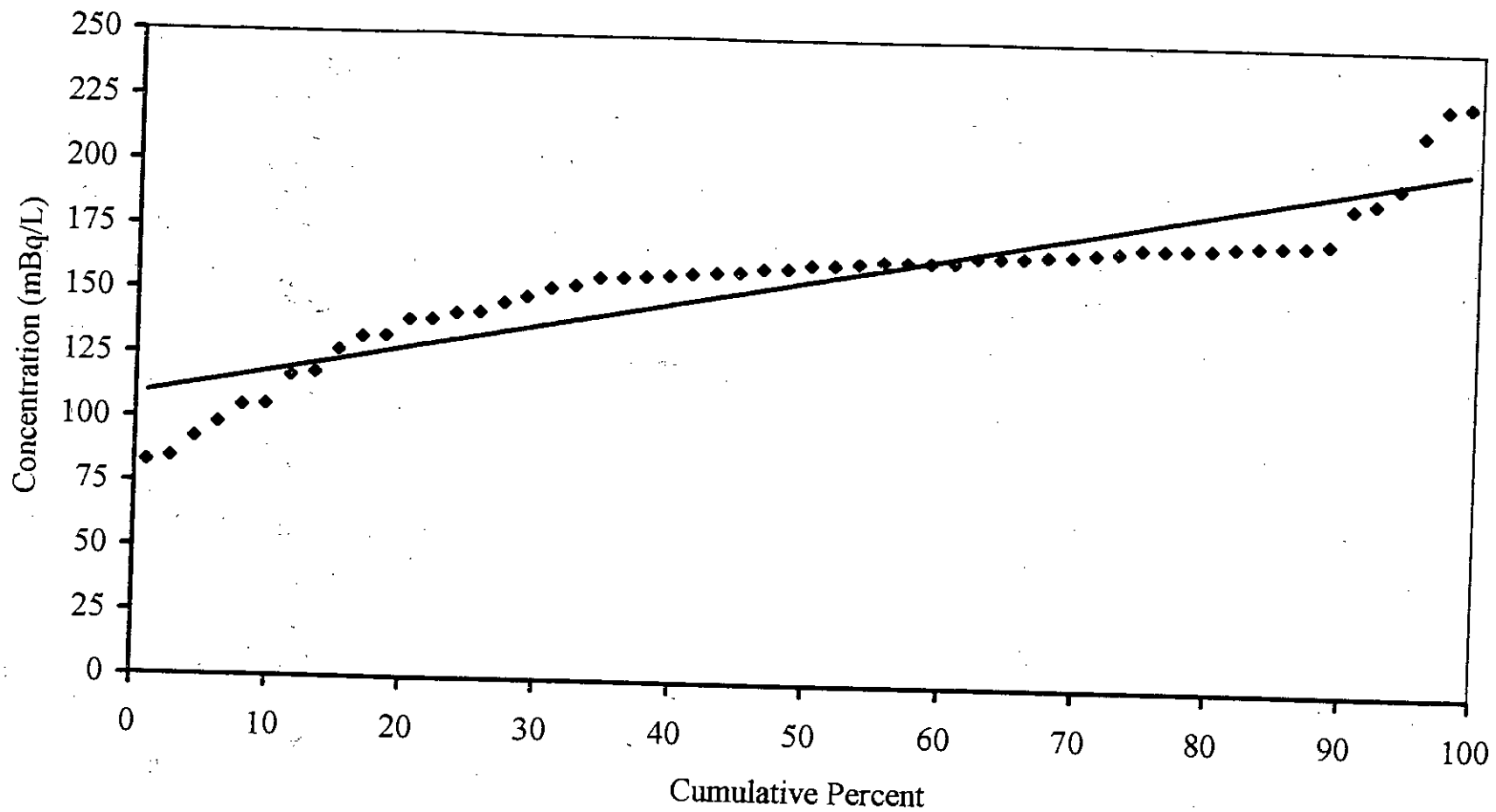


Figure 4.12: Probability Plot (cumulative frequency plot) for U-238 in Water samples.

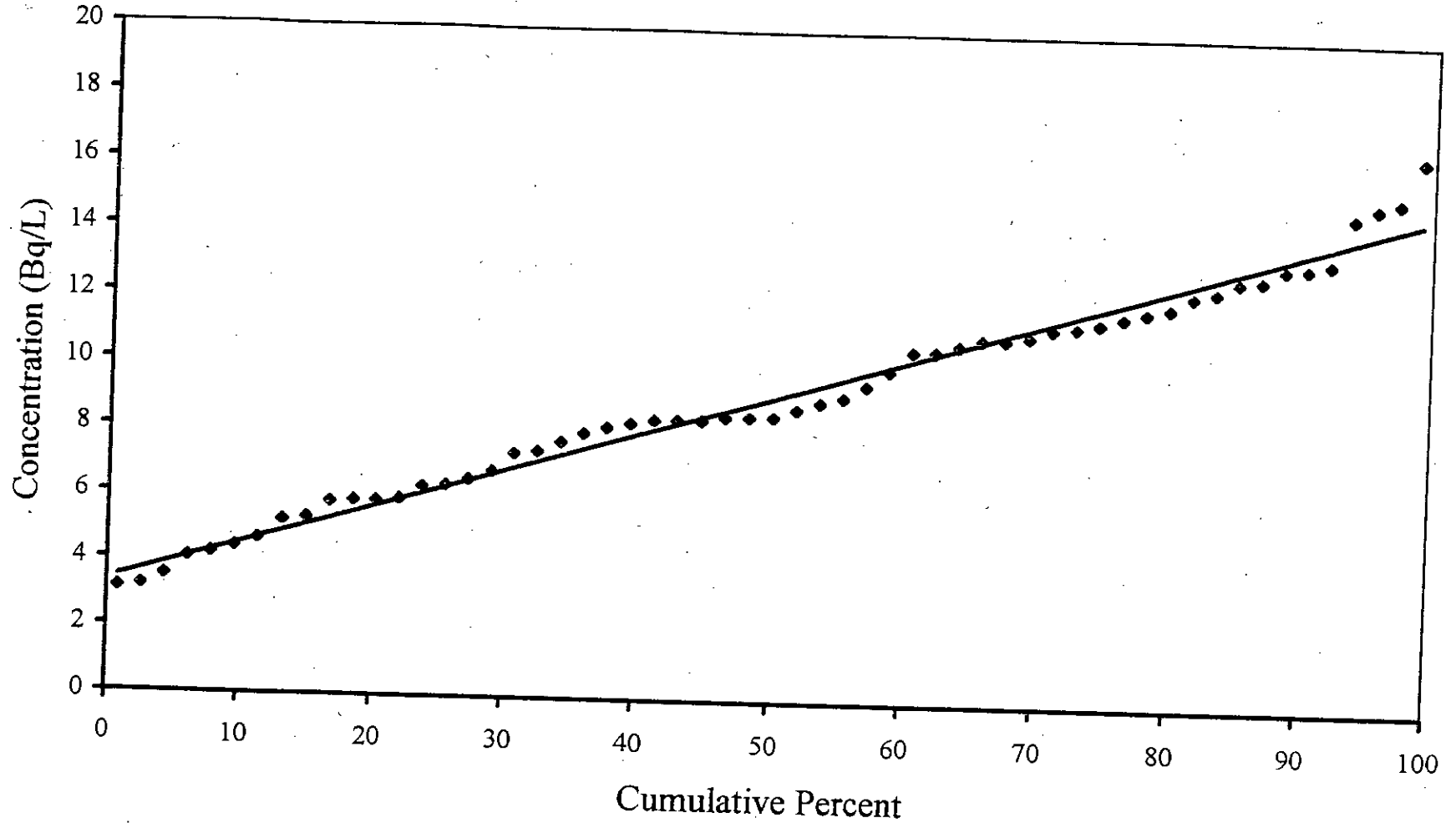


Figure 4.13: Probability Plot (cumulative frequency plot) for K-40 in Water Samples.

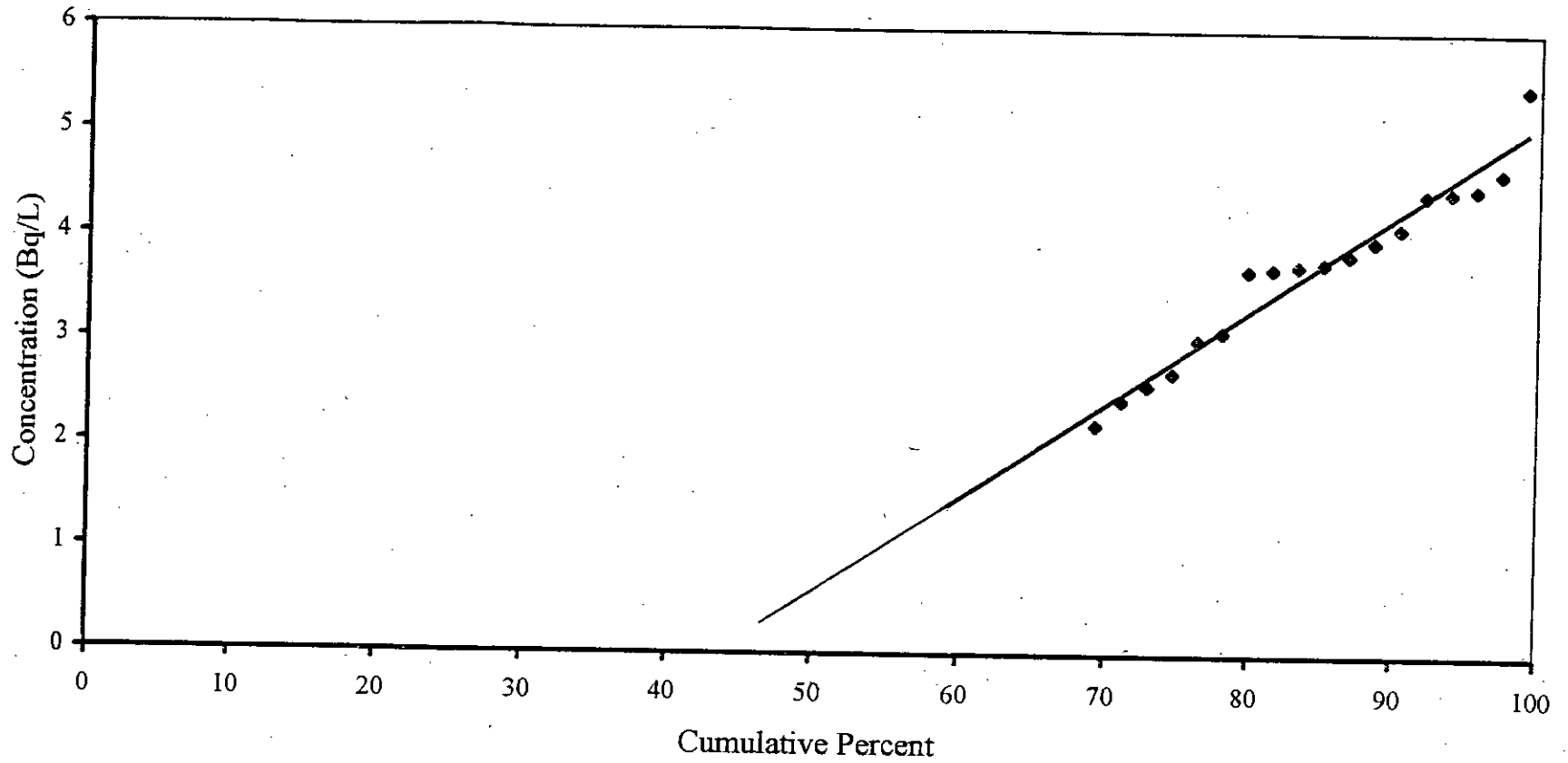


Figure 4.14: Probability Plot (cumulative frequency plot) for Cs-137 in Water Samples

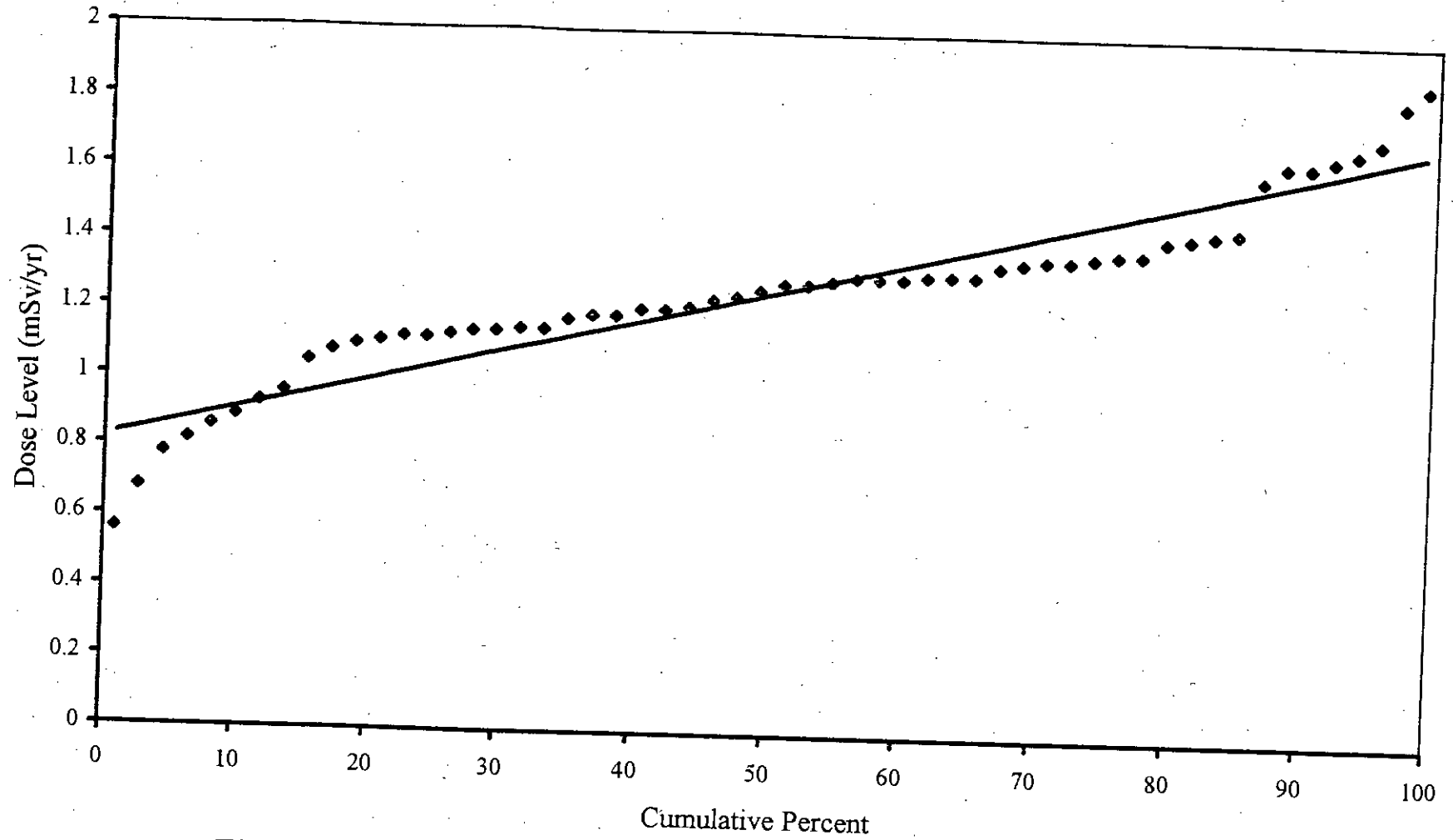


Figure 4.15: Cumulative Frequency Plot for Terrestrial Radiation Dose Throughout Bangladesh.

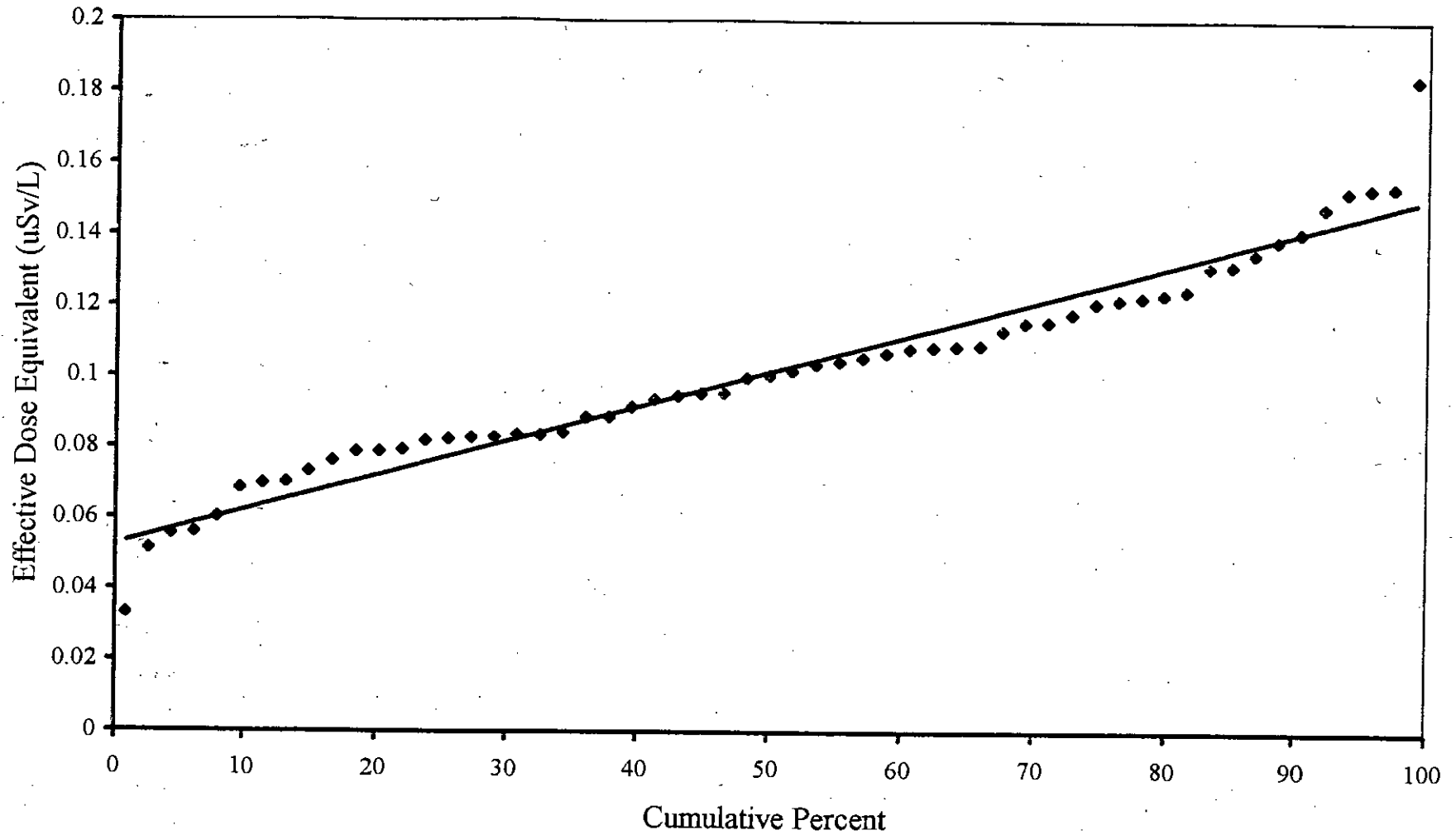


Figure 4.16: Cumulative Frequency Plot for Average Radiation Dose Received Due to Intake of 1L Water.

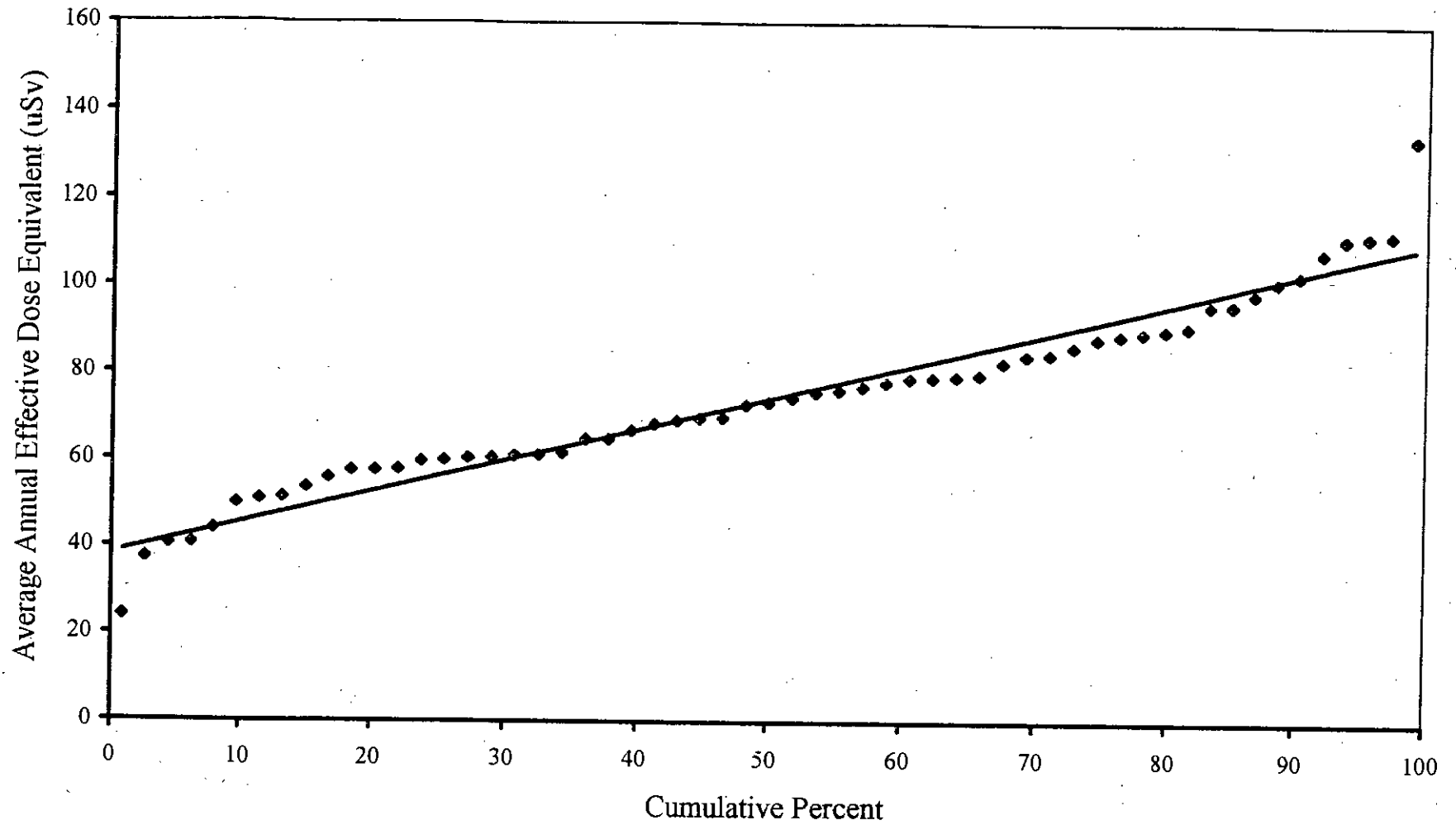


Figure 4.17: Cumulative Frequency Plot (Probability Plot) for Average Annual Radiation Dose Due to Intake of Water Throughout Bangladesh.



REFERENCES



REFERENCES

- [1] "*Sources and Effects of Ionizing Radiation*", United Nations Scientific Committee on the Effects of Atomic Radiation (*UNSCEAR*), 1993 Report to the General Assembly, with Scientific annexes, United Nations; New York, 1993.
- [2] **G. P. Hanson** and **E. Komarov**, "*Health Effects in Residents of High Background Radiation Regions*", published in: *Biological Effects of Low Level Radiation, Proceedings of an International Symposium on the Effects of Low-Level Radiation*, Vienna, IAEA; IAEA-SM-266/81, pp.211-230, IAEA 1983.
- [3] **W. A. Kolb** and **M. Wojcik**, "*Enhanced Radioactivity Due to Natural Oil and Gas Production and Related Radiological Problems*", *The Science Of The Total Environment*; Vol. 45(October), pp.77-84, 1985.
- [4] "*Sources, Effects, and Risks of Ionizing Radiation*", United Nations Scientific Committee on the Effects of Atomic Radiation (*UNSCEAR*), 1988 Reports to the General Assembly, United Nations; 1988.
- [5] **Pei-Huo Lin**, **Ching-Jiang Chen**, **Ching-Chung Huang**, and **Yu-Ming Lin**, "*Measurement of Cosmic-Ray Induced Ionization Intensity*", *Radiation Protection Dosimetry*; Vol. 15, pp.185-189, 1986.
- [6] **Merril Eisenbud**, "*Environmental Radioactivity*" 3rd Edition, Academic Press, Orlando, USA, 1987.
- [7] **W. H. Carlton**, **C. E. Murphy, Jr.**, and **A. G. Evans**, "*Radiocesium in the Savannah River Site Environment*", *Health Physics*; Vol. 67(3), pp.233-234, 1994.
- [8] "*National Council on Radiation Protection, Environmental Radiation Measurements*", Washington DC, NCRP; NCRP Report No. 50; 1976.
- [9] **Y. Shimada**, **S. Morisawa**, and **Y. Inoue**, "*A Numerical Model for the Analysis and Evaluation of Global ¹³⁷Cs Fallout*", *Health Physics*; Vol. 70(2), pp.171-179, 1996.
- [10] "*Ionizing Radiation : Sources and Biological Effects*", United Nations Scientific Committee on the Effects of Atomic Radiation (*UNSCEAR*), 1982 Reports to the General Assembly, United Nations; New York, 1982.
- [11] **R. V. Clark**, "*Marine Pollution*", Second Edition; Clarendon Press, Oxford 1989.

- [12] **Masaharu Hoshi et al.**, "*Fallout Radioactivity in Soil and Food Samples in the Ukraine: Measurements of Iodine, Plutonium, Cesium, and Strontium Isotopes*", Health Physics; Vol. 67(2), pp.187-191, 1994.
- [13] "*One Decade After Chernobyl (Summing up the Consequences of the Accident)*", Proceedings of an International Conference: Vienna, 8–12 April, 1996; IAEA – 1996.
- [14] **S. Gopalkrishnan and C. Rangarajan**, "*Nuclear Explosions and Radioactive Fallout*", Published in *Methods of Analysis of Radionuclide Contaminants in Foods*, Pollution Monitoring Section, Bhabha Atomic Research Centre, Bombay, India 1989.
- [15] **Herman Cember**, "*Introduction to Health Physics*", 3rd Edition, Pergamon Press Ltd. UK, 1995.
- [16] **B. Mason**, "*Principles of Geochemistry*", John Wiley & Sons Inc., New York; USA, 1966.
- [17] **J. Manuel Pérez Iglésias, M. Cruz Alvarez Alvarez, M. Teresa Dopico Vivero, and León Garzón Ruipérez**, "*Indoor ^{222}Rn Concentrations in Central Austrias*", Health Physics; Vol. 70(5), pp.689-694, 1996.
- [18] **H. J. Albering, J. A. Hoogewerff, and J. C. S. Kleinjans**, "*Survey of ^{222}Rn Concentrations in Dwellings and Soils in the Dutch-Belgian Border Region*", Health Physics; Vol. 70(1), pp.64-69, 1996.
- [19] **F. T. Cross, N. H. Harley, and W. Hofmann**, "*Health Effects and Risks from ^{222}Rn in Drinking Water*", Health Physics; Vol. 48, pp.649-670, 1985.
- [20] **Robert Granier and Denis-Jean Gambini**, English Translator- **Roy Lisker**, "*Applied Radiation Biology and Protection*" Ellis Horwood, England, 1990.
- [21] **Eric J. Hall**, "*Radiobiology for the Radiologist*", 3rd Edition; Harper & Row Publisher, Philadelphia, 1992.
- [22] "*International Commission on Radiological Protection (ICRP) Publication 60*", Annals of the ICRP, 1990 Recommendations of the ICRP; Published as Vol. 21(1-3), Pergamon Press Ltd., UK, 1991.
- [23] **K. Sriram**, "*Nuclear Measurement Techniques*", Affiliated East West Press Pvt. Ltd., New Delhi, India, 1986.
- [24] **H. E. Johns and J. R. Cunningham**, "*The Physics of Radiology*" 4th Edition, Charles C. Thomas Publisher, USA, 1980.

- [25] **Abel J. Gonzalez**, "*Biological Effects of Low Doses of Ionizing Radiation : A Fuller Picture*", Quarterly Journal of the IAEA; Vol. 36, Bulletin 4, pp.37-45; IAEA 1984.
- [26] **S. Khalilullah**, "Radiation Injury and its Management : A Guideline for Physicians", Appendix of the Medical Preparatory Plan of the TRF; AERE Dhaka Publication, pp.1-5, September 1986.
- [27] **Ramzi S. Cotran, Vinay Kumer and Stanley L. Robbins**, "*Robbins Pathologic Basis of Disease*" 4th Edition; W. B. Saunders Company, pp.9-12 (cellular injury and adaptation), Canada 1989.
- [28] **William F. Ganong**, "*Review of Medical Physiology*", 17th Edition; Prentice-Hall International Inc., pp.1-18 (The General and Cellular Basis of Medical Physiology) USA 1995.
- [29] **J. B. Walter and M. S. Israel**; "*General Pathology*", 6th Edition, Churchill Livingstone; Page-63 (Cell Responses to Injury), Hongkong 1987.
- [30] **Alan Martin and Samuel A. Harbison**, "*An Introduction to Radiation Protection*", 3rd Edition, Chapman and Hall, London; 1986.
- [31] "*IAEA-RCA Course on Safety Aspects in the Industrial Application of Radiation Sources, Bombay, December 2-13, 1991: Lecture Notes*", Division of Radiological Protection, Bhabha Atomic Research Centre, Bombay, India 1991.
- [32] **M. A. Rab Molla, A. Jalil, F. Nasreen, and S. F. Mahal**, "*Maximum Units of Radioactivity in Foodstuffs in Bangladesh*", Nuclear Science and Applications; Bangladesh Atomic Energy Commission, Dhaka, Bangladesh; Vol. 1(1), page- 75, 1989.
- [33] "*Measurement of Radionuclides in Food and the Environment, A Guide Book*", Technical Reports Series No. 295, IAEA, Vienna, 1989.
- [34] **M. A. Rab Molla and A. F. M. Salahuddin Chowdhury**; Annual Scientific Report, Health Physics Division, AECD; pp.48-58; 1974-1976.
- [35] **M. A. Rab Molla et al.**; Final Report; IAEA/BAEC research Contract No. 1325/RB AECD/HP/B, 1978.
- [36] **M. Asikainen and H. Kahlos**, "*Natural Radioactivity of Drinking Water in Finland*", Health Physics; Vol. 39(1), pp.77-83, 1980.
- [37] **David E. McCurdy and Russel A. Mellor**, "*The Concentration of ^{226}Ra and ^{228}Ra in Domestic and Imported Bottled Waters*", Health Physics; Vol. 40(2), pp.250-253, 1981.

- [38] **Siro Abe, Kazunobu Fujitaka, Michiko Abe, and Kenzo Fujimoto**, "*Extensive Field Survey of Natural Radiation in Japan*", Journal of Nuclear Science and Technology; Vol. 18(1), pp.21-45, 1981.
- [39] **Kazunobu Fujitaka, Siro Abe, and Kenzo Fujimoto**, "*Distribution of Natural Radiation in Japan in Relation to Geologic properties*", Journal of Nuclear Science and Technology; Vol. 18(3), pp.222-232, 1981.
- [40] **C. S. Chong and G. U. Ahmad**, "*Gamma Activity of ^{40}K , ^{226}Ra , and ^{232}Th in Building Materials in Penang*", Health Physics; Vol. 43(2), pp.272-273, 1982.
- [41] **Louis B. Kriege and Rolf M. A. Hahne**, " *^{226}Ra and ^{228}Ra in Iowa Drinking Water*", Health Physics; Vol. 43(4), pp.543-559, 1982.
- [42] **William Cline, Susan Adamovitz, and Clifford Blackman**, "*Radium and Uranium Concentrations in Georgia Community Water System*", Health Physics; Vol.44(1), 1983.
- [43] **C. Richard Cothorn and William L. Lappenbusch**, "*Occurance of Uranium in Drinking water in the US*", Health Physics; Vol. 45(1), pp.89-99, 1983.
- [44] **T. E. Myrick, B. A. Berven and F. F. Haywood**, "*Determination of Concentrations of Selected Radionuclides in Surface Soil in the US*", Health Physics; Vol. 45(3), 1983.
- [45] **Malcolm E. Cox and Barry L. Fankhauser**, "*Distribution of Fallout Cesium-137 in Hawaii*", Health Physics; Vol. 46(1) pp.65-71, 1984.
- [46] **C. Richard Cothorn and William L. Lappenbusch**, "*Compliance Data for the Occurrence of Radium and Gross α -particle Activity in Drinking Water Supplies in the United States*", Health Physics; Vol. 46(3), pp.503-510, 1984.
- [47] **Philippe Martin**, "*On the Natural Radioactivity of Potable waters in Saudi Arabia*", Health Physics; Vol. 46(4), pp.947-949, 1984.
- [48] **C. Papastefanou, M. Manolopoulou, and S. Charalambous**, "*Exposure from Radioactivity in Building Materials*", Health Physics; Vol. 47(5), pp.775-783, 1984.
- [49] **I. Gans**, "*Natural Radionuclides in Mineral Waters*", The Science. Of The Total Environment; Vol. 45(October), pp.93-99, 1985.
- [50] **J. G. Ackers, J. F. Den Boer, P. De Jong, and R. A. Wolschrijn**, "*Radioactivity and Radon Exhalation Rates of Building Materials in the Netherlands*", The Science Of The Total Environment; Vol. 45(October), pp.151-156, 1985.

- [51] **G. Keller and H. Muth**, "*Radiation Exposure in German Dwellings, Some Results and Proposed Formula for Dose Limitation*", *The Science Of The Total Environment*; Vol. 45(October), pp.299-306, 1985.
- [52] **H. Schimier and A. Wicke**, "*Results from a Survey of Indoor Radon Exposures in the Federal Republic of Germany*", *The Science Of The Total Environment*; Vol. 45(October), pp.307-310, 1985.
- [53] **I. R. McAulay and J. P. McLaughlin**, "*Indoor Natural Radiation Levels in Ireland*", *The Science Of The Total Environment*; Vol. 45(October), pp.319-325, 1985.
- [54] **A. Sørensen, L. Bøtter-Jensen, B. Majborn, and S. P. Nielsen**, "*A Pilot Study of Natural Radiation in Danish Houses*", *The Science Of The Total Environment*; Vol. 45(October), pp.351-356, 1985.
- [55] **A. Battaglia, E. Bazzano, and G. Bonfanti**, "*Indoor Dose in Milano (Italy)*", *The Science Of The Total Environment*; Vol. 45(October), pp.365-371, 1985.
- [56] **R. Van Dongen and J. R. D. Stoute**, "*Outdoor Natural Background Radiation in the Netherlands*", *The Science Of The Total Environment*; Vol. 45(October), pp.381-388, 1985.
- [57] **H. W. Julius, and R. Van Dongen**, "*Radiation Doses to the Population in the Netherlands, Due to External Natural Sources*", *The Science Of The Total Environment*; Vol. 45(October), pp.449-458, 1985.
- [58] **B. M. R. Green, L. Brown, K. D. Cliff, C. M. H. Driscoll, J. C. H. Miles, and A. D. Wrixon**, "*Surveys of Natural Radiation Exposure in UK Dwellings with Passive and Active Measurement Techniques*", *The Science Of The Total Environment*; Vol. 45(October), pp.459-466, 1985.
- [59] **A. Rannou, C. Madelmont, and H. Renouard**, "*Survey of Natural Radiation in France*", *The Science Of The Total Environment*; Vol. 45(October), pp.467-474, 1985.
- [60] **C. Richard Cothorn, William L. Lappenbusch, and Jacqueline Michel**, "*Drinking - water Contribution to Natural Background Radiation*", *Health Physics*; Vol. 50(1), pp.33-47, 1986.
- [61] **C. Papastefanou, M. Manolopoulou, E. Savvides, and S. Charalambous**, "*Natural Radiation Dose in Petralona Cave*", *Health Physics*; Vol. 50(2), pp.281-286, 1986.

- [62] **A. S. Mollah, G. U. Ahmad, S. R. Hussain, and M. M. Rahman**, "The Natural Radioactivity of Some Building Materials in Bangladesh", *Health Physics*; Vol. 50(6), pp.849-851, 1986.
- [63] **R. D. Delaune, G. L. Jones, and C. J. Smith**, "Radionuclide Concentrations in Louisiana Soils and Sediments", *Health Physics*; Vol. 51(2), pp.239-244, 1986.
- [64] **James E. Watson, Jr., and Barry F. Mitsch**, "Ground Water Concentrations of ^{226}Ra and ^{222}Rn in North Carolina Phosphate Lands", *Health Physics*; Vol. 52(3), pp.361-365, 1987.
- [65] **K. S. V. Nambi and S. D. Soman**, "Environmental Radiation and Cancer in India", *Health Physics*; Vol. 52(5), pp.653-657, 1987.
- [66] **Yu-Ming Lin, Pei-Huo Lin, Ching-Jiang Chen, and Ching-Chung Huang**, "Measurement of Terrestrial γ -Radiation in Taiwan, Republic of China", *Health Physics*; Vol. 52(6), pp.805-811, 1987.
- [67] **P. Corvisiero, C. Salvo, P. Boccacci, G. Ricco, A. Pilot, G. Taccini, G. Scielzo, M. Corso, F. Valerio, and D. Bordo**, "Radioactivity Measurements in North-West Italy After Fallout from the Reactor Accident at Chernobyl", *Health Physics*; Vol. 53(1), pp.83-87, 1987.
- [68] **Isabel M. Fisenne, Pamela M. Perry, Karin M. Decker, and Helen W. Keller**, "The Daily Intake of ^{234}U , ^{235}U , ^{238}U , ^{228}Th , ^{230}Th , ^{232}Th , and ^{226}Ra by New York City Residents", *Health Physics*; Vol. 53(4), pp.357-363, 1987.
- [69] **C. Papastefanou, M. Manolopoulou, and S. Charalambous**, "Cesium-137 in Soils from Chernobyl Fallout", *Health Physics*; Vol. 55(6), pp.985-987, 1988.
- [70] **Tieh-Chi Chu, Pao-Shen Weng, and Yu-Ming Lin**, "Changes in Per Capita and Collective Dose Equivalent Due to Natural Radiation in Taiwan (1950-1983)", *Health Physics*; Vol. 56(2), pp.201-217, 1989.
- [71] **Chien Chung**, "Environmental Radioactivity and Dose Evaluation in Taiwan After the Chernobyl Accident", *Health Physics*; Vol. 56(4), pp.465-471, 1989.
- [72] **Olafur Arnalds, Norman H. Cutshall and Gerald A. Nielsen**, "Cesium-137 in Montana Soils", *Health Physics*; Vol. 57(6), pp.955-958, 1989.
- [73] **T. Yesin and N. Cakir**, "Caesium-137 and Caesium-134 levels in Soil in a Tea Plantation in Turkey After the Chernobyl Accident", *Applied Radiation And Isotopes*; Vol. 40(3), pp.209-211, 1989.

- [74] **S. E. Simopoulos**, "Soil Sampling and ^{137}Cs Analysis of the Chernobyl Fallout in Greece", *Applied Radiation And Isotopes*; Vol. 40(7), pp.607-613, 1989.
- [75] **R. J. de Meijer, F. J. Aldenkamp, M. J. A. M. Brummelhuis, J. F. W. Jansen, and W. Put**, "Radionuclide Concentrations in the Northern Part of The Netherlands After The Chernobyl Reactor Accident", *Health Physics*; Vol. 58(4), pp.441-452, 1990.
- [76] **Narayani P. Singh, David P. Burleigh, Herbert M. Ruth, and McDonald E. Wrenn**, "Daily U Intake in Utah Residents from Food and Drinking Water", *Health Physics*; Vol. 59(3), pp.333-338, 1990.
- [77] **H. Florou and P. Kritidis**, "Natural Radioactivity in Environmental Samples from an Island of Volcanic Origin (Milos, Aegean Sea)", *Marine Pollution Bulletin*; Vol. 22(8), pp.417-419, 1991.
- [78] **Man-yin W. Tso and Chung-chen Li**, "Terrestrial Gamma Radiation Dose in Hong Kong", *Health Physics*; Vol. 62(1), pp.77-81, 1992.
- [79] **V. Bansal, A. Rawat, P. J. Jojo, and Rajendra Prasad**, "Analyzing Uranium Concentrations in Drinking Water Samples in India Using the Fission-Track Technique", *Health Physics*; Vol. 62(3), pp.257-259, 1992.
- [80] **B. A. Marouf, A. S. Mohamad, J. S. Taha, and I. K. Al-Haddad**, "Population Doses from Environmental Gamma Radiation in Iraq", *Health Physics*; Vol. 62(5), pp.443-444, 1992.
- [81] **M. Brai, S. Bellia, R. Di Liberto, G. Dongarra, S. Hauser, F. Parello, P. Puccio, and S. Rizzo**, "Environmental Gamma Radiation Measurements on the Island of Pantelleria", *Health Physics*; Vol. 63(3), pp.356-359, 1992.
- [82] **L. Zikovsky and G. Kennedy**, "Radioactivity of Building Materials Available in Canada", *Health Physics*; Vol. 63(4), pp.449-452, 1992.
- [83] **T. Ren, Z. Wang, and C. Zhu**, "Population Doses from Terrestrial Gamma Exposure in China", *Radiation Protection Dosimetry*; Vol. 45(1/4), pp.431-434, 1992.
- [84] **Ching-Jiang Chen, Pao-Shan Weng, and Tich-Chi Chu**, "Evaluation of Natural Radiation in Houses Built with Black Schist", *Health Physics*; Vol. 64(1), pp.74-78, 1993.
- [85] **P. Schuller, Ch. Løvengreen, and J. Handl**, " ^{137}Cs Concentration in Soil, Prairie Plants, and Milk from Sites in Southern Chile", *Health Physics*; Vol. 64(2), pp.157-161, 1993.

- [86] **N. M. Ibrahim, A. H. Abd El Ghani, S. M. Shawky, E. M. Ashraf, and M. A. Farouk**, "*Measurement of Radioactivity Levels in Soil in the Nile Delta and Middle Egypt*", Health Physics; Vol. 64(6), pp.620-627, 1993.
- [87] **Alberto Malanca, Valerio Pessina, and Giuseppe Dallara**, "*Assessment of the Natural Radioactivity in the Brazilian State of Rio Grande Do Norte*", Health Physics; Vol. 65(3), pp.298-302, 1993.
- [88] **A. P. Radhakrishna, H. M. Somashekarappa, Y. Narayana, and K. Siddappa**, "*A New Natural Background Radiation Area on the Southwest Coast of India*", Health Physics; Vol. 65(4), pp.390-395, 1993.
- [89] **L. S. Quindós, P. L. Fernández, J. Soto, C. Ródenas, and J. Gómez**, "*Natural Radioactivity in Spanish Soils*", Health Physics; Vol. 66(2), pp.194-200, 1994.
- [90] **Man-yin W. Tso, Chor-yi Ng, and John K. C. Leung**, "*Radon Release from Building Materials in Hong Kong*", Health Physics; Vol. 67(4), pp.378-384, 1994.
- [91] **Y. Narayana, H. M. Somashekarappa, A. P. Radhakrishna, K. M. Balakrishna, and K. Siddappa**, "*External Gamma Radiation Dose Rates in Coastal Karnataka*", Journal Of Radiological Protection; Vol. 14(3), pp.257-264, 1994.
- [92] **A. S. Mollah, S. Roy, A. F. Kuddus, K. Alam, and M. M. Rahman**, "*Environmental Radioactivity Monitoring*", AERE, Technical Report 1990 and 1991; No. AERE/TR-3, Savar, Dhaka; page-45, June 1994.
- [93] **K. E. Holbert, B. D. Stewart, and P. Eshraghi**, "*Measurement of Radioactivity in Arizona Ground Water Using Improved Analytical Techniques for Samples with High Dissolved Solids*", Health Physics; Vol. 68(2), pp.185-194, 1995.
- [94] **John R. Meriwether, Scott F. Burns, Ronald H. Thompson, and James N. Beck**, "*Evaluation of Soil Radioactivities Using Pedologically Based Sampling Techniques*", Health Physics; Vol. 69(3), pp.406-409, 1995.
- [95] **T. K. Ball, D. G. Cameron, T. B. Colman, and P. D. Roberts**, "*Behaviour of Radon in the Geological Environment: A Review*", Quarterly Journal Of Engineering Geology; Vol. 24, pp.169-182, 1991.
- [96] **Ilya Likhtariov, Lionella Kovgan, Dmitriy Novak, Sergey Vavilov, Peter Jacob, and Herwig G. Paretzke**, "*Effective Doses Due to External Irradiation from the Chernobyl Accident for Different Population Groups of Ukraine*", Health Physics; Vol. 70(1), 1996.

- [97] Masayoshi Yamamoto, Tsuneco Tsukatani, and Yukio Katayama, "Residual Radioactivity in the Soil of the Semipalatinsk Nuclear Test Site in the Former USSR", Health Physics; Vol. 71(2), pp.142-148, 1996.
- [98] Kiyoshi Shizuma, Kazuo Iwatani, Hiromi Hasai, Masaharu Hoshi, Takamitsu Oka, and Masaharu Okano, "¹³⁷Cs Concentrations in Soil Samples from an Early Survey of Hiroshima Atomic Bomb and Cumulative Dose Estimation from the Fallout", Health Physics; Vol. 71(3), pp.340-346, 1996.
- [99] Shu-Ying Lai, Pao-Shan Weng, and Teh-Chi Chu, "Concentrations of ¹³⁷Cs in Soils and Selected Forest Plants in Taiwan", Applied Radiation And Isotopes; Vol. 47(2), pp.159-164, 1996.
- [100] Z. Pietrzak-Flis, E. Chrzanowski, S. Dembinska, "Intake of ²²⁶Ra, ²¹⁰Pb, and ²¹⁰Po with Food in Poland", The Science Of The Total Environment; Vol. 203(2), pp.157-165, 6th September, 1997.
- [101] J. Uyttenhove, S. Pommé, B. Van Waeyenberge, F. Hardeman, J. Buysse, and J. -P. Culot, "Survey of the ¹³⁷Cs Contamination in Belgium by In-Situ Gamma Spectrometry, A Decade After the Chernobyl Accident", Health Physics; Vol. 73(4), pp.644-646, 1997.
- [102] S. Bellia, M. Brai, S. Hauser, P. Puccio, and S. Rizzo, "Natural Radioactivity in a Volcanic Island: Ustica, Southern Italy", Applied Radiation And Isotopes; Vol. 48(2), pp.287-293, 1997.
- [103] G. Manjon, I. Vioque, H. Moreno, R. Garcia- Tenoria, and M. Garcia- Leon, "Determination of ²²⁶Ra and ²²⁴Ra in Drinking Waters by Liquid Scintillation Counting", Applied Radiation And Isotopes; Vol. 48(4), pp.535-540, 1997.
- [104] E. Gomez, F. Garcias, M. Casas, and V. Cerda, "Determination of ¹³⁷Cs and ⁹⁰Sr in Calcareous Soils: Geographical Distribution on the Island of Majorca", Applied Radiation And Isotopes; Vol. 48(5), pp.699-704, 1997.
- [105] Yen-Chuan Kuo, Shu-Ying Lai, Ching Chung Huang, and Yu-Ming Lin, "Activity Concentrations and Population Dose from Radium-226 in Food and Drinking Water in Taiwan", Applied Radiation And Isotopes; Vol. 48(9), pp.1245-1249, 1997.
- [106] F. K. Miah, S. Roy, M. Touhiduzzaman, and B. Alam, "Distribution of Radionuclides in Soil Samples In and Around Dhaka City", Applied Radiation And Isotopes; Vol. 49(1-2), pp.133-139, 1998.

- [107] **John Jagger**, "*Natural Background Radiation and Cancer Death in Rocky Mountain States and Gulf Coast States*", *Health Physics*; Vol. 75(4), pp.428-430, 1998.
- [108] **N. N. Jibiri**, and **I. P. Farai**, "*Assessment of Dose Rate and Collective Effective Dose Equivalent Due to Terrestrial Gamma Radiation in the City of Lagos, Nigeria*", *Radiation Protection Dosimetry*; Vol. 76(3), pp.191-198, 1998.
- [109] **B. Baggoura**, **A. Nouredine**, and **M. Benkrid**, "*Level of Natural and Artificial Radioactivity in Algeria*", *Applied Radiation And Isotopes*; Vol. 49(7), pp.867-873, 1998.
- [110] **R. H. Higgy**, and **M. Pimpl**, "*Natural and Man-made Radioactivity in Soils and Plants Around the Research Reactor of Inshass*", *Applied Radiation And Isotopes*; Vol. 49(12), pp.1709-1712, 1998.
- [111] **M. M. Rahman**, "*Fallout and Natural Radioactivity in the Sand Samples of Coastal Areas and in the Rock Samples of North-Eastern Part of Bangladesh*", M. Sc. Thesis; Department of Physics, Jahangirnagar University, Dhaka, December-1991.
- [112] **Muhammad Anwar Uddin**, "*Study of Natural and Anthropogenic Radionuclides in Drinking Water Using High Resolution Gamma Spectrometry*", M. Sc. Thesis; Department Of Physics, University Of Chittagong, Chittagong; August-1996.
- [113] **Tutul Kanti Saha**, "*Study of Environmental Radiation by Thermoluminescence Dosimetry (TLD), β - γ Survey Meter, and Gamma Spectrometry*", M. Sc. Thesis; Department Of Physics, University Of Chittagong, Chittagong; August-1996.
- [114] **James A. Sorenson** and **Michael E. Phelps**, "*Physics in Nuclear Medicine*", 2nd Edition, Grune & Stratton Inc. Harcourt Brace Jovanovich Publishers, Orlando-Florida, USA 1987.
- [115] **H. Bauser** and **W. Ronge**, "*The Electret Ionization Chamber: A Dosimeter for Long Term Personnel Monitoring*", *Health Physics*; Vol. 34, pp.97-102, 1978.
- [116] **J. R. Greening**, "*Fundamentals of Radiation Dosimetry*" 2nd Edition, Medical Physics Handbooks 15, Institute of Physics Publishing (IOP), Bristol, London; 1992.
- [117] *Dosimetry in Radiotherapy*, Vol. 2, "Proceedings of a Symposium, Vienna, 31 August-4 September, 1987": IAEA, Vienna; pp.339-342, 1988.
- [118] **V. K. Mehta**, "*Principles of Electronics*", 5th Edition, S Chand & Company Ltd., New Delhi; 1993.
- [119] **A. F. McKinlay**, "*Thermoluminescence Dosimetry*", Medical Physics Handbooks 5, Adam Hilger Ltd., Bristol, Great Britain; 1981.

- [120] **Glenn F. Knoll**, "*Radiation Detection and Measurement*" 2nd Edition, John Wiley & Sons, Inc.; USA, 1989.
- [121] **William J. Price**, "*Nuclear Radiation Detection*", 2nd Edition, McGraw Hill Series in Nuclear Engineering, McGraw Hill Inc, USA, 1964.
- [122] **C. Rangarajan**, "*Natural Radioactivity and Radiation Exposure*", Published in *Methods of Analysis of Radionuclide Contaminants in Foods*, Pollution Monitoring Section, Bhaba Atomic Research Centre, Bombay, India 1989.
- [123] **K. Debertain and R. G. Helmer**, "*Gamma and X-ray Spectrometry with Semiconductor Detectors*", North Holland, Elsevier Science Publishers B.V., Netherlands, 1988.
- [124] **R. K. Varma and B. S. Negi**, "*Scintillation and Solid State Detectors*", Published in *Methods of Analysis of Radionuclide Contaminants in Foods*, BARC, Bombay, India, 1989.
- [125] *Instruction Manual for Portable Dose Ratemeter PDR1Sv*, NE Technology Limited, England, 1990.
- [126] *Operating Manual (with Datasheet), SILENA Detektor Systeme GmbH*, Germany, 1994.
- [127] *High Voltage Power Supply: Nucleus Model - ORTEC 495*, Operating and Service Manual.
- [128] *ORTEC Spectroscopy Amplifier Model - 570*, Operating And Service Manual.
- [129] *EMCAPLUS MCA EMULTION Software*, Instruction Manual, June-1994.
- [130] **William R. Hendee**, "*Medical Radiation Physics*", 2nd Edition, Year Book Medical Publishers, Inc., Chicago-London, 1979.
- [131] **Klaus Debertain and Ren Jianping**, "*Measurement of the Activity of Radioactive Samples in Marinelli Beakers*", Nuclear Instruments and Methods in Physics Research, Sec.-A, Vol. 278, pp.541-549; 1989.
- [132] **B. S. Pasternack and N. H. Harley**, "*Detection Limits for Radionuclides in the Analysis of Multi-component Gamma Ray Spectrometry Data*", Nuclear Instruments & Methods, Vol. 91, pp.533-540; 1971.
- [133] "*International Commission on Radiological Protection (ICRP) Publication 68*", Vol. 24(4), ICRP; Pergamon Press Ltd., UK, 1994.
- [134] "*Statistical Pocketbook of Bangladesh 1997*", Bangladesh Bureau of Statistics, Statistics Division, Ministry of Planning, Government of the People's Republic of Bangladesh; January 1998.

- [135] **D. A. Waite**, "*Interpretation of Environmental Radioactivity Measurements*" in: CRC Handbook of Environmental Radiation, Alfred W. Klement (Editor), CRC Press Inc. Boca Raton, Florida, 2nd Printing; USA, 1991.
- [136] **M. Brai, S. Hauser, S. Bellia, P. Puccio, and S. Rizzo**, "*Natural γ -Radiation of Rocks and Soils from Vulcano (Aeolian Islands, Mediterranean Sea)*", Nuclear Geophysics; Vol. 9, pp.121-127, 1995.
- [137] **Dr Amartya Kumar Sen**, Nobel Laureate in Economics in 1998, "*Interview with Bangladesh Television*", Telecasted at ~ 9.00 pm of Monday, December 21, 1998.
- [138] **Alison P. Casarett**, "*Radiation Biology*", Prentice Hall, Inc. Englewood Cliffs, New Jersey, Published by United States Atomic Energy Commission, 1968.
- [139] "*Dosimetry for Criticality Accidents*", Technical Reports Series No. 211, IAEA, Vienna, 1982.



ANNEXURE



ANNEXURE

UNITS AND FACTORS CONSIDERED IN RADIATION DOSIMETRY AND RADIOLOGICAL PROTECTION

In radiation dosimetry and in radiological protection, several factors and units are considered. These are described in brief in following paragraphs.

1. Dosimetry Units

There are two different considerations in radiation dosimetry, viz.: (1) to describe a radiation beam itself, and, (2) to describe the amount of energy it may impart to any medium.

1.1. The Quantities Describing a Radiation Beam

The terms describing a radiation beam are briefly explained below.

Fluence: If the beam is monoenergetic, and if the number of particles (say photons) dN that cross an area da taken at right angles to the beam, then the ratio of these two quantities is called "fluence or photon fluence"^[24] which is denoted by Φ

$$\text{i.e., Fluence or Photon Fluence } \Phi = \frac{dN}{da}$$

The SI unit of Fluence is particles/m².

Fluence Rate: The number of photons or any radiant particles that passes through unit area per unit time is called the fluence rate^[24], which is denoted by ϕ

$$\text{i.e., Fluence Rate } \phi = \frac{d\Phi}{dt}$$

The SI unit of Fluence Rate is particles/m²- sec.

Energy Fluence: Let dN be the number of photons crossing the area da taken perpendicular to the direction of the beam of photons then the Energy Fluence is the amount of energy crossing per unit area^[24]. It is denoted by the symbol Ψ ;

$$\text{i.e., the Energy Fluence } \Psi = \frac{dN}{da} \cdot h\nu$$

where $h\nu$ is the effective energy of the photons considered. The SI unit of Energy Fluence is Joules/m².

Energy Fluence Rate: The amount of energy carried by the photons or radiant particles crossing through unit area per unit time is called the Energy Fluence Rate, or Energy Flux Density or Intensity^[24]. It is represented by the symbol ψ

$$\text{i.e., Energy Fluence Rate } \psi = \frac{dY}{dt}$$

The SI unit of Energy Fluence Rate is Watt/m².

1.2. The Quantities Related to the Amount of Energy Impart to Any Medium

The quantities related to the amount of energy impart to any medium are briefly explained below.

Exposure: The purpose of ionizing radiation dosimetry is the measurement of the physical and biological consequences of exposure to radiation. As these consequences are proportional to the local absorption of energy, the dosimetry of ionizing radiation is based on the measurement of this quantity.

Exposure is a quantity expressing the amount of ionization caused in air by X-or γ -radiation. The special unit is the (Röntgen) Roentgen (R) which corresponds to the production of ions (of one sign) carrying a charge of 2.58×10^{-4} coulomb per kilogram (kg) of air^[30], i.e., 1 e.s.u charge per cc of air, at NTP^[138]. The absorption of energy in air corresponding to an exposure of 1R is 0.008694 Joules/kg

Since the Roentgen applies only to X- and γ -radiation and their effect on air, so it is not appropriate as a common radiation unit. In the human tissue the energy deposition corresponding to the exposure of 1R γ -radiation of commonly encountered range of photon energy is 0.0096 J/kg. Exposures are commonly expressed in two ways.

Acute Exposure: It is the exposure to a large dose of radiation within a relatively short time. The radiation damages are much more severe in cases of acute exposure.

Chronic Exposure: The chronic exposure is the long term, low level overexposure. The total amount of radiation received may be the same as received in the acute exposure but the radiation damages are of much low severity.

Kerma: Kerma stands for “Kinetic Energy Released in Material”. At a point P, it is defined as the ratio of the transferred energy from photons to electrons dE_{tr} , in the element of volume centred on P to the mass dm contained in the volume element^[20].

$$\text{i.e., Kerma } K = \frac{dE_{tr}}{dm}$$

It is expressed in J/kg i.e., in Gray(Gy).

Linear Energy Transfer (LET): The LET is defined as the energy lost by a radiant particle in traversing a unit distance^[116] i.e., if dE be the energy lost by a charged radiant particle in traversing a distance dl , then the linear energy transfer (LET)

$$\text{i.e., } L = \frac{dE}{dl}$$

commonly used unit of LET is keV/micron.

Roentgen Equivalent Physical (REP): 1 REP is defined as that dose of ionizing radiation which produces an energy absorption of 0.0094 J/kg (94 erg/gm) in tissue^[23].

REP also has the disadvantage that it is applicable only to tissue. This disadvantage has been removed by introducing another unit called Rad, which is discussed in the following paragraph.

Absorbed Dose: Absorbed dose is a measure of energy deposition in any medium by all types of ionizing radiation. Absorbed dose at a point P of any medium is defined as the ratio of the energy, dE , effectively absorbed by an element of volume dv centred on P to the mass contained in that volume element^[20].

$$\text{i.e., Absorbed dose } D = \frac{dE}{dm}$$

The original unit of absorbed dose was Rad (Radiation absorbed dose) and was defined as an energy deposition of 0.01 J/kg^[30].

$$\text{i.e., } 1 \text{ Rad} = 0.01 \text{ J/kg.}$$

$$\text{So that, } 1 \text{ J/kg} = 100 \text{ Rad.}$$

Again, we have the exposure of IR results in an energy deposition of 0.008694 J/kg in air and 0.0096 J/kg in tissue, therefore

$$\text{IR} = 0.8694 \text{ Rad in air}$$

and, $1R = 0.96 \text{ Rad in tissue}$

In the SI units, the unit of absorbed dose is Gray (Gy) and is defined as an energy deposition of 1 J/kg

i.e., $1 \text{ Gy} = 1 \text{ J/kg} = 100 \text{ Rad}$

Therefore the absorbed dose corresponding to the exposure of $1R$ radiation in air and tissue is respectively given by

$1 R = 0.008694 \text{ Gy in air}$

$1 R = 0.0096 \text{ Gy in tissue.}$

Quality Factor: Since the probability of “stochastic effects” is found to be dependent on the quality of the radiation, a weighting factor has been traditionally introduced to modify the absorbed dose and to define the dose equivalent. This dimensionless factor is called the quality factor $QF^{[30]}$.

The quality factor measures the ability of a particular type of radiation to cause biological damage depending on LET and consequently on specific ionization.

The term “Quality Factor” is nowadays replaced by a more precise term “Radiation Weighting Factor” which will be discussed later.

Dose Equivalent: Dose equivalent is a measure of biological effect of radiation. The more precise term “Equivalent Dose” in modern use is substituted for the term “Dose Equivalent”. The dose equivalent (DE) is defined by^[30].

$$DE = D \times QF \times DF$$

where the terms D & QF are defined in the previous paragraphs and DF is the distribution factor. In the SI units, the unit of DE is Sievert (Sv)

$$\text{i.e., } DE (\text{in Sv}) = D (\text{in Gy}) \times QF \times DF$$

The unit of DE will be in Rem when the absorbed dose is measured in Rad.

$$\text{i.e., } DE (\text{in Rem}) = D (\text{in Rad}) \times QF \times DF.$$

Since $1 \text{ Gy} = 100 \text{ Rad}$, so $1 \text{ Sv} = 100 \text{ Rem}$. But in earlier days, Rem was defined as follows.

Roentgen Equivalent Man (Rem): 1 Rem is defined as that amount of any ionizing radiation which produces the same biological damage as $1R$ of X -or γ -radiation^[23]. Thus

$$\text{Dose (in Rem)} = \text{Dose (in Rad)} \times RBE.$$

Where RBE is the Relative Biological Effectiveness, a term related to “Radiation Biology” and is equivalent to “Radiation Weighting Factor” or “Quality Factor”.

2. Units of Radioactivity

Another quantity that is necessary to study the dosimetry is the unit of radioactivity. There are two units of radioactivity in common use, one is the Becquerel (Bq) and the other is Curie (Ci).

Becquerel: Becquerel is the SI unit of radioactivity and 1 Bq is equal to 1 disintegration per second (1 dps).

Curie: 1 Ci is equal to 3.7×10^{10} dps.

$$\text{i.e., } 1 \text{ Ci} = 3.7 \times 10^{10} \text{ Bq.}$$

3. Quantities used in Radiological Protection

Some of the most common quantities used in radiological protection are- (1) Radiation weighting factor (W_R), (2) Equivalent dose (H_T), (3) Tissue weighting factor (W_T), (4) Effective dose equivalent (H_E), (5) Organ dose (D_T), (6) Lethal dose ($LD_{50/30}$), (7) As low as reasonably achievable (ALARA), and, (8) Dose Limits. A short description of these are given below.

Radiation Weighting Factor (W_R): In radiological protection, to find the absorbed radiation energy average over a tissue or organ rather than a point, the absorbed dose is weighted by a factor related to the energy and type of the radiation causing the dose in the tissue or organ of interest. This dimensionless quantity is called the radiation weighting factor^[22] and is denoted by the symbol (W_R). The radiation weighting factor is equivalent the quality factor (Q) to account the dose equivalent (H) at a specified point. The radiation weighting factor (W_R) for different types of radiation are given in Table A1; where all values relate to the radiation incident on the body or, for internal sources, emitted from the source.

Table A1: Radiation weighting factors^[22]

Type and energy range	Radiation weighting factor (W_R)
Photons, all energies	1
Electrons and muons, all energies*	1
Neutrons, energy < 10 KeV	5
10 KeV to 100 KeV	10
> 100 KeV to 2 MeV	20
> 2 MeV to 20 MeV	10
> 20 MeV	5
Protons, other than recoil protons, energy > 2 MeV	5
Alpha particles, fission fragments, heavy nuclei	20

* Excluding Auger electrons emitted from nuclei bound to DNA.

Equivalent Dose (H_T): In radiological protection, the Equivalent dose is the absorbed dose averaged over a tissue or organ and weighted for the radiation quality that is of interest^[22] i.e., the radiation weighting factor W_R . It is denoted by the symbol H_T . The “Equivalent dose” is equivalent to the “dose equivalent”. H_T is formed by weighting the mean absorbed dose D_T , in a tissue or organ, by the weighting factor W_R . i.e.,

$$H_T = W_R \times D_T$$

When various types of energy of radiation exist, then H_T is expressed as a summation over the all types and energy of radiation. i.e.,

$$H_T = \sum_R W_R \times D_{T,R}$$

Where $D_{T,R}$ is the absorbed dose averaged over the tissue or organ T, due to radiation R. The unit of equivalent dose is Sievert (Sv).

Tissue Weighting Factor (W_T): The factor by which the equivalent dose in tissue or organ T is weighted is called the Tissue weighting factor⁽²²⁾. It is denoted by the symbol W_T , which represents the relative contribution of that organ or tissue to the total detriment due to these effects resulting from uniform irradiation of the whole body. The sum of the tissue weighting factors is unity. The Tissue weighting factor W_T for different organs and tissues are shown in Table A2.

Table A2: Tissue weighting factors^[22]

Tissue or Organ	Tissue Weighting Factor (W_T)
Gonads	0.20
Bone marrow (red)	0.12
Colon	0.12
Lung	0.12
Stomach	0.12
Bladder	0.05
Breast	0.05
Liver	0.05
Oesophagus	0.05
Thyroid	0.05
Skin	0.01
Bone surface	0.01
Remainder*	0.05

* The remainder is composed of the following additional tissues and organs: adrenals, brain, upper large intestine, small intestine, kidney, muscle, pancreas, spleen, thymus and uterus.

Effective Dose Equivalent (H_E): Effective dose equivalent or simply the “effective dose” is the sum of the weighted equivalent doses in all the tissues and organs of the body^[22]. It is denoted by the symbol H_E and is given by-

$$H_E = \sum_T W_T \times H_T$$

Where H_T is the equivalent dose in tissue or organ T and W_T is the weighting factor for tissue T. The unit of effective dose is Sievert (Sv).

Organ Dose (D_T): For radiation protection purposes, a tissue or organ average absorbed dose D_T is defined as^[22]:

$$D_T = \frac{E_T}{m_T}$$

where E_T is the total energy imparted in a tissue or organ and m_T is the mass of that tissue or organ, m_T may range from less than 10 gm for the ovaries to over 70 kg for the whole body.

Lethal Dose: Lethal dose is the absorbed dose required to kill 50% of the exposed subjects within 30 days post-irradiation. It is denoted by $LD_{50/30}$ (50%, 30 days). For human subjects, the $LD_{50/30}$ for whole body photon irradiation is typically assigned a value of 4 Gy^[139].

Serious exposures not resulting in death are frequently called Sublethal (value of, say, 1 Gy or less). Such exposures may cause milder symptoms of the acute radiation syndrome, including loss of appetite, loss of hair, inflammation of throat, pallor, haemorrhage, and diarrhoea. No deaths are expected to occur in the absence of complications.

As Low As Reasonably Achievable (ALARA): ALARA concept is the radiologic operating philosophy considering the economic and social factors; the radiologic operation processes, equipment and other operating factors such that shielding, ventilation etc. are so designed that all exposures can be kept as low as reasonably achievable^[15].

Dose Limits: ICRP gave the definition of Dose Limits or “Maximum permissible dose (MPD)” as that dose for an individual, accumulated over a long period of time or resulting from a single exposure, which carries a negligible probability of severe somatic or genetic injuries. In ICRP 60 the dose limits are intended to be a level of dose above which the consequences for the individual would be widely regarded as unacceptable^[22]. After evaluating several aspects of radiation detriment, ICRP has recommended the values which are shown in Table A3.

Table A3: Recommended dose limits^[22]

Application	Dose limit	
	Occupational	Public
Effective dose (whole body exposure)	20 mSv per year averaged over defined periods of 5 years*	1 mSv in a year**
Annual equivalent dose in		
the lens of eye	150 mSv	15 mSv
the skin (1 cm ²)	500 mSv	50 mSv
the hands and feet	500 mSv	—

* With the further provision that the effective dose should not exceed 50 mSv in any single year, the excess dose must be adjusted within the next four years so that the average annual dose limit should not exceed 20 mSv. Additional restrictions apply to the occupational exposure of pregnant women.

** In special circumstances, a higher value of effective dose could be allowed in a single year, provided that the average over 5 years does not exceed 1 mSv per year.

